Evaluation of Methods to Assess the Strength of Soil Cement Base

By

Justin Blake McLaughlin

A thesis submitted to the Graduate Faculty of
Auburn University
in partial fulfillment of the
requirements for the Degree of
Master of Science

Auburn, Alabama
August 5, 2017

Keywords: compressive strength, steel-molded cylinders, core, dynamic cone penetrometer, plastic mold cylinders

Approved by

J. Brian Anderson, Chair, Associate Professor of Civil Engineering
Anton K. Schindler, Co-Chair, Professor of Civil Engineering
Jack Montgomery, Assistant Professor of Civil Engineering

Abstract

Soil cement is a mixture of soil, portland cement, and water that, once compacted and cured, forms a strong and durable pavement base. Construction practices and variance among core strength data have led to questions concerning proper quality control practices and strength testing protocol regarding soil cement. A major concern in this area is strength assessment of the fully cured soil-cement roadbed. This concern has led to the following questions: Is it plausible to use field-molded specimens to evaluate the strength of soil-cement base? Is it plausible to use the dynamic cone penetrometer to evaluate the in-place strength of soil-cement base?

In order to answer these questions, a field testing program was developed to evaluate the suitability of using the dynamic cone penetrometer based on ASTM D 6951, molded cylinder method based on ASTM D 1632, and the plastic mold method (Sullivan et al. 2014). The results from this research are aimed at providing guidance to ALDOT when specifying strength assessment parameters of soil-cement base.

Based on the results from this research, the plastic mold method should be used for qualification of the soil-cement mixture along with field inspection testing. If the plastic mold compressive strength is less than or greater than the ALDOT specification on strength of soil cement base, the dynamic cone penetrometer should be used to determine the in-place strength of soil-cement base.

Acknowledgments

First, I would like to thank my advisors Dr. J. Brian Anderson and Dr. Anton Schindler for their patience, guidance, and instruction throughout this research project and my collegiate career. Without their help, this thesis would not have been completed. I also like to thank Dr. J. Brian Anderson for helping me obtain a job with Hayward Baker; without your help I do not know what I would have done. Also, I would like to thank Dr. Jack Montgomery for time and participation as one of my committee members and for the knowledge he has given me in the classroom.

I would also like to thank my research partner Jordan Nemiroff for all her hard work and patience with me. It was my pleasure to get to know you over the past two years. My utmost appreciation goes to the Alabama Department of Transportation (ALDOT) and the Highway Research Center (HRC) at Auburn University for their financial support on this research project. Also, I would like to thank Lee Yelverton and Kevin Jones, of the Alabama Department of Transportation, for their assistance and collaboration on this project.

Finally, I would like to thank my mother (Sonya McLaughlin), father (Charles McLaughlin), and my brother (Nick McLaughlin) for their love, encouragement, and amazing support throughout my entire life. I would also like to thank my girlfriend (Katie Poole) for helping me extract and bag cylinders late at night.

Table of Contents

List of Tables

List of Figures

Chapter 1

Introduction

1.1 Background

Soil cement is a mixture of native soils with a measured amount of portland cement and water that hardens after compaction and curing to form a strong, durable, frost resistant paving material (Halsted et al. 2006). Soil-cement can be mixed in place using on site materials or mixed in a central plant using selected materials (Halsted et al. 2006). Mixed in-place soil-cement is compacted after blending small amounts of cement with native soils and central plant mixed soil cement is hauled to the placement area in dump trucks and placed on the roadway using a grader, paver, or Jersey-type spreader (Halsted et al. 2006). Soil cement is used throughout the industry as a pavement base for highways, roads, streets, parking areas, airports, industrial facilities, and material hauling and storage areas (Halsted et al. 2006). The Alabama Department of Transportation (ALDOT) uses soil-cement as a base for roadway construction in areas where crushed stone is unavailable or costs too much to transport to the site.

By mixing portland cement with weak native soils, the cement-stabilized base are tightly bound together by the cement. The entire mass is then hardened into a slab with an enough rigidity and strength to spread the loads over a large area of the subgrade, whereas the unstabilized granular soils have a more concentrated load on a small area shown in Figure 1.1. The stronger uniform support, provided by the soil cement, reduces the stress applied to the subgrade preventing subgrade failure, potholes, and road roughness.

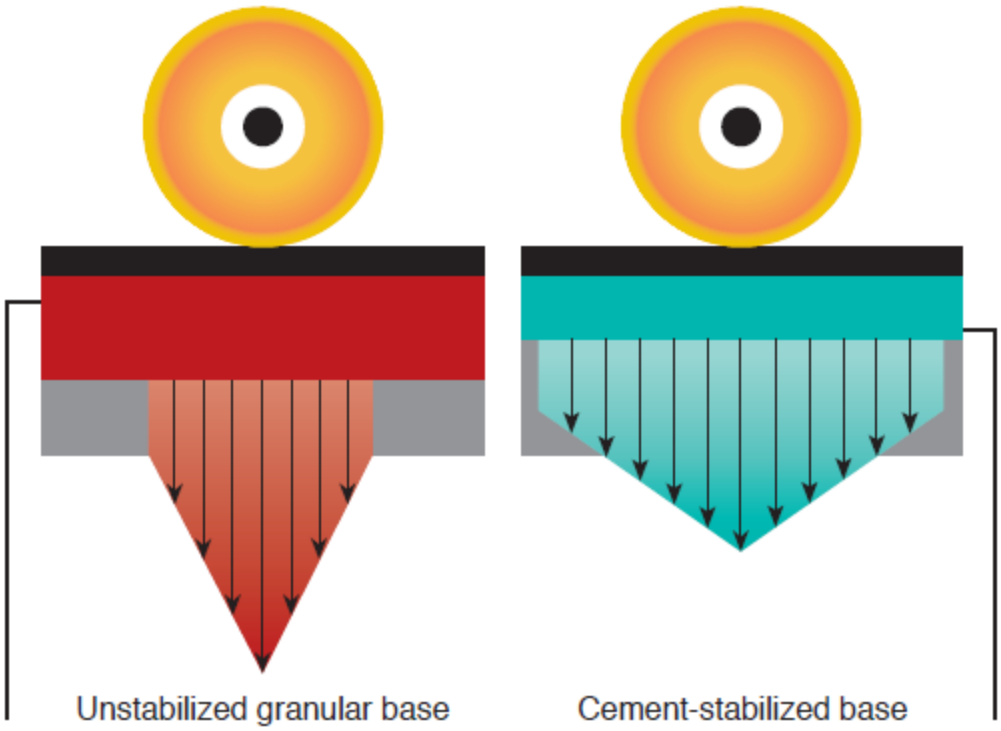

Figure 1.1: Unstablized granular base versus soil-cement base (Halsted et al. 2006)

Advantages of using soil-cement bases include (Halsted et al 2006):

- Provides a stronger, stiffer base that reduces deflections due to traffic loads, delaying the onset of surfaces distress such as fatigue cracking and extended pavement life,
- Thickness of the base are less than those required for granular bases carrying the same traffic load because the loads are distributed over a large area,
- A wide variety of in-situ soils can be used, eliminating the need to haul in expensive select granular aggregates,
- The construction operation progresses quickly with little disruption of the traveling public,
- Rutting is reduced due to the resistance of consolidation and movement of the cement stabilized base,

- Forms a moisture-resistant base that keeps water out and maintains higher levels of strength, even when saturated, thus reducing the potential for pumping of subgrade soils,
- Provides a durable, long-lasting base in all types of climates, designed to resist damaged caused by cycles of wetting and drying and freeze-thaw conditions, and
- Continues to gain strength with age.

Although there are many advantages to using soil cement, there are also some downfalls to using soil cement. Research has shown that a soil-cement base requires an upper and lower bound on strength requirements, in order to produce a quality product. When soil-cement strengths are too low, soil cement will not provide adequate support for traffic, resulting in rutting and large deflections (George 2002). When the strengths are too high, excessive amounts of cement may lead to wide shrinkage cracks that can cause reflective cracking in the hot mix asphalt surface (George 2002).

ALDOT 304 (2014) requires seven-day compressive strengths of cores to be between 250 and 600 psi to receive full payment for the construction of the roadbed. If the compressive strength is less than 250 psi, a price reduction will be imposed following Equation 1.1 (ALDOT 304 2014). If the compressive strength of the core is greater than 600 psi, a price reduction will be imposed following Equation 1.2 (ALDOT 304 2014). For compressive strengths less than 200 psi or greater than 650 psi, the soil-cement layer shall be removed and replaced by the contractor without addition compensation (ALDOT 304 2014). A summary of these ALDOT requirements is presented in Table 1.1.

$$Price\ Reduction = (\ 0.4\ \%\ per\ psi\ )\ x\ (\ 250psi - \ f_c\ ) \quad \text{(Equation 1.1)}$$

$$Price\ Reduction = 20\% - (\ 0.4\ \%\ per\ psi\ )x\ (650psi - \ f_c) \quad \text{(Equation 1.2)}$$

Where:

Price Reduction = reduction in pay (%), and

f_c = Compressive strength of the soil-cement cores

Table 1.1: ALDOT (2014) compressive strength specifications

Average 7-day Compression Strength (f_c)	**Action**
f_c < 200 psi	Remove and Replace
200 ≤ f_c < 250 psi	Price Reduction
250 ≤ f_c ≤ 600 psi	No Price Reduction
600 ≤ f_c < 650 psi	Price Reduction
f_c > 650 psi	Remove and Replace

Construction practices and variance among core strength data have led to questions concerning the proper quality control practices and testing protocol. An ALDOT current practice consists of allowing the soil-cement roadbed to cure for at least seven days before placement of the top layer of asphalt. Cores are typically cut on the sixth day and delivered to the testing laboratory for final curing protocols and compressive strength test are conducted on the seventh day. Results from past ALDOT projects have shown high variability in core strength values, and has led to an increase in concern of the in place strength and the use of coring as a pay item. Figure 1.2 shows 7-day core strengths from ALDOT projects STPAA-0052 (504) in Houston and Geneva Counties in Alabama. Cores taken just a few feet apart show strengths that differed by more than 200 percent. Strength limits are shown on the graph showing the pay scale that ALDOT uses. The contractor was required to remove and replace multiple sections without additional compensation, and some sections resulted in a reduction in pay.

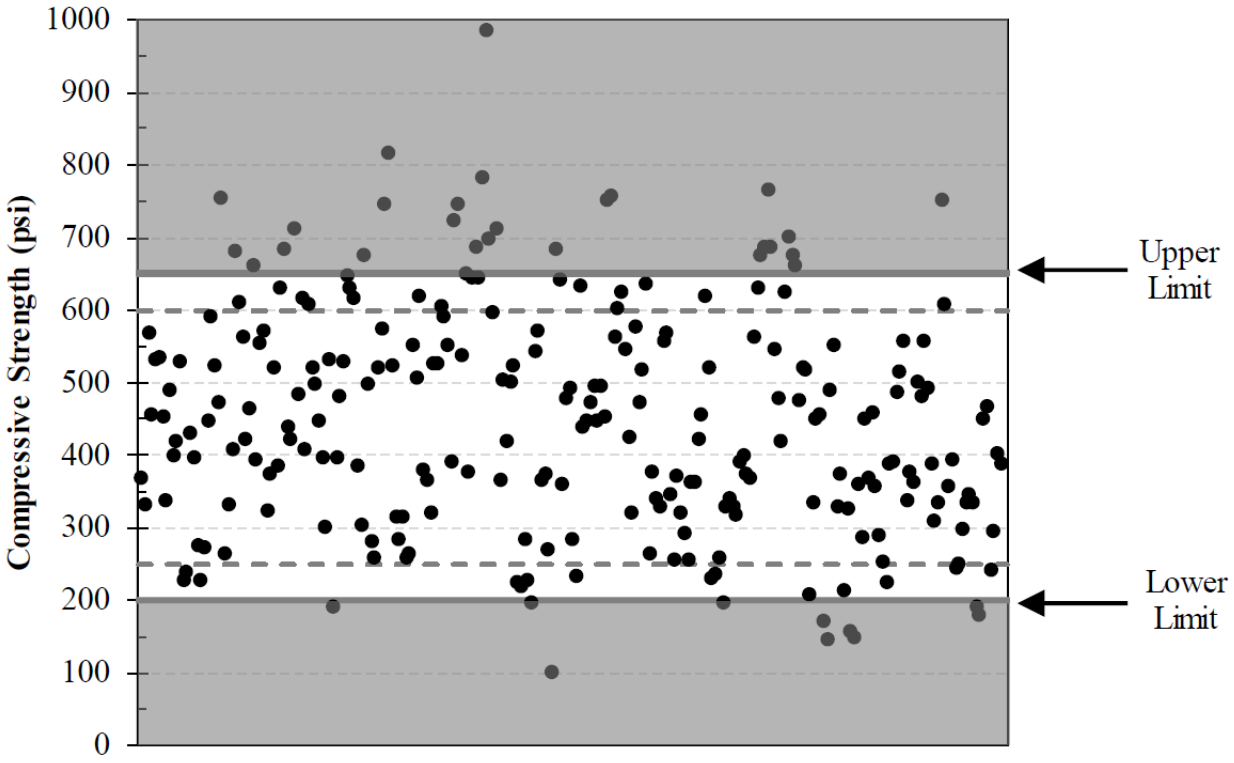

Figure 1.2: Compressive strengths of cores from ALDOT project STPAA-0052 (504)

Due to the high variability in core strengths in past ALDOT projects, other techniques have been developed in an effort to create a reliable method to assess the strength of soil cement. One method used on this project was created by Wilson (2013) utilizing a modified method of ASTM D 1632 (2007), *Standard Practice for Making and Curing Soil Cement Compressive and Flexure Test Specimens in the Laboratory*. ASTM D 1632 (2007) is a laboratory specification on how to make laboratory soil cement cylinders for compressive strength analysis. Wilson (2013) modified this method to treat soil cement like conventional concrete cylinders that are made at the job-site with the material that will be used for the soil-cement placement as a check for the strength of the finished product. This method will be referred to throughout the paper as the steel mold method.

Another method of testing used during this research was the plastic mold (PM) method developed by Sullivan et al. (2014) at Mississippi State University. Sullivan et al. (2014) created his own method to test the strength of the finished product. The method consists of using a modified proctor hammer and a standard 3 by 6 in. plastic mold, which meets the requirements of ASTM C 470 for single-use concrete molds, to compact a soil-cement specimen inside a PM split mold attached to a steel plate. This method is discussed in detail in Chapter 2.5.4.

Another method used for testing soil-cement strength in this research project was the dynamic cone penetrometer (DCP). The procedure used for testing is based on ASTM D 6951 (2009), *Standard Test Method for Use of the Dynamic Cone Penetrometer in Shallow Pavement Applications*. The DCP has been correlated to a variety of engineering properties such as the California Bearing Ratio (Mohammadi et al. 2008), soil classification (Huntley 1990), and compressive strength (McElvaney and Djatnika 1991; Patel and Patel 2012; Nemiroff 2016). This DCP was used to test the seven day in-place strength of the soil-cement base, where the Wilson (2013) molded cylinder method and Sullivan (2014) plastic mold method test seven-day compressive strength of sampled material.

1.2 Research Objectives

The objective of this research effort was to develop a method to reliably assess the strength of soil cement base. Is it plausible to use field-molded samples such as molded cylinders (Wilson 2013) or plastic molds (Sullivan 2014) as control samples to evaluate the strength of soil cement base? Or should the in-place strength of the soil cement base be tested using the DCP presented by Nemiroff (2016)? The primary objectives of this thesis were to:

- Evaluate the suitability of using the molded cylinder samples based on ASTM D 1632 as control samples in the field to assess the strength of soil cement,

- Evaluate the suitability of using the plastic mold method in the field as control samples to assess the strength of soil cement,
- Evaluate the suitability of using the dynamic cone penetrometer in the field to assess the in-place strength of soil cement.
- Recommend a testing protocol that the Alabama Department of Transportation (ALDOT) should implement to assess the strength of soil cement.

1.3 Research Approach

At the time of research, U.S. Highway 84 bypass project in Elba, Alabama was being constructed with an eight inch thick soil-cement base. To develop a method that would reliably assess the strength of the soil cement base, three different test methods were evaluated. One method used was developed by Wilson (2013) whom modified ASTM D 1632, *Standard Practice for Making and Curing Soil Cement Compression and Flexural Test Specimens in the Laboratory*, as a basis for preparing molded soil cement cylinders in the field. The second method used was developed by Sullivan et al. (2014) that developed the plastic-mold method to prepare soil cement cylinders in the field. The third method used was as per ASTM D 6957 (2009) with the DCP to strength correlation proposed by Nemiroff (2016). All three methods were conducted in the field on U.S Highway 84 and results were obtained in order to determine how each test method compared to each other and the seven-day core results collected on the project.

After all these studies were conducted, the suitability of the dynamic cone penetrometer for determining the in-place strength of soil cement base was evaluated. DCP test were conducted over the whole eight inch layer, and the most efficient penetration depth was chosen.

Based on the findings of this research, a strength testing method was developed for ALDOT using the plastic mold (PM) method as a qualification of the soil cement mixture along with field inspection tool. If the plastic mold compressive strength is less than or greater than the ALDOT specification on strength of soil-cement base, the dynamic cone penetrometer should be used to determine the in-place strength of soil-cement base.

1.4 Thesis Outline

An overview of previous research and literature concerning all aspects of this research project is summarized in Chapter 2 of this report. First, the materials that are used in the production of soil cement are presented and discussed. Next, the influence of important engineering properties such as density, compressive strength, and durability are discussed. Next, an overview of soil-cement base construction is discussed pertaining to the different mixing methods, compaction, curing, and quality control. The last section discusses different strength evaluations that were used during the research such as coring, molded cylinders, plastic molds, and the dynamic cone penetrometer.

The experimental plan developed for this research project is presented in Chapter 3. First, the location of the field project is presented. Next, a detailed description of the testing procedure that was developed is presented along with the different testing apparatus and methods that were used.

The results obtained from this study are presented and discussed in Chapter 4. Results from the molded cylinder method and plastic mold method are presented and discussed. Also results and statistical analysis of the dynamic cone penetrometer are discussed along with results determining the most efficient penetration depth.

A summary of the research performed is presented in Chapter 5. Also, all conclusion and recommendations made from this research are summarized.

Appendices A through I follow Chapter 5. Appendix A contains Proctor density curves to make the molded cylinders in the field. Appendix B shows the laboratory procedure done to determine the number of blows to obtain 98 percent density using the plastic mold method. Appendix C contains all the individual compressive strength data obtained from the molded cylinder method, plastic mold method, DCP method, and cores. Appendices D through H contain the DCP penetration results for different depths when the penetration is plotted against blow count. Finally, shown in Appendix I is a plot of all the cores taking from U.S Highway 84 bypass project in Elba, Alabama.

Chapter 2

Literature Review

2.1 Introduction

In this chapter, a literature review of the materials used in production of soil cement base is presented, as well as the soil cements properties such as density and compressive strength. Next, an overview of the process and quality control of soil cement base construction are discussed. Also, testing concerns related to comparison of soil cement with conventional concrete are discussed. Lastly, the evaluation of strength using the dynamic cone penetrometer, molded cylinders, plastic mold method, and coring is discussed.

2.2 Materials

2.2.1 Soil

Soil is defined as the relatively loose agglomerate of minerals, organic materials and sediments found above the bedrock (Holtz and Kovacs 1981). According to ACI 230 (2009), almost all soil types can be used in the construction of soil cement except for organic soils, highly plastic clays, and poorly reacting sandy soils. In general, even though all soil types can be used, granular soils are preferred because they pulverize and mix easier than fine-grained soils. The most common soils used in the production of soil cement are silty sand, processed crushed or uncrushed sand and gravel, and crushed stone (ACI 230 2009). Previous research by Robbins and Mueller (1960) showed that some types of sandy soils may have an adverse effect on the performance of soil cement. The study showed that sandy soils with more than 2 percent organic content or a pH lower than 5.3 will react abnormally with cement. The study also showed that

acidic organic material often had adverse effects of strength development in soil cement mixtures (Robbins and Mueller 1960).

2.2.1.1 Particle Size

For this research, the AASHTO terminology was used to distinguish the boundary between coarse and fine-grained soils. Coarse-grained soils are soils with more than 35% retained on or above the No. 200 sieve and fin-grained soils are soils with 35% or more passing the No. 200 sieve (Halsted et al. 2008).

All types of soil can be hardened with portland cement, because its stability is obtained from the hydration of the cement and not by the cohesion and internal structure of the material (PCA 1995). Coarse-grained soils, such as sands and gravels, are the recommended choice for soil-cement base construction (PCA 1995). Small quantities of cement do not improve fine-grained soils sufficiently to make them satisfactory as base material (PCA 1995). The most preferred choice of soil-cement base are coarse-grained soils because of their ability to pulverize and mix more easily than fine-grained soils (ACI 230 2009). Fine-grained soils require more cement than coarse-grained soils for adequate strength of soil-cement base (PCA 1995). Typically, fine-grained soils tend to have a higher optimum moisture contents. Soils which have high moisture demands also require more cement, making them more prone to drying shrinkage issues (Kuhlman 1994). According to ACI 230 (2009) coarse-grained soils containing between 5% and 35% fines passing the No. 200 sieve produce the most economical soil-cement base.

Sands and gravels that contain 55 percent or more material passing the No. 4 sieve, 37 percent passing the No. 10 sieve, and a maximum nominal size aggregate less than or equal to 2 inches work the best for soil-cement base (ACI 230 2009). These soils are readily pulverized,

easily mixed, and can be built under a wide range of conditions (PCA 1995). According to PCA (1995) sands and gravels with 45 percent or more retained on the No. 4 sieve are being used successfully. To achieve the most economical cement factor for durable cement-treated base, it is recommended to use soil/aggregates that provide dense, well-graded blends with a nominal maximum aggregate size not to exceed three inches in order to help minimize segregation and produce a smooth finished surface (Halsted et al. 2006). ALDOT requires 100 percent passing the 1.5 inch sieve, 80 - 100 percent passing the No. 4 sieve, 15 - 65 percent passing the No. 50 sieve, 0 - 25 percent passing the No. 200 sieve, and 4 - 25 percent clay (ALDOT 304 2014).

Figure 2.1 shows the aggregate gradation band recommended by PCA to minimize the cement content. This band shows the desired range of particle size that will require the least amount of cement necessary to produce a quality soil-cement base. Gradations that fall outside the recommended band could require more cement to be used due to the material being too fine or the material being to coarse to provide the structural interlocks necessary for strength. Too much coarse material interferes with compaction of the matrix of finer particles (Halsted et al. 2006). Gap-graded soil mixes that are dominated by two or three aggregate sizes are not desirable for soil-cement applications (Halsted et al. 2006).

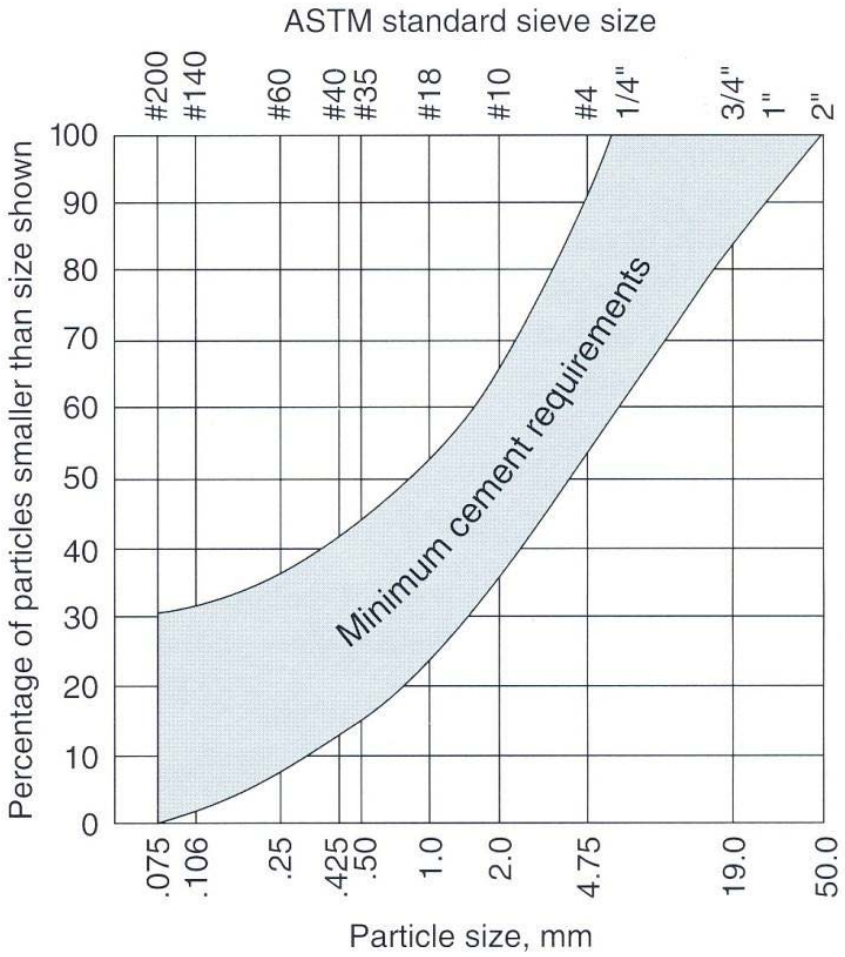

Figure 2.1: Aggregate gradation band for minimum cement requirements (Halsted et al. 2006)

2.2.2 Portland Cement

For most soil-cement applications, Type I or Type II portland cement conforming to ASTM C 150 is normally used (ACI 230 2009). However, other cementitious materials such as fly ash, slag cement, and hydrated lime have been successfully used in soil-cement base operations. The required amount of cement varies depending on the desired properties and soil type (ACI 230 2009). Cement contents may range from as low as 4 to as high as 16 percent by dry weight of soil (ACI 230 2009). Table 2.1 provides a typical estimate for the mixture proportioning procedure based on soil type. This table is not to be used as a rigid requirement, but merely as an estimate of cement content needed based on soil type.

Table 2.1: Typical cement requirements for various soil types (ACI 230 2009)

AASHTO soil classification	ASTM soil classification	Typical range of cement requirement, *percent by weight	Typical cement content for moisture-density test (ASTM D558), percent by weight	Typical cement contents for durability tests (ASTM D559 and D560), percent by weight
A-1-a	GW, GP, GM, SW, SP, SM	3 to 5	5	3-5-7
A-1-b	GM, GP, SM, SP	5 to 8	6	4-6-8
A-2	GM, GC, SM, SC	5 to 9	7	5-7-9
A-3	SP	7 to 11	9	7-9-11
A-4	CL, ML	7 to 12	10	8-10-12
A-5	ML, MH, CH	8 to 13	10	8-10-12
A-6	CL, CH	9 to 15	12	10-12-14
A-7	MH, CH	10 to 16	13	11-13-15
* Does not include organic or poorly reacting soils. Also, additional cement may be required for severe exposure conditions such as slope protection				

2.2.3 Water

Water is necessary in soil cement to help obtain maximum compaction and for hydration of the portland cement (ACI 230 2009). Potable water or other relatively clean water, free from harmful amounts of alkalis, acid, or organic matter may be used (ACI 230 2009). Seawater has been used successfully, however the presence of chlorides in seawater may increase early strengths (ACI 230 2009). Typically water from the city is acceptable and used in soil-cement applications without being tested (ALDOT 2012). Moisture contents of soil cement are usually in the range of 5 to 13 percent by weight of oven-dry soil cement. ALDOT (2012) Section 807 recommends that water used shall be fresh, free from oil, and shall not contain impurities in excess of the limits shown in Table 2.2

Table 2.2: Maximum Limit for Impurities in Water Used for Soil-Cement Applications (adapted from ALDOT 2012)

Item	Limit
Acidity or alkalinity in terms of calcium carbonate	500 mg/L AASHTO T 26
Total organic solids	500 mg/L AASHTO T 26
Total inorganic solids	500 mg/L AASHTO T 26
Chloride Ion Concentration	250 mg/L AASHTO T 26
Sulfate Ion Concentration	250 mg/L AASHTO T 26
pH	Min. 6.0m Max 8.0 ASTM D 1293

2.3 Soil Cement Properties

2.3.1 Density

The Standard Proctor Test, outlined in ASTM D 558 (2004) or AASHTO T 134 is used to determine the optimum moisture content and the maximum dry density. A typical moisture-density curve is shown in Figure 2.2.

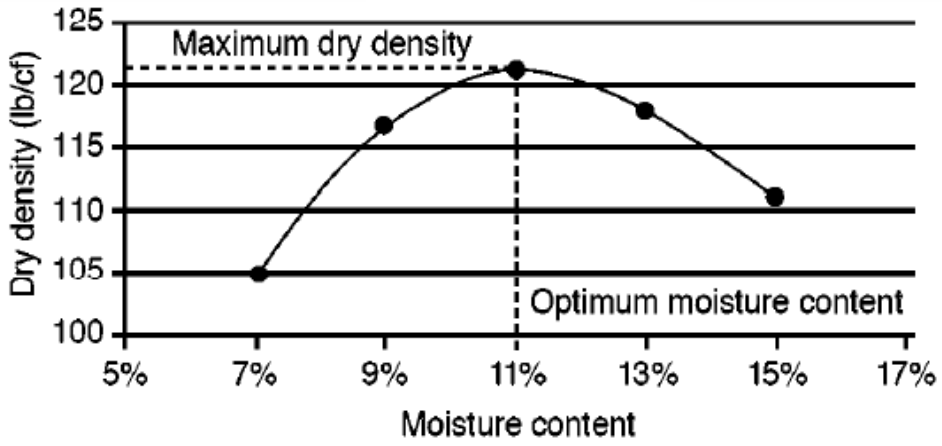

Figure 2.2: Maximum Dry Density and Optimum Moisture Content (Halsted et al. 2006)

Density of soil is usually measured in terms of dry density (ACI 230 2009). Adding cement to a soil generally causes change in both the optimum moisture content and maximum dry density for a given compactive effort, however the direction of the change is unpredictable

(ACI 230 2009). The high specific gravity of the cement relative to the soil tends to produce a higher density, while the flocculating action of the cement tends to produce an increase in optimum moisture content (ACI 230 2009). Shen and Mitchell (1966) showed that generally for a given cement content, the higher the density of the specimen was the higher the compressive strength of the cohesionless soil-cement mixture. Prolonged delays between the mixing of soil cement and compaction have an influence on both density and strength (ACI 230 2009). Research by West (1959) showed that a delay of more than 2 hours between mixing and compaction results in a significant decrease in both density and compressive strength. Research by Felt (1955) showed similar findings, but showed that this effect of time delay could be minimized, providing the mixture was mixed several times an hour, and the moisture content at the time of compaction was at or slightly above optimum moisture.

2.3.2 Compressive Strength

ASTM D 1633 (2007) is used to measure the unconfined compressive strength of soil-cement mixtures. The unconfined compressive strength, f_c, is the most widely referenced property of soil-cement (ACI 230 2009). Unconfined compressive strength indicates the degree of reaction of the soil-cement-water mixture, rate of hardening, and serves as a criterion for determining the amount of cement requirements for proportioning soil-cement (ACI 230 2009). Soaking specimens prior to testing is recommended in ASTM D 1633 since most soil-cement structures may become permanently saturated during their service life and exhibit lower strength under saturated conditions (ACI 230 2009). Examples of 7 and 28 day unconfined compressive strengths for soaked soil cement specimens are shown in Table 2.3.

Table 2.3: Range of unconfined compressive strengths of soil cement (ACI 230 2009)

Soil type	Soaked compressive strength,* psi	
	7-day	28-day
Sandy and gravelly soils: AASHTO Groups A-1, A-2, A-3 Unified Groups GW, GC, GP, GM, SW, SC, SP, SM	300 to 600	400 to 1000
Silty soils: AASHTO Groups A-4 and A-5 Unified Groups ML and CL	250 to 500	300 to 900
Clayey soils: AASHTO Groups A-6 and A-7 Unified Groups MH and CH	200 to 400	250 to 600

*Specimens moist-cured 7 or 28 days, then soaked in water before strength testing.
Note: 1 psi = 0.0069 MPa.

The range of values given is representative for a majority of soils normally used in the United States for soil-cement construction (ACI 230 2009). Figure 2.3 shows that a linear relationship can be used to approximate between compressive strength and cement content.

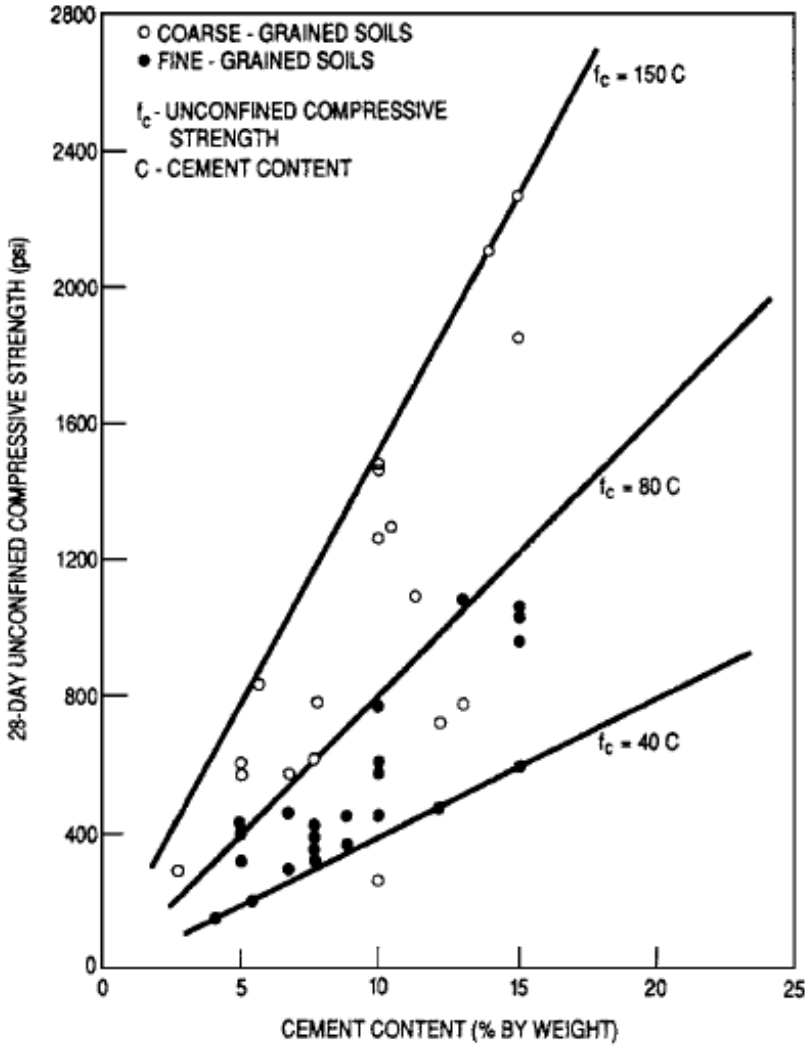

Figure 2.3: Relationship between cement content and unconfined compressive strength for soil-cement (ACI 230 2009)

Curing time affects the strength gain of soil-cement mixture differently depending on the type of soil used in the mixture. Figure 2.4 shows that strength increase is greater for granular soil cement than for fine-grained soil cement.

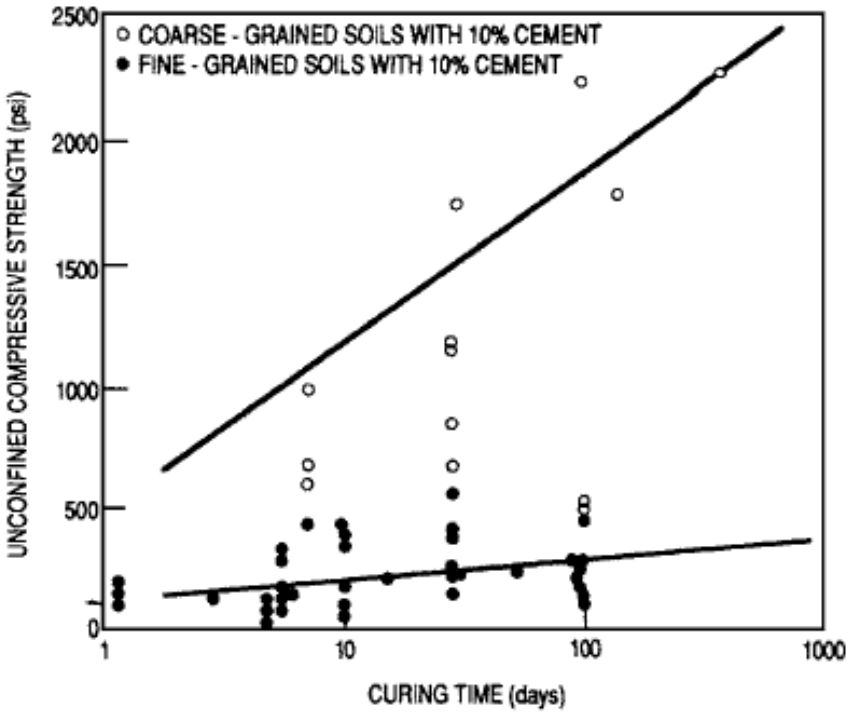

Figure 2.4: Effects of curing time on unconfined compressive strength of soil-cement mixtures (FHWA 1979)

2.3.3 Shrinkage and Reflective Cracking

Shrinkage cracks may develop in the soil cement base over time and result in reflective cracking in the upper asphalt surface layer. Cement-treated soils undergo shrinkage during drying of the soil-cement layer. The shrinkage and subsequent cracking depend on cement content, soil type, water content, degree of compaction, and curing time (ACI 230 2009). Soil cement made of fine-grained soils crack differently than coarse-grained soils. Soil cement made with clays develops higher total shrinkage, but crack widths are smaller and individual cracks are usually spaced 2 to 10 feet apart (ACI 230 2009). Coarse-grained soil cement produce less shrinkage, but larger cracks spaced 10 to 20 feet apart (ACI 230 2009). Figure 2.5 shows some shrinkage cracks of the soil cement base on US Highway 84 in Elba, Alabama.

Figure2.5: Transverse and Longitudinal Cracking on U.S. Highway 84

George (2002) stated that despite shrinkage cracks, soil cement performance has been good or better than other base materials. George (2002) concluded that crack spacing and crack width are influenced by the following factors;

1. Volume change (shrinkage) resulting from drying and/or temperature change,
2. Tensile strength of the stabilized material,
3. Stiffness and creep of stabilized material, and
4. Subgrade restraint.

Shrinkage cracking in the soil-cement base may lead to reflective cracking in the asphalt pavement. ACI 230 (2009) states that reflective cracking in asphalt pavements, induced by base

cracking in soil cement, may or may not be a performance problem. Many miles of soil-cement pavements have performed well even though narrow reflective cracks developed in the asphalt pavement (ACI 230 2009). Overall crack-related degradation can be mitigated by adopting materials and/or methods that bring about a desirable crack pattern (George 2002). It is stated that numerous fine cracks would ensure adequate interlocking and, in turn, superior load transfer across crack faces (George 2002). When the cracks are large enough to admit moisture and degrade the base and subgrade while reducing the load transfer cracking can become a performance problem (ACI 230 2009). Large cracks can cause raveling, pumping/loss of subgrade material, pavement faulting, surface deterioration, and poor ride quality (ACI 230 2009). Methods to control cracking and achieve good performance include proportioning to minimize shrinkage, use of secondary additives, observing quality construction procedures, and controlling the cracking through bituminous surfaces (ACI 230 2009). Some specific techniques include: compacting at slightly less than optimum moisture content, limiting the fines content in the soil, using interlayers to inhibit propagation of cracks from the base layer, delayed surfacing and allow prolonged curing for 14 to 28 days to allow initial cracks to form, using thicker base slab with less cement, prescribing materials/methods that promote numerous microcracks to form, adding fly ash to reduce overall shrinkage, use of expansive cement, and using specification parameters that help provide a desirable crack pattern (ACI 230 2009).

2.3.4 Durability

Durability of soil-cement mixtures and adequate strength are the principal structural requirements of a hardened soil-cement mixture and a good service life. ASTM D 559 (2015), *Standard Test Method for Wetting and Drying Compacted Soil-Cement Mixtures*, and ASTM D 560, *Standard Test Method for Freezing and Thawing Compacted Soil-Cement Mixtures*, are

used to determine the durability of the soil-cement mixture. The Portland Cement Association (PCA) criteria for wet-dry and freeze-thaw durability are shown in Table 2.4. Cement contents sufficient to prevent weight losses greater than the values indicated after 12 cycles of wetting-drying-brushing or freezing-thawing-brushing are considered adequate to produce a durable soil cement.

Table 2.4: PCA criteria for soil-cement as indicated by wet-dry and freeze-thaw durability tests (PCA 1971)

AASHTO soil group	Unified soil group	Maximum allowable weight loss, %
A-1-a	GW, GP, GM, SW, SP, SM	14
A-1-b	GM, GP, SM, SP	14
A-2	GM, GC, SM, SC	14*
A-3	SP	14
A-4	CL, ML	10
A-5	ML, MH, CH	10
A-6	CL, CH	7
A-7	OH, MH, CH	7

*Ten percent is maximum allowable weight loss for A-2-6 and A-2-7 soils.
Additional criteria:
1. Maximum volume changes during durability test should be less than 2% of initial volume.
2. Maximum water content during test should be less than quantity required to saturate sample at time of molding.
3. Compressive strength should increase with age of specimen.
4. Cement content determined as adequate for pavement, using the aforementioned PCA criteria, will be adequate for soil cement slope protection that is 5 ft (1.5 m) or more below the minimum water elevation. For soil cement that is higher than that elevation, cement content should be increased two percentage points.

The U.S. Army Corps of Engineers (USACE) follows its technical manual, *Soil Stabilization for Pavements,* to produce an adequate soil cement base. Table 2.5 shows the criterion of the USACE.

Table 2.5: USACE durability requirements (ACI 230 2009)

Type of soil stabilized	Maximum allowable weight loss after 12 wetting-and-drying or freezing-and-thawing cycles, % of initial specimen weight
Granular, $PI < 10$	11
Granular, $PI > 10$	8
Silt	8
Clays	6

2.4 Overview of Soil-Cement Base Construction

2.4.1 Soil-Cement Base Construction

ACI 230 (2009) states that in the construction of soil cement, the objective is to obtain a thoroughly mixed, adequately compacted, and cured material. Soil cement should not be mixed or placed when the soil or subgrade is frozen or when the air temperature is below 45° F (ACI 230 2009). ALDOT (2014) states that mixing and placement will not be allowed when the air temperature is below 40°F in the shade, when the temperature of the soil is below 50°F, and during rain or when rain is imminent. When the air temperature is expected to reach the freezing point, the soil cement should be protected from freezing for at least seven days (ACI 230 2009). The soil cement shall not be placed unless the mixing, placement, and compaction can be completed within two hours without interruption (ALDOT 2014). There are two main types of mixing methods, mixed in-place and mixing at a central-mixing plant and these will be discussed first. Next, the processes of compacting, finishing, and curing are presented.

2.4.1.1 Mixed In-Place Method

Mixed in-place soil-cement operations are performed with transverse single-shaft mixers. All soil types, from granular to fine-grained, can adequately be pulverized and mixed using a

single-shaft mixer; however, some soils may require multiple passes of the mixer to achieve adequate pulverization (ACI 230 2009). Soil-cement base construction may be performed with material already in-place or by borrowed material. Uniformity of the soil material throughout the borrow site should be monitored for purposes of quality control for cement requirements, optimum moisture, and density (ACI 230 2009).

Before mix in-place operations begin all soft or wet subgrade areas are located and corrected. All deleterious material such as stumps, roots, organic soils, and aggregates larger than 3 inches should be removed (ACI230 2009). Once all material is removed, the soil is shaped to the approximate lines and grades. Next, bulk distribution of cement is obtained by using a mechanical spreader. The main intent of the cement-spreading operation is to provide a uniform distribution of cement. For a uniform cement spread, the mechanical spreader must be operated at a uniform speed with a constant level of cement in the hopper (ACI 230 2009). Generally, the amount of cement required is specified as a percentage by weight of oven-dry soil, or in pounds of cement per cubic foot of compact soil cement (ACI 230 2009). The mechanical spreader can be attached to either a dump truck or a bulk-cement truck as shown in Figure 2.6. When a bulk-cement truck is utilized, cement is moved pneumatically from the truck through an air-separator cyclone that dissipates the air pressure; the cement then falls into the hopper of the spreader (ACI 230 2009).

Figure 2.6: Bulk-cement truck with mechanical spreader used to place cement

Once the cement has been evenly applied to the roadbed, a single-shaft mixer like the one shown in Figure 2.7 is used to pulverize and mix the cement with the soil. Agricultural-type equipment is not recommended due to their relatively poor mixing uniformity (ACI 230 2009). Soils with higher fine contents are generally more difficult to pulverize and mix. In-place mixing efficiency, as measured by the strength of the treated soil, may be less than that obtained in the laboratory (ACI 230 2009). When these circumstances arise, an increase in 1 or 2 percent cement content may compensate for the in efficiency of the mixing method (ACI 230 2009).

Figure 2.7: Single-shaft mixer used in mixed-in-place construction

Next, a water truck is used to apply the appropriate amount of water to the surface of the mixture to obtain the desired water content. This may take a couple of passes before the desired water content is reached. The water truck used will typically have a spray bar mounted on the back as shown in Figure 2.8. Then, the single-shaft mixer mixes the material again to ensure a properly mixed material. The soil and cement must be sufficiently blended when water contacts the mixture to prevent the formation of cement balls (Halsted et al. 2006).

Figure 2.8: Water truck used in mixed-in-place construction

ACI 230 (2009) recommends that fine-grained soils be mixed at moisture content near optimum for the most effective pulverization. Granular soils should be mixed at a moisture content less than optimum to prevent the formation of cement balls (ACI 230 2009). After, the cement has been added and mixed, and water applied and re-mixed, the compaction process begins.

2.4.1.2 Central-Mixing Plant Method

The plant-mixed method can be divided into two types: the pug mill mixer and the rotary mixer. Pug mill mixers can further be divided into continuous flow or batch mixers. Batch pug mill mixers and rotary drum mixers have been used satisfactorily, the most common central plant mixing method is the continuous-flow pug mill mixer (ACI 230 2009). Continuous-flow pug mil mixers have a production rate that varies between 200 and 800 ton/hour (ACI 230 2009).

A typical continuous-flow pug mill plant, shown in Figure 2.9, consists of a soil bin or stockpile, a cement silo with surge hopper, a conveyor belt to deliver the soil and cement to the

mixing chambers, a mixing chamber, a water storage tank for adding water during mixing, and a holding hopper to temporarily store the mixed soil cement prior to loading (ACI 230 2009).

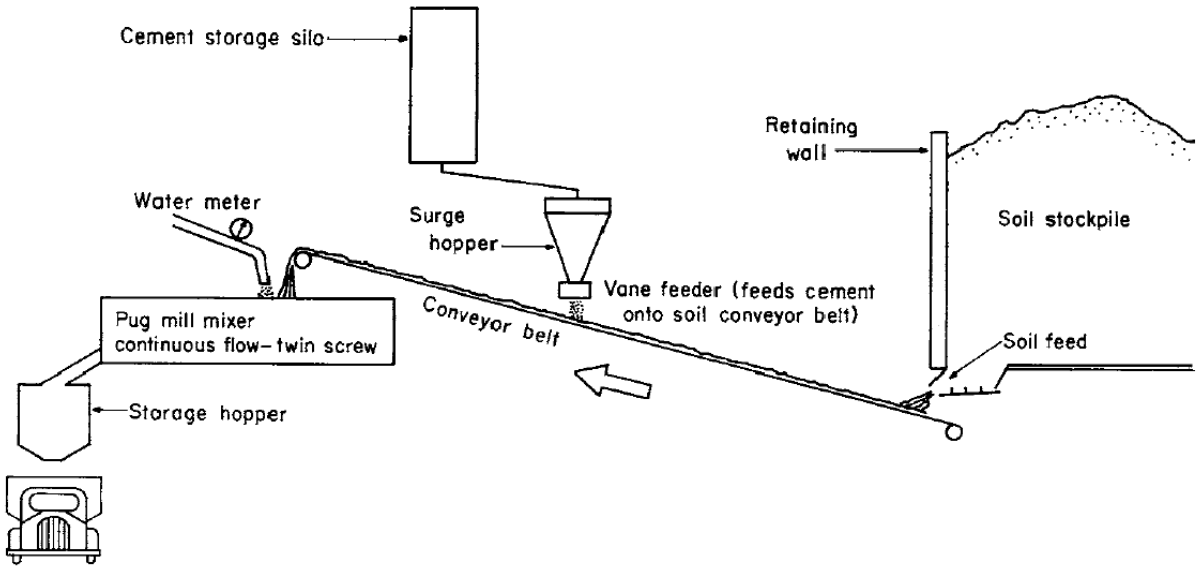

Figure 2.9: Diagram of continuous-flow pug mill plant (ACI 230 2009)

A pug mill mixing chamber consists of two parallel shafts equipped with paddles along each shaft as shown in Figure 2.10. The twin shafts rotate in opposite directions, and the soil cement is moved through the mixer by the pitch of the paddles (ACI 230 2009).

Figure 2.10: Twin-shaft pug mill mixing chamber (Halsted et al. 2006)

Central-mixing plants are generally used for projects which involve the use of borrow materials. Granular borrow materials are preferred due to their low cement requirements and ease in mixing (ACI 230 2009). Clayey soils are avoided because they are difficult to pulverize (ACI 230 2009). Most soil borrow sites are located near the construction site or roadways. Natural soil deposits usually do not consist of homogenous and uniform materials. If the material in the borrow area varies with depth, full-face cuts should be made with excavation machinery to ensure that some material from each layer is obtained (ACI 230 2009). If the material varies laterally across the borrow pit, loads from different locations in the borrow area should be mixed (ACI 230 2009). Mixing for gradation uniformity can be done at the plant location with the help of a bulldozer and front-end loader. Excavated material dumped at the base of the stockpile can be pushed up the stockpile using a bulldozer and a front-end loader can be used to load the soil feed (ACI 230 2009). An adequate check for unsuitable materials, such as clay lenses, cobbles or cemented conglomerates, should be performed routinely to ensure that large particles and clay balls are removed. Most plants will have a 1 to 1-1/2 inch mesh to screen the material before mixing.

Freshly mixed soil cement is typically transported using dump trucks. To reduce evaporation losses during hot, windy conditions and to protect against sudden showers, rear and bottom dump trucks are often equipped with protective covers (ACI 230 2009). ACI 230 (2009) recommends that no more than 60 minutes should elapse between the start of moist mixing and the start of compaction. They also recommend the haul time be limited to 30 minutes. ALDOT (2012) states that cement treated bases shall be delivered and spread within 45 minutes after mixing, and if a mixture has not been compacted within three hours of placement is to be rejected and removed at the contractor’s expense.

ACI 230 (2009) recommends that the mixed soil cement be placed on a firm subgrade, without segregation, in a quantity that will produce a compacted layer of uniform thickness and density. The subgrade and all adjacent surfaces should be moistened before placing soil cement. Even though there are a variety of spreading devices and methods, the use of a motor grader, a spreader box, or asphalt-type pavers are the most common (ACI 230 2009). Figure 2.11 shows a motor grader spreading the plant mixed soil cement before compaction efforts take place. Some pavers are equipped with one or more tamping bars that provide initial compaction. Soil cement is usually placed in a layer 10 to 30 percent thicker than the final compacted thickness (ACI 230 2009).

Figure 2.11: Spreading operations

2.4.1.3 Compaction of Soil Cement Base

Compaction should begin as soon as possible and should be completed within 2 hours of initial mixing (West 1959). The detrimental effects of delayed compaction on density and strength are discussed in sections 2.3.1 and section 2.2.2. No section should be left unworked for

longer than 30 minutes during the compaction operation. In order to obtain maximum density, it is standard practice to compact the soil-cement mixture at or near optimum moisture content as determined by ASTM D 558. Standard practice requires soil-cement base to be compacted to a minimum of between 95 and 98 percent of maximum density. ALDOT requires soil-cement base to be compacted to within two percentage points of optimum moisture content and 98 percent density or above as determined by the required laboratory test (ALDOT 2012).

After soil cement is thoroughly mixed the compaction process begins. The first compaction method was used to provide initial compaction to the soil-cement base, as shown in Figure 2.12. The main types of rollers used for compaction of soil cement are sheepsfoot rollers, multiple-wheel rubber-tired roller, vibratory steel-wheeled roller, and heavy rubber-tired roller.

Figure 2.12: Front-end loader used for initial compaction

Standard practice for fine-grained mixtures requires a sheepsfoot roller for initial compaction, followed by a rubber tire roller for finishing as shown in Figure 2.13 and Figure 2.14, respectively.

Figure 2.13: Sheepsfoot roller used to compact fine-grained soil-cement base

Figure 2.14: Multiple-wheel, rubber-tire roller used to compact soil-cement base

Coarse-grained soils or granular soils require the vibratory roller for compaction. Finishing usually requires a steel-wheeled roller without vibration. Most designs require a layer thickness in the range of 6 to 9 inches (ACI 230 2009). Compactive efforts continues until the required density is achieved (ACI 230 2009). A vibratory steel-wheel roller is shown in Figure 2.15.

Figure 2.15: Steel-wheel vibratory roller used for granular soil compaction

2.4.1.4 Curing

Once the density requirement is obtained and compaction is nearing completion, grade requirements and cross sections are finalized and curing is started. Proper curing of soil cement is important because strength gain is dependent upon time, temperature, and the presence of water (ACI 230 2009). Strength gain due to the hydration of the cement requires a moist environment. Curing has to start once compaction and finishing have been completed. Typically,

the soil-cement base is allowed to cure for 3 to 7 days before construction is allowed to continue. During this time, light traffic is generally allowed on the soil-cement base as long as the curing seal is not compromised (ACI 230 2009).

Water sprinkling and applying of a bituminous coating are two popular methods of curing (ACI 230 2009). By keeping the surface sprinkled with water, along with light rolling to seal the surface, the soil-cement base can maintain moisture levels adequate to promote appreciable strength gains. The most common method of curing is done with the use of a bituminous coating. With bituminous curing, the soil cement is commonly sealed with emulsified asphalt. The rate of application is dependent on the particular emulsion, but typically varies from 0.15 to 0.30 gal/yd^2 (ACI 230 2009). Before the bituminous material is applied, the surface of the soil cement should be moist and free of dry, loose material. If traffic is allowed on the soil cement during the curing period, it is desirable to apply sand over the bituminous coating to minimize the tracking of the bituminous material (ACI 230 2009). Figure 2.16 shows a layer of bituminous material placed on the soil-cement base on U.S. Highway 84.

Figure 2.16: Asphalt emulsion placed on the soil-cement base

2.4.2 Quality Control Testing and Inspection

Quality control is essential to ensure that the soil-cement base will be adequate for its intended use. It is also an in-place check system to ensure that the contractor has performed work that meets the requirements of the design plans and specifications. Field inspections of soil-cement base construction involve controlling the following properties (ACI 230 2009):

- Cement content,
- Moisture content,
- Mixing uniformity,
- Compaction,
- Lift thickness and surface tolerance, and
- Curing.

2.4.2.1 Cement Content

For mixed in-place construction, the inspector must check the accuracy of the cement spread by the bulk spreaders to ensure the proper quantity is being applied. The two ways to check bulk cement are a spot check or an overall check. Spot check is done by placing a sheet of canvas, usually 1 yd^2 in area, ahead of the cement spreader. After the spreader has passed the canvas, the cement is carefully collected and weighed (ACI 230 2009). The cement application rate is then calculated and adjusted if necessary. The other method is by performing an overall check. This is done by measuring the distance or area which a truckload of cement with a known weight is spread. The actual area covered is then compared to the theoretical area (ACI 230 2009).

In a central mixing plant operation, it is necessary to proportion the cement and soil before they enter the mixing chamber. When soil cement is mixed in a batch-type pug mill or

rotary-drum mixing plant, the proper quantities of soil, cement, and water for each batch are weighed before being transferred to the mixer (ACI 230 2009). These type plants are calibrated by checking the accuracy of the scales used to weigh each material. For continuous-flow mixing plants, two methods can be used to check for accuracy. The first method consists of running soil through the plant for a given amount of time and collecting the material in a truck, while cement is diverted directly from the feeder into a truck. Both the cement and soil are then weighed and adjusted until the correct amount of cement is released (ACI 230 2009). The second method consists of feeding soil directly onto a conveyor belt, and the soil on a selected length is collected and its dry weight is determined. Then the plant is operated with only cement feeding onto the conveyor belt, and the cement feeder is then adjusted until the correct amount of cement is being discharged (ACI 230 2009). Typically, central mixing plants are calibrated at least daily at the beginning of each project. For more accurate testing method ASTM D 558 may be used to determine the cement content of freshly mixed soil cement. The test, can be conducted within 15 minutes in the field and is reliable to within 1 percent of the actual cement content (ACI 230 2009).

2.4.2.2 Moisture Content

Optimum moisture content obtained by ASTM D 558 is typically used for field control of moisture content during construction. As previously stated, adequate moisture content is important to achieve adequate compaction and for hydration of the cement. One approach is moisture content estimation, which is fairly empirical. Estimations of moisture content by look and feel are quite common practice in quality control of soil-cement base construction. A quick way to check the moisture content is by collecting a sample in one's hand. The mixture will be at or near optimum moisture content if the hand is dampened when it is tightly squeezed. Mixtures

above optimum will leave excess water on the hands, while mixtures below optimum will tend to crumble easily (ACI 230 2009). Another way to estimate the moisture content is by breaking the soil cement into two pieces, if the soil cement brakes into two pieces with little or no crumbling the sample is at optimum moisture content.

If the surface of the soil cement begins to turn grey in color during compaction or finishing, it is a sign that the surface is becoming too dry (ACI 230 2009). When this occurs, very light fog spray applications of water should be applied made to bring the moisture content back to optimum (ACI 230 2009).

2.4.2.3 Mixing Uniformity

For mixed in-place construction uniformity is checked by digging trenches or a series of holes at regular intervals for the full depth of treatment. The material is checked to ensure uniform color and texture from top to bottom (ACI 230 2009). A mixture that has a streaked appearance has not been mixed sufficiently (ACI 230 2009).

The uniformity can be checked visually at central mixing plants, but can also be checked during placement using similar methods used for mixed in-place construction. The mixing time necessary to achieve an uniform mixture will depend on the soil gradation and mixing plant used. Usually 20 to 30 seconds of mixing are required (ACI 230 2009).

2.4.2.4 Compaction

Standard practice requires the soil-cement mixtures to be compacted at or near optimum moisture content to a specified minimum percent of maximum density. Field density requirements range from 95 to 100 percent of the maximum density obtained in the laboratory by ASTM D 558. The three most common methods for determining in-place density are: Nuclear method (ASTM D 2922 and ASTM D 3017), Sand-cone method (ASTM D 1556), and balloon

method (ASTM D 2167). In-place densities are determined daily at frequencies that vary widely, depending on the application, and should be conducted immediately after rolling (ACI 230 2009). By comparing in-place density measures with the results obtained from the moisture-density test, any adjustment in compaction procedures can be determined (ACI 230 2009). ALDOT (2012) requires in-place density measurements to be taken with a nuclear density gauge as shown in Figure 2.17.

Figure 2.17: Nuclear density gauge for field density measurements

2.4.2.5 Lift Thickness and Surface Tolerance

Lift thickness is usually checked by digging small holes in the soil cement to determine the bottom of the treated material or when field density checks using the sand-cone or balloon methods are used. Depth can be determined by using a 2 percent solution of phenolphthalein squirted down the side of cut face of the soil cement. The soil cement will turn pinkish-red, while

the untreated material will retain its natural color (ACI 230 2009). Another method to check for lift thickness is to core a hardened soil-cement sample. ALDOT checks for lift thickness by cutting cores for compressive strength, and required that the compacted lift thickness of the layer shall not be more than ½ of an inch less or 1 inch more than the required thickness (ALDOT 304 2014).

Surface tolerance are usually specified for soil-cement pavement applications (ACI 230 2009). Surface tolerances or smoothness is usually measured with 10 or 12 feet straightedge or surveying equipment. Most state DOT's limit the maximum departure from a 12 or 10 feet straightedge to about 3/8 of an inch, although, departures from design grade of up to 5/8 inch are usually allowed (ACI 230 2009). ALDOT states that the finished surface shall not vary more than ½ of an inch in any 25 foot section (ALDOT 2012).

2.5 Strength Evaluation

2.5.1 Core Testing

ALDOT quality control and acceptance requirements mandated that cores be taken on the sixth or seventh day after completion of the soil-cement roadbed for in-place compressive strength testing. Figure 2.18 shows a typical core once removed from the core hole.

Figure 2.18: Core taken from U.S. Highway 84 in Elba, Alabama

There are different methods used to cut cores and condition a core from the time it has been removed from the roadbed until the time of testing. The locations the cores are to be taken are designated by the Engineer in accordance with ALDOT 304 (2014). The coring operation is to be done by the contractor meeting the requirements set for by ALDOT 419 (2008) and under the supervision of the engineer. Cores shall be 6 inches in diameter for soil cement layers greater than 7 inches in thickness (ALDOT 304 2014). According to ALDOT 419 (2008) coring should be done dry, but can be performed with a minimum amount of water at a low flow. Figure 2.19 shows a picture of the coring operation.

Figure 2.19: Coring operation on U.S. Highway 84 in Elba, Alabama

All cores once removed from the in-place soil-cement bed are to be placed in a plastic bag to minimize moisture loss. If water was used during the coring operation, the surface of the cores samples shall be let to air dry in the shade for 30 minutes before placing them in a plastic bag (ALDOT 419 2008). Once the cores are bagged they are to be placed in a horizontal position with at least half of their diameter embedded in a pre-dampened bed of sand in a covered wooden box provided by the contractor and immediately transferred to the testing location (ALDOT 419 2008). When the sample has arrived at the testing location it is removed from the plastic bag, and dry sawed to remove any irregularities to the bottom surface. Both ends of the cores are to be capped per AASHTO T 231 using sulfur mortar only (ALDOT 419 2008). Cores

shall be tested for compressive strength when they have obtained a constant mass and the sulfur mortar caps have been allowed to harden according to AASHTO T 231 (ALDOT 419 2008). Testing equipment shall meet the requirements of AASHTO T 22 and the person performing the compressive strength testing shall be an ALDOT Concrete Strength certified technician (ALDOT 419 2008). ALDOT 419 (2008) states that the loading rate during testing shall be applied continuously and at the same rate throughout the testing procedure. The compressive strength shall be reported to the nearest tenth psi and if the specimen length-to-diameter ratio is less than 2, a correction factor as shown in AASHTO T 22 shall be applied to the compressive strength results (ALDOT 419 2008).

After the cores have been removed from the core holes they shall be repaired immediately by the contractor. Core holes shall be filled with the same mixture of soil cement used during placement (ALDOT 419 2008). The soil-cement mixture shall be placed in increments of three-inch layers at a time and each layer shall be packed in place with small tools and consolidated by tamping (ALDOT 419 2008). Figure 4.20 shows a typical core section ready to be repaired.

Figure 2.20: Cored section of soil cement ready to be repaired on U.S. Highway 84

2.5.2 Dynamic Cone Penetrometer

The dynamic cone penetrometer (DCP) is an in-situ testing device used in field exploration and quality control of compacted soils during construction. The DCP is simple to operate, inexpensive, and produces repeatable results. The DCP was originally developed in South Africa for in-situ evaluation of pavement layer strength (Scala 1956). It is now used in South Africa, the United Kingdom, Australia, New Zealand, and several states in the United States such as California, Florida, Minnesota, Mississippi, Texas and North Carolina (Ahsan

2014). The DCP has been correlated to engineering properties such as the California Bearing Ratio (Mohammadi et al. 2008), soil classification (Huntley 1990), and unconfined compressive strength (McElvaney and Djatnika 1991; Patel and Patel 2012; Nemiroff 2016).

Dynamic cone penetrometers come in various different weights and drop heights depending on their intended use. The ASTM-standard device for use in shallow pavement applications consists of a 17.6 lb. (8 kg) or a 10.1 lb. (4.6 kg) hammer with a drop height of 22.6 inches (575 mm) (ASTM D 6951 2009). Figure 2.21 shows a schematic of ASTM-standard DCP. The device consist of a 5/8 inch (16 mm) diameter steel drive rod with a replaceable point or disposable cone tip, a coupler, a handle, and a vertical scale (ASTM D 6951 2009). Schematic drawings of a replaceable point tip and a disposable cone tip are shown in Figures 2.22 and 2.23. The tip has an included angle of 60 degrees and a diameter at the base of 20mm.

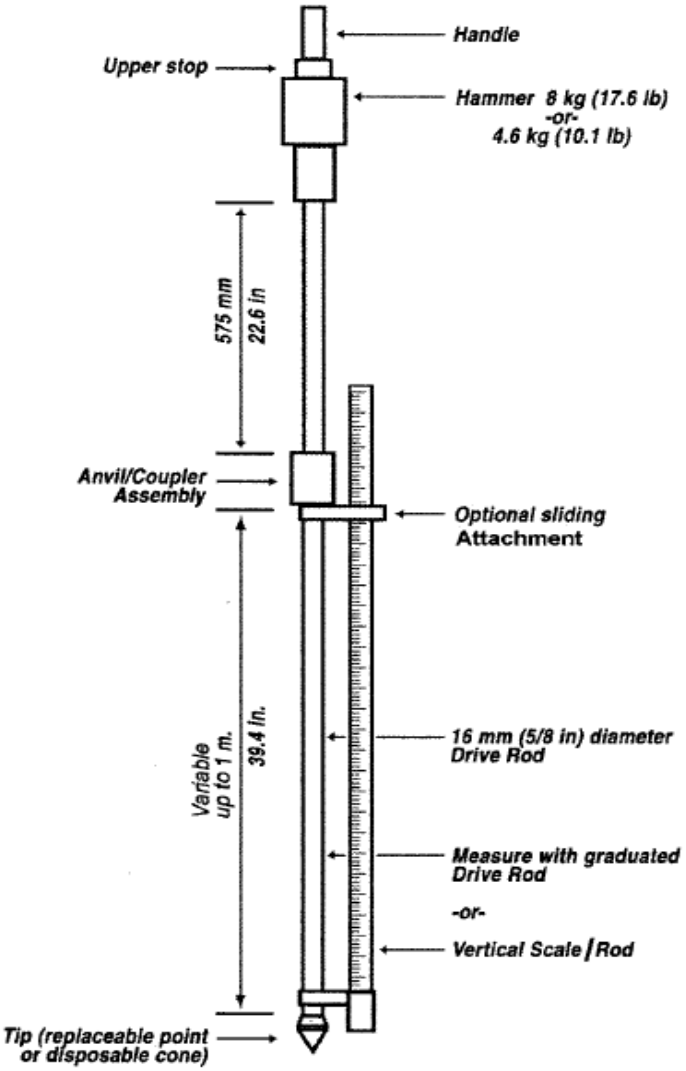

Figure 2.21: Schematic drawing of dynamic cone penetrometer (ASTM D 6951 2009)

In order to operate the DCP, the device is held plum with one hand and the hammer is raised with the other to the maximum height and dropped. The penetration distance can either be read on the scale and recorded manually, typically after every 5 blows, or a magnetic ruler can be used to read and obtain every blow. The readings obtained are then used to calculate the dynamic cone penetration index (DCPI) using Equation 2.1

$$DCPI = \frac{PR_2 - PR_1}{BC_2 - BC_1} \qquad \text{(Equation 2.1)}$$

Where:

PR = the penetration reading (mm),

BC = the blow count,

$PR_2 - PR_1$ = the difference between two consecutive readings at different depths (mm),

and

$BC_2 - BC_1$ = the difference between two consecutive blow counts.

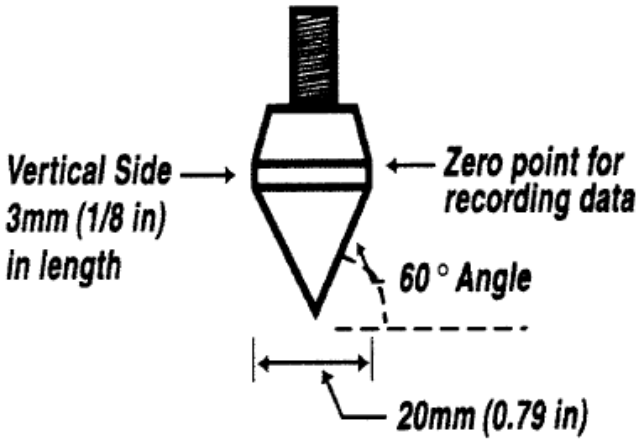

Figure 2.22: Replaceable point tip for dynamic cone penetrometer (ASTM D 6951 2009)

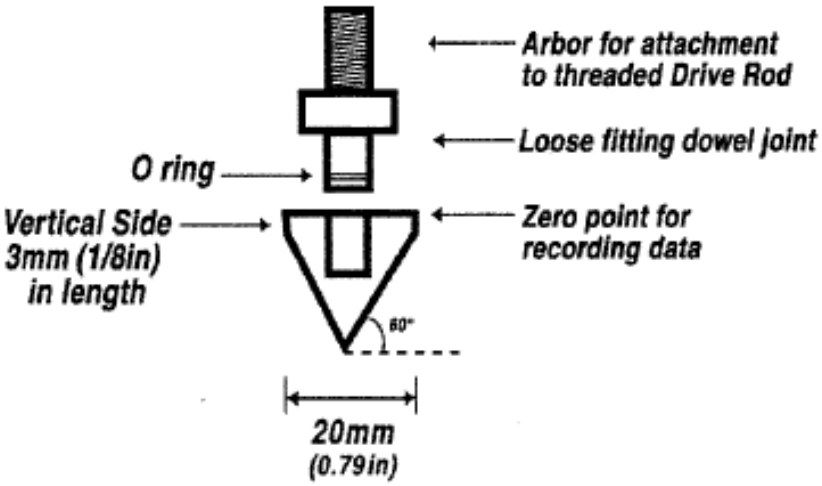

Figure 2.23: Disposable cone tip for dynamic cone penetrometer (ASTM D 6951 2009)

The DCPI can be calculated after every 5 drops or can be calculated based on the total penetration depth and blow count using a magnetic ruler. Figure 2.24 shows a picture of a DCP with a magnetic ruler used for testing. The unconventional units used were chosen for several reasons. When collecting the data using the dynamic cone penetrometer, it is more accurate and easier to recorded penetration in millimeters than in inches. The unit convention has been previously used by Ahsan (2014) during his investigation using the dynamic cone penetrometer to determine strength of stabilized soils.

Figure 2.24: DCP equipped with a magnetic ruler for recording penetration readings

Extensive research has been performed to determine factors that can affect the measurements of the DCP on unstabilized materials. Kleyn and Savage (1982) concluded that the plasticity, density, moisture content, and gradation affect the measurements. Hassan (1996) showed that the moisture content, AASHTO soil classification, confining pressures, and dry density of fine grained soils affected the measurements obtained by the DCP. George (2000) concluded that the maximum aggregate size and the coefficient of uniformity could affect DCP results.

Researchers have found that the penetration slope of the DCP in penetration per blow is inversely related to the strength of the specimen being tested (Patel and Patel 2012; McElvaney and Djatnika 1991; Nemiroff 2016). Therefore, if a specimen has a very low strength the penetration rate will be larger than when compared to a specimen with a high strength.

2.5.2.1 Location of the DCP Strength Evaluation

North Carolina Department of Transportation (NCDOT) uses dynamic cone penetrometer test to evaluate the strength of chemical stabilized subgrade or base. Locations are chosen at random location using the procedure outlined in NCDOT Chemical Stabilization Subgrade/Base QA Field Manual (2013). NCDOT (2013) uses random sampling techniques to locate test sites to avoid biased testing. Process is done by using a table of random numbers. Once a number has been used it is marked through and not used again. Random sampling is done in two dimensions by location a station (length) and a pull distance from the edge (width) (NCDOT 2013). The first step is to determine the number of test locations in a test section. The length of the test section is multiplied by number of 12-foot lanes in the section, divided by 440, and rounding up to the nearest whole number. This number indicates the number of test location the dynamic cone penetrometer must be performed in a section. The second step is to divide the section length by

the total number of testing locations to get the length between each location. In the third step, a random sample multiplier is chosen from the random sample number table and divided by 100 to obtain a decimal value. In the fourth step a random sample number is then multiplied by the equal sections length determined in step 2. The fifth step is to add the distance determined in step 4 to the value determined in step 2. A second set of random sample multipliers are then used to determine the distance from the edge of the section where the tests are to be performed. Either the left or the right edge is chosen as a reference point, it does not matter but must be consistent throughout testing. The sixth step is to divide the random sample multiplier by 100 to convert to a decimal and multiply by the width of the section to determine the location the DCP must be performed.

The dynamic cone testing pattern used by NCDOT (2013) is shown in Figure 2.25. Five DCP's are to be performed at each testing location and averaged to achieve a single CBR value at each station (NCDOT 2013). The CBR is then converted to strength by using Equations 2.2 and 2.3, respectively.

$$\text{CBR} = 10^{[1.53-(Log\ X)*1.066]} \quad \text{(Equation 2.2)}$$

Where;

CBR = California Bearing Ratio, and

X = Penetration in centimeters.

$$\text{psi} = \left(\left(\frac{\text{CBR}}{0.70}\right)^{.658}\right) * 1.171 \quad \text{(Equation 2.3)}$$

Where;

psi = compressive strength, and

CBR = California Bearing Ratio.

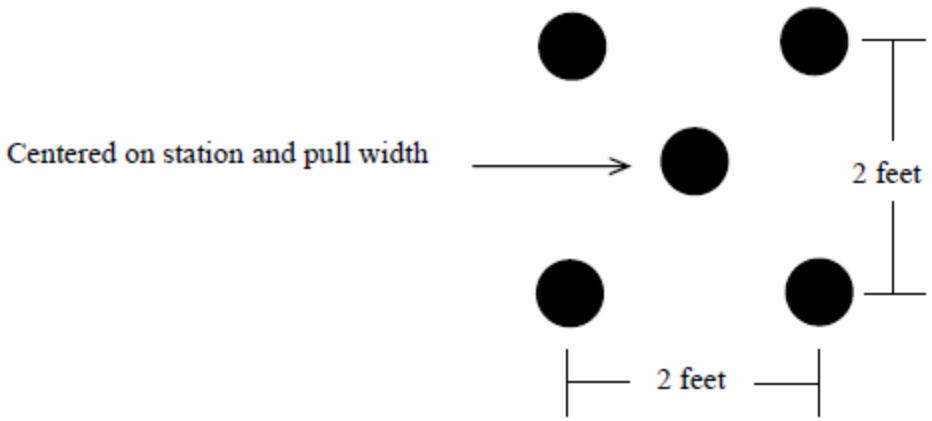

Figure 2.25: NCDOT dynamic cone penetration testing pattern

2.5.2.2 Correlation between DCP and Unconfined Compressive Strength

Research has been performed to determine a relationship between the dynamic cone penetration index and the unconfined compressive strength on various unstabliized and stabilized-soil types. McElvaney and Djatnika (1991) performed laboratory studies on silty clay, clay, and sandy clay with and without the addition of lime. The test were performed using the ASTM standard DCP hammer of 17.6 lb. on specimens that were 5.98 inches (152mm) in diameter and 4.57 inches (116 mm) tall. The test specimens were penetrated a total of 50 mm. The unconfined compressive strength tests were conducted using BS 1924, on specimens with a L/D ratio of 2.0. They concluded that the laboratory test results indicated that the DCP provided a reasonable estimate of the unconfined compressive strength of the soil-lime mixtures. The inclusion of data from material with zero lime content has negligible effect on the regression analysis, suggesting that the correlation obtained is primarily a function of strength and is not influenced by the way in which strength is achieved (McElvaney and Djatnika 1991). McElvaney and Djatnika (1991) developed three correlations.

50% probability of underestimation:

$$\log(UCS) = 3.56 - 0.807\log(DN) \qquad \text{(Equation 2.4)}$$

95% confident that probability of underestimation will not exceed 15 percent:

$$\log(UCS) = 3.29 - 0.809 \log(DN) \quad \text{(Equation 2.5)}$$

99% confident that probability of underestimation will not exceed 15 percent;

$$\log(UCS) = 3.21 - 0.809 \log(DN) \quad \text{(Equation 2.6)}$$

Where:

UCS = the unconfined compressive strength (kPa), and

DN = the DCP reading (mm/blow).

Figure 2.26 shows the correlation from McElvaney and Djatnika (1991) between the unconfined compressive strength and the dynamic cone penetrometer results. The figure includes both stabilized and unstabilized material.

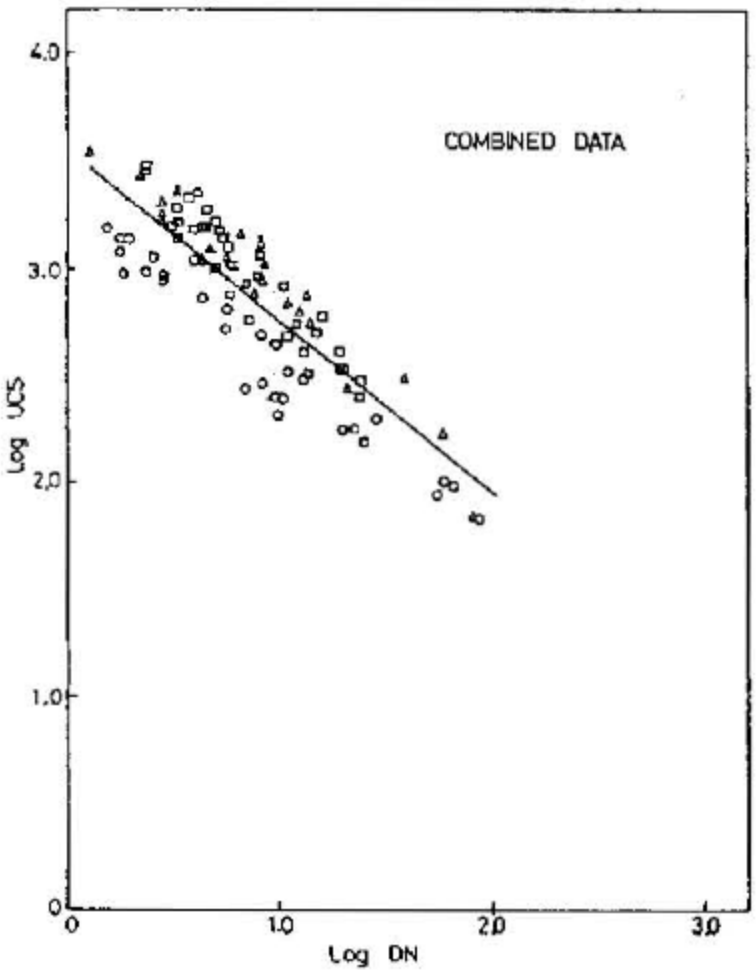

Figure 2.26: Correlation between UCS and DCP results from McElvaney and Djatnika (1991)

Patel and Patel (2012) conducted tests on in-situ conditions simulated in the laboratory on CH, CI, CL, CL-ML, MI, SC, AND SM-SC soils. They also conducted tests by stabilizing these soils with cement, lime, and flyash. The test were performed with an ASTM standard DCP hammer of 17.6 lb. on soaked and unsoaked specimens using an automated DCP device. The penetration was recorded up to 300 mm. Unconfined compressive strength was tested in accordance with Indian Standard: 2720, using a L/D ratio of 2.0. Patel and Patel obtained the following equation for unstabilized and stabilized soils:

$$UCS = 3.1237 \times DCPI^{-0.865} \quad \text{(Equation 2.7)}$$

Where:

UCS = the unconfined compressive strength (N/mm^2), and

DCPI = the dynamic cone penetration index (mm/blow).

Figure 2.27 shows the correlation between the unconfined compressive strength and the dynamic cone penetrometer index for a wide variety of soils that were stabilized using cement, lime, and flyash and unstabilized soil. Patel and Patel (2012) concluded that the correlation between the unconfined compressive strength and the dynamic cone penetrometer index were independent of soil type and the use of cement, lime, or flyash.

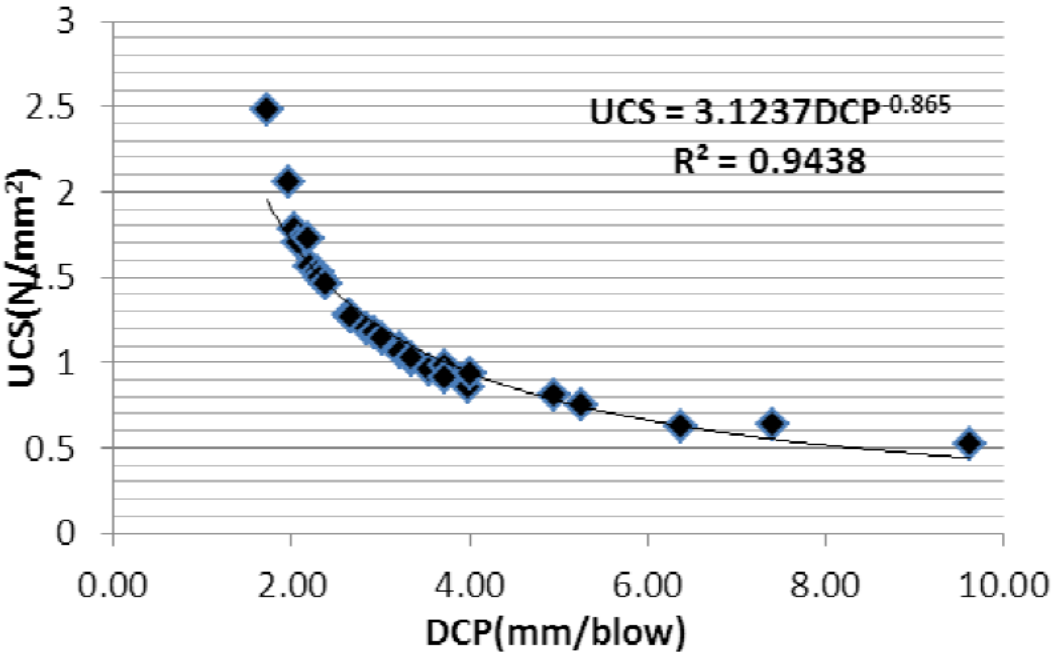

Figure 2.27: Correlation between UCS and DCP results from Patel and Patel (2012)

Nemiroff (2016) conducted test on in-situ conditions simulated in the laboratory on SC, SP, and SP-SC soil types stabilized with cement. The tests were performed with an ASTM standard DCP hammer of 17.6 lb. on three and seven-day cured soil cement specimens. The specimens were made in a five-gallon bucket that was confined by a cast in-place concrete block.

The specimens were made 8 inches thick to simulate the lift thickness of US Highway 84 soil-cement placement. The first inch (25 mm) of penetration was discarded as per ASTM D 6951 to allow the DCP to seat in the surface and the next 160 mm of penetration were recorded. The study was done in millimeters instead of inches due to the ease of testing. Nemiroff (2016) determined that because the strength of the soil cement specimen was linear with depth, that a depth of 75 mm (3 in.) would be ideal penetration depth because it produced the best results and least amount of technician effort. Unconfined compressive strengths were conducted followed the modified ASTM D 1632 (2007) method created by Wilson (2013) using a L/D of 2.0. A total of 185 cylinders and 57 DCP specimens were produced and tested to determine the relationship recommended by Nemiroff (2016). Nemiroff (2016) determined that the most practical molded cylinder strength to DCP slope correlation, based on ease of use for field applications and best fit, was the logarithmic function. Nemiroff (2016) recommended Equation 2.8 for soil-cement applications. The equation is valid for a strength range between 100 and 800 psi.

$$MCS = 926e^{-0.615DCP} \quad \text{(Equation 2.8)}$$

Where:

MCS = molded cylinder strength (psi), and

DCP = dynamic cone penetrometer slope (mm/blow).

Figure 2.28 shows the correlation between unconfined compressive strength and the dynamic cone penetrometer slope for typical soils used soil-cement applications. Nemiroff (2016) concluded that the correlation between unconfined compressive strength and the dynamic cone penetrometer was independent of soil type and the amount of cement that was used to stabilize the material.

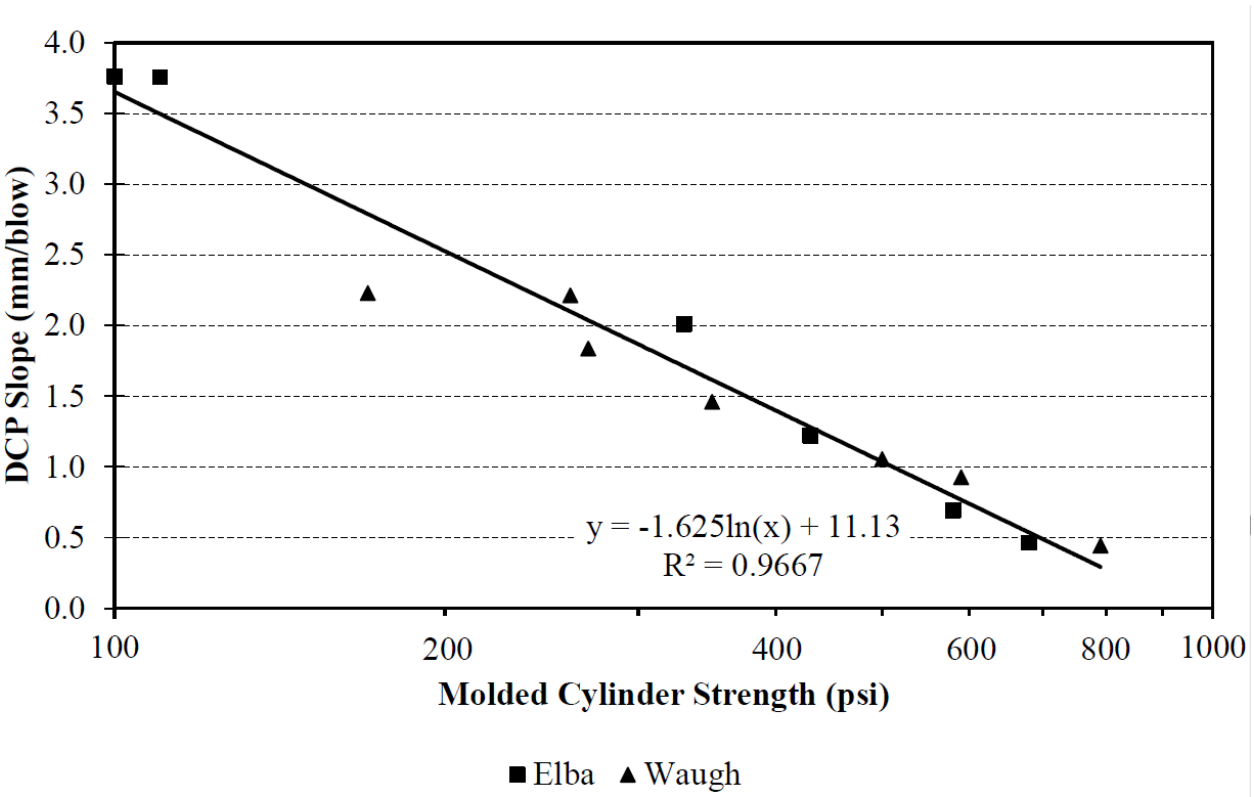

Figure 2.28: Correlation between MCS and DCP slope results from Nemiroff (2016)

Enayatpour et al. (2006) performed a series of laboratory tests on cement- and lime-stabilized soils to correlate the unconfined compressive strength with the dynamic cone penetrometer. Their results showed that the DCP could be calibrated to predict the unconfined compressive strengths of subgrades. Enayatpour et al. (2006) concluded that a linear relationship existed between the DCP and the UCS. They did stress that field studies needed to be conducted to provide reliable strength interpretations in real field conditions.

Nemiroff (2016) shows how all the different correlations between DCP, penetration rate and unconfined compressive strength, compare to each other.

2.5.3 Molded Cylinder Strength

2.5.3.1 Proctor Molded Specimens

The majority of past research dealing with soil cement compressive strength was conducted using a specimen size of 4.0 inches in diameter and 4.58 inches in height with a length-to-diameter (L/D) ratio of 1.15 (ASTM D 559 2015). This method gives a “relative measure of the strength rather than a rigorous determination of compressive strength” (ASTM D 1633 2007). This method makes use of the same compaction equipment and molds commonly available in soil laboratories.

To make a soil-cement specimen, there are specific production techniques and procedures to follow. The production of the four-inch diameter specimen is described in ASTM D 698 (2012). This method uses a Proctor mold and a standard Proctor hammer weight of 5.5 pounds. The soil cement is placed in the mold in three equal lifts and compacted by dropping the hammer 25 times per lift around the specimen. After the three lifts are completed, the top ring of the Proctor mold is removed, and the top and bottom of the mold are trimmed level with the Proctor mold. Figure 2.29 shows a Standard Proctor mold.

Figure 2.29: Standard Proctor mold and hammer used to make soil-cement specimens

After making the specimen, ASTM D 1633 (2007) states the specimen should be cured according to ASTM D 1632 (2007). ASTM D 1632 (2007) states that the molded specimen remain in the mold while curing in a moist room for 12 hours or longer, then it shall be removed and extruded using a sample extruder. Once extruded, the specimens are placed back into the continuous moist-curing room. At the end of the moist-curing period, the specimens are immersed in water for four hours and tested immediately after.

2.5.3.2 Wilson (2013) Steel Mold Specimen

Wilson (2013) studied the use of a modified version of ASTM D 1632 (2007) to produce and cure soil cement specimens made in the laboratory or field. The modified version of the ASTM D 1632 uses a specimen with a 2.8-inch diameter and a height of 5.6-inches resulting in a L/D ratio of 2.0. Relative to the Proctor specimen this specimen size gives a better measure of the compressive strength since it reduces the complex stresses that may occur during the shearing of the smaller L/D ratio specimens (ASTM D 1633 2007).

Figure 2.30 and 2.31 show the dimensions and equipment used for production. The cylindrical steel molds used had an inside diameter of 2.8 ± 0.01 inches and a height of 9 inches. The mold also included a machined steel top and bottom piston having a diameter 0.005 inches less than the mold, a 6 inch mold extension, spacer clips, two aluminum separating disks 1/16 inch thick by 2.78 inches in diameter, and two ultra-high molecular weight polyethylene (UHMW) plugs with a diameter 0.005 inches less than the mold, which ensures an air tight seal.

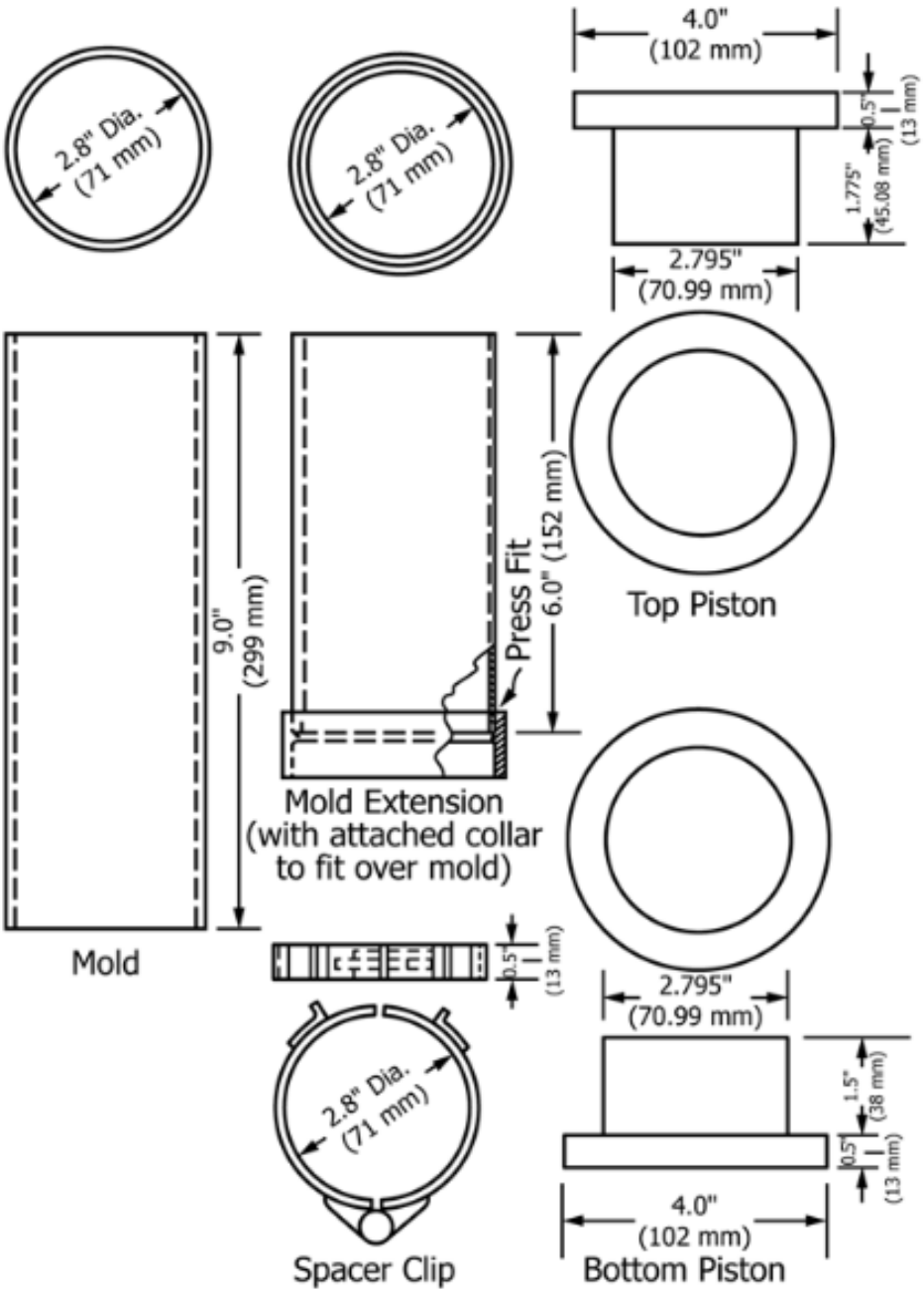

Figure 2.30: Soil cement cylinder mold (ASTM D 1632 2007)

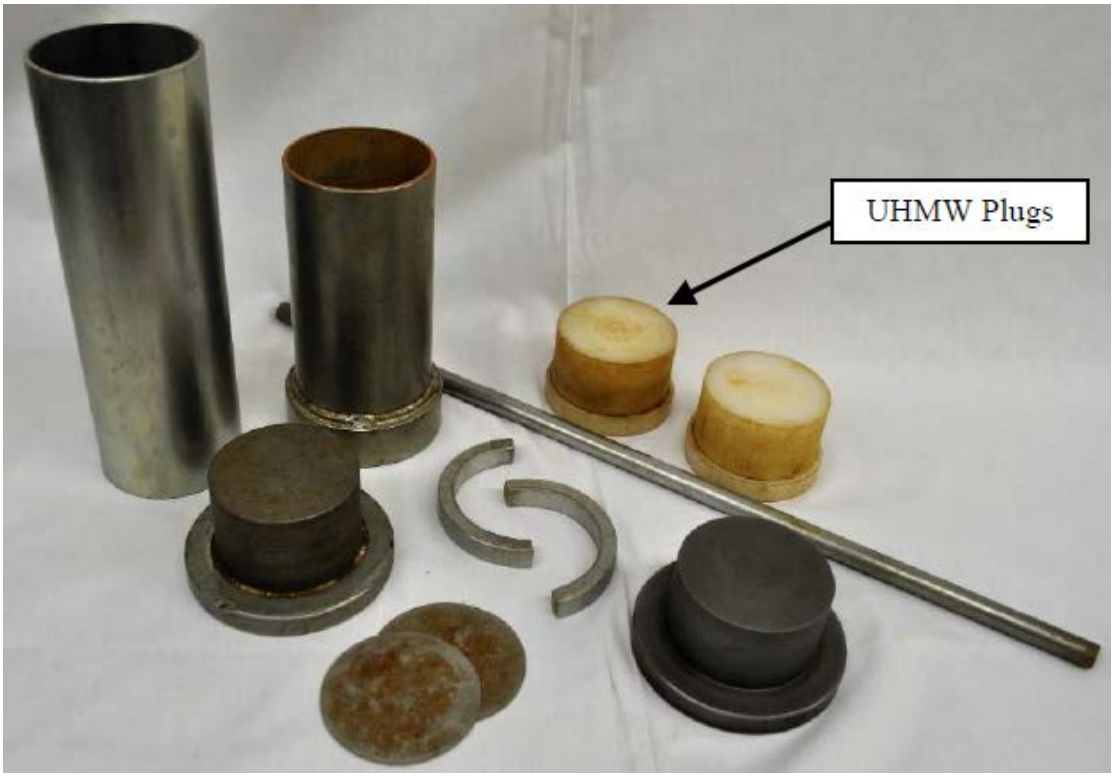

Figure 2.31: Soil cement molding equipment

In order to produce a specimen, a moisture-density curve was produced corresponding with the soil-cement being tested. Once the moisture-density curve was determined, a small sample of freshly mixed soil-cement was tested to determine the moisture content. Based on this moisture content and the moisture-density curve already produced, a target mass was determined using Equation 2.9 to create a specimen with at least 98% density.

$$M_{sc} = 9.06\,\gamma_{dry}\,\frac{lb}{ft^3} \qquad \text{(Equation 2.9)}$$

Where:

M_{sc} = mass of soil cement, and

γ_{dry} = dry unit weight corresponding to composite sample moisture content (lb/ft^3).

After the mass of the soil-cement was determined, the mold and separating disks were lightly coated with a low-viscosity oil and placed on the bottom piston. Once assembled, the six-

inch mold extension was placed on top of the mold and the predetermined amount of soil cement was placed inside the mold. The soil cement was then tampered with a smooth steel rod until the specimen was below the level of the 6 inch mold extension. Then the mold extension was removed along with the separating disks placed at the bottom of the mold and the top piston placed on top of the mold. The specimen was then compacted until the lip of the piston touched the end of the mold using a compacting drop-weight machine, shown in Figure 2.32. Once compaction was complete, the pistons and separating disk were removed and a UHMW polyethylene mold plug was placed on each end to reduce moisture loss. Metal foil tape was placed around the UHMW polyethylene plugs and the mold as an extra barrier to prevent moisture loss during the initial curing stage. Figure 2.33 shows steel mold cylinders once completed.

Figure 2.32: Dropping-weight compacting machine (Wilson 2013)

Figure 2.33: Molded specimens during initial curing period (Wilson 2013)

Once the UHMW polyethylene plugs and metal foil tap were placed on the specimen, the initial curing period began. Molds were placed in a location in the laboratory or on-site where they had limited exposure to sun, wind, and other environmental hazards for at least 12 hours. After the initial curing stage was complete, specimens were transported to the laboratory where they were extruded using a vertical specimen extruder. Once the specimens were extruded they were placed in a continuously moist-curing room until the time of testing.

2.5.3.3 Strength Correction Factors for Length-to-Diameter Ratios

For cylindrical concrete cylinders, ASTM C 39 (2016) states that if a specimen's length-to-diameter ratio (L/D) is 1.75 or less, the compressive strength needs to be multiplied by the appropriate strength correction factor. These strength correction factors are suggested for use for soil-cement specimens in ASTM D 1633 (2007). In the study performed by Wilson (2013), the L/D strength correction factors commonly used for correcting the compressive strength of soil-cement cylinders were investigated. Wilson (2013) showed that the ASTM C 39 (2016) L/D strength correction factors were not applicable to soil-cement cylinders when made and tested

using ASTM D 1632 (2007) and ASTM D 1633 (2007). Wilson (2013) recommended that no L/D strength correction factor be applied for L/D ratios between 1.0 and 2.0.

2.5.4 Plastic Mold Method (PM)

Sullivan et al. (2014) developed a method using plastic molds to produce and cure soil-cement specimens in the laboratory and field. This method uses specimens mold that were constructed from standard 3 in. (76.2 mm) by 6 in. (152.4 mm) plastic molds which meets the requirements of ASTM C 470 (2015) for single-use concrete molds. The standard molds were modified by sanding the bottoms to remove the plastic ridge around the edge to provide a flush surface for compaction. After the molds were sanded down, a drill-press was used to produce a 1.4 in. (35 mm) diameter hole through the center of the molds bottom. The 1.4 in. (35 mm) hole allows for the specimen to be extruded without damage. After the hole was cut in the bottom of the mold, an aluminum plate 3 in. (76.2 mm) in diameter and 0.06 in. (1.6 mm) thick was inserted into the bottom of the mold to cover the hole and provide a rigid surface for extrusion. The plastic cut-outs form the drilling process were placed back over the cut-out and tapped to provide a solid compaction surface. The modification process to the molds is shown in Figure 2.34.

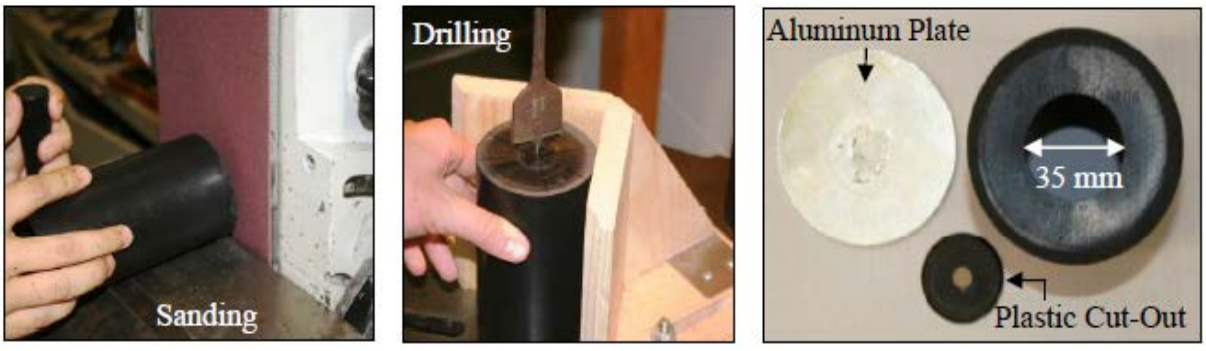

Figure 2.34: Plastic Mold Modification (Sullivan et al. 2014)

A steel mold was design that allowed a 3 in. (76.2 mm) diameter by 5.9 in. (150.8 mm) tall specimen to be compacted inside. The mold was then mounted to a 11.4 by 9.5 by 0.5 in. steel plate. Figure 2.35 shows the PM specimen preparation apparatus. The split mold inner diameter is the same as the outer diameter of the plastic mold. This helps facilitate alignment and prevents the plastic mold from being struck during compaction. The collar helps contain soil during the compaction process.

Figure 2.35: PM specimen preparation apparatus (Sullivan et al. 2014)

Soil-cement specimens are produced by compacting three pre-weighed lifts with the PM apparatus shown in Figure 2.35 and a modified Proctor hammer (10 pounds dropped 18 inches). Each lift was compacted using 5 blows of the modified Proctor hammer, and then scarified each lift before adding the rest of the material. Sullivan et al. (2014) found that this method produces densities between 92 and 100 percent of the target max dry density. Equation 2.10 shows how the weight of each lift was determined (Sullivan et al. 2014).

$$W_{s-c} = 3.8\ x\ \gamma_d x(\frac{100+OMC}{100}) \qquad \text{(Equation 2.10)}$$

Where:

$W_{s\text{-}c}$ = Weight of soil-cement material per lift (g),

γ_d = Maximum dry density of soil-cement mixture (lb/ft^3), and

OMC = Optimum moisture content of soil-cement mixture (%).

Chapter 3

Experimental Plan

3.1 Introduction

The main objective of this research project was to evaluate different methods to assess the strength of soil-cement base in the field. To accomplish this, a field experimental testing plan was developed to evaluate the compressive strength of soil cement. At the time of this research project, the U.S. Highway 84 bypass in Elba, Alabama was been constructed with soil-cement as the base of the roadway. Several trips were made to Elba, Alabama to assess the strength of the soil-cement base being placed by Newell Construction out of Hope Hull, Alabama.

This chapter provides an overview of the field experimental testing program. The soil-cement mixture used are described and its mixture proportions are defined. The rationale for selection of testing locations for soil cement is discussed. The procedures for making soil-cement compression test specimens and performing DCP tests in the field are discussed. A detailed description of the testing procedures and apparatus are presented. In addition, details of sample preparation and curing procedures are covered.

3.2 Experimental Testing Program

In order to evaluate different soil-cement testing methods, an experimental testing program was developed. Figure 3.1 shows a summary of the field testing plan. Four strength-testing methods were evaluated in the field: Modified ASTM D 1632 (Wilson 2013) for steel mold cylinder strength, a modified version of the Plastic Mold Method (Sullivan et al. 2014) for molded cylinder strength, core testing (ALDOT 419 2008), and Dynamic Cone Penetrometer Method (ASTM D 6951 2009). The molded cylinders developed by Wilson (2013) and Sullivan

et al. (2014) were tested for their unconfined compressive strength at seven days. The DCP tests were performed for penetration at seven days. Cores were removed on the sixth day and tested on the seventh day in accordance with ALDOT 419 (2008).

The results from DCP testing were converted to unconfined compressive strength by a relationship recommended by Nemiroff (2016). By using this relationship, the strengths estimated from the DCP results could be compared to those obtained from testing molded cylinders and cores.

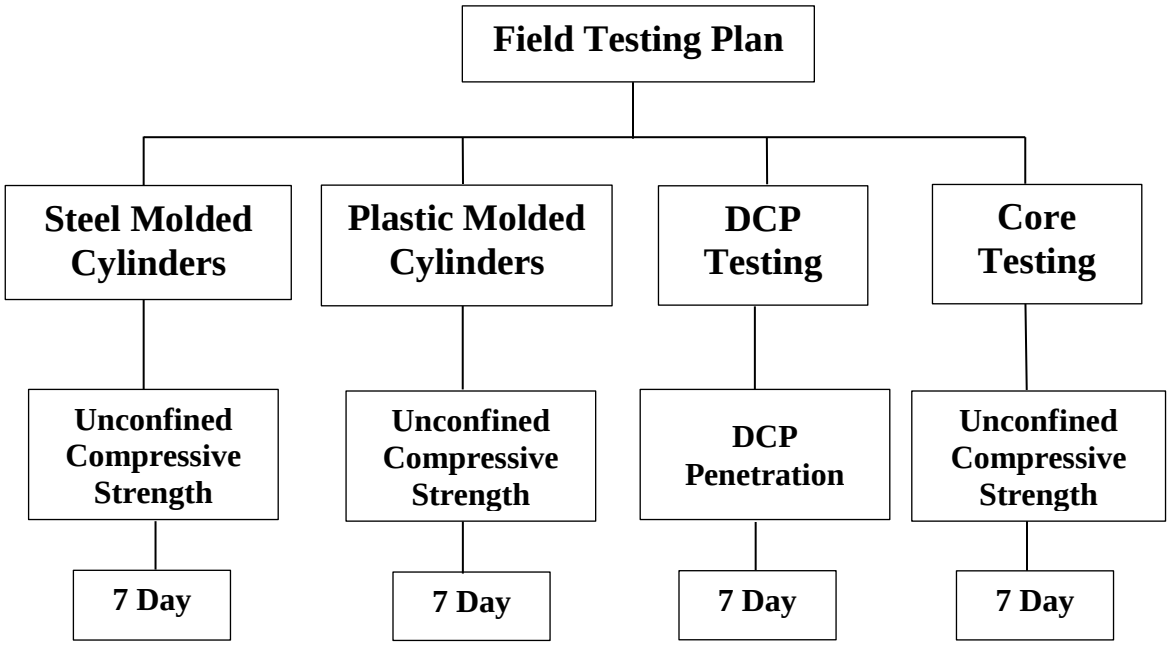

***Note: All core testing done by ALDOT**

Figure 3.1: Summary of field testing plan

3.2.1 Field Mixtures

The field mixture evaluated for this research project is shown in Table 3.1 and was developed by the contractor. These data were obtained from design studies performed by Building and Earth Sciences, Inc. This information was present at the time of making field

molded specimens at the jobsite and was used in the production of field molded specimens. According to AASHTO soil classification, the soil used during project testing was A-2-4 (0). Additional information including design curves and gradation analyses can be found in Appendix A.

Table 3.1: Mixture properties of field mixture

Project Location	Mixture properties of field mixture		
	Cement Content, %	Optimum Moisture Content, %	Maximum Dry Density, lb/ft^3
Elba, AL	7	14.3	113.2

3.2.2 Location of Project Site

The field testing took place in Elba, Alabama on the U.S. Highway 84 bypass constructed by Newell Construction out of Hope Hull, Alabama. The ALDOT project number was NHF-0203(523), and both eastbound and westbound lanes were tested. The project location is shown in Figure 3.2 with beginning coordinates of 31°24’12” N, 86°02’06” W and ending coordinates of 31°25’28” N, 86°03’40” W.

Figure 3.2: U.S. Highway 84 bypass project location (Google Maps 2017)

3.2.3 Testing Strategy Within a Section

Much discussion went into how to perform testing within a placed soil-cement section. After careful consideration, it was decided each section of soil-cement placement would have three testing locations for the DCP and two locations for the molded cylinders and plastic molds. Figure 3.3 shows a schematic of the field testing plan. A section for the U.S Highway 84 bypass project was considered to be a 528 feet (1/10 mile) in length. Soil was sampled at the beginning and end of each section for the production of molded cylinders (Wilson 2013) and plastic molded cylinders (Sullivan et al. 2014). At each testing location for the molded cylinders, five specimen were made. The DCP was tested at each sampling location for the molded cylinders and at the core testing location. The core location was unknown until the soil cement had been in place for six days, so no molded samples could be made at this location. Only DCP tests could be

conducted within three feet of known core locations, because DCP testing was performed after the cores were extracted.

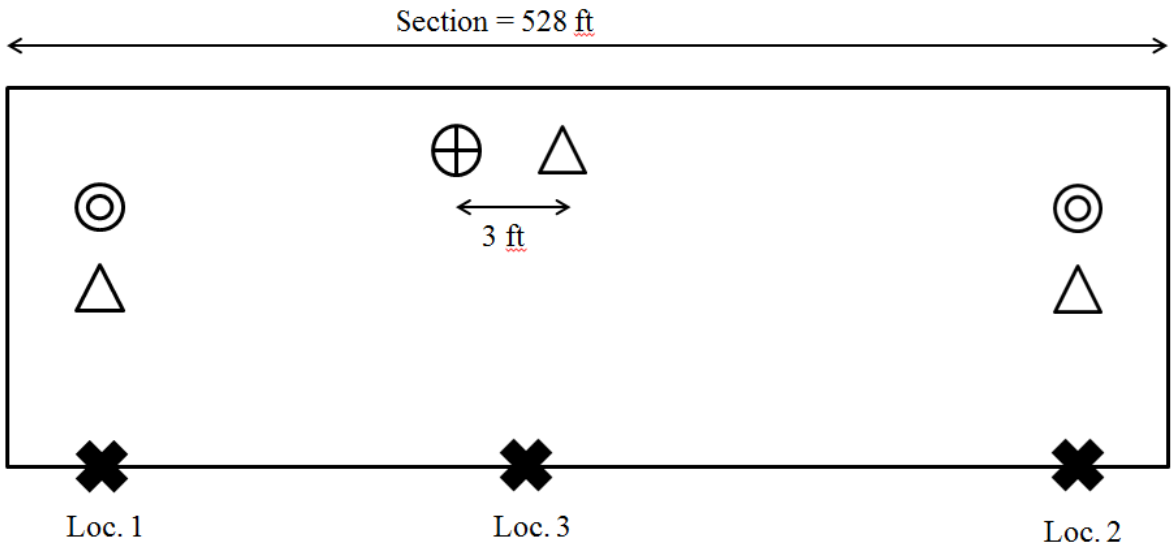

Figure 3.3: Field Testing Plan

Where:

Sample location of cylinder material

Location where 3 dynamic cone penetrometer tests will be performed

Coring location performed by Newell and tested by ALDOT

At each testing location for the dynamic cone penetrometer three tests were conducted. To reduce the number of DCP blows and thus technician effort, this was altered from the NCDOT (2013) document that conducted five tests at each testing location. The test was arranged in a triangular pattern, as shown in Figure 3.4 that shows a schematic of dynamic cone testing plan. Each test was conducted two feet from the other one so the test location would not be impacted by the previous test; however, these three tests are close enough to each other so that their average would characterize the in-place strength at this location.

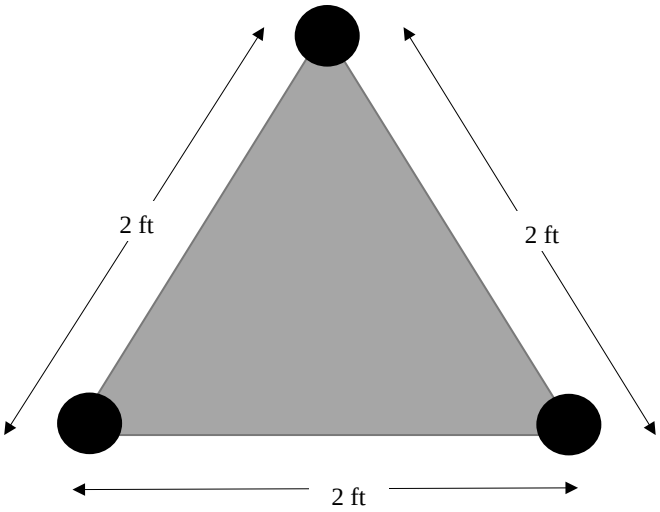

Figure 3.4: DCP testing pattern

3.2.4 Field Testing

The objective of the field testing program was to evaluate different test methods to determine the in-place strength of soil-cement base. The research took place in Elba, Alabama on the U.S. Highway 84 bypass. This research involved travelling to the jobsite and making steel-molded cylinders and plastic molded cylinders from mix in-place soil-cement as shown in Figure 3.5. The project also involved driving back to the project site on the seventh day to conduct DCP test on the section of soil-cement placed the week prior at the three locations shown in Figure 3.3.

All cylinders were initially cured at the jobsite and transported back to the laboratory the following day. Samples were de-molded using a vertical hand jack, sealed in plastic bags, and placed in a moist room for final curing. Samples were tested on the seventh day for compressive strength.

Figure 3.5: Steel-molded cylinder on-site

3.3 Field Experimental Procedures

3.3.1 In-Place Sampling of Mixed Soil Cement

The material was sampled after the soil-cement mixture was mixed in-place. Samples were taken in shovel-sized quantities from the beginning and end of each section as defined in Figure 3.3. Figure 3.6 shows material that is ready to be sampled.

3.6: Material ready to be samples for molded specimen production

To prevent moisture loss, a 5-gallon bucket was filled with freshly mixed soil-cement and the lid was placed on the bucket directly after the last portion of the sample was obtained. The sample buckets were then transported to the area where molded specimens were made. The sample buckets where kept out of direct sunlight and protected from wind and other sources of evaporation and contamination during the preparation of the molded cylinders. A typical bucket with soil cement to make field molded specimens is shown in Figure 3.7.

Figure 3.7: Sample of soil-cement mixture in 5-gallon bucket

3.3.2 Determining the Moisture Content of Soil-Cement Specimens

After the soil cement has been sampled in a 5-gallon bucket and transported to the area were the soil-cement molded cylinders will be made, the moisture content was determined. A

small sample of the soil-cement was taken from the 5-gallon bucket of freshly sampled soil-cement. Figure 3.8 shows a sample of soil-cement used to determine the moisture content. In order to determine the moisture content ASTM D 4959 (2016): *Standard Test Method for Determination of Water Content of Soil By Direct Heating* was followed. A test sample of approximately 200 grams was used. Once the representative portion of the soil mass was collected it was placed on a hot plate shown in Figure 3.9 to remove all moisture.

Figure 3.8: Representative sample of soil-cement used to determine moisture content

Figure 3.9: Hot plate used to evaporate all of the water out of the soil-cement mixture

To determine the mass of water in the soil-cement mixture the specimen was heated and weighed, on a scale conforming to ASTM D 4753 (2015), until the specimen did not change mass. Figure 3.10 shows the scale used for all moisture content testing. When the specimen no longer changes mass, all the water has been evaporated from the soil-cement mixture. The water content can then be determined once the mass of the dry specimen is known. Equation 3.1 shows how the moisture content was calculated.

Figure 3.10: Scale used to determine the moisture content

$$w = [(M_1 - M_2) / (M_2 - M_c)] \times 100 \qquad \text{(Equation 3.1)}$$

Where:

w = water content, %,

M_1 = mass of container and moist specimen, g

M_2 = mass of container and dried specimen, g, and

M_c = mass of container, g.

3.3.3 Determining the Mass of a Steel Molded Cylinder (Wilson 2013)

Once the moisture content is known, the mass of material for a specimen can be computed volumetrically to target a specific compaction level. The moisture density curve of the

project soil cement (Appendix A) was used to determine whether the moisture content of the sample fell within the 98 percent range of optimum moisture content (OMC). The tested moisture content of the sample was used to determine the mass of soil cement, by using the dry unit weight from the moisture density curve corresponding to the samples moisture content in lb/ft^3 and converting it to g/in^3. The volume of the specimen molds is 2.8 inches in diameter by 5.6 inches high, therefore a sample volume of 34.5 in^3 is created. Wilson (2013) provides Equation 3.2 and 3.3 to determine the mass of soil-cement material needed to make the test specimens. Figure 3.11 shows a test specimen being weighed out to the correct mass.

$$M_{sc} = \left(\gamma_{Dry}\,\frac{lb}{ft^3}\right) x \left(\frac{ft^3}{1728\ in.^3}\right) x \left(\frac{kg}{2.2046lb}\right) x \left(34.5in^3 x \frac{1000g}{1kg}\right) \qquad \text{(Equation3.2)}$$

Which reduces to:

$$M_{sc} = 9.06 \times \gamma_{dry} \qquad \text{(Equation 3.3)}$$

Where:

M_{sc} = mass of soil-cement (grams), and

γ_{dry} = dry unit weight corresponding to composite sample moisture content, lb/ft^3.

Figure 3.11: Specimen being weighed out to its correct mass

3.3.4 Steel Molded Cylinder Production

Steel molded cylinder production followed the modified ASTM D 1632 created by Wilson (2013). Once the mass of the soil-cement mixture was known, the mold and separating disks were lightly coated with low-viscosity oil and placed on the bottom piston. The 6-inch high

mold extension was placed on top of the mold and the predetermined amount of soil cement from Equation 3.3 was placed inside the mold. The soil cement was then tamped with a smooth steel rod until the specimen was below the level of the mold extension. Figure 3.12 shows the tamping process used to make steel molded cylinders.

Figure 3.12: Steel molded specimen being tamped with a steel rod

Once the soil was below the mold extension, the extension was removed along with the separating disk placed at the bottom of the mold and the top piston was placed on the top of the mold. The specimen was then compacted until the lip of the top piston touch the end of the steel mold using a compacting drop-weight hammer. The compaction process typically took 5-7 blows with the drop-weight hammer. Figure 3.13 shows a specimen being compacted with the drop-weight hammer. Once compacted the pistons and separating disk were removed and a UHMW polyethylene mold pug was placed on each of the specimen and taped with foil tape to prevent any moisture loss. The process was repeated until five molded cylinders were made at each testing location as shown in Figure 3.13.

Figure 3.13: Steel molded cylinder being compacted using a drop-weight hammer

3.3.5 Plastic-Mold Cylinder Production

Plastic-mold cylinder production closely followed the method that Sullivan et al. (2014) from Mississippi State University however, a few changes were made with the input of ALDOT. The plastic molds used for testing were standard 3 in. (76.2 mm) by 6 in. (152.4 mm) plastic molds. Sullivan et al. (2014) suggested modifying the standard molds by sanding the bottom of the molds to remove the plastic ridge, and then using a drill-press to produce a 1.4 in (35 mm) diameter hole through the center of the mold. Once the whole was cut an aluminum disk was to be placed at the bottom of the hole and the plastic cut-out tapped back to the bottom of the mold. Figure 3.14 shows portions of the modified plastic mold.

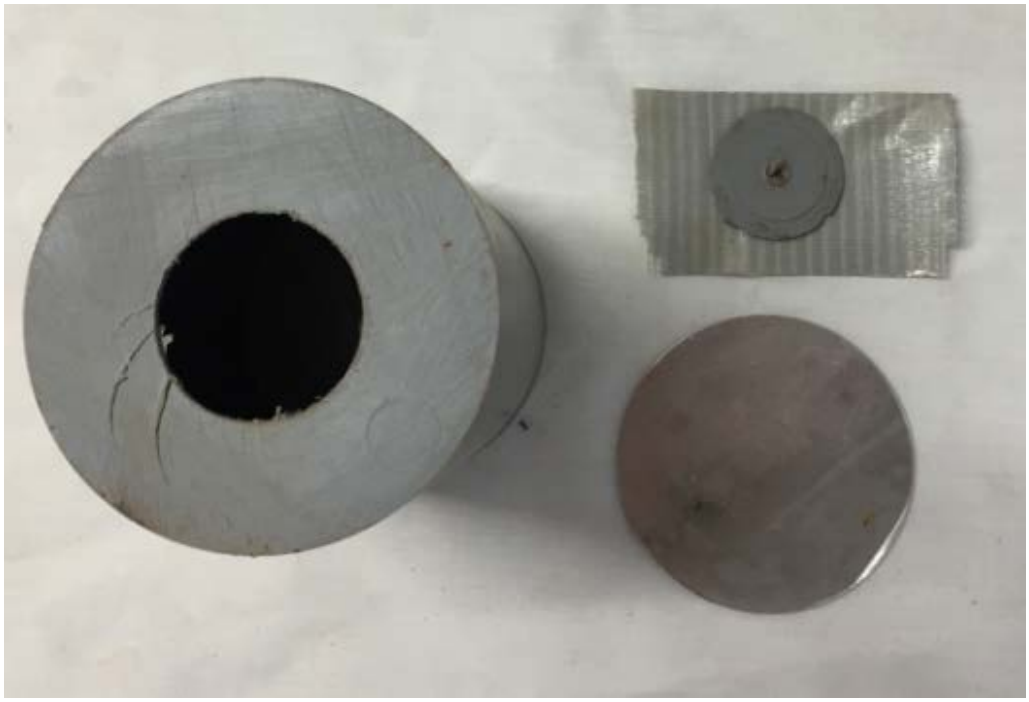

Figure 3.14: Modified plastic mold as proposed by Sullivan et al. (2014)

Plastic molded specimens were originally made as described by Sullivan et al. (2014); however it was found that many of the test specimens were coming out damaged during the extrusion process. Figure 3.15 shows a plastic mold specimen that was damaged during the extrusion process when the specimen was 24-hours old. It was noticed from the beginning of

testing that some of the plastic molded cylinders had horizontal cracks when they were extruded like the one shown in Figure 3.15. Damage to the test specimens lead to a change in the plastic-mold method suggested by Sullivan et al. (2014).

Figure 3.15: Plastic-mold specimen damaged by the extrusion process

After discussion with ALDOT it was decided to make the following change to the plastic-mold method. Instead of drilling a hole in the bottom of the mold, the mold would be cut down the side with a box blade. After cutting, the mold was taped together to allow the cut to remain sealed after the specimen fabrication. After removing the tape, the cut in the side allowed the specimen to be pulled out of the plastic mold instead of using a jack. Figure 3.16 shows the new

modification to the standard plastic molds. After this change, no specimens were damaged using this method.

Figure 3.16: New method used to make plastic-mold cylinders

Once the plastic molds where modified, specimens were prepared with this method. The soil-cement mixture that was sampled in the 5-gallon bucket was used for the production of the plastic-mold cylinders. The plastic-mold method does not depend on the water content of the soil-cement mixture like the steel molded cylinder method. Therefore, the plastic molds were ready to be made as soon as the soil-cement mixture was transported back to the testing location. Using the testing apparatus constructed by Sullivan et al. (2014) and a modified proctor hammer, five test specimens were made at each testing location. The modified plastic cylinders were placed in the testing apparatus and soil was placed into the mold and compacted using a modified proctor hammer in three equal lifts. Figure 3.17 shows a plastic-mold cylinder being constructed.

Figure 3.17: Plastic-mold cylinder being compacted using a modified Proctor hammer

At the beginning of the testing process the plastic molds were constructed using five blows per lift in accordance with the recommendations of Sullivan et al. (2014). However, after noticing that the density was below the 98 percent required by ALDOT, seven blows per lift

were used. This was established by laboratory testing. A laboratory study was done using five, seven, and nine blows and the density was measured to see how many blows it would take to obtain 98 percent density required by ALDOT. This study showed that for this soil-cement mixture, seven blows per lift should be used. Seven blows with the hammer used is also the equivalent amount of energy input for a Proctor sized mold. After the plastic molds had been compacted, the molds were removed from the testing apparatus and trimmed flush with the top of the plastic mold using a straightedge as shown in Figure 3.18. After the specimen was trimmed flush, a plastic cap was placed on the mold and a strip of duct tape was placed over the slit in the side of the mold to prevent moisture loss, shown in Figure 3.19. Duct tape was used instead of foil tape to be consistent with ALDOT practices.

Figure 3.18: Straightedge used to make the soil-cement specimen flush with the mold

Figure 3.19: Duct tape placed on the side of the specimen to prevent moisture loss

3.3.6 Initial Curing

3.3.6.1 Steel Molded Cylinders

Research performed by Wilson (2013), showed that specimens were too weak to be removed from their steel cylindrical mold immediately after production and that the soil cement needed to remain in the mold until initial curing was complete. Wilson (2013) stated that field specimen were to be cured in the molds under conditions that limit exposure to sun, wind, and other sources of rapid evaporation, and from contamination for 12 hours or longer if required. In this research project, specimens were made on one day and retrieved the following day to conform to the findings from Wilson (2013). Steel molded specimens were stored in a shaded area, and in a location where they would be safe until they could be transported back to the laboratory for extrusion. Typical field curing can be seen in Figure 3.20. After the initial curing period of 12 hours or longer, cylinders were transported back to the laboratory at Auburn

University where final curing occurred. During transportation, the cylinders were protected with suitable cushioning material to prevent damage.

Figure 3.20: Molded specimen during initial curing stage

3.3.6.2 Plastic-Mold Cylinders

Sullivan et al. (2014) suggested that plastic-mold cylinders be stored on site for one day and transported back to the lab the following day. In this research project specimens were initially cured the same way as the steel molded cylinders. Test specimens were stored in a shaded area, and in a location where they would be safe until they could be transported back to the laboratory for removal. Typically the specimens were on site for 24 hours, being picked up and brought back to the laboratory at Auburn University the day after production. Figure 3.21 shows initial curing of plastic-mold cylinders. During transportation back to the laboratory the plastic molded cylinders were protected to prevent damage to the test specimens.

Figure 3.21: Plastic molded cylinders during the initial curing stage

3.3.7 Specimen Extrusion

3.3.7.1 Extrusion of Steel Molded Cylinders

Once the initial curing was completed and the specimens had been transported back to the laboratory, the UHMW polyethylene mold plugs were removed and the specimens were extruded from the specimen molds. A standard vertical hand jack was used to extrude the specimens. This jack showed minimal signs of causing edge cracking during extrusion which was a problem when a horizontal jack was used (Wilson 2013). Figure 3.22 shows the vertical hand jack used to extrude the steel molded cylinders.

Figure 3.22: Vertical hand jack used to extrude molded specimens

Once the specimens were extruded, each cylinder was weighed and measurements were taken to determine the density of the specimens.

3.3.7.2 Extrusion of Plastic-Mold Cylinders

At the beginning of the project plastic molded cylinders were extruded using the method developed by Sullivan et al. (2014). Once the initial curing was complete, the plastic caps were removed along with the plastic cut-out tapped to the bottom. The specimens were extruded using the same vertical jack used to extrude the steel molded cylinders with a slight modification. The diameter of the plastic-mold cylinders was larger than the steel molded cylinders so a top plate was machined to fit the plastic molds. The top plate was needed because the plastic-mold specimen diameter was three inches and the top plate of the extrusion jack was made to extrude the steel molded specimens which are 5.6 inches in diameter. A bottom plate with a 1.4 in. (35 mm) diameter was also machined for the extrusion jack to push through the bottom of the plastic mold and extrude the specimen. Figure 3.23, shows the modifications made to vertical hand jack to extrude the plastic molded cylinders.

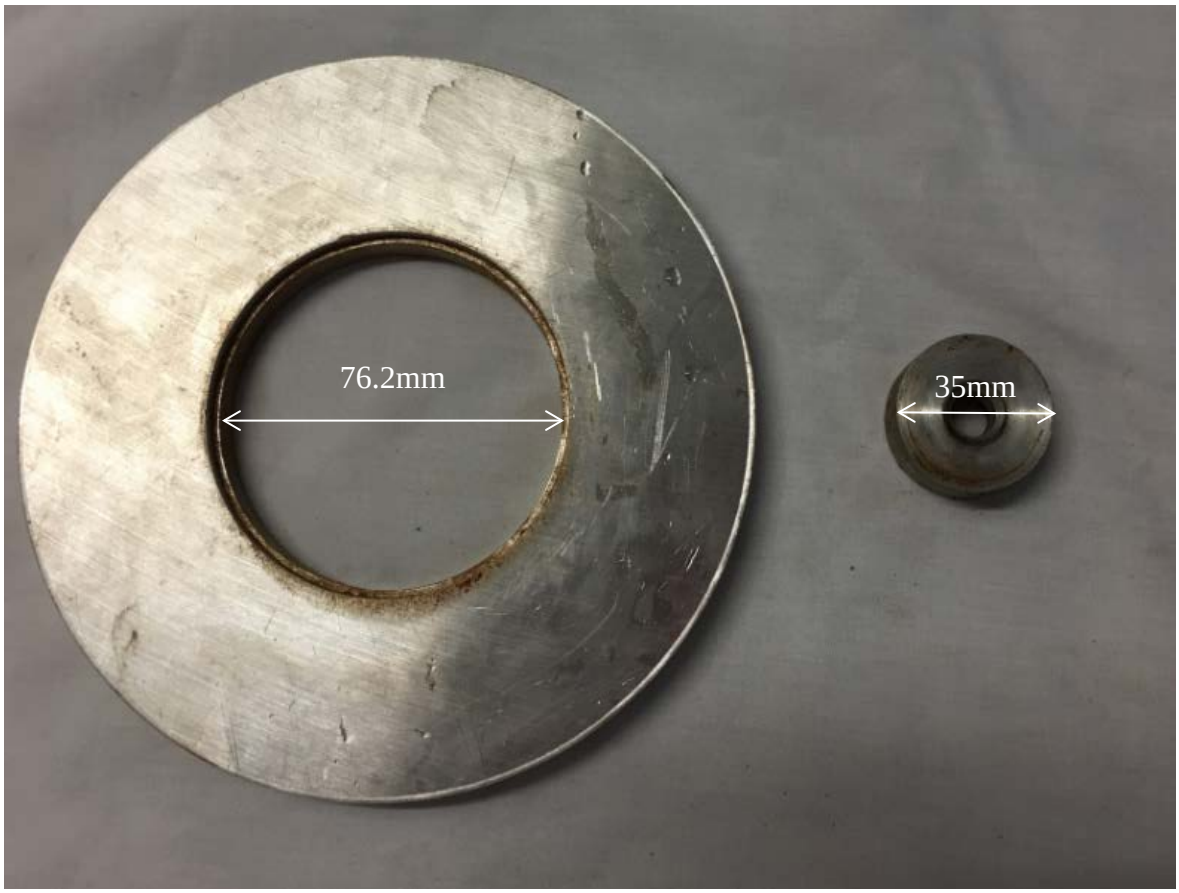

Figure 3.23: Modifications made to extrude the plastic molded cylinders

Once the molds were extruded, each cylinder was weighed and measurements were taken to determine the density of the specimen. The measurements consisted of taking three diameter readings, one at the top one in the middle and one at the bottom, and three length readings. In order to determine the diameter the middle diameter was multiplied by two and was added to the top and bottom diameter then divided by four to determine the weighted average diameter. Three length readings were averaged together to determine the height. Cylinders were weighed and measured to determine their density. Figure 3.24, shows measure being taken to determine the plastic-mold specimen's density.

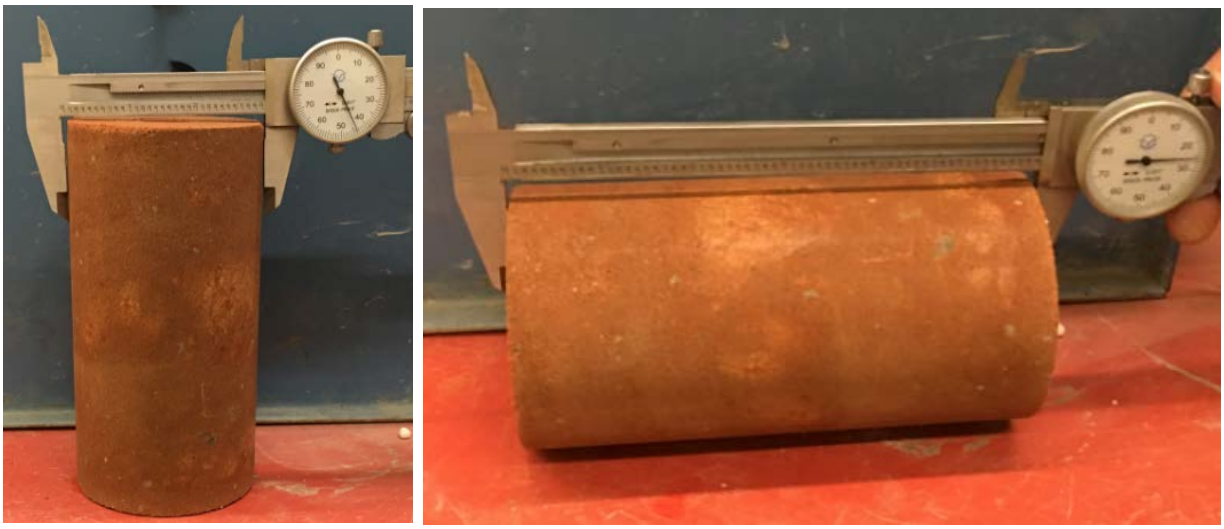

Figure 3.24: Diameter and length readings to determine the density of the PM specimens

As mentioned earlier, using the vertical jack to extrude the plastic-mold specimen caused damage to the specimens and this method was thus modified during the project. Instead of using a vertical jack to extrude the specimens, the molds were cut along the side and extruded by pulling the mold apart and sliding the cylinder out of the plastic mold by hand as shown in Figure 3.25. After removal, the cylinders were weighed and measurements taken to determine their density as mentioned above. Diameter measurements were taken with both methods and no difference in diameter was shown by cutting the plastic mold, when compared to the method Sullivan (2013) recommended.

Figure 3.25: New extrusion method for the plastic-mold cylinders

3.3.8 Final Curing

3.3.8.1 Steel Molded Cylinders

Final curing began as soon as the specimens were extruded from the steel molds. Cylinders were placed in a sealed plastic bag corresponding to the findings presented by Nemiroff (2016). All of the air was removed from the bags and the bag was sealed. By sealing the bags, no moisture was added or removed from the specimens. Once the specimens were bagged, they were placed in the moist-curing room, which was kept at a temperature of 73 °F ± 3

°F, as shown in Figure 3.26, specimens remained in the moist-curing room until it was to test their compressive strength.

Figure 3.26: Final curing of the steel molded cylinders in the moist-curing room

3.3.8.2 Plastic-Mold Cylinders

Plastic-mold cylinders were left in the plastic mold and sealed in a plastic bag the same way the steel molded cylinders were cured. All air was removed from the bags and the bags were sealed shut. Plastic molds were then placed in the moist curing room as described in Section 3.3.8.1. Final curing is shown in Figure 3.27.

Figure 3.27: Final curing of the plastic molded cylinders in the moist-curing room

3.3.9 Testing

3.3.9.1 Steel Molded Cylinder Strength

Compression testing followed the modified ASTM D 1633 (2007) method created by Wilson (2013) during previous research at Auburn University. The differences include

- Specimens were not immersed in water for 4 hours prior to final curing,
- Specimens were not capped, and
- The loading rate of 20 ± 10 psi/s was changed to 10 ± 5 psi/s

The molded cylinder specimens were not immersed in water for 4 hours prior to testing based on recommendations made by Wilson (2013). Specimens were not capped because of the recommendations from Wilson (2013) that showed that the method of making soil cement cylinders provided the planeness and perpendicularity tolerances necessary to meet the criteria of ASTM C 1633 (2007). The loading rate was reduced to 10 ± 5 psi/s due to the recommendations Wilson (2013) made that suggested that the lower rate was more suitable for the low strength requirements of soil cement.

For compression testing, a 100-kip compression testing machine was used for precise control of the loading rate. The 100-kip compression testing machine used for this research is shown in Figure 3.28.

Figure 3.28: 100-kip compression testing machine

After the specimens were removed from the moist-curing room they were removed from the plastic bag and tested in the compression machine shown above. Figure 3.29 shows a test

specimen with in the compression testing machine. Precautions were taken to ensure that the vertical axis of the specimen was aligned with the center of thrust of the upper plate.

Figure 3.29: Soil-cement cylinder in the compression testing machine

The load was applied at a constant rate of 10 ± 5 psi/s until failure occurred. The total load was recorded to the nearest 10 lb. The compressive strength was then calculated by dividing the failure load by the cross-sectional area of the test specimen.

To determine if any outliers existed among the set of five cylinders tested at each age, the acceptable range among results method outlined in ASTM C 670 (2015): *Standard Practice for Preparing Precision and Bias Statements for Test Methods for Construction Materials* was used. In research performed by Wilson (2013) a coefficient of variation of 7.1% for no capping for strength was determined. The multiplier of coefficient of variation from ASTM C 670 (2015)

shown in Table 3.2 was multiplied by a coefficient of variation of 7.1% to produce an acceptable range of results. The range was determined by taking the difference between the maximum strength and the minimum strength and dividing by the average strength of the five cylinders. Five cylinders were made at each location, from which a multiplier of 3.9 is found from Table 3.2. A coefficient of variation of 7.1% times a multiplier of 3.9 gives a maximum acceptable range of 27.7% to determine if any outliers existed in the testing process. This method of identifying outliers was used to be consistent with the way Wilson (2013) identified outliers in his research project.

Table 3.2: Multiplier of Standard Deviation or Coefficient of Variation (Adapted from ASTM C 670 2015)

Number of Test Results	Multiplier of Standard Deviation or Coefficient of Variation
2	2.8
3	3.3
4	3.6
5	3.9
6	4
7	4.2
8	4.3
9	4.4
10	4.5

3.3.9.2 Plastic-Mold Cylinders Strength

The plastic molded cylinder method followed the same testing practices presented in Section 3.3.9.1 for the steel molded cylinders. ASTM C 670 (2015) was also used to determine

the outliers in each test batch. The plastic molded cylinder method used the same coefficient of variation of 7.1% that Wilson (2013) suggested for the steel molded cylinder method.

3.3.9.3 DCP Testing

All dynamic cone penetrometer testing followed the procedure of ASTM D 6951 (2009). A 17.6 lb hammer with a 5/8-inch diameter steel rod with a 22.6-inch drop height was used meeting the requirements set forth in ASTM D 6951 (2009). All tests were completed using a replaceable point tip with a 60° angle, shown in Figure 3.30. The tip was replaced after every 100 tests.

Figure 3.30: Replaceable DCP tip

Before testing began, the DCP was assembled and checked for any damaged parts. After the DCP was checked, testing could begin. The testing locations are explained in Section 3.2.3 and shown in Figure 3.3. Three tests were conducted at each testing location in the pattern shown in Figure 3.31and Figure 3.4. With the DCP held vertically, the tip was first seated by driving the

tip 1 in. (25 mm) into the soil-cement base, such that the top of the widest part of the tip was flush with the surface of the soil cement. At the beginning of the research project, an initial reading was manually recorded from the ruler, shown in Figure 3.32. In January 2017, a Kessler Magnetic Ruler was purchased for the research project allowing DCP testing to be conducted by one person. While holding the DCP in a vertical plumb position the operator raised the hammer until it made a light contact with the top handle and released the hammer to initiate a blow. Using the manual ruler, the penetration was read off from a millimeter scale and recorded after every five blows of the hammer. The Magnetic Ruler recorded penetration readings in mm after every blow of the hammer. This process continued until at least 175 mm of total penetration was obtained. Since the soil-cement layer was eight inches (200 mm) thick, one inch (25 mm) of seating followed by seven inches (150 mm) of penetration allowed the DCP to penetrate thru the entire soil-cement layer. In accordance with ASTM D 6951 (2009), if the penetration was less than 2 mm after five blows or the handle deflected more than 3 inches from the vertical position, testing was stopped. After 175 mm of penetration, the DCP was removed by driving the hammer upwards against the handle.

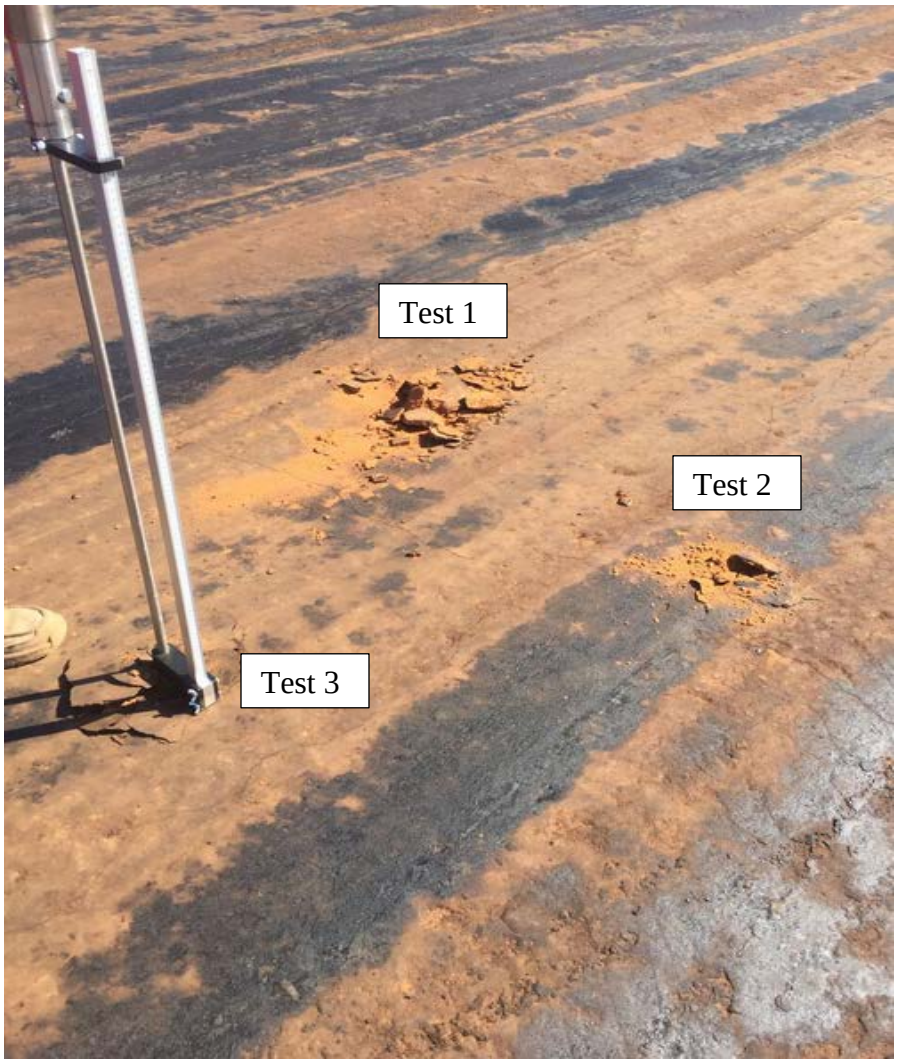

Figure 3.31: Triangular testing pattern conducted at each DCP testing location

Manual Ruler Magnetic Ruler

Figure 3.32: Manual ruler and magnetic ruler used for DCP penetration readings

Figure 3.33: DCP tested conducted at a core hole location equipped with a magnetic ruler

When the test was completed and all the data were collected, penetration depth versus blow-count was plotted. To determine if there were outliers at any testing location, the acceptable range among DCP results were determined and evaluated as discussed in Section 4.6.2. The compressive strength from the DCP data was found by determining the trend line using the slopes of each of the three tests conducted. Once the trend line was found, the slope of

the trend line was used in Nemiroff's (2016) equation. Equation 3.4 shows the relationship between penetration strength and compressive strength that Nemiroff (2016) determined.

$$MCS = 926e^{-0.615DCP} \quad \text{(Equation 3.4)}$$

Where:

MCS = molded cylinder strength (psi), and

DCP = dynamic cone penetrometer slope (mm/blow).

3.3.9.4 Core Strength Testing

ALDOT mandates that cores be cut on the sixth or seventh day after completing a section of the soil-cement roadbed for compressive strength testing. Figure 3.34 shows a typical core hole. Each section consists of 528 feet of soil-cement base 8 inches thick. The location within each 528 foot section from which cores are to be taken was designated by the Engineer in accordance with ALDOT-210 (ALDOT 304 2014). Once the core location was selected by the Engineer, Newell Construction cut three cores out of each section. Once the cores where cut they were removed from the ground as shown in Figure 3.35. After removal, cores were placed in a plastic bag to minimize moisture loss. After the cores were bagged they were then transported by ALDOT back to the testing facility in Troy, Alabama. ALDOT performed all compressive strength testing on the cores obtained for this project. All results reported herein were obtained from ALDOT seventh division.

Figure 3.34: Core hole on U.S. Highway 84 bypass project in Elba, Alabama

Figure 3.35: Core sample being removed from the soil-cement base on the Elba project

Chapter 4

Presentation and Analysis of Results

4.1 Introduction

In this chapter, results from the experimental work described in Chapter 3 are presented and discussed. The compressive strength results for the steel molded cylinder, plastic-mold cylinder soil-cement specimens, and core strength are presented and evaluated. An in-depth analysis of the dynamic cone penetrometer results is presented and discussed along with a penetration depth analysis to determine the most efficient penetration depth. All the data collected from the Elba soil-cement base project can be found in Appendices B through I.

4.2 Dynamic Cone Penetrometer Data Analysis

In this section, discussion on the reason for performing an extensive analysis on the DCP is discussed. Next discussion on how to perform a check for outlier in a test data set is presented. Then a discussion on how the most efficient penetration depth was chosen is presented.

4.2.1 Reasons for Analyzing DCP Results

The main reason for assessing the nature of the DCP results was to have a consistent method to obtain reliable results with this method. When tests were conducted in the field, the majority of the tests had strong trends between blow count and penetration depth with little variability in the testing procedure. However, when analyzing the data some of the test results were highly variable when comparing the three tests done at one location. Two types of highly variable results were observed in the findings. Figure 4.1 shows the first type of highly variable results.

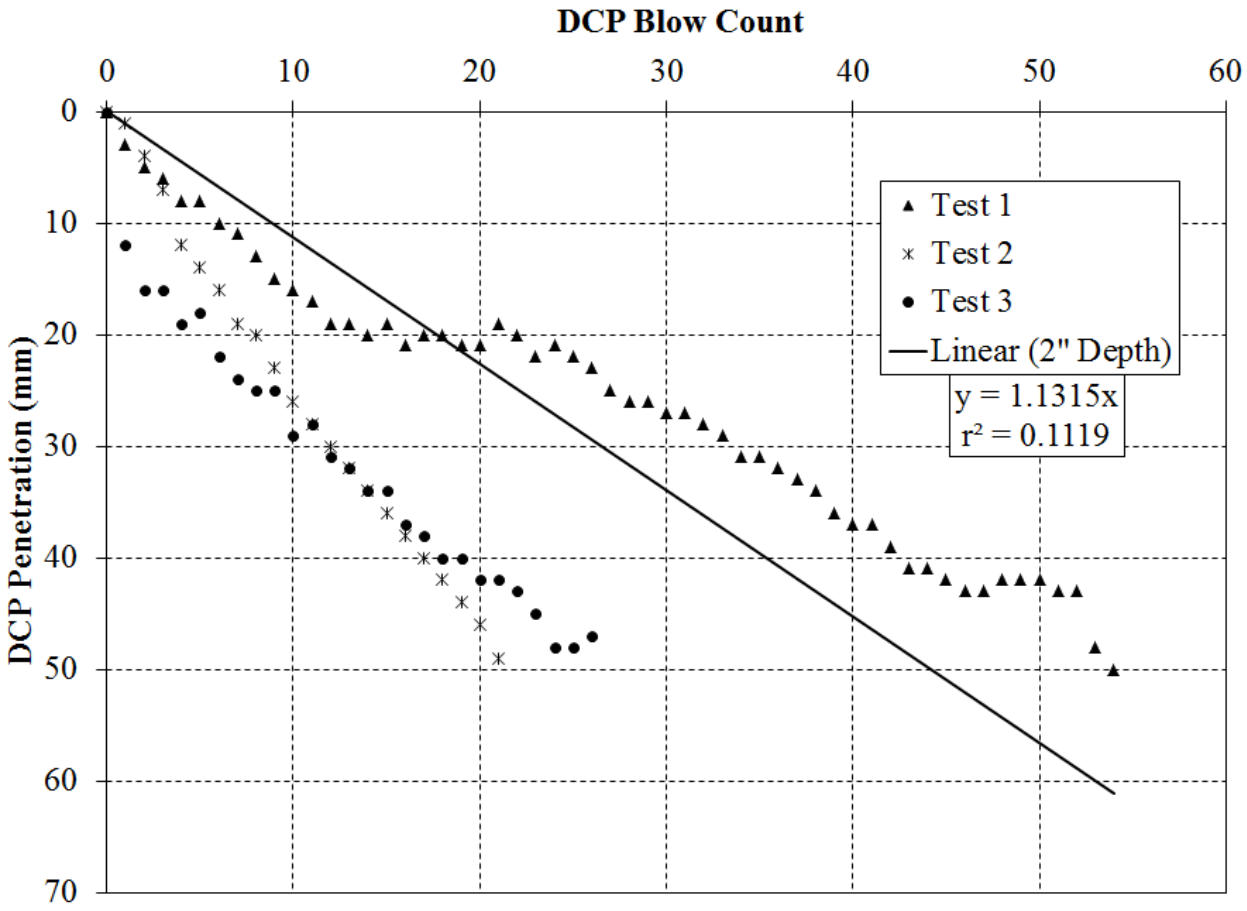

Figure 4.1: First example of highly variable DCP test results encountered on the Elba project

Figure 4.1 shows a weak correlation when comparing all three tests conducted at this location. However, looking closely at the data, Test 2 and Test 3 show very similar results. Looking at Test 1 one can see two linear portions of the line from 0 to 11 and 25 to 45 blows. However, from 11 to 25 blows the trend is almost flat. The almost flat trend indicates that the DCP most likely encountered a hard object, maybe a large aggregate particle, at a depth of apprximately18 mm. The other type of results that presented highly variable results is shown in Figure 4.2.

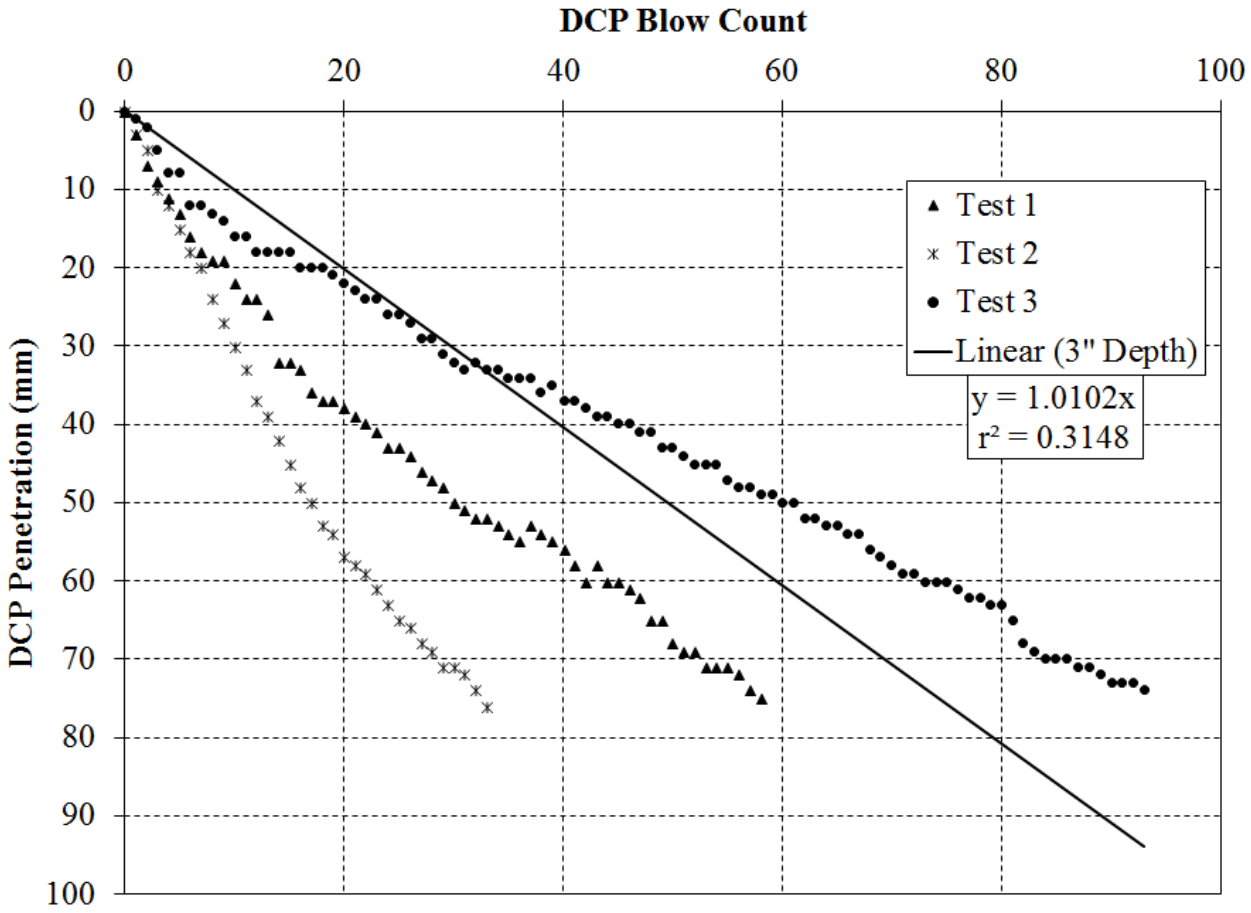

Figure 4.2: Second example of highly variable DCP test results encountered on the Elba project

Figure 4.2 shows three distinctly different slopes for three tests conducted at this location. Test 1 needed 58 blow counts to get to 75 mm of penetration, where Test 2 and 3 needed blow counts of 30 and 92, respectively to get to this same depth.

The examples of two types of irregularity in DCP results presented above help justify the need to use a systematic approach to identify these outliers in the DCP data. This led to a statistical analysis on the dynamic cone penetrometer and is outlined in Section 4.2.2.

4.2.2 Determining Outliers in DCP Results

An in depth analysis of the DCP results was conducted to an approach to identify outliers in the results. A statistical evaluation of the acceptable range among results method was performed on the DCP following ASTM C 670 (2015): *Standard Practice for Preparing Precision and Bias Statements for Test Methods for Construction Materials*. It was determined by assessing at all the data collected during this research project that the maximum acceptable range of 50 percent eliminated some of the outliers while also being high enough not to eliminate too many DCP results. Any data that exhibited a range greater than 50 percent were deemed to contain an outlier test incorporated in the testing location.

Three DCP tests were conducted at each testing location. After completing the tests, results were entered into a spreadsheet for analysis, in terms of blow count and penetration depth in millimeters. Next, the blow count was linearly interpolated to show the blow count at every 5 mm of penetration. This was done for two reasons: so the linear regression line would not be bias to the data set that had the most data points and so that the data that were obtained with a standard ruler at every five blows could properly be compared to the data that was obtained with the magnetic ruler that was collected at every blow. Once all three tests were linearly interpolated at every 5 mm of penetration, the slope of each individual DCP test was determined using the least squares method to calculate a straight line. This was done by using the linest function within Excel. Once all three slopes were determined, the three slopes were averaged together. ASTM C 670 (2015) was used to determine the percent range of the three slopes collected for a test location. In doing this the maximum slope and the minimum slope are needed along with the average slope of the three tests. The acceptable range of 50 percent was then used to determine outliers. The maximum slope minus the minimum slope divided by the average

slope of the three test times 100 percent indicates the range of three conducted tests. If the range was less than 50 percent, then no outlier existed and all three tests results were analyzed by plotting blow count on the x-axis and depth of penetration in mm on the y-axis, as shown in Figure 4.3.

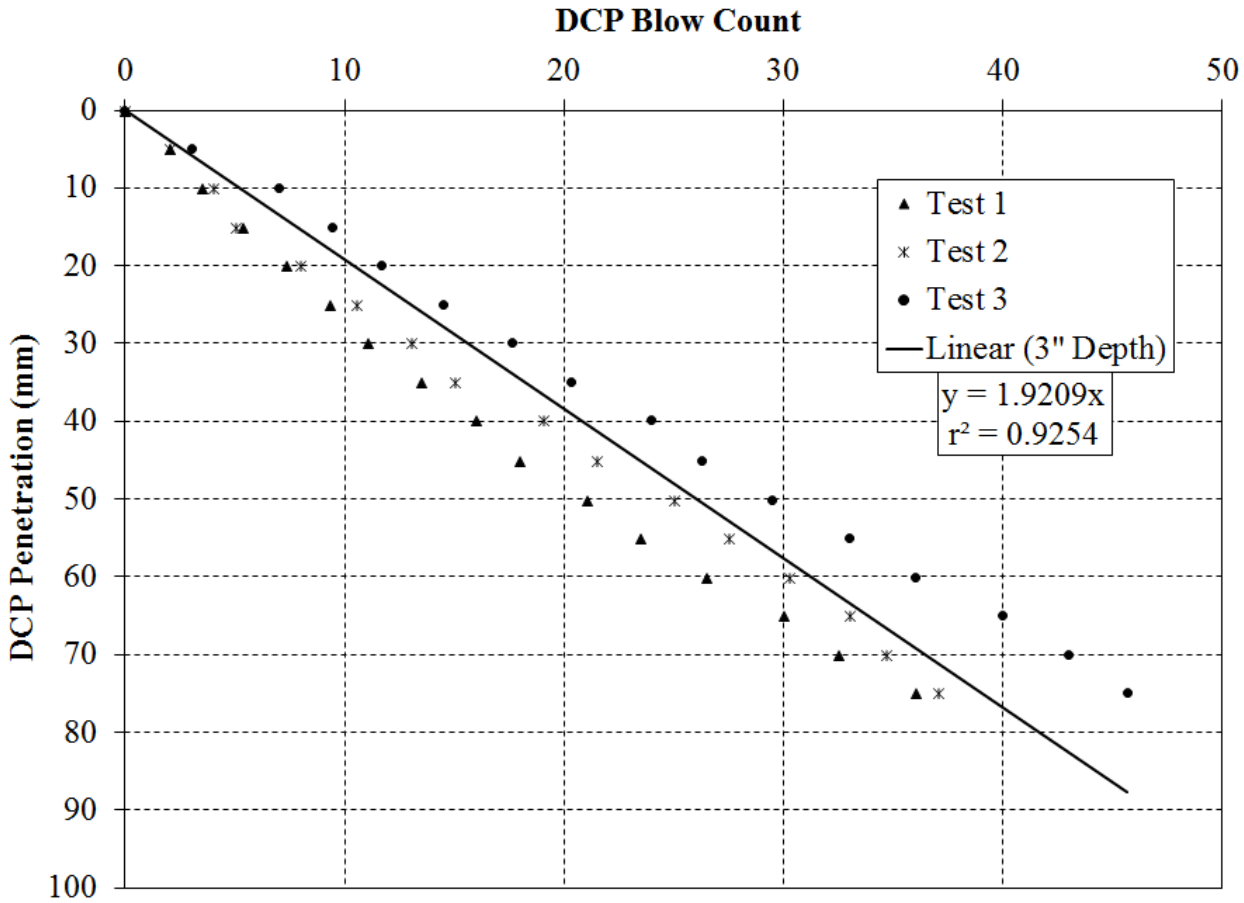

Figure 4.3: DCP test conducted on soil-cement layer and analyzed for outliers

If the range of the three tests conducted was greater than 50 percent then an outlier exists in the dataset. The second step in identifying an outlier in the dataset was done by the absolute value of the difference between the slope of each test conducted and the average slope of the dataset. Once this difference was calculated, the test with the largest difference was deemed the outlier and was removed from the dataset. The next step was to re-calculate the average slope of the remaining two tests and identify the maximum and minimum slope. The same process as

previously stated was then used again to determine the percent range of the data set. If the range was less than 50 percent, then the remaining two results could be analyzed by plotting the blow count on the x-axis and depth of penetration in mm on the y-axis. If the range of the remaining two tests was larger than 50 percent, the DCP tests were disregarded all three tests results differed too much from each other. The number of tests with one outlier totaled 57 and the number disregarded was 18 out of 205 tests.

4.2.3 DCP Penetration Depth Analysis

After a method was established to determine outliers in the DCP data, an extensive analysis was performed to determine the depth of penetration over which to analyze the DCP data. Nemiroff (2016) concluded that the most efficient penetration depth was 75 mm (3 in.). However this needed to be repeated in the field to ensure that 75 mm of penetration was the best depth for DCP test. For ease of presentation, all graphs shown are for the same location of testing for the DCP: however, overall conclusions are based on all the tests performed during the research project. The figures presented in Figures 4.5 through 4.9 represent a demonstration of the process used to analyze each testing location.

For each testing location, data from the three DCP tests were plotted using the procedure outlined in Section 4.2.2. The blow count was plotted on the x-axis and the depth of penetration on the y-axis in mm. Soil cement was placed with an 8 inch (200 mm) layer thickness and the DCP was seated 25 mm (1 in.) before data were recorded. Five penetration depths were evaluated: 25 mm, 50 mm, 75 mm, 100 mm, and full-depth (175 mm). A summary of these penetration depths is shown in Figure 4.4.

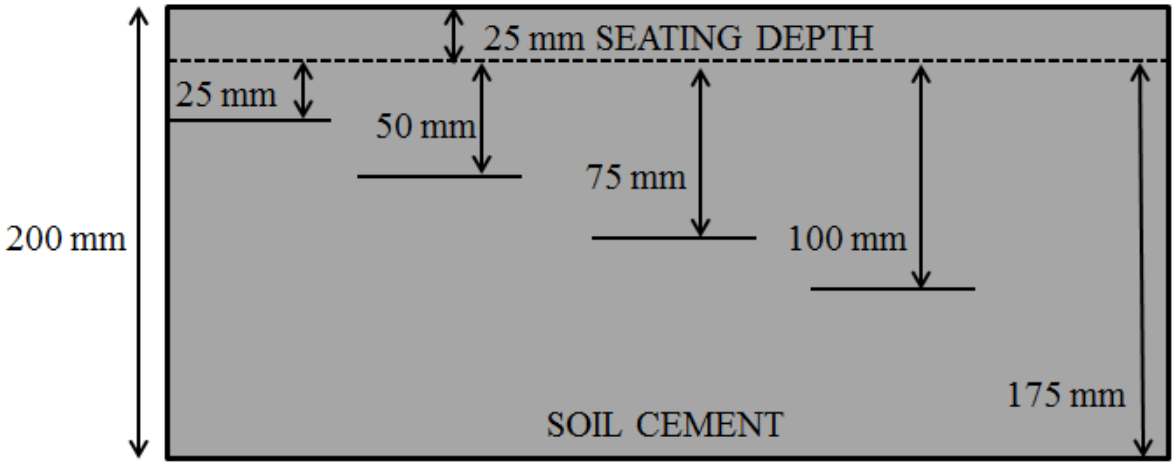

Figure 4.4 Penetration depth summary

The results obtained from these penetration depths were analyzed and compared to each other in order to determine which penetration depth produced the most accurate results with the least amount of technician effort when performing DCP test. A summary of all the data from the testing locations can be found in Appendices D through H.

4.2.3.1 Twenty-five-Millimeters Penetration Depth Analysis

An analysis was performed on 25 mm (1 in.) of penetration to determine if it would be appropriate to only penetrate the soil cement layer 1 in. Webster et al. (1992) suggested that a minimum penetration of 25 mm (1 in.) was sufficient. The depth is approximately 15 percent of the full penetration depth, excluding the seating depth. Example 25 mm penetration depth results at location 19 are shown in Figure 4.5.

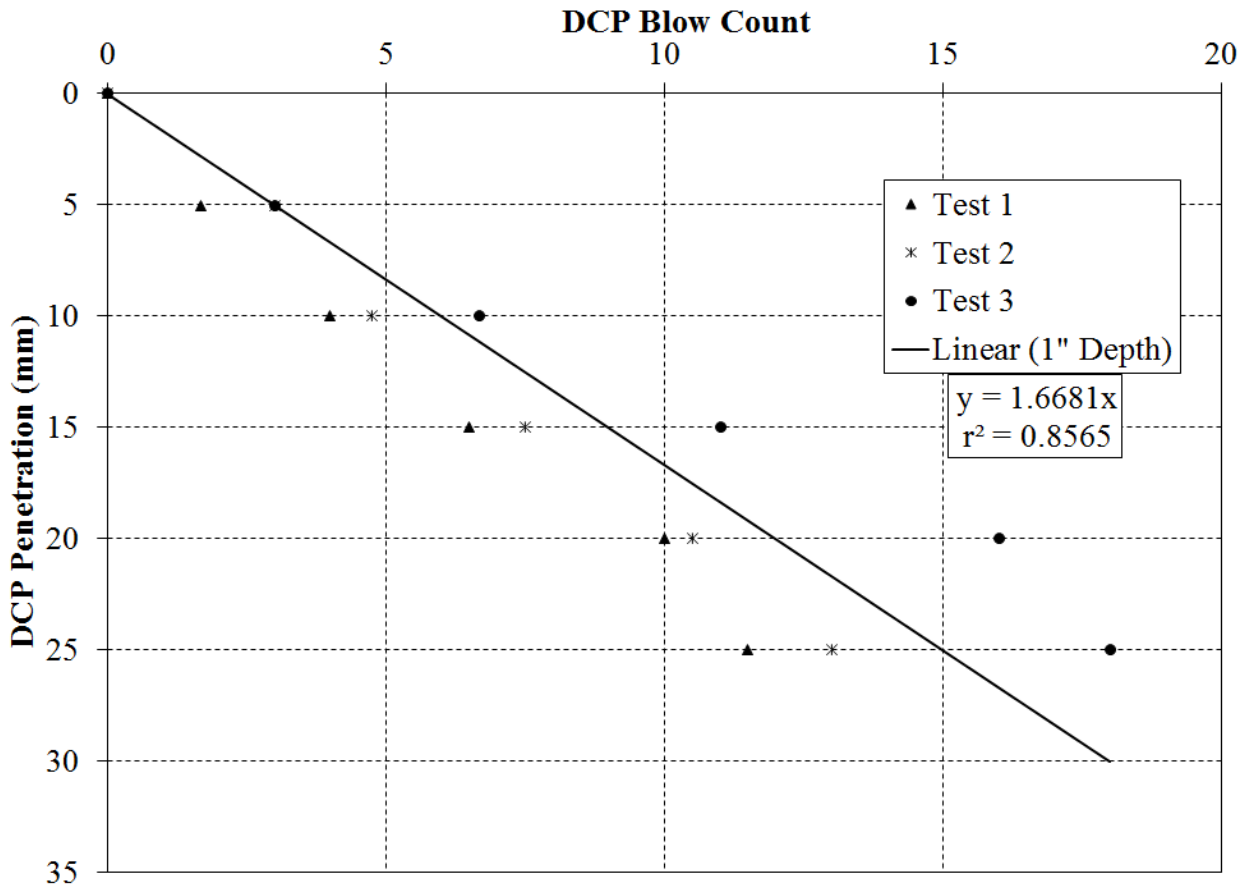

Figure 4.5: Example 25 mm penetration depth result at location 19

Nemiroff (2016) suggested that a depth of 25 mm (1 in.) did not produce enough data points to ensure quality data. However, 25 mm was still analyzed to see if 25 mm of penetration would be enough data to produce quality test. The coefficient of determination (R^2) indicated a reasonably high linear correlation; however, as will be seen deeper penetration depth provide even stronger correlations.

4.2.3.2 Fifty-Millimeters Penetration Depth Analysis

The next a penetration depth of 50 mm (2 in.) was analyzed to determine if less technician effort than Nemiroff (2016) suggestion of 75 mm would still produce accurate results. Shown in Figure 4.6, is the relationship developed for an example penetration depth of 50 mm collected at location 19 for the Elba project.

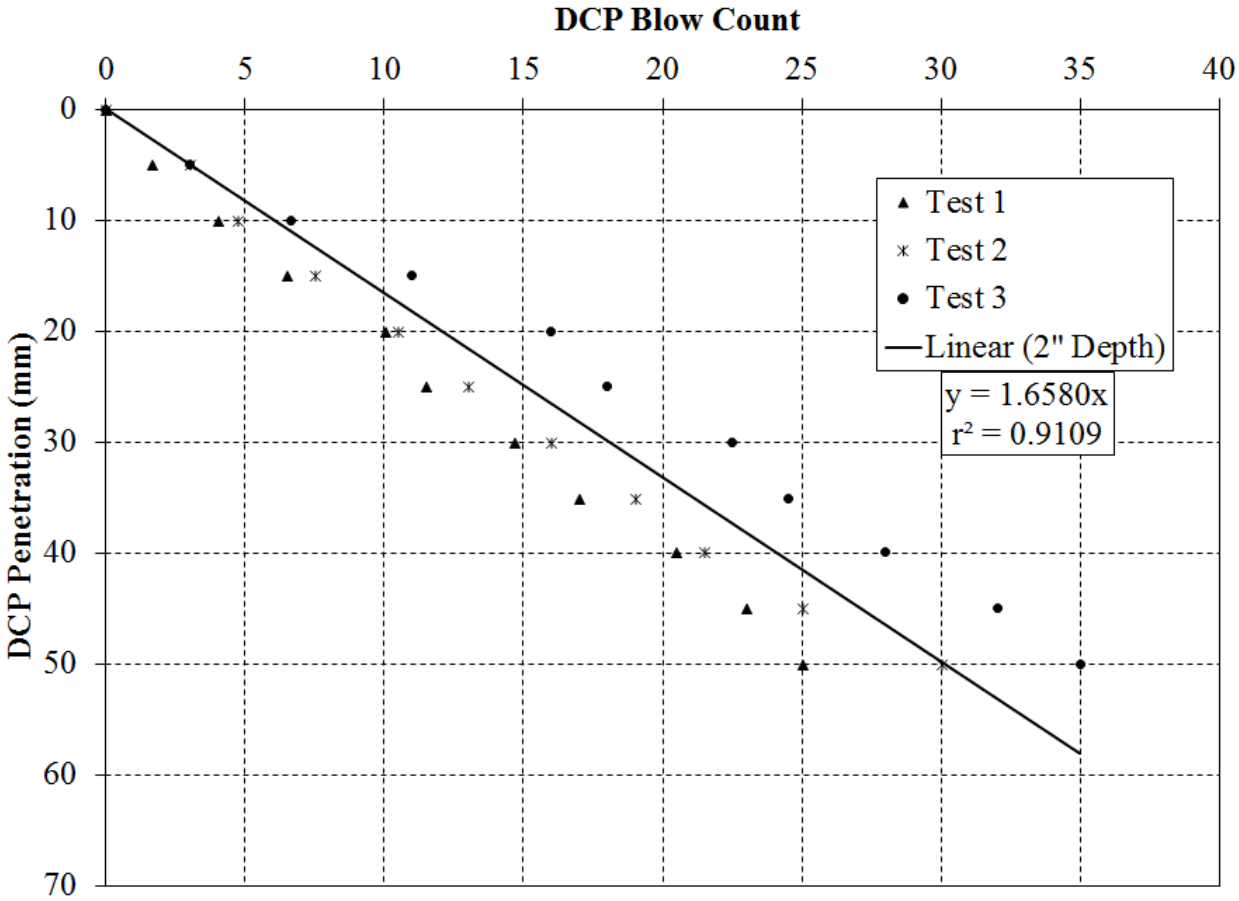

Figure 4.6: Example 50 mm penetration depth at location 19

As suspected, the relationship remained linear with depth. The penetration slope decreased by 0.6 percent compared to the 25 mm penetration slope indicating that they are very similar. The coefficient of determination (R^2) increased from 0.86 to 0.91, indicating a stronger linear relationship exists between DCP blow count and an increase in penetration.

4.2.3.3 Seventy-Five-Millimeters Penetration Depth Analysis

Next, a penetration depth of 75 mm (3 in.) was analyzed to determine if the Nemiroff (2016) recommendation of 75 mm was the most efficient penetration depth. A 75 mm penetration depth was chosen since it is exactly half of the 200 mm (8-inches) soil-cement base layer thickness when a 25 mm (1 in.) seating depth is included. Figure 4.7 shows an example of a 75 mm penetration depth at location 19. The penetration slope decreased by 3.6 percent

compared to the 50 mm slope. The coefficient of determination (R^2) increased from 0.91 to 0.92 indicating an even stronger linear relationship existed between DCP blow count and penetration than existed with the 50 mm depth.

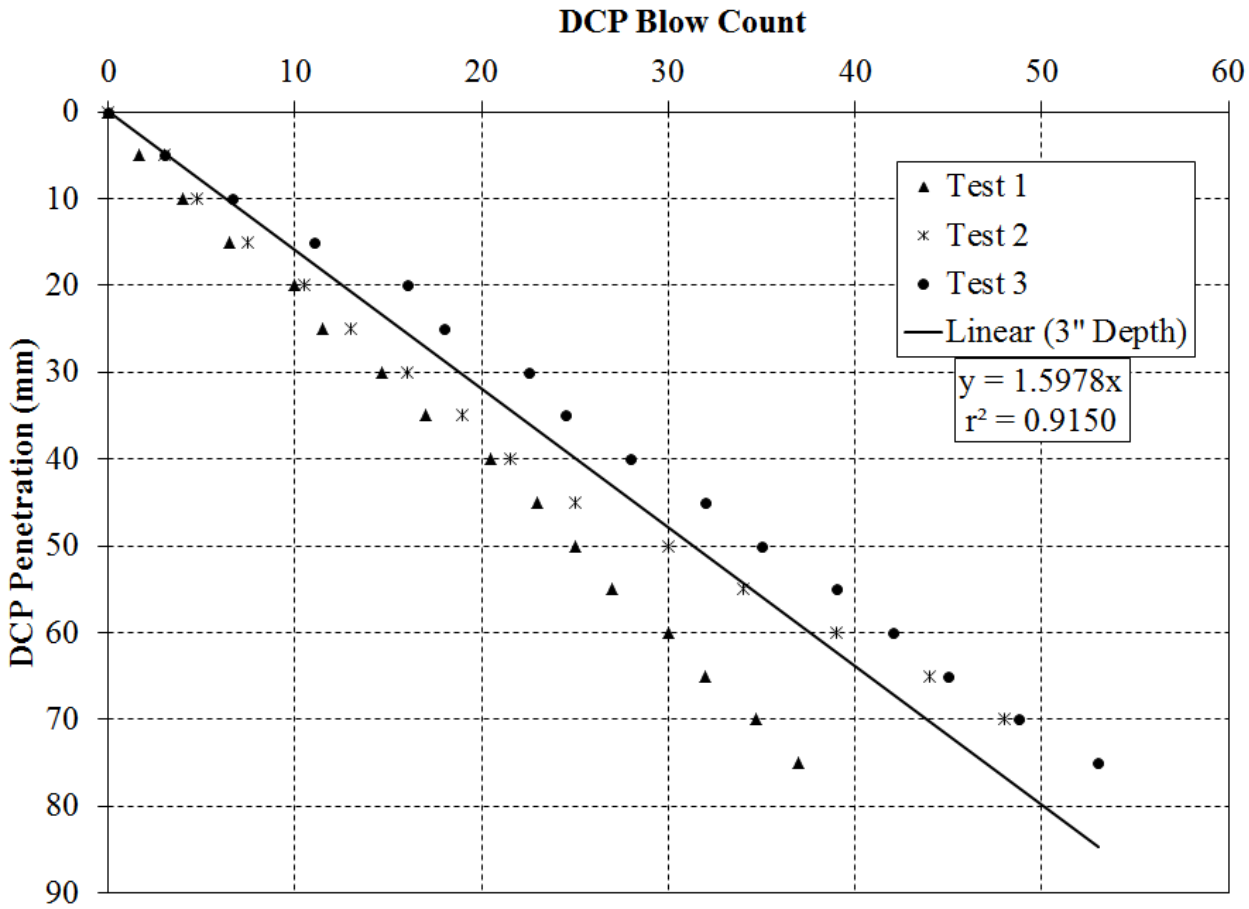

Figure 4.7: Example 75 mm penetration depth at location 19

4.2.3.4 One-Hundred-Millimeter Penetration Depth Analysis

An analysis was performed on 100 mm (4 in.) penetration depth to determine if penetrating the soil cement layer an addition inch would produce more accurate results. A 100 (4 in.) mm penetration was chosen because it is an additional inch from the recommended penetration depth of 75 mm (3 in.) by Nemiroff (2016) and its approximately 60 percent of the total soil cement layer. Figure 4.8, shows the relationship produced by a penetration depth of 100 mm for location 19. As expected, the relationship remained linear with depth. The percent

difference of the slope is 1.5 percent when compared to 75 mm slope. The coefficient of determination (R^2) depth decreased from 0.92 to 0.91 when compared to 75 mm penetration. From this example alone, the extra inch of penetration did not significantly improve the coefficient of determination.

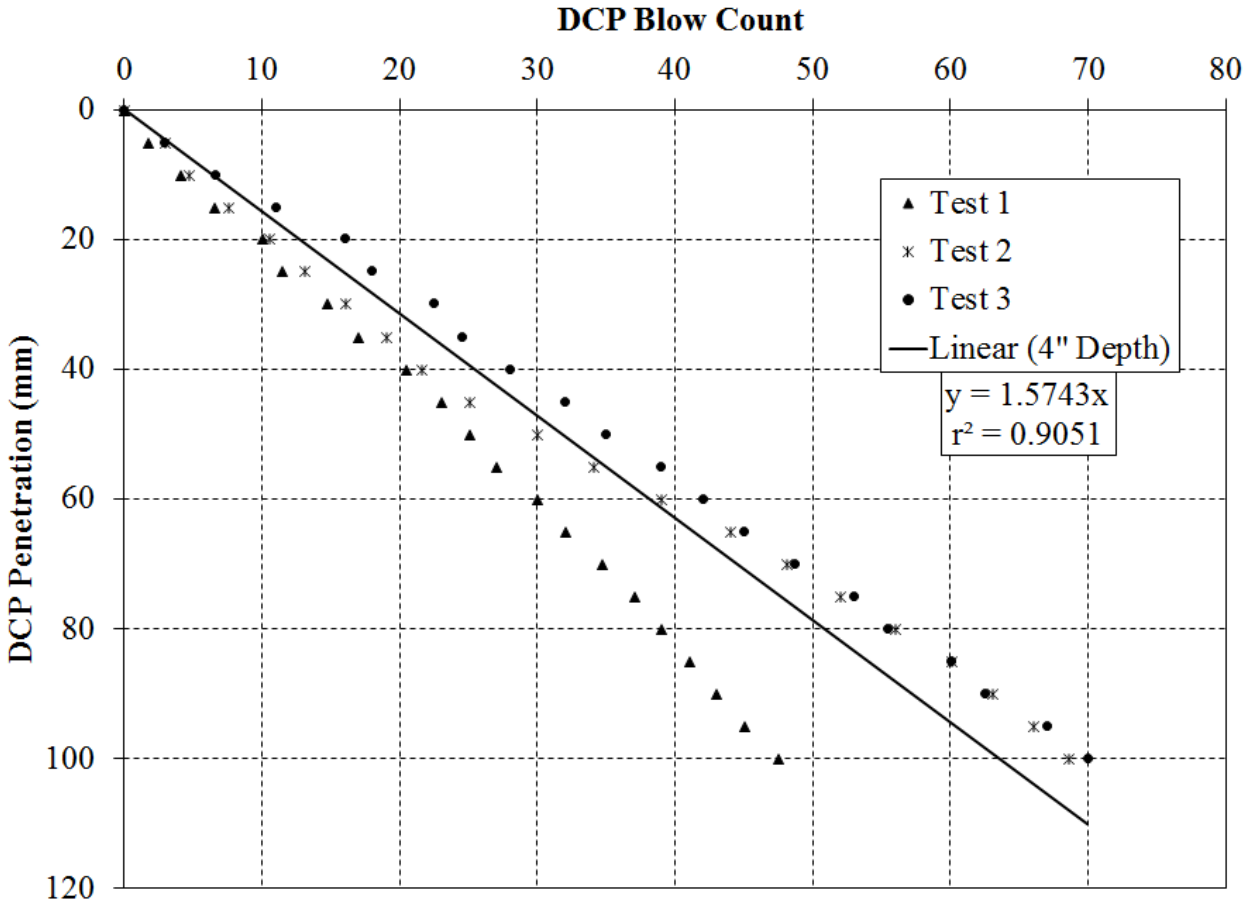

Figure 4.8: Example 100 mm penetration depth at location 19

4.2.3.5 Full-Depth (175 mm) Penetration Analysis

Finally, a full set of data collected over a penetration range of 0 to 175 mm was plotted to determine if analyzing the full-depth of data improved the correlation between blow count and penetration depth. An example of a full-depth penetration analysis of the DCP is presented in Figure 4.9 in location 19. Figure 4.9 shows a strong linear relationship between the blow count

and the penetration depth, however the coefficient of determination is lower when compared to 50 mm, 75 mm, and 100 mm penetration depths.

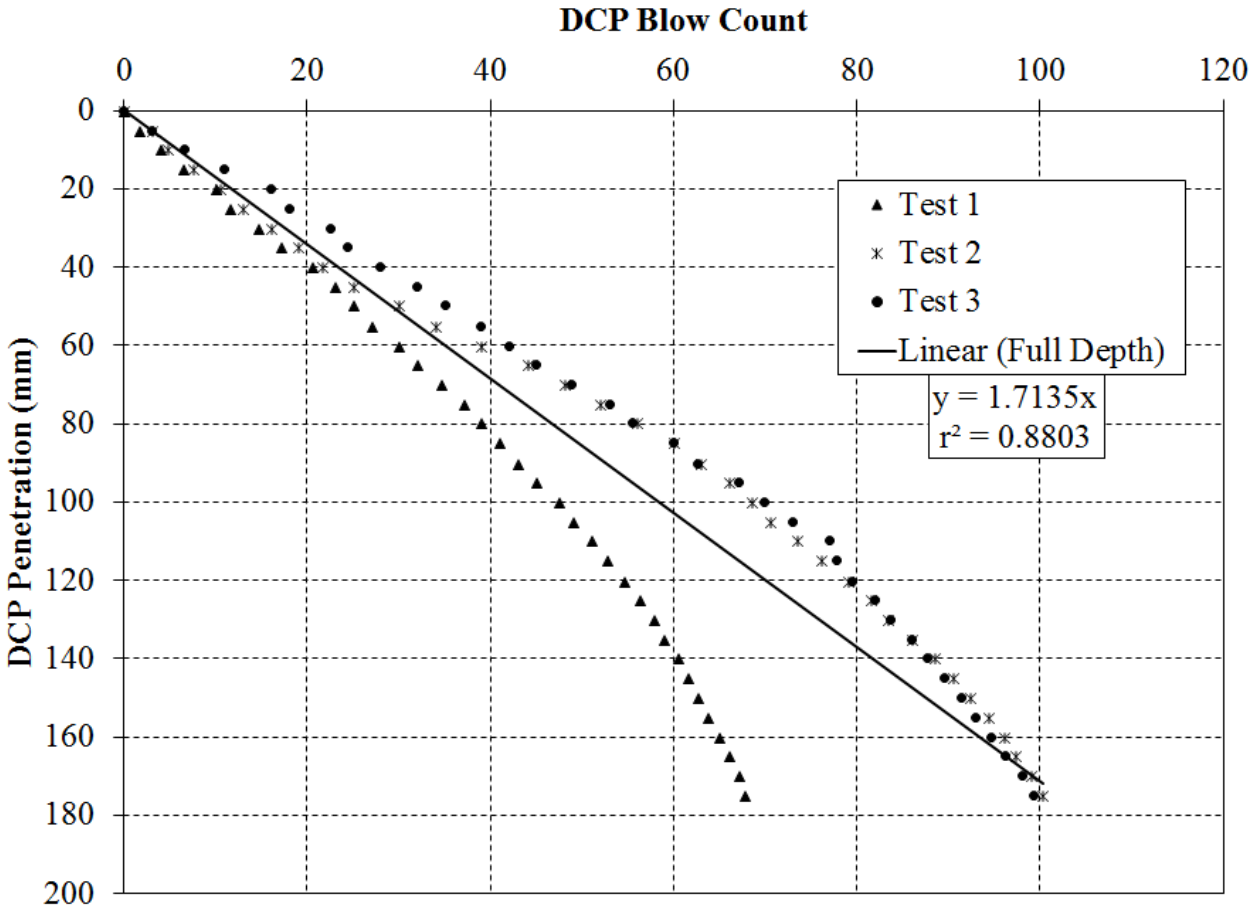

Figure 4.9: Example of full depth penetration at location 19

As expected, the relationship remained linear throughout the entire depth. However, Figure 4.16 shows that the soil cement layer did become weaker starting around 100 mm which is evident in how the curve starts to turn downward below the 100 mm mark. This could be due to compactive effort not reaching the entire 8 inches of the soil cement lift. The percent difference of slope is only 2.7 percent compared to the 25 mm slope; however it is 7.2 percent different when compared to the 75 mm penetration depth. The coefficient of determination (R^2) decreased from 0.92 to 0.88 when compared to the result from the 75 mm penetration depth.

4.2.3.6 Summary and Discussion of the Penetration Analysis

The average coefficient of determination (R^2) for each penetration depth was determined for all the data gathered during the research and is shown in Figure 4.10. Shown in Figure 4.10 are range bars that indicated the minimum and maximum coefficient of determination obtained for each penetration depth.

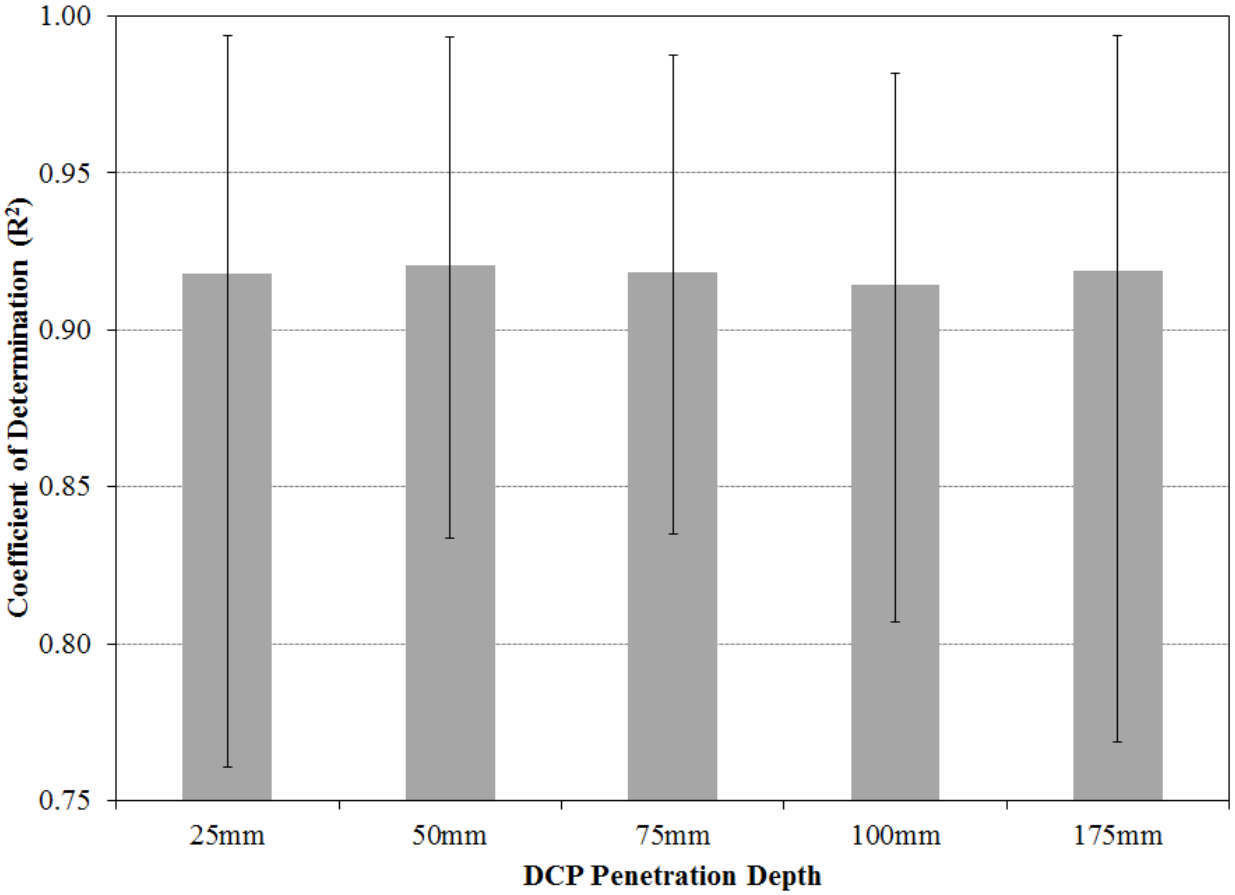

Figure 4.10: Coefficient of determination for all DCP test results collected

The results from the penetration summarized shown in Figure 4.10 generally show a very high coefficient of determination for a linear relationship, meaning that the DCP penetration rate is linear with depth. Penetration depths of 25 mm and 175 mm show the largest degree of variability when compared to the results obtained at 50 mm, 75 mm, and 100 mm. Penetration depths of 50 mm and 75 mm show the smallest variability in the coefficient of determination.

The two penetration depths with the highest value of average coefficient of determination was also the depths of 50 mm and 75 mm. A depth of 75 mm was chosen as the most efficient penetration depth for two main reasons. One, a depth of 75mm was chosen by Nemiroff (2016) to be the most efficient penetration depth when conducting laboratory test on soil cement. Nemiroff (2016) penetration analysis is presented in Figure 4.11. The other reason for choosing 75 mm is that it allows the technician performing the test to penetrate exactly half of the 8-inch thick soil cement layer when the DCP is seated 25 mm before data are collected.

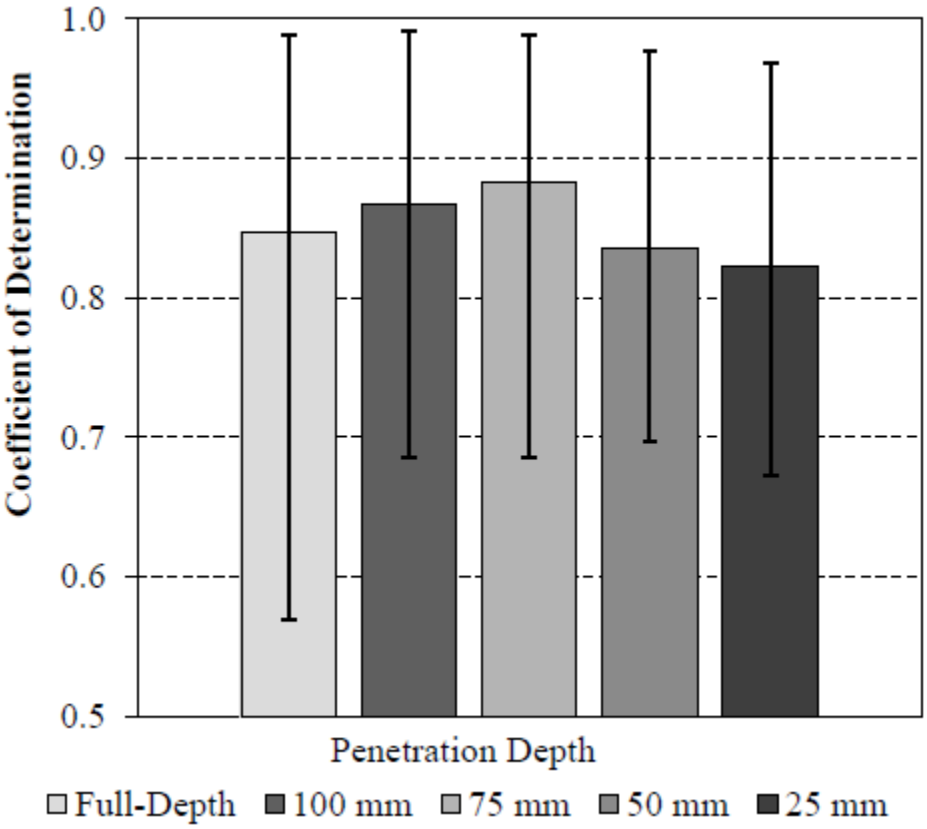

Figure 4.11: Coefficient of determination for all DCP tests conducted in the laboratory (Nemiroff 2016)

Using the penetration analysis that was performed during the research, Table 4.1 was compiled to summarize the quantity of DCP blows need to penetrate 75 mm (3 in.) depending on the strength of the soil cement base. The strength range chosen was based on the ALDOT 304

(2014) specification requirements for in-place strength of soil cement base. Based on the recommendation of this research project and the research performed by Nemiroff (2016), 75 mm is the only penetration depth summarized in Table 4.1. Using Table 4.1, when a technician is conducting DCP test in the field he or she will immediately know if the desired strength of the soil cement base was reached. If the average blow count falls within 35 to 106 blows full pay will be allotted from the guidelines set forth in ALDOT 304 (2014). If the average blow count falls within 30 to 34 or 107 to 130 blows, a pay reduction should be incorporated indicating the strength falls with the pay reduction range of ALDOT 304 (2014). If the average blow count falls under 30 blows or over 130 blows the section should be removed and replaced.

Table 4.1: Summary of blow counts for 75 mm of penetration

Penetration Depth	Blow Count				
	200 psi	250 psi	425 psi	600 psi	650 psi
75 mm	30	35	59	106	130

4.3 Results of the Steel-Mold Cylinder Test Method

As stated previously one method evaluated for determining the compressive strength of soil cement was the steel-mold cylinder method developed by Wilson (2013). Figure 4.12 shows the average seven-day compressive strength test results obtained with this method for each testing location. The values presented in Figure 4.12 are the averages of five cylinders made at each testing location. Any outliers were removed from the data set by the method stated in Section 3.3.9.1 before plotted in Figure 4.12.

Figure 4.12 shows ALDOT 304 (2014) guidelines on soil-cement strength ranges. Any samples testing below 200 psi and above 650 psi were to be removed and replace without compensation. Samples testing between 200-250 psi and 600-650 psi are subject to pay reduction

as stated in Section 1.1. Any other test specimens between 250 and 600 psi would receive 100% pay.

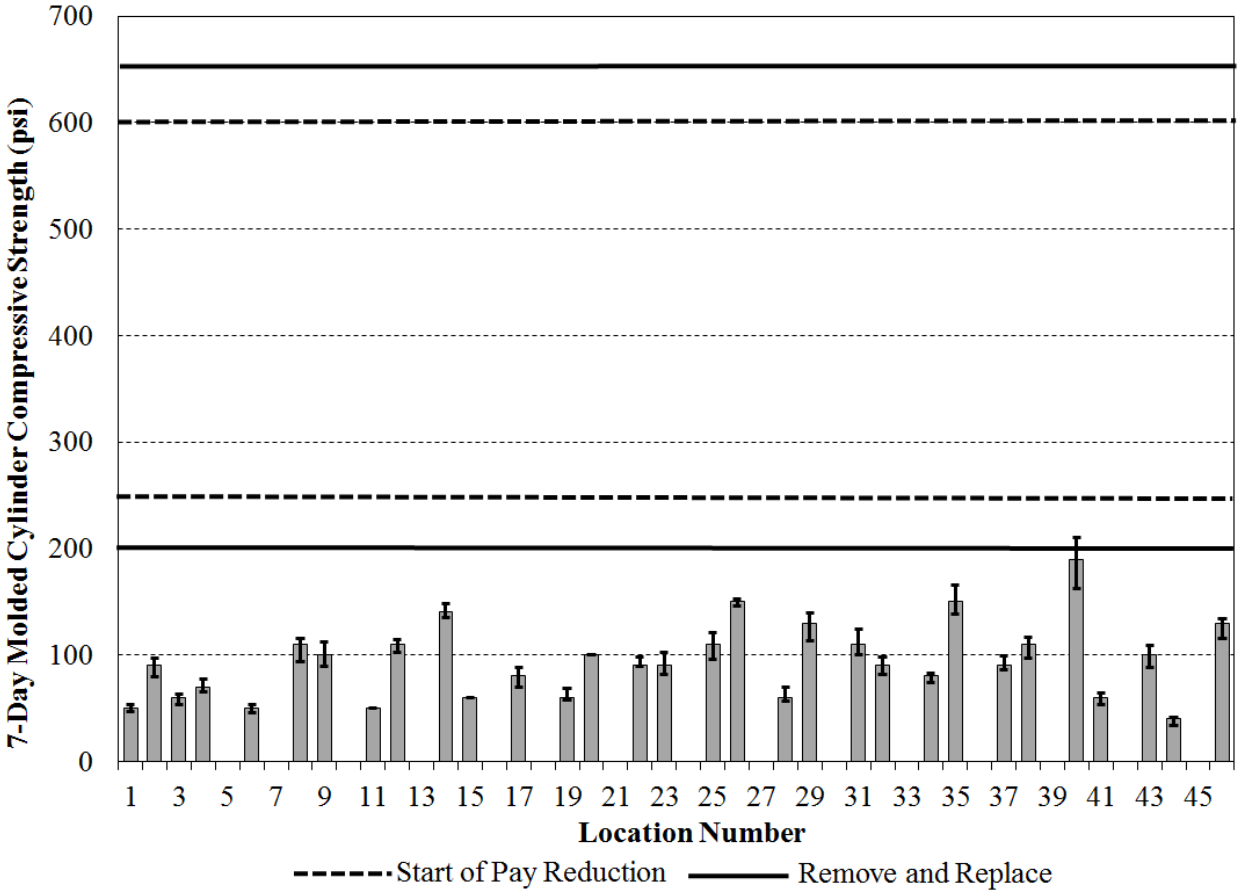

Figure 4.12: Seven-day compressive test results for steel-mold cylinders

As seen in Figure 4.12 all results from steel-mold cylinders were very low when compared to ALDOT strength requirements. Minimum and maximum tests results at each location are shown by the range bars added to figure 12. Range bars, in Figure 4.12, indicate very little within test variation results in the testing method; however, the molded cylinders indicated very low strength soil cement. Using this test method, results from locations showed that the soil cement should be removed and replaced, which is not the case as will be seen from the results of the other test methods. Since, the molded cylinder strength was so low, this test will not be used in comparison to other methods. Wilson (2013) steel mold cylinder method was

never used in the field during his research and has limitations when used in the field and not the laboratory. The method was deemed insufficient for field testing and should only be used when testing molded cylinders in the laboratory.

Density was checked for each steel-molded cylinder made during the Elba project as described in Section 3.3.7.1 Figure 4.13 shows the density results for the steel-molded cylinders at each testing location during the Elba soil-cement project. Values presented in Figure 4.13 are the average density values for the five test specimens made at each testing location. The secondary y-axis, deviation from optimum moisture content range, indicates zero when the water content measured in the field fell within the moisture content needed to achieve 98 % density. However, the secondary y-axis show a positive deviation from zero when soil cement in a location was too wet to achieve 98 % density, and a negative value when soil cement in a location was too dry to achieve 98 % density.

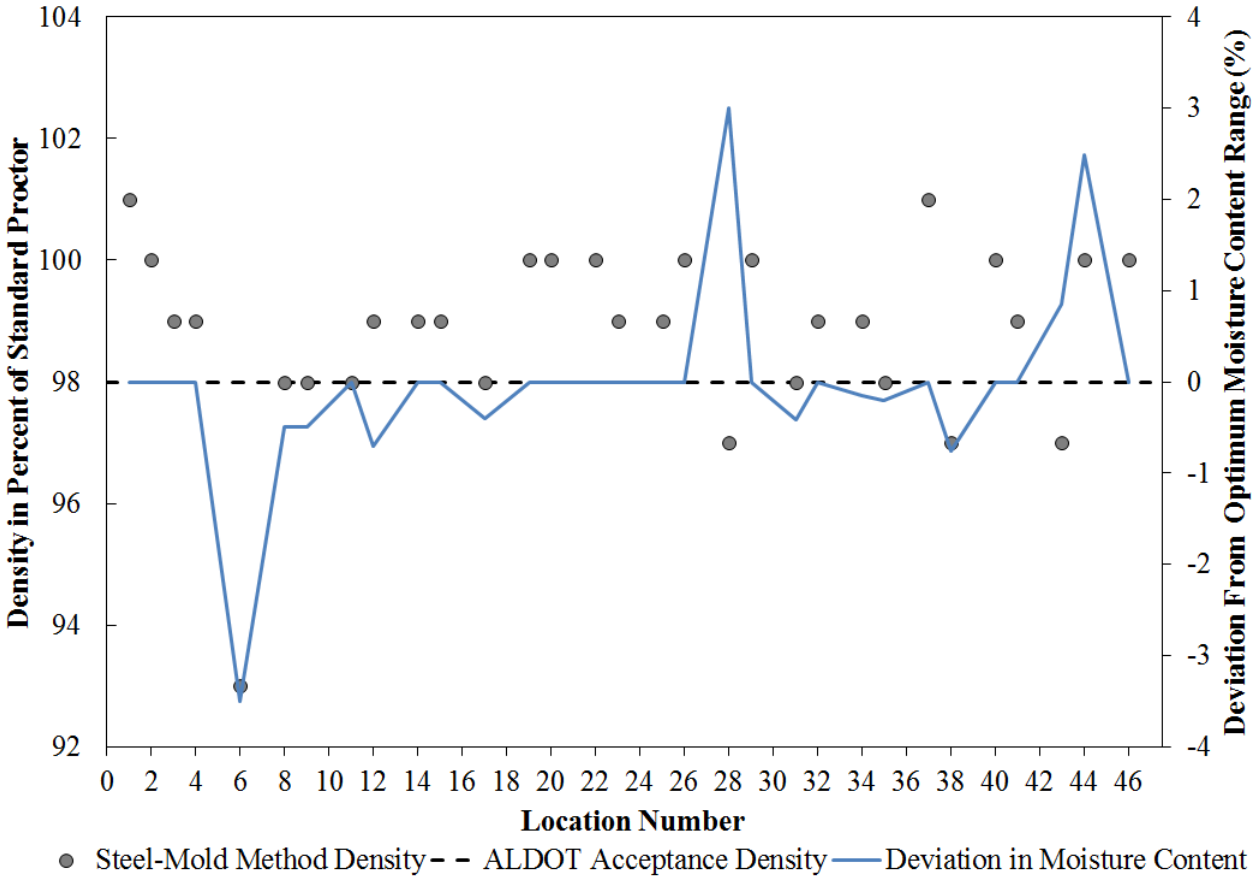

Figure 4.13: Molded cylinder method average density values at each testing location

Figure 4.13 shows that the density of the steel-molded cylinders out of all testing locations except for three met ALDOT 304 (2014) density requirements for soil-cement base. The three locations that did not meet density occurred where the moisture content of the testing location fell outside the range needed to achieve 98 % density

4.4 Results of the Plastic-Mold Method

As stated previously, another method used to determine the strength of soil cement base was the plastic-mold method developed by Sullivan et al. (2014) and slightly modified as described Section 3.3.5. Figure 4.14 shows the average seven-day compressive strength test results for each testing location obtained for the plastic-mold method. The values presented in Figure 4.14 are the averages of five plastic-mold cylinder results made at each testing location.

Any outliers were removed from the data set by the method stated in Section 3.3.9.2 before plotted in Figure 4.14.

Figure 4.14 also shows the ALDOT 304 (2014) strength requirements for soil cement. Specimens testing below 200 psi and above 650 psi indicated sections to be removed and replaced without compensation. Specimens testing between 200-250 psi and 600-650 psi indicate sections are subject to pay reduction as defined in Section 1.1. All strength results between 250 and 600 psi would result in 100% pay for the section.

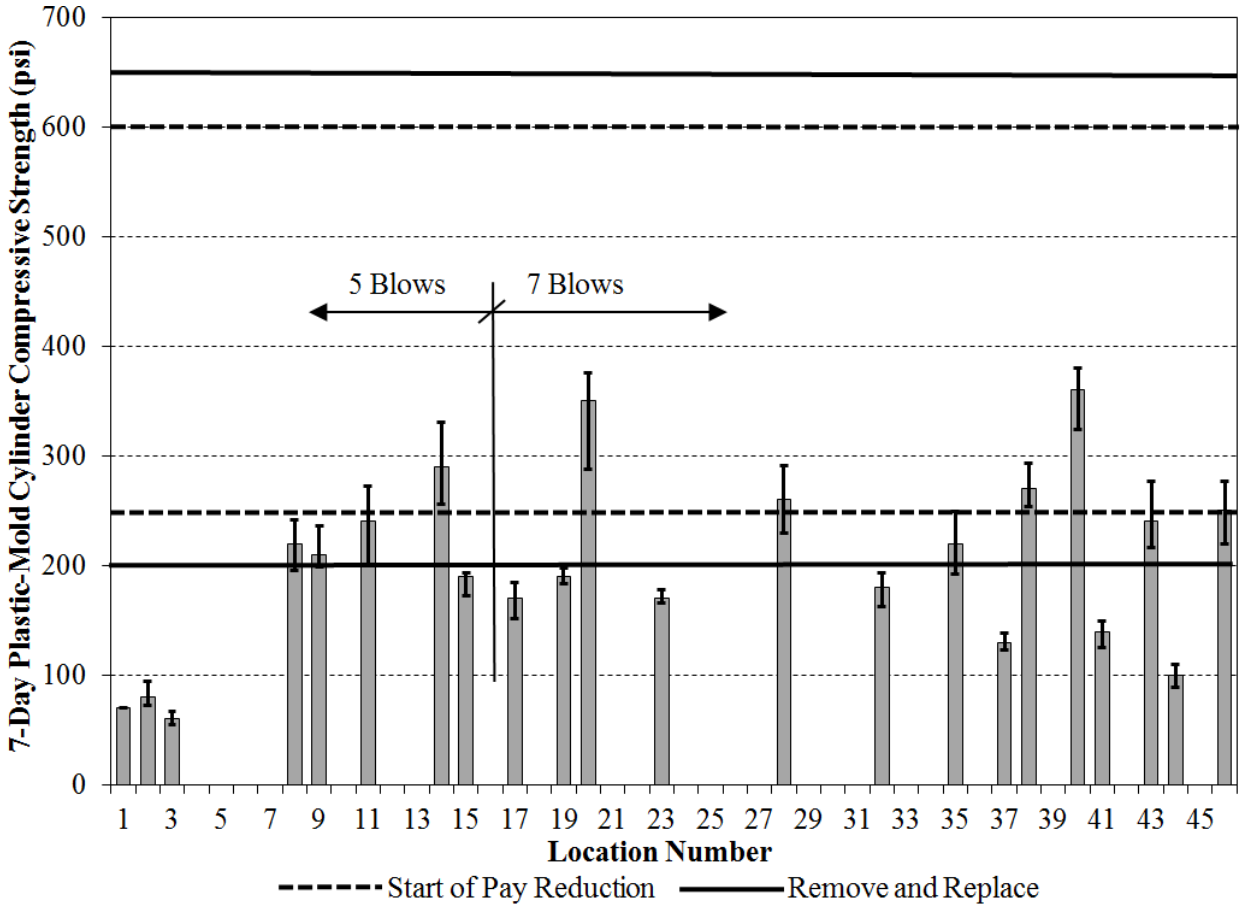

Figure 4.14: Seven-day compressive strength results for the plastic-mold method

Fewer plastic molds were tested due to lack of equipment needed to make the plastic-mold specimens. Shown in Figure 4.14, the plastic-mold method was altered to seven blows

instead of five blows in order to achieve 98 % density required by ALDOT 304 (2014). The study conducted that requires seven blows to achieve 98 % density can be found in Appendix B.

Density was determined for each plastic-mold cylinder made during the Elba project following procedure outlined in Section 3.3.7.2. Figure 4.15 shows the density of the plastic-mold cylinders at each testing location collected during the Elba project. Values presented in Figure 4.15 are the average value of density for the five test specimens made at each testing location. Also shown in Figure 4.15 are the deviations from optimum moisture content range.

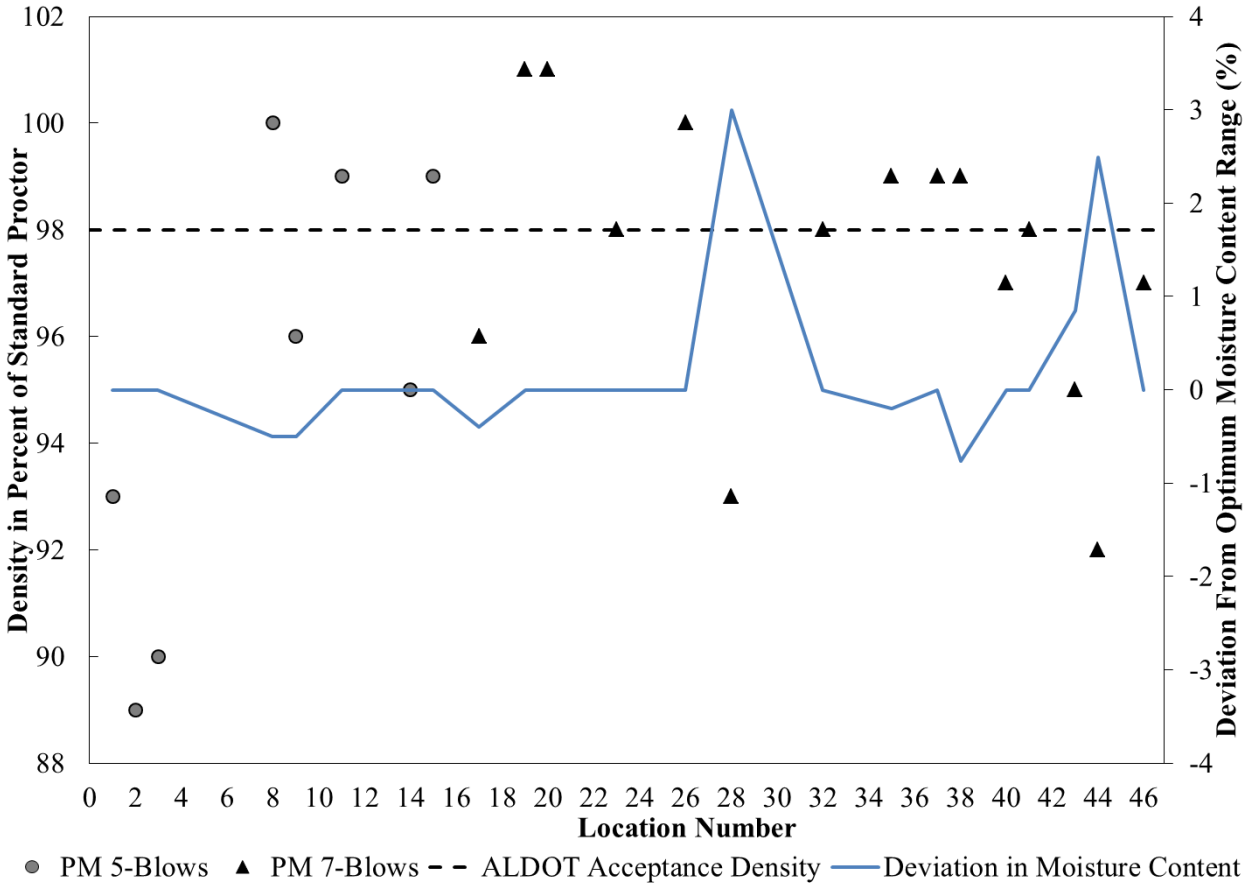

Figure 4.15: Plastic-mold method average density values at each testing location

Figure 4.15 shows that when five blows were used and the water content was in the optimum water content range, the density of the plastic-mold cylinders did not meet the 98 % density requirement set forth by ALDOT 304 (2014). When seven blows were used, most of the

plastic molds meet the density requirement of 98 % when the water content fell inside the optimum water content range. As expected, fewer plastic molds meet density than the steel-mold method.

4.5 Results of the Dynamic Cone Penetrometer

The third method used to evaluate the strength of soil-cement base was the DCP used in accordance with ASTM D 6951 and the correlation between strength and DCP result developed by Nemiroff (2016). Figure 4.16 shows the compressive strength of the soil cement base using the equation developed by Nemiroff (2016), shown in Section 2.5.2.1. The strength estimates shown in Figure 4.16 are the average of three DCP tests conducted at each testing location. The minimum and maximum strength estimated from the DCP data are also shown with range bars at each testing location. Outliers were removed before the data were plotted in Figure 4.16. The procedure used to analyze DCP data was covered in Section 4.2.

More DCP tests were conducted in order to compare the DCP with the steel-molded cylinder method and the plastic-mold method, while also having the ability to compare the SCP strength results to the core strength obtained by ALDOT. The range bars in Figure 4.16 show more variability in the test method compared to plastic-mold cylinder method; however, the DCP shows the strength of the in-place soil cement, whereas the plastic molds are sampled and compacted by the technician. Variability in-place will be greater than variability of plastic-mold cylinders made and cured under controlled conditions.

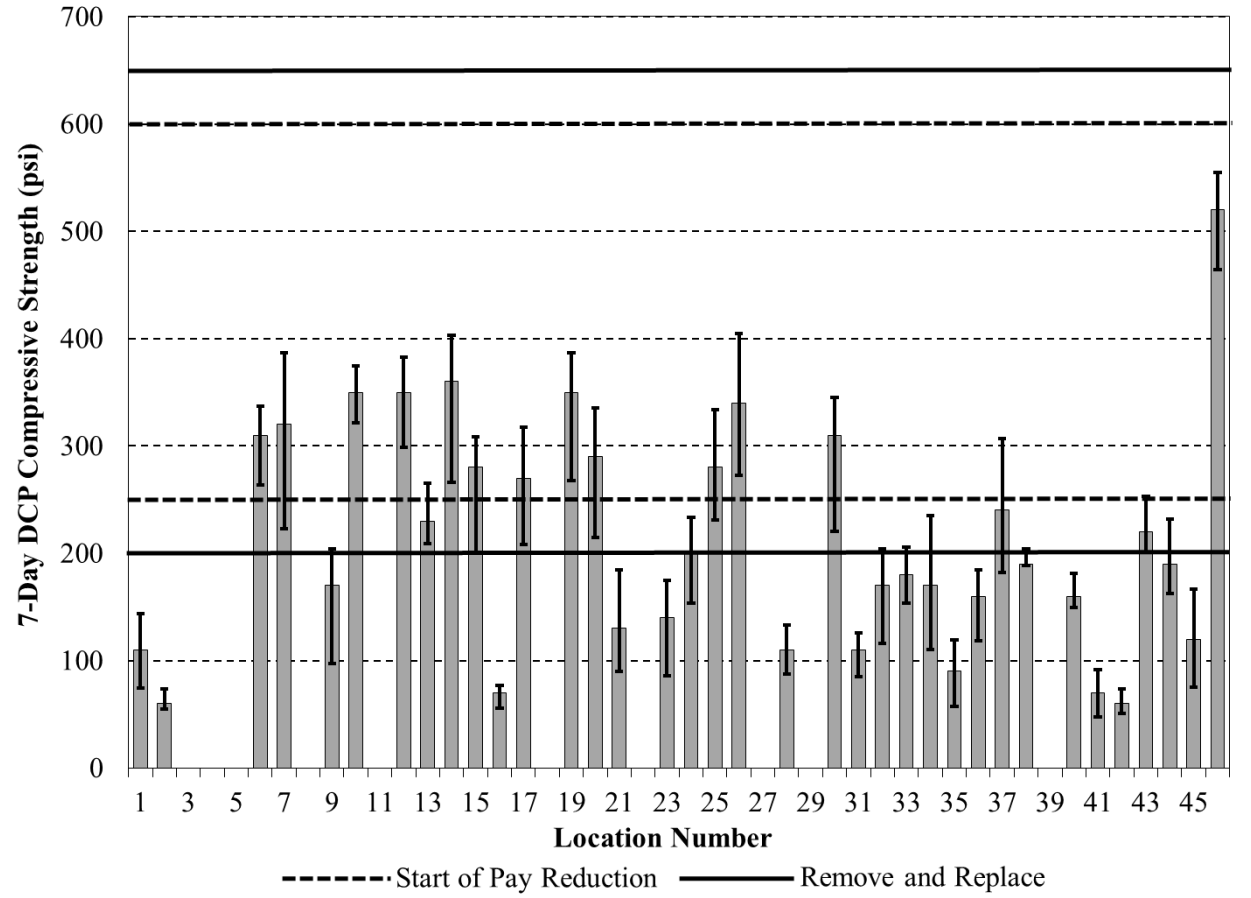

Figure 4.16: Seven-day compressive strength results from DCP results

4.6 Core Strength Results

Cores were extracted by Newell construction and tested by ALDOT on the seventh day. Three cores were extracted from each 1/10 of a mile section. Figure 4.6 shows the average seven-day compressive strength for each testing location. The values shown in Figure 4.17 are the average of three cores that were taken from each location. Also shown are range bars that show the minimum and maximum core strength obtained at each location.

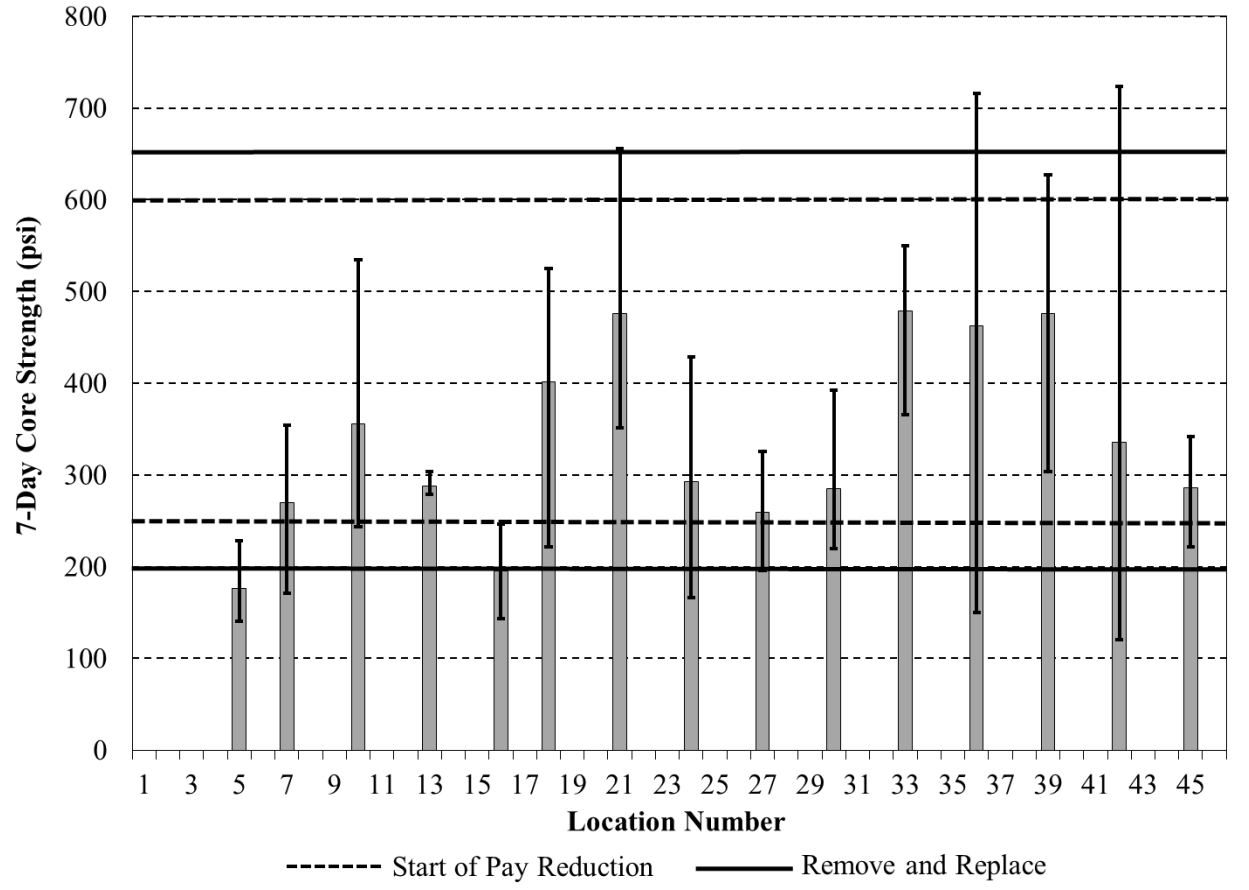

Figure 4.17: Seven-day compressive strength results from cores taken on U.S Highway 84

Figure 4.17 indicates that all but two sections received full pay for the soil cement placement. The two sections that did not receive full pay should be removed and replaced by ALDOT 304 (2014) guidelines. Range bars in the figure indicate that compressive testing of cores is a highly variable test method which is similar to what was found on past ALDOT projects. Core testing was the most variable test method used in the research project. Cores do test the in-place strength of the soil-cement base; however, the DCP test method also tests the in-place strength of the soil-cement and has a lot less variability. A graph of all the core strength results extracted during the Elba project can be found in Appendix I.

4.7 In-Place Density Results

The in-place density of the tested section was measured using a nuclear density gauge by ALDOT. Figure 4.18 shows the density obtained at each testing location during the soil cement project. Figure 4.18 shows the in-place density of the soil cement base after compaction was complete.

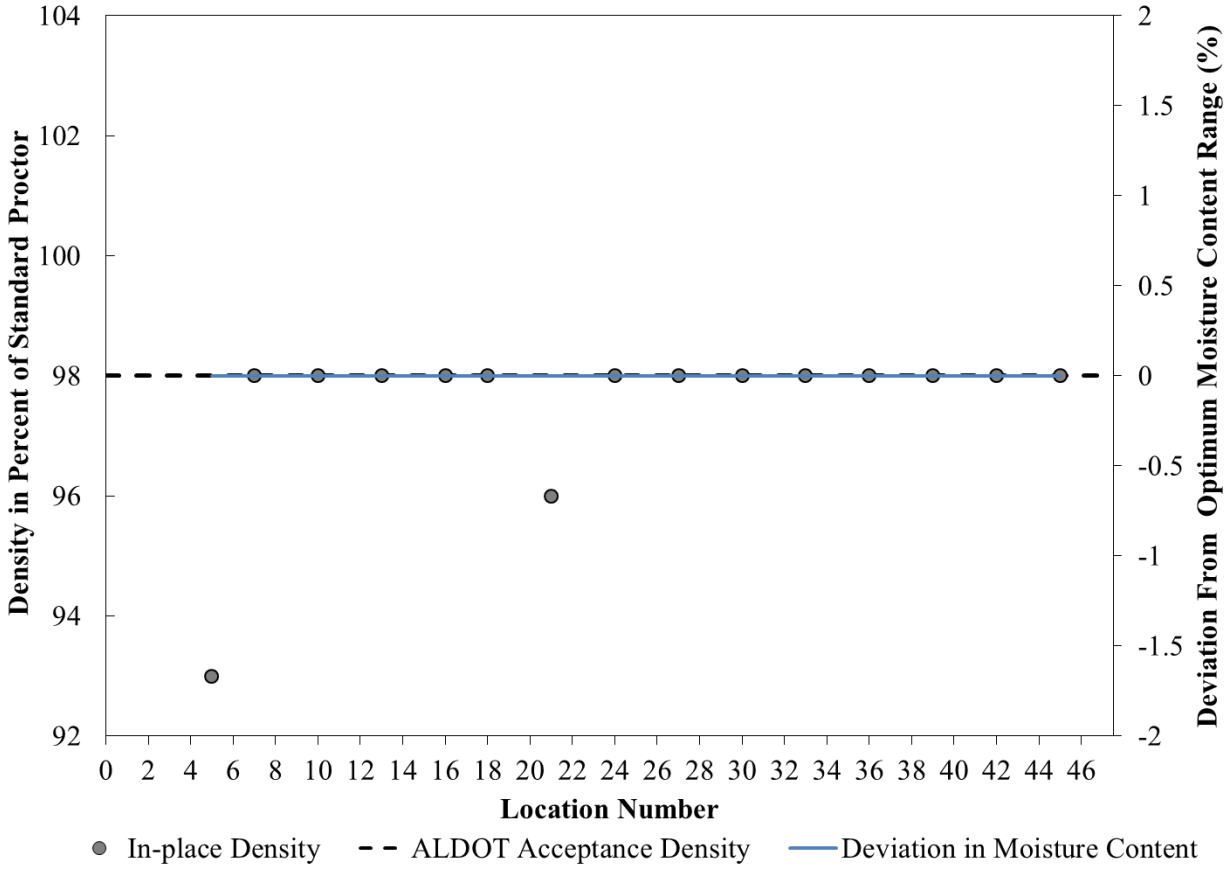

Figure 4.18: Density of the in-place soil cement base on U.S. Highway 84 in Elba, AL

4.8 Comparison of the Test Methods Evaluated

In this section, the results of each of the test methods evaluated during this research project are compared to each other. First the variability of each test method is compared against the variability of the other test method. Then an evaluation of the strength of the soil cement base in a section calculated using each of the test methods is presented and discussed. A section is

determined from the average of nine DCP tests, ten plastic-mold tests, and ten steel-mold cylinder tests. Then a location comparison of the strength of each test method is presented and discussed. This was explained in detail in Section 3.2.3.

4.8.1 Variability of Each Test Method

The variability of each test method was analyzed to determine which methods had the least amount of variability. The reason for this research project was the amount of variability that was encountered during post compressive tests of the specimens cored from the soil cement roadbed. Four different test methods were analyzed during this research project for their variability. Specimens for the steel-mold (SM) cylinder method developed by Wilson (2013) and the plastic-mold (PM) method by Sullivan et al. (2014) are made from material sampled at the project site during placement of the base, whereas the DCP test and cores tested in-place strengths. Figure 4.19 shows the average range in strength obtained from each test method. All the data presented in Figure 4.19 include outlier tests to fairly compare the variability of all these test methods.

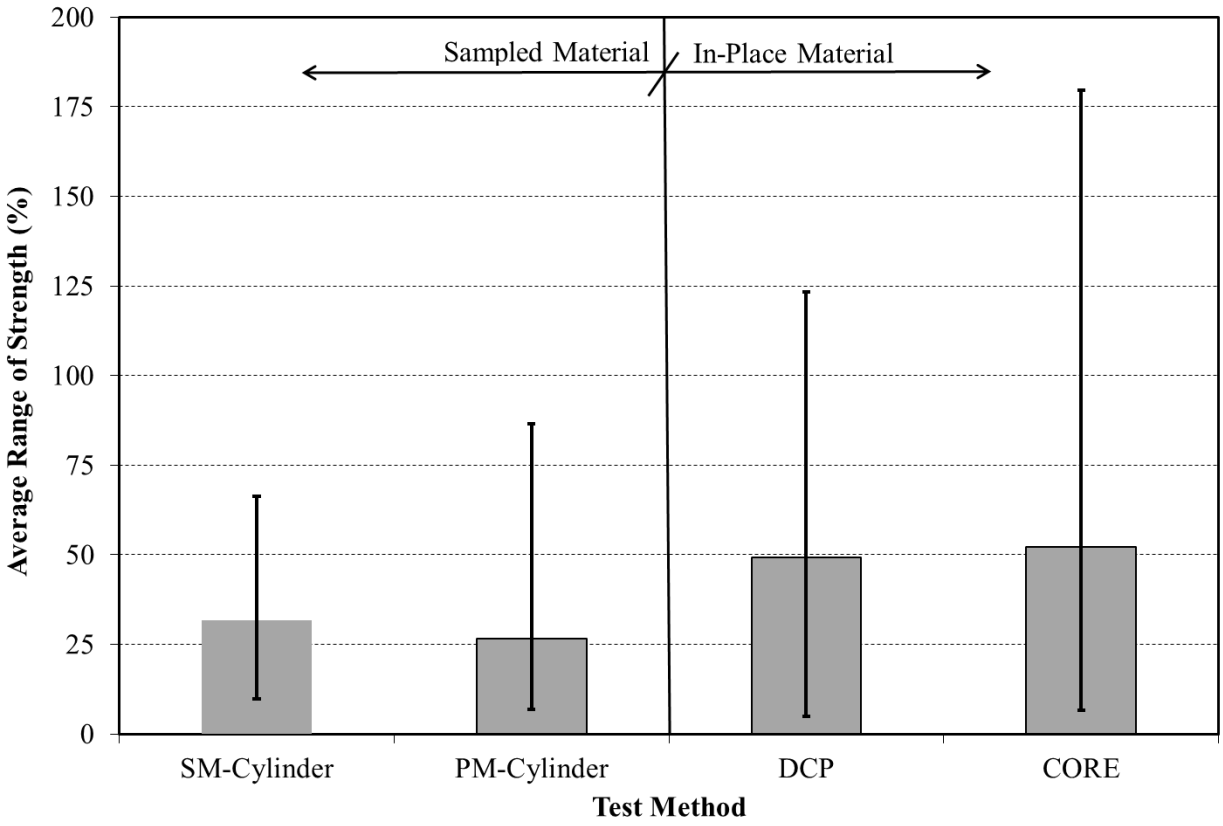

Figure 4.19: Range of strength using each test method

Plotted in Figure 4.19 is the average range of strength the test method produced over the entire project. The range was calculated by averaging the strength results determined at each testing location and identifying the maximum and minimum values. The average of all these results were determined for each test and plotted. In Figure 4.19 the range bars indicate the maximum range of test results and the minimum range of test results obtained for each test method. As expected, tests on sampled material produced smaller strength range values than tests performed on the in-place base. Figure 4.19 shows that the core results produced the largest variability in test results of the methods evaluated. The steel-mold cylinder and the plastic-mold cylinder tests have the least variability. The DCP produced the least amount of variability when comparing in-place strength assessment methods.

4.8.2 Section Comparison

As previously mentioned, ALDOT passes or fails soil cement mixtures based on seven-day core strengths for each 1/10 of a mile section of soil-cement. Section 3.2.3 discusses how each section was tested. The results plotted are an average over then entire 1/10 of a mile section for each set of three core tests, ten plastic mold tests, and nine DCP tests. Figure 4.20 shows the relationship between the test method evaluated and ALDOT current standard strength measurement. Therefore, in this evaluation the core strength were used as the control sample and each of the other methods were compared to the core results. It should be noted that steel-mold cylinder method developed by Wilson (2013) was not compared to the other methods because of the low strength values the method produced as shown in Section 4.3.

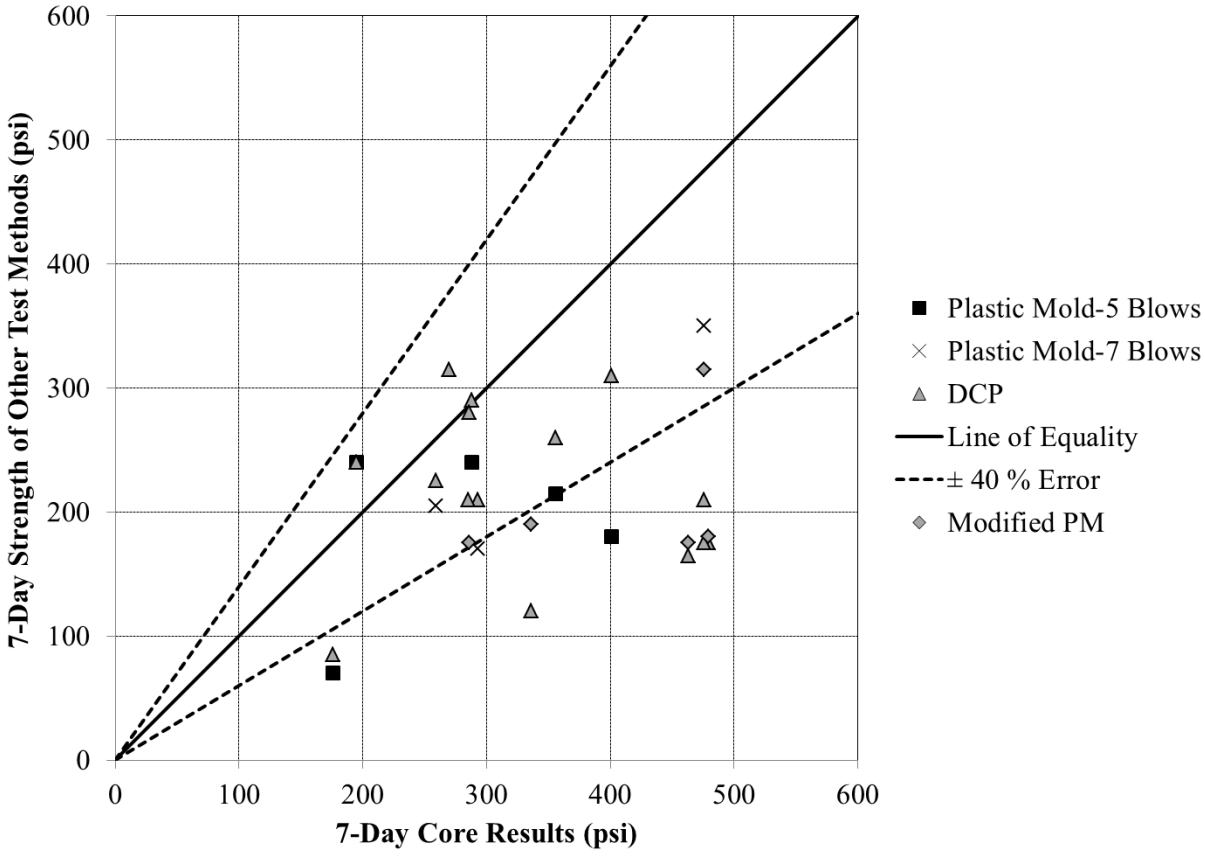

Figure 4.20: Core results versus all other strength test methods evaluated

Figure 4.20 shows that most of the data fell below line of equality. This is an indication that within a section the cores produced a higher strength than the plastic-mold method or the DCP. Plastic molds made with seven blows of a modified Proctor hammer were always weaker than core results within that section. A majority of the data fell within the ±40 percent error margins. Since the cores produced the most variable results and the reason for this research is to find a less variable test method to analyze the in-place strength of soil cement, the DCP was used as the control in Figure 4.21.

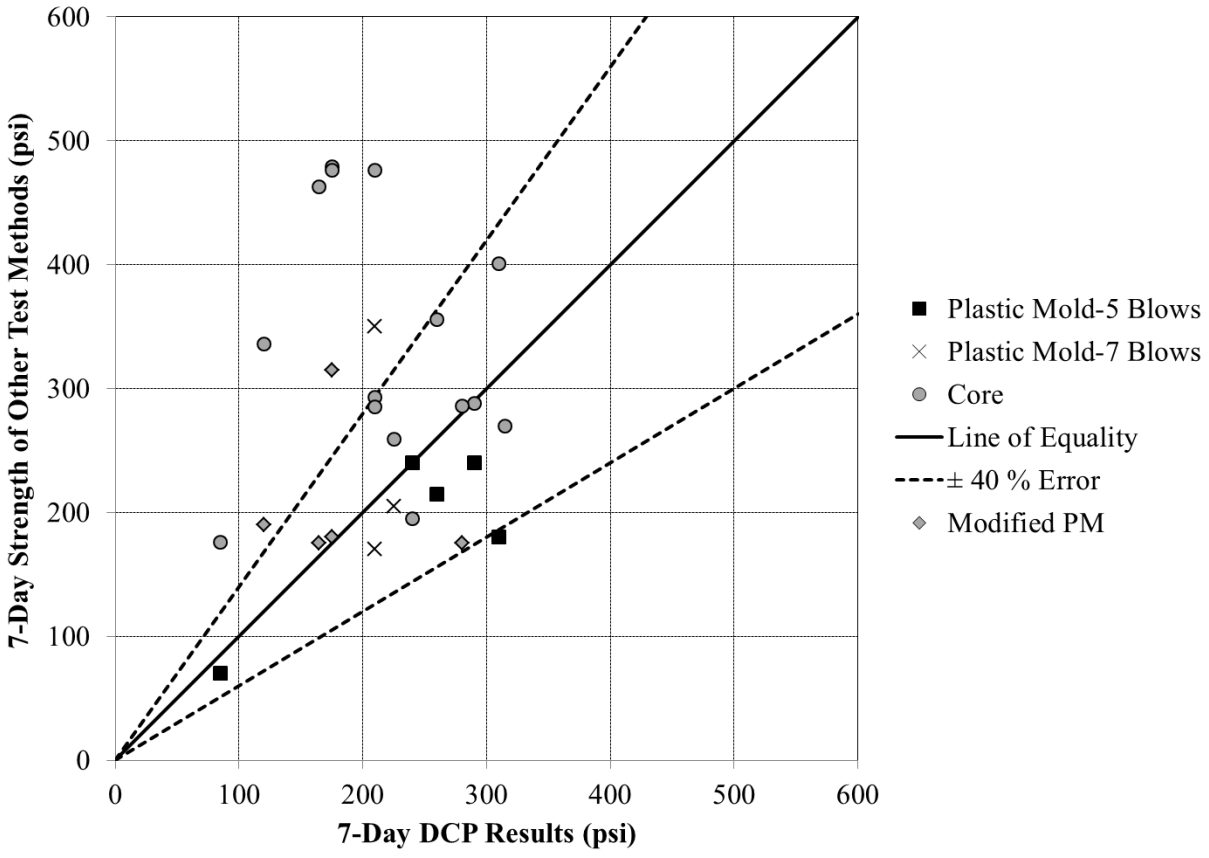

Figure 4.21: DCP results versus all other test methods evaluated

Figure 4.21 indicates a strong correlation between the plastic-mold method and the DCP within a test section. Concluded in the previous section, the majority of the core results produced higher values than the DCP within a test section. All but four results of the cylinder test method plastic-mold fell within the ±40 percent error margins plotted in Figure 4.21.

4.8.3 Location Comparison

Since the plastic-mold cylinder test method and DCP were performed at two locations within a section, they can be compared based on their matching test locations. At each location there were five plastic-mold cylinder tests made and three DCP tests conducted. Figure 4.22 shows the DCP as the control test method.

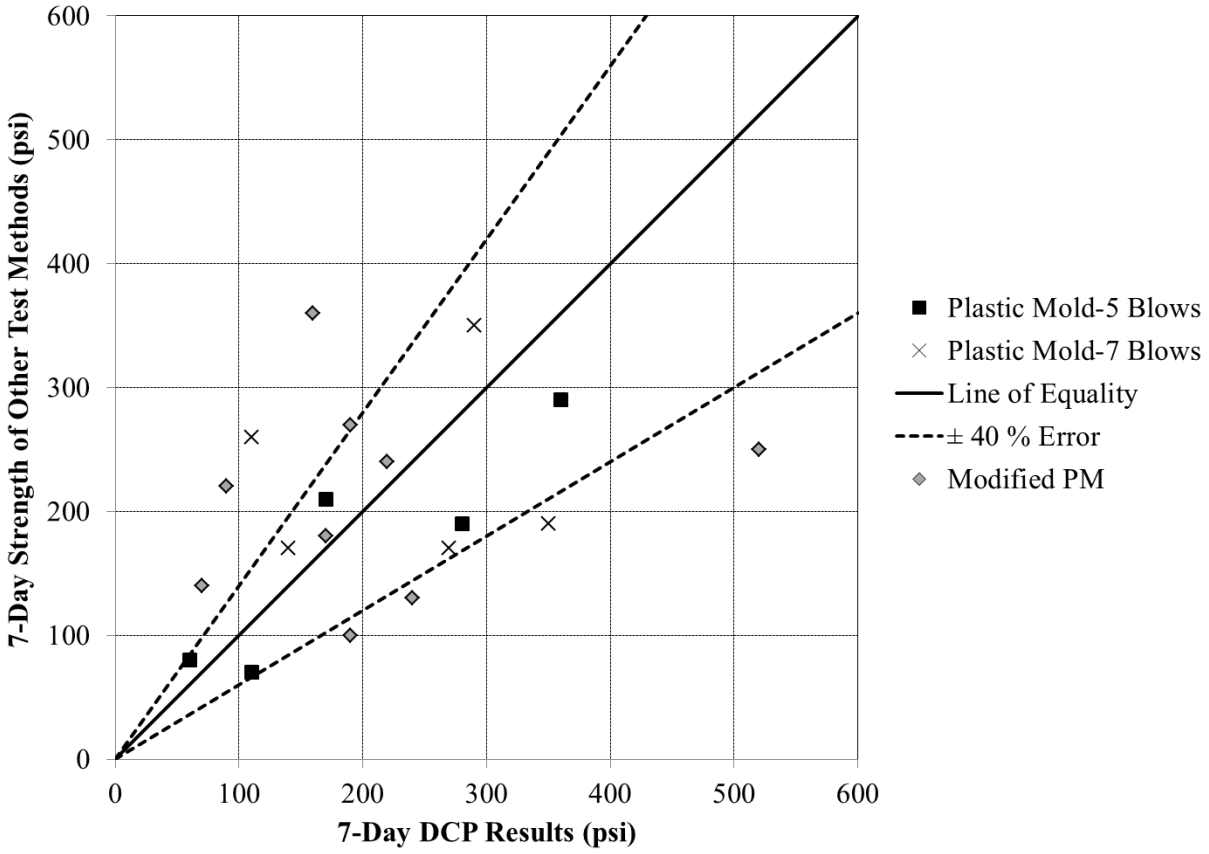

Figure 4.22: DCP results versus the plastic-mold method at each testing location

Figure 4.22 shows a comparison between the plastic-mold method and the DCP. When comparing the results one has to keep in mind that the PM cylinder test the strength of the soil cement mixed on-site, whereas, the DCP actually tested the strength of the in-place soil-cement base. Based on this, the average plastic-mold method and the DCP showed similar comparisons of strength.

Chapter 5

Summary, Conclusions, and Recommendations

5.1 Summary

Soil cement is a mixture of soil, portland cement and water that once compacted and cured can act as a strong, durable, frost-resistant pavement base layer. Soil-cement can be mixed in-place using on site materials or it can be mixed in a central plant using selected materials. A few advantages of using soil-cement base are that it (Halstad et al. 2006):

- Provides a stronger, stiffer base that reduces deflections due to traffic loads, delaying the onset of surfaces distress such as fatigue cracking which extends pavement life,
- Eliminates the need to haul in expensive select granular aggregates by using a wide variety of in-situ soils,
- Reduces rutting due to the resistance of consolidation and movement of the cement stabilized base, and
- Provides a durable, long-lasting base in all types of climates, designed to resist damaged caused by cycles of wetting and drying and freeze-thaw conditions

Although there are advantages to using soil-cement, variability among core strength data used to assess the in-place strength for quality assurance base has led to questions concerning the most appropriate method to test this important property. Therefore the goal of this research project was to develop a method to reliably asses the strength of soil-cement base. Is it plausible to use field-molded samples such as steel-mold cylinders (Wilson 2013) or plastic-mold cylinders (Sullivan et al. 2014) from quality assurance tests to evaluate the strength of soil-cement base? Or should the in-place strength of the soil cement base be tested using the DCP

method (ASTM D 6951 2009) of evaluating the strength of soil cement presented by Nemiroff (2016)?

During this research project, several test methods were evaluated to assess the strength of soil cement base. The molded cylinder method by Wilson (2013) and the plastic mold method by Sullivan (2014) were evaluated as controls in order to determine the strength of soil cement. The dynamic cone penetrometer method by Nemiroff (2016) and the standard ALDOT compression testing of cores method were evaluated as in-place strength measures of the soil cement base. Approximately 155 steel-mold cylinders and 110 plastic-mold cylinders were made and tested over the course of this research project. There were 45 core compressive strength test evaluated and 123 DCP tests, totaling 10,263 hammer blows were conducted on U.S. Highway 84 soil-cement project in Elba, Alabama.

5.2 Conclusions

The research yielded the following key findings:

- The steel-mold cylinder test method (Wilson 2013) is neither a practical nor accurate test to be performed in the field. Due to the amount of time it takes to determine the water content and desired weight of the test specimens. This method also consistently produced strengths lower than any of the other methods evaluated in this study. The method should only be used in the laboratory where the moisture-density relationship of the soil cement is known for the specific soil tested.
- The plastic-mold method (Sullivan et al. 2014) is a very simple to conduct and can be a viable option to determine the strength of soil-cement base.
- However, instead of drilling a hole in the bottom the plastic mold method should be modified by cutting a slit in the side of the plastic mold before the cylinder is made.

After the cylinder is made, it should be taped with metal foil tape to ensure no moisture escapes the specimen. This will allow for easier extrusion of the mold than the method Sullivan et al. (2014) recommended that produced extruded cylinders with extensive horizontal cracks.

- The dynamic cone penetrometer is able to efficiently penetrate mixed in-place soil cement bases in the field.
- Field data from the dynamic cone penetrometer shows that that the penetration of the soil cement is linear with depth up to 100 mm penetration or 5/8 of the 8 in. layer depth.
- The most efficient penetration depth of the dynamic cone penetrometer is 75 mm (3 in.) because it produces the efficient results, matches the findings Nemiroff (2016) made in the laboratory, provides less amount of technician effort than full-depth penetration, and penetrates exactly half of the soil cement layer after accurately seating of the DCP.
- The DCP versus strength equation recommended by Nemiroff (2016), shown in Section 2.5.2.2 Equation 2.5, should be used to evaluate the strength of soil-cement base with 75 mm (3 in.) of DCP penetration.
- The dynamic cone penetrometer is a more reliable test method to determine the in-place strength of soil-cement base compared to compression testing of cores, which is the standard practice that ALDOT currently uses to determine strength.

5.3 Recommendations

It is recommended that ALDOT implement a new testing procedure to assess the strength of soil-cement base. The recommendation from this research would be to use plastic-mold method by Sullivan et al. (2014)as modified in this study for mixture qualification in soil-cement base applications. The plastic-mold cylinder method would also be used as the initial test

in the field to assess the soil cement strength. Sections will still be passed or failed on a 1/10 of a mile stretch of soil cement, and it is recommended that this be based on DCP test results. The process would include picking one random location and make three specimens with the modified plastic-mold cylinder method during the placement of the soil-cement base. Next, the cylinders should be placed in a shaded area, free of rain or any other contamination, and allowed to cure on site for 24-hours before they are transported to the laboratory for final curing and testing. After the molds are transported back to the laboratory, they should be sealed in a plastic bag while still in their plastic molds, all the air shall be removed from the bag, and placed in a moist-curing room or curing tank for final curing. The plastic-mold specimens shall be removed from the bag and the plastic mold tested using a compression machine on the seventh day. The average of the three compression tests on plastic mold specimens shall be used as indicator of the strength of the soil cement mixed on-site. . If the plastic-mold cylinder strength results fall between 250 and 600 psi, full pay shall be awarded. If the cylinder strength falls below 250 psi or above 600 psi, dynamic cone penetrometer tests shall be conducted on the soil-cement base section from which these cylinders were made. When conducting dynamic cone penetrometer test, three random locations shall be picked by the Engineer. Three DCP test shall be conducted at each of the three random locations chosen, penetrating 75 mm (3 in.) into the soil cement layer once the DCP is properly seated 25 mm (1 in.) in the soil-cement base, and the data should be processed as discussed in Section 4.2.2 to insure there are not any outliers among the DCP tests at a location. Once this is done, the average DCP strength of the three locations shall be taken as the strength of the soil cement base using Nemiroff (2016) equation shown in Section 2.5.2.2 Equation 2.5. If the strength falls with 250 psi to 600 psi full pay shall be awarded. If the strength falls with 200 to 250 psi or 600 to 650 psi pay reduction shall be incorporated following Equations 1.1 and 1.2.

If the strength falls under 200 psi or over 650 psi, the section of soil-cement base shall be removed and replaced at the expense of the contractor.

A recommendation for future work would be to confirm that the DCP to strength relationship recommended by Nemiroff (2016) is applicable for the plastic-mold cylinder test method. A strong correlation between laboratory made molded cylinders and the dynamic cone penetrometer was found by Nemiroff (2016). A correlation between the steel-mold cylinder method and the plastic-mold method can be done by making both types of cylinders in the lab from the same uniformly mixed soil cement and tested for strength on the same day. Another recommendation would be to test the dynamic cone penetrometer using different soil types to ensure that the strength of the soil cement base is independent of the soil type used during construction.

References

AASHTO T 22. 2010. Standard Test Method for Compressive Strength of Cylindrical Concrete Specimens. *AASHTO - Standard Specifications for Transportation Materials and Methods of Sampling and Testing,* American Association of State Highway and Transportation Officials, Washington, DC.

AASHTO T 134. 2013. Standard Method of Test for Moisture-Density Relations of Soild-Cement Mixtures. *AASHTO - Standard Specifications for Transportation Materials and Methods of Sampling and Testing,* American Association of State Highway and Transportation Officials, Washington, DC.

ACI 230. 2009. *Report on Soil Cement*. (ACI 230.1R-09), American Concrete Institute, Farmington Hills, MI.

Alabama Department of Transportation. 2012. *Standard Specifications for Highway Construction*. Alabama Department of Transportation.

ALDOT 304. 2014. *Soil-Cement*. Alabama Department of Transportation, Special Provision No. 12-1167.

ALDOT 419. 2008. *Extracting, Transporting, and Testing Core Samples from Soil-Cement*. Alabama Department of Transportation.

Ashan, Ahmed. 2014. “Pavement Performance Monitoring Using Dynamic Cone Penetrometer and Geogauge During Construction.” Masters Thesis, The University of Texas at Arlington.

ASTM C 39. 2016. *Standard Test Method for Compressive Strength of Cylindrical Concrete Specimens*. ASTM International. West Conshohocken, PA.

ASTM C 470. 2015. *Standard Specification for Molds for Forming Concrete Test Cylinders Vertically.* ASTM International, West Conshohocken, PA.

ASTM C 670. 2010. *Standard Practice for Preparing Precision and Bias Statements for Test Materials for Construction Materials*. ASTM International. West Conshohocken, PA.

ASTM D 558. 2004. *Standard Test Methods for Moisture-Density (Unit Weight) Relations of Soil-Cement Mixtures.* ASTM International. West Conshohocken, PA.

ASTM D 559. 2015. *Standard Test Method for Wetting and Drying Compacted Soil-Cement Mixtures*. ASTM International. West Conshohocken, PA.

ASTM D 560. 2015. *Standard Test Methods for Freezing and Thawing Compacted Soil-Cement Mixtures*. ASTM International. West Conshohocken, PA.

ASTM D 698. 2007. Standard Test Methods for Laboratory Compaction Characteristics of Soil Using Standard Effort. *ASTM International*. West Conshohocken, PA.

ASTM D 1556. 2015. *Standard Test Method for Density and Unit Weight of Soil in Place by Sand-Cone Method.* ASTM International. West Conshohocken, PA.

ASTM D 1632. 2007. *Standard Practice for Making and Curing Soil-Cement Compression and Flexure Test Specimens in the Laboratory*. ASTM International. West Conshohocken, PA.

ASTM D 1633. 2007. *Standard Test Methods for Compressive Strength of Molded Soil-Cement Cylinders*. ASTM International. West Conshohocken, PA.

ASTM D 2167. 2015. *Standard Test Method for Density and Unit Weight of Soil in Place by the Rubber Balloon Method.* ASTM International. West Conshohocken, PA.

ASTM D 2922. 2005. *Standard Test Methods for Density of Soil and Soil-Aggregate in Place by Nuclear Methods (Shallow Depth).* ASTM International. West Conshohocken, PA .

ASTM D 3017. 2005. *Standard Test Methods for Water Content of Soil and Rock in Place by Nuclear Methods (Shallow Depth).* ASTM International. West Conshohocken, PA.

ASTM D 4735. 2015. *Standard Guide for Evaluating, Selecting, and Specifying Balances and Standard Masses for Use in Soil, Rock, and Construction Materials Testing.* ASTM International. West Conshohocken, PA.

ASTM D 4959. 2007. *Standard Test Method for Determination of Water (Moisture) Content of Soil By Direct Heating.* ASTM International. West Conshohocken, PA.

ASTM D 6951. 2009. *Standard Test Method for Use of the Dynamic Cone Penetrometer in Shallow Pavement Applications.* ASTM International. West Conshohocken, PA.

Enayatpour, Saeid, Anand J. Puppala, and Hariharan Vasudevan. 2006. "Dynamic Cone Penetrometer to Evaluate Unconfined Compressive Strength of Stabilized Soils." *Geotechnical Special Publication,* American Society of Civil Engineers, pp.285-292.

Felt, E. J. 1955. "Factors Influencing Physical Properties of Soil-Cement Mixtures." *Bulletin No. 108,* Highway Research Board, Washington, D.C., pp. 138-162.

Federal Highway Administration (FHWA). 1979. *Soil Stabilization in Pavement Structures: A User's Manual,* V.2. Report No. FHWA-IP-80-2, Washington, DC.

George, K.P. and W. Uddin. 2000. *Subgrade Characterization for Highway Pavement Design Final Report,* Mississippi Department of Transportation, Jackson, MS.

George, K.P. 2002. “Minimizing Cracking in Cement-Treated Material for Improved Performance.” *Research and Development Bulletin RD123,* Portland Cement Association. Skokie, IL.

Google Maps. 2017. https://www.google.com/maps/

Halsted, G.E., Luhr, D.R., Adaska, W.S. 2006. *Guide to Cement-Treated Base (CTB). Portland Cement Association.* Skokie, IL.

Halsted, G.E., Adaska, W. S., McConnell, W. T. 2008. *Guide to Cement-Modified Soil (CMS).* Portland Cement Association. Skokie, IL.

Hassan, A.B. 1996. “The Effects of Material Parameters on Dynamic Cone Penetrometer Results for Fine-Grained Soils and Granular Materials.” PhD diss., Oklahoma State University.

Holtz, R.D., Kovacs, W.D., 1981. *An Introduction to Geotechnical Engineering*. 1st Edition, Englewood Cliffs, NJ: Prentice Hall.

Huntley, S.L. 1990. “Use of a dynamic penetrometer as a ground investigation and design tool in Hertfordshire.” *Field Testing in Engineering Geology*. Geological Society Engineering Geology Special Publications No. 6.

Kleyn, E.G. and P.E. Savage. 1982. “The Application of the Pavement DCP to Determine the Bearing Properties and Performance of the Road Pavements”. *International Symposium on Bearing Capacity of Roads and Airfields*, Trondheim, Norway.

Kuhlman, R. H., 1994. Cracking in Soil Cement-Cause, Effect, and Control. *Concrete International*, pp. 56-59.

McElvaney, J. and IR. Bunadi Djatnika. 1991. “Strength Evaluation of Lime-Stabilized Pavement Foundations Using the Dynamic Cone Penetrometer.*”* *Australian Road Research*, Vol. 21, No. 1, pp. 40-52.

Mohammadi, S.D., M. R. Nikoudel, H. Rahimi, and M. Khamechchiyan. 2008. “Application of the Dynamic Cone Penetrometer (DCP) for determination of the engineering parameters of sandy soils.” *Engineering Geology*, 101 (3): 195-203.

North Carolina Department of Transportation. 2013. *Chemical Stabilization QA Subgrade/Base Field Testing.* North Carolina Department of Transportation.

Nemiroff, J. 2016. “Strength Assessment of Soil Cement”. *Master’s Thesis*. Auburn University.

Patel, Mukesh A. and H.S. Patel. 2012. “Experimental Study to Correlate the Test Results of PBT, UCS, and CBR with DCP on Various Soils in Soaked Condition.” *International Journal of Engineering*, Vol. 6, Issue 5, pp. 244-261.

Portland Cement Association (PCA). 1971. “Soil Cement Laboratory Handbook.” *Engineering Bulletin*, Portland Cement Association. Skokie, IL.

Portland Cement Association (PCA). 1995. “Soil-Cement Construction Handbook.” Engineering Bulletin, *Portland Cement Association.* Skokie, IL.

Robbins, E.G., and Mueller P.E. 1960. “Development of a Test for Identifying Poorly Reacting Sandy Soils Encountered in Soil-Cement Applications.” Highway Research Board, *Bulletin 267*, pp.46-49.

Scala, A.J. 1956. “Simple Methods of Flexible Pavement Design Using Cone Penetrometer.” *N.Z. Eng.* 11 (2).

Shen, C.K. and J.K. Mitchell. 1966. “Behavior of Soil-Cement in Repeated Compression and Flexure.” Highway Research Board, *Highway Research Record*, No. 128. Washington, DC., pp. 68-100.

Sullivan, W, I. Howard, and B. Anderson. 2014. “Development of Equipment for Compacting Soil-Cement into Plastic Molds for Design and Quality Control Purposes.” 94th Annual Meeting of the Transportation Research Board.

Webster, S., R. Grau, and T. Williams. 1992. *Description and Application of Dual Mass Dynamic Cone Penetrometer*. Project AT40. US Army Corps of Engineers, Washington, DC.

West, G. 1959. "A Laboratory Investigation into the Effect of Elapsed Time After Mixing on the Compaction and Strength of Soil-Cement." *Geotechnique*, Vol. 9, No. 1, pp. 22-28.

Wilson, William Herbert Jr. 2013. Strength Assessment of Soil Cement. Master's Thesis, Auburn University.

Appendix A

Proctor Density Curve

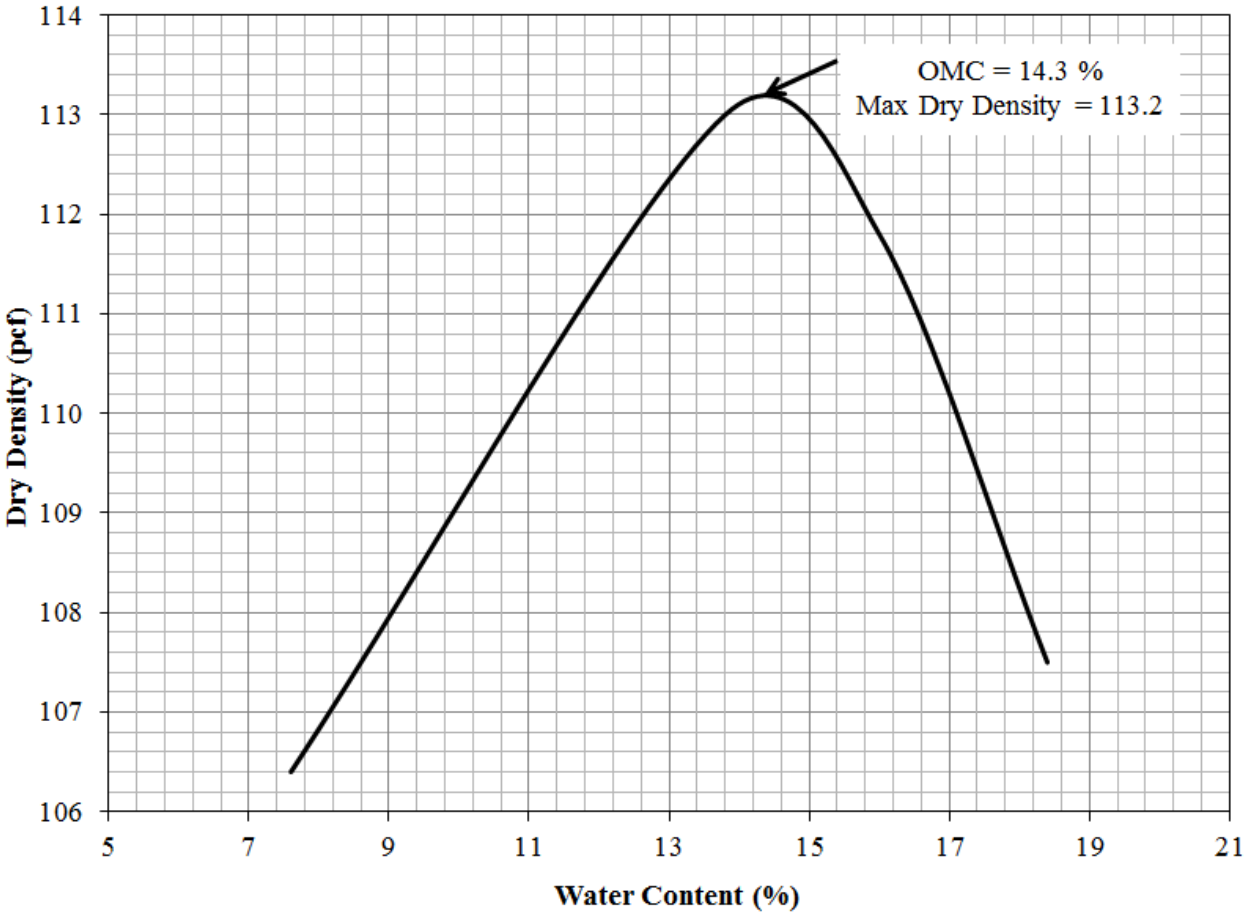

Figure A.1: Design curve used to construct molded cylinder method in the field

Appendix B

Plastic Mold Density Evaluation in the Laboratory

Table B.1: 5 blow evaluation

Cylinder No.	D (in)	H (in)	Weight (g)	Weight (lb)	Density (pci)	Wet Density (pcf)	Dry Density (pcf)	% Lab Density
1	3.0308	5.8520	1427.9	3.1480	0.0746	128.8	115.0	96
2	3.0223	5.8520	1474.8	3.2514	0.0774	133.8	119.5	100
3	3.0253	5.8453	1419.3	3.1290	0.0745	128.7	114.9	96
4	3.0303	5.8477	1420.3	3.1312	0.0742	128.3	114.6	95
5	3.0305	5.8760	1431.6	3.1561	0.0745	128.7	114.9	96

Table B.2: 7 blow evaluation

Cylinder No.	D (in)	H (in)	Weight (g)	Weight (lb)	Density (pci)	Wet Density (pcf)	Dry Density (pcf)	% Lab Density
1	3.0300	5.8663	1497.2	3.3008	0.0780	134.8	120.4	100
2	3.0313	5.8730	1477.2	3.2567	0.0768	132.8	118.6	99
3	3.0298	5.8713	1506.5	3.3213	0.0785	135.6	121.1	101
4	3.0258	5.8833	1504.1	3.3160	0.0784	135.4	120.9	101
5	3.0308	5.8693	1496.8	3.2999	0.0779	134.7	120.2	100

Table B.3: 9 blow evaluation

Cylinder No.	D (in)	H (in)	Weight (g)	Weight (lb)	Density (pci)	Wet Density (pcf)	Dry Density (pcf)	% Lab Density
1	3.0333	5.8823	1507.5	3.3235	0.0782	135.1	120.6	101
2	3.0308	5.8783	1505.3	3.3186	0.0783	135.2	120.7	101
3	3.0293	5.8620	1506.5	3.3213	0.0786	135.8	121.3	101
4	3.0342	5.8667	1492.8	3.2911	0.0776	134.1	119.7	100
5	3.0288	5.8507	1493.7	3.2930	0.0781	135.0	120.5	100

Appendix C

Summary of All the Strength Obtained from Different Test Methods

Table C.1: Test conducted on locations 1 through 8

Test Method	Location							
	1	2	3	4	5	6	7	8
	Compressive Strength (psi)							
Steel Mold	50	90	60	70	-	50	-	110
Plastic Mold	70	80	60	-	-	-	-	220
DCP	110	60	-	-	-	310	320	-
Core	-	-	-	-	176	-	270	-

Table C.2: Test conducted on location 9 through 16

Test Method	Location							
	9	10	11	12	13	14	15	16
	Compressive Strength (psi)							
Steel Mold	100	-	50	110	-	140	60	-
Plastic Mold	210	-	240	-	-	290	190	-
DCP	170	350	-	350	230	360	280	70
Core	-	356	-	-	288	-	-	195

Table C.3: Test conducted on locations 17 through 24

Test Method	Location							
	17	18	19	20	21	22	23	24
	Compressive Strength (psi)							
Steel Mold	80	-	60	100	-	90	90	-
Plastic Mold	170	-	190	350	-	-	170	-
DCP	270	-	350	290	130	-	140	200
Core	-	401	-	-	476	-	-	293

Table C.4: Test conducted on locations 25 through 32

Test Method	Location							
	25	26	27	28	29	30	31	32
	Compressive Strength (psi)							
Steel Mold	110	150	-	60	130	-	110	90
Plastic Mold	-	-	-	260	-	-	-	180
DCP	280	340	-	110	-	310	110	170
Core	-	-	259	-	-	285	-	-

Table C.5: Test conducted on locations 33 through 40

Test Method	Location							
	33	34	35	36	37	38	39	40
	Compressive Strength (psi)							
Steel Mold	-	80	150	-	90	110	-	190
Plastic Mold	-	-	220	-	130	270	-	360
DCP	180	170	90	160	240	190	-	160
Core	479	-	-	463	-	-	476	-

Table C.6: Test conducted on locations 41 through 46

Test Method	Location					
	41	42	43	44	45	46
	Compressive Strength (psi)					
Steel Mold	60	-	100	40	-	130
Plastic Mold	140	-	240	100	-	250
DCP	70	60	220	190	120	520
Core	-	336	-	-	286	-

Appendix D

25 mm Penetration

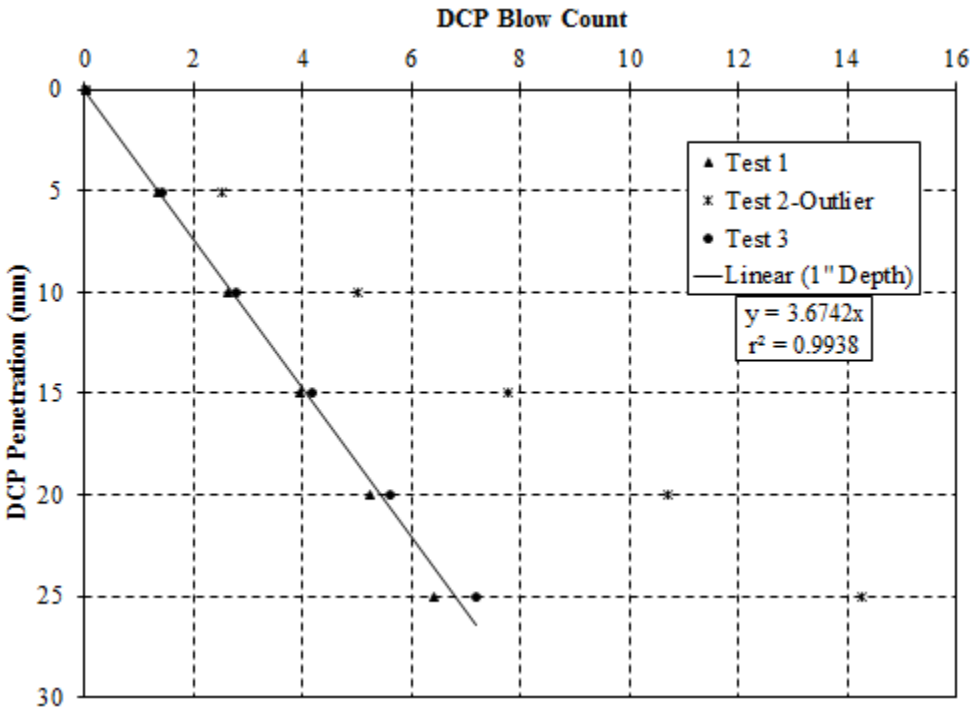

Figure D.1: Test conducted on November 1, 2016 Location 1 – compressive strength of 100 psi

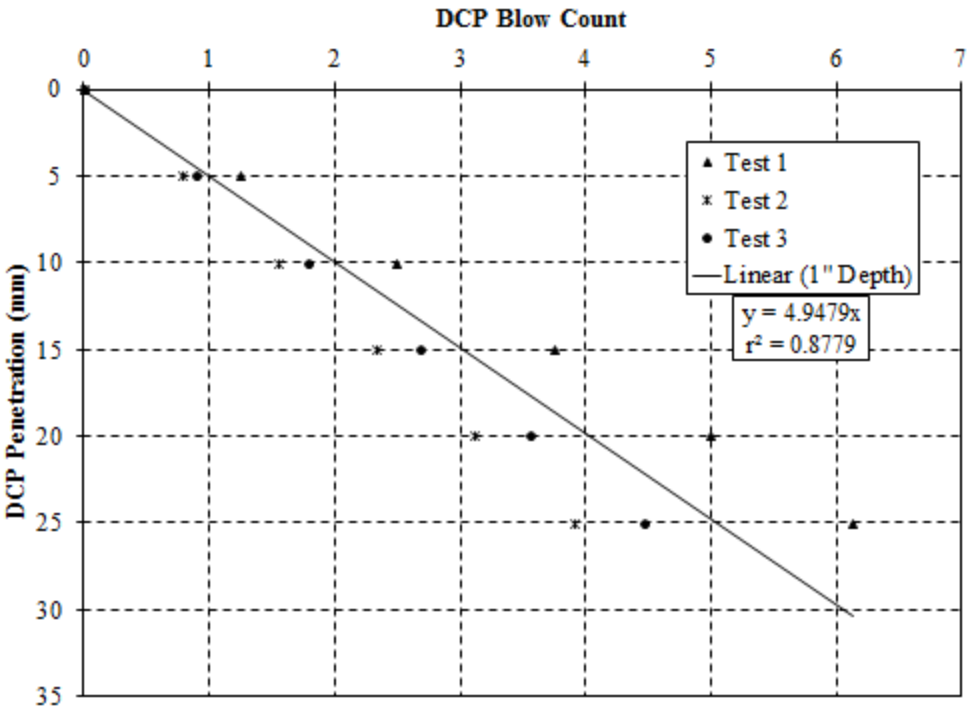

Figure D.2: Test conducted on November 1, 2016 Location 2 – compressive strength of 50 psi

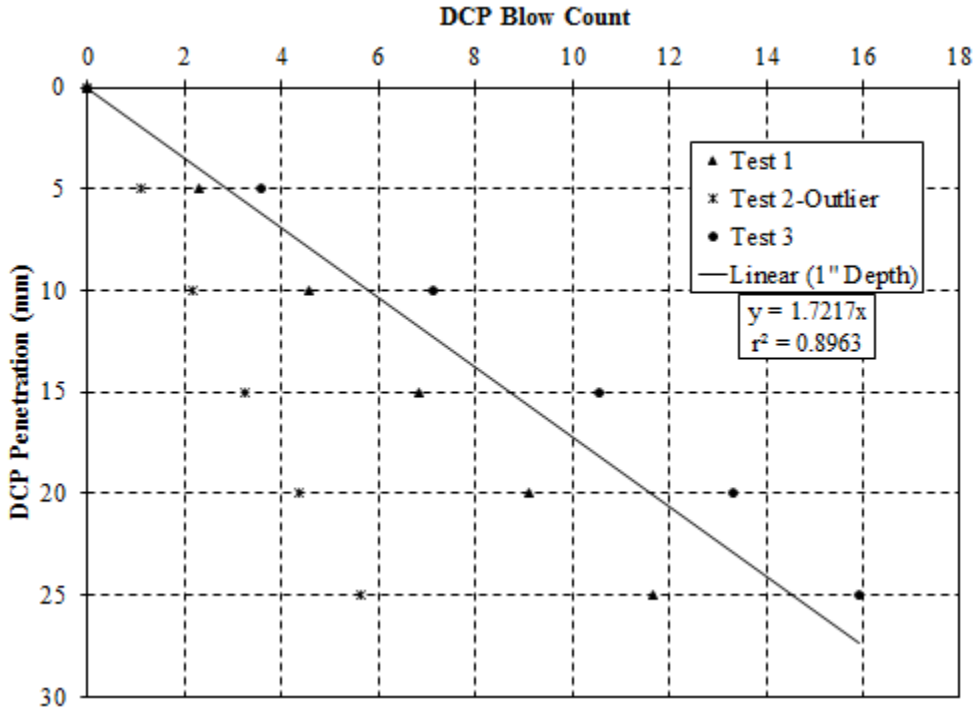

Figure D.3: Test conducted on November 7, 2016 Location 6– compressive strength of 320 psi

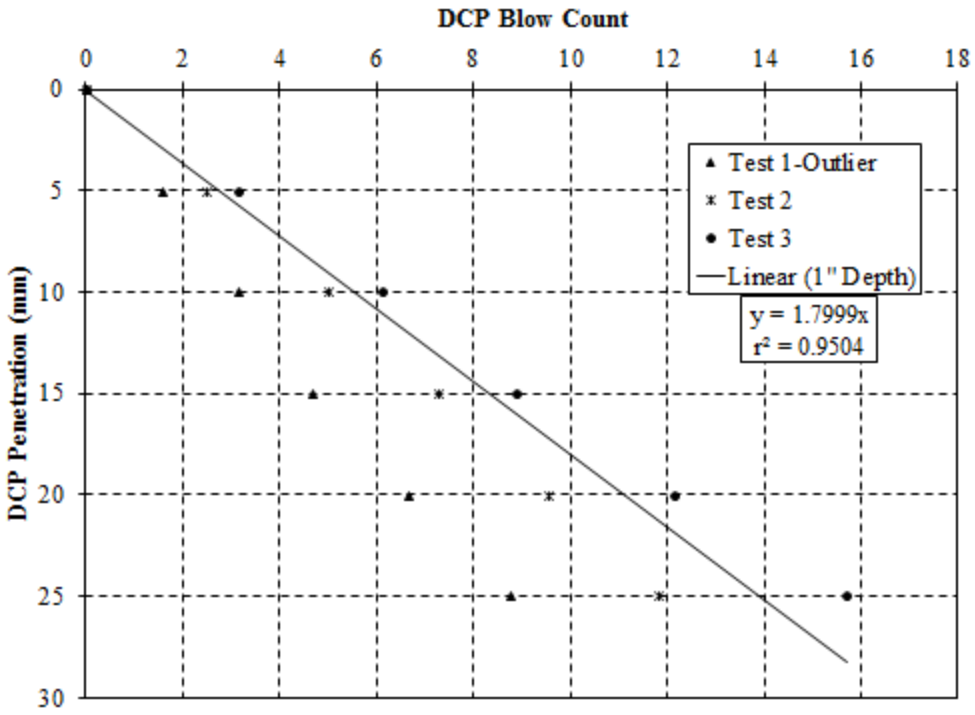

Figure D.4: Test conducted on November 7, 2016 Location 7– compressive strength of 310 psi

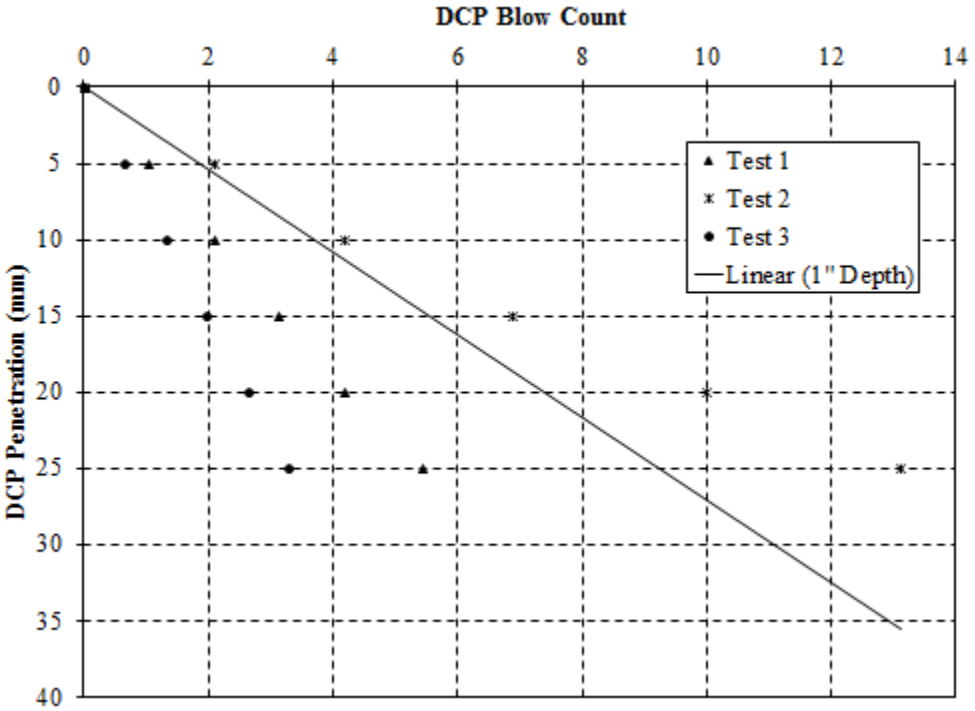

Figure D.5: Test conducted on November 22, 2016 Location 8 – range greater than 50%

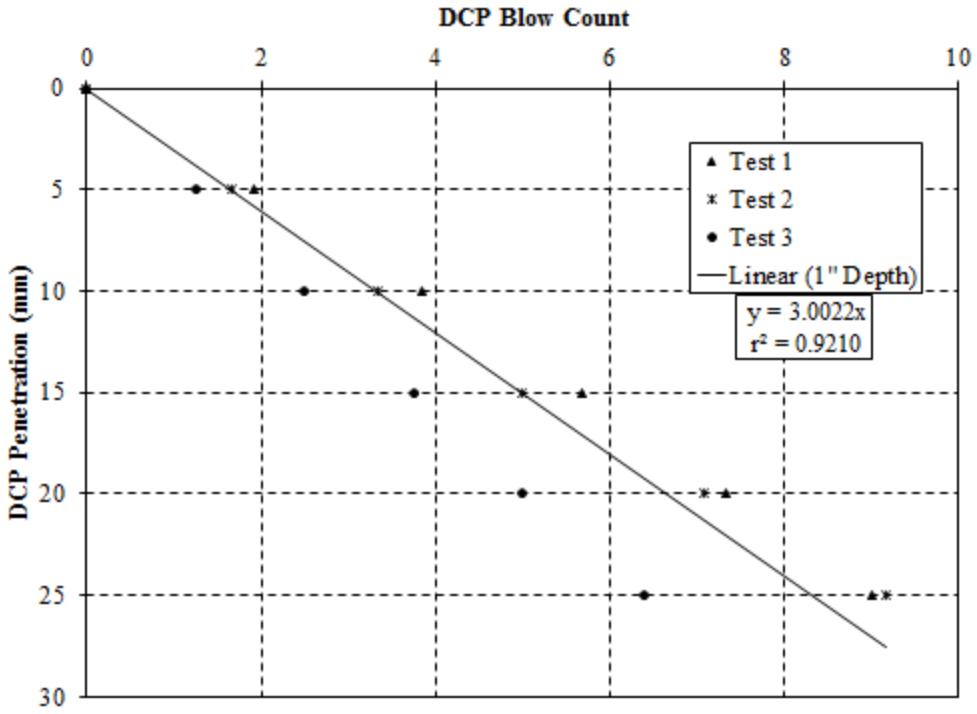

Figure D.6: Test conducted on November 22, 2016 Location 9 – compressive strength of 150 psi

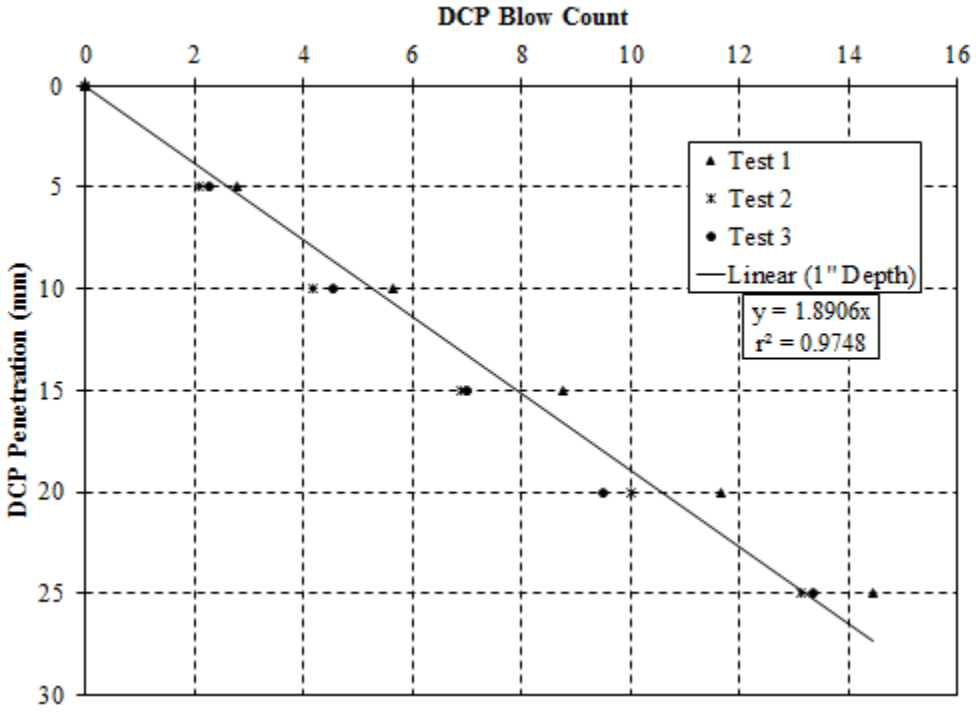

Figure D.7: Test conducted on November 22, 2016 Location 10–compressive strength of 290 psi

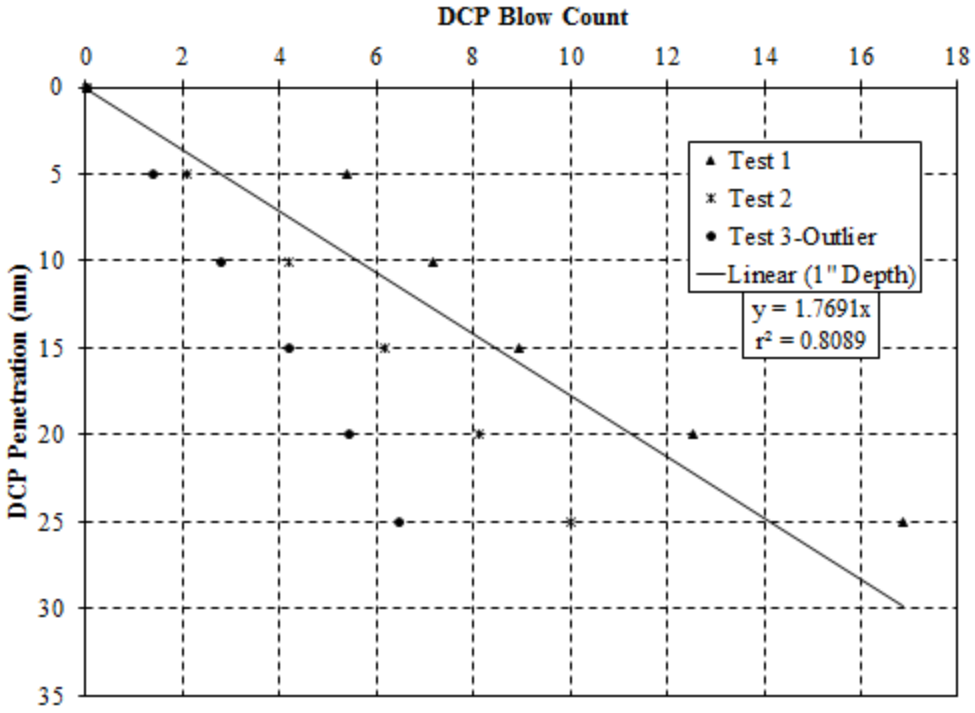

Figure D.8: Test conducted on November 22, 2016 Location 12–compressive strength of 310 psi

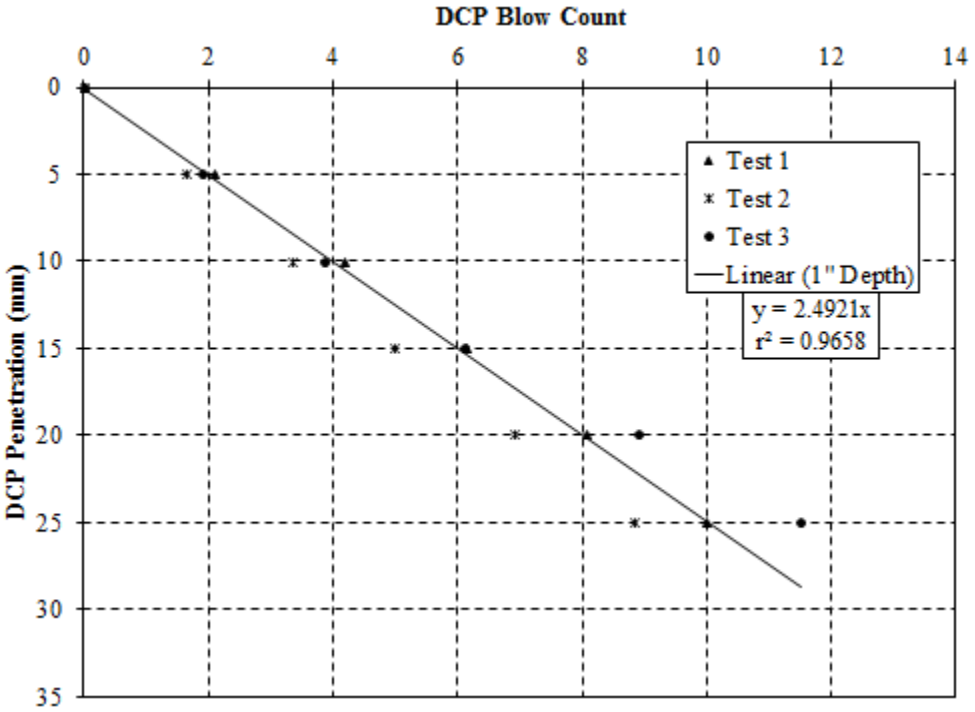

Figure D.9: Test conducted on November 22, 2016 Location 13–compressive strength of 200 psi

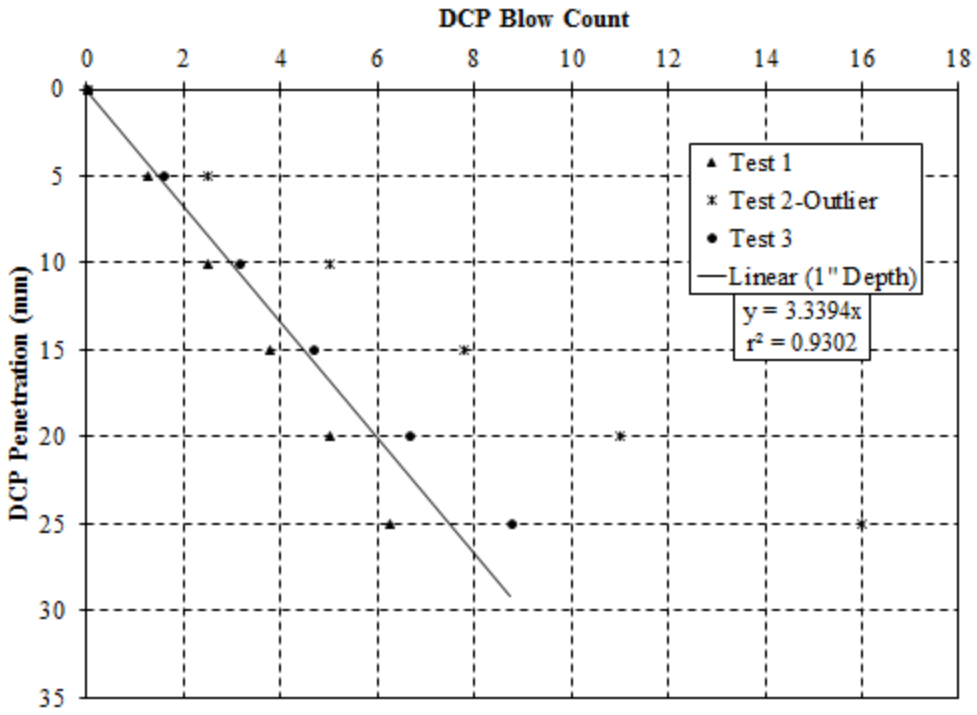

Figure D.10: Test conducted on November 23, 2016 Location 14–compressive strength of 120 psi

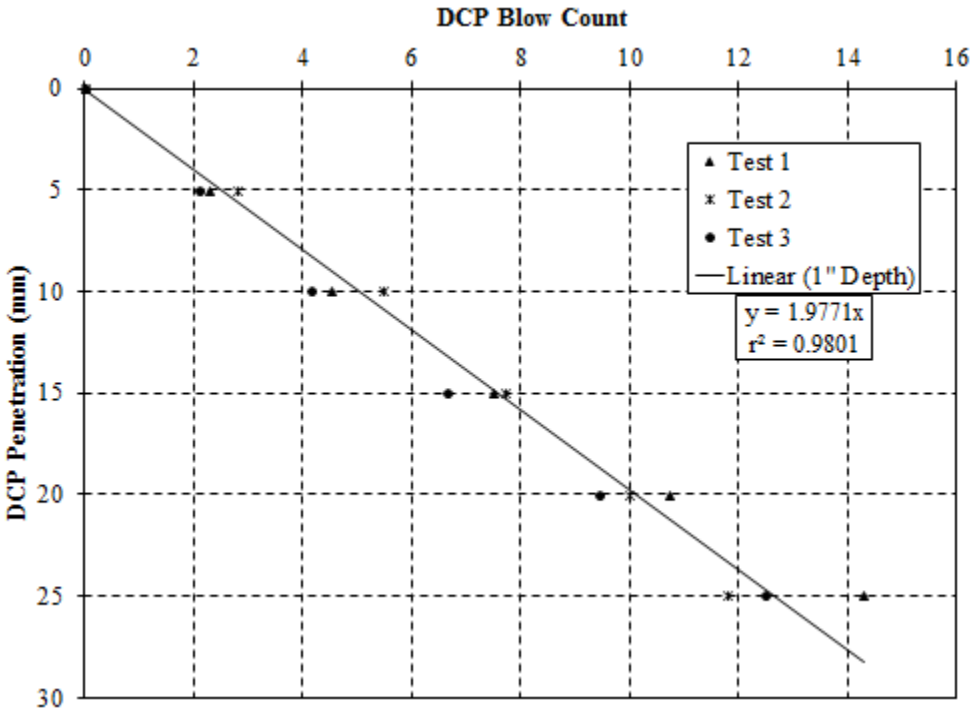

Figure D.11: Test conducted on November 23, 2016 Location 15–compressive strength of 270 psi

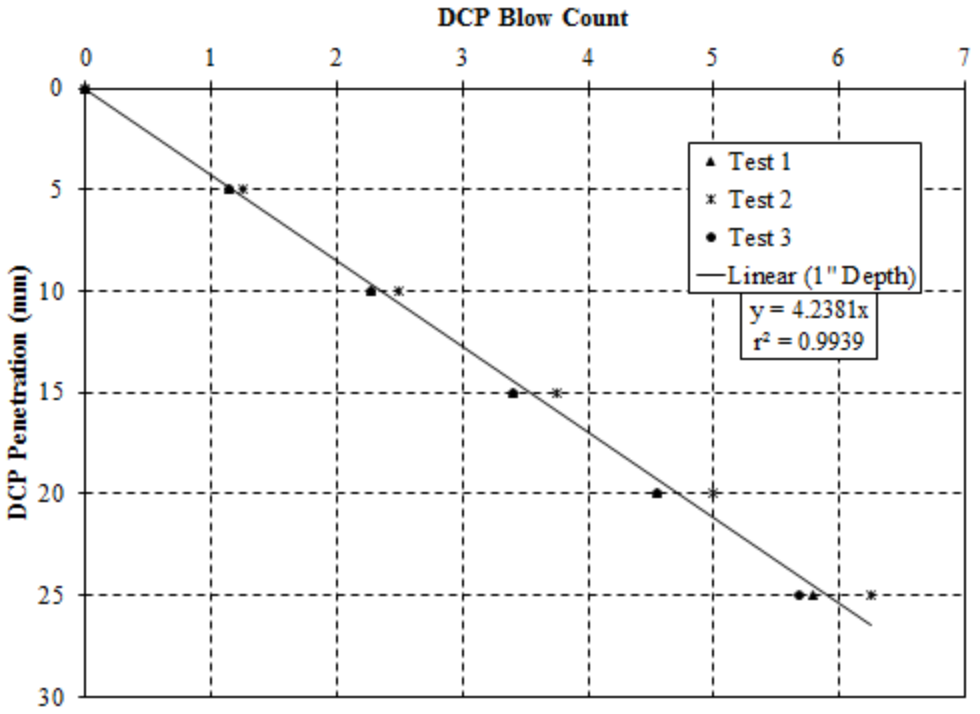

Figure D.12: Test conducted on November 23, 2016 Location 16–compressive strength of 70 psi

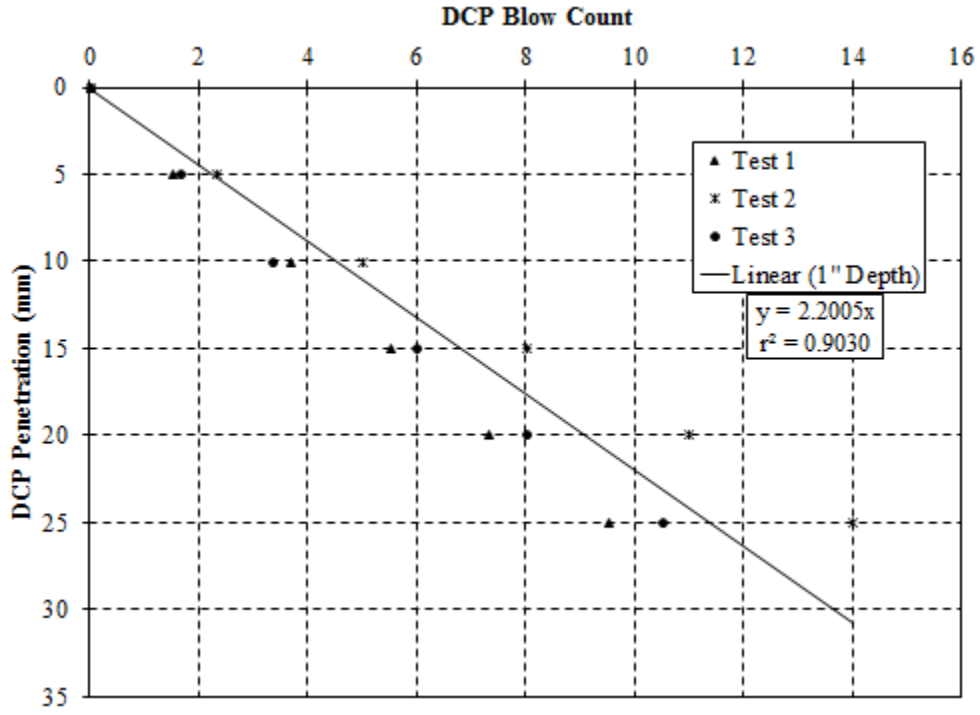

Figure D.13: Test conducted on March 23, 2017 Location 17 – compressive strength of 240 psi

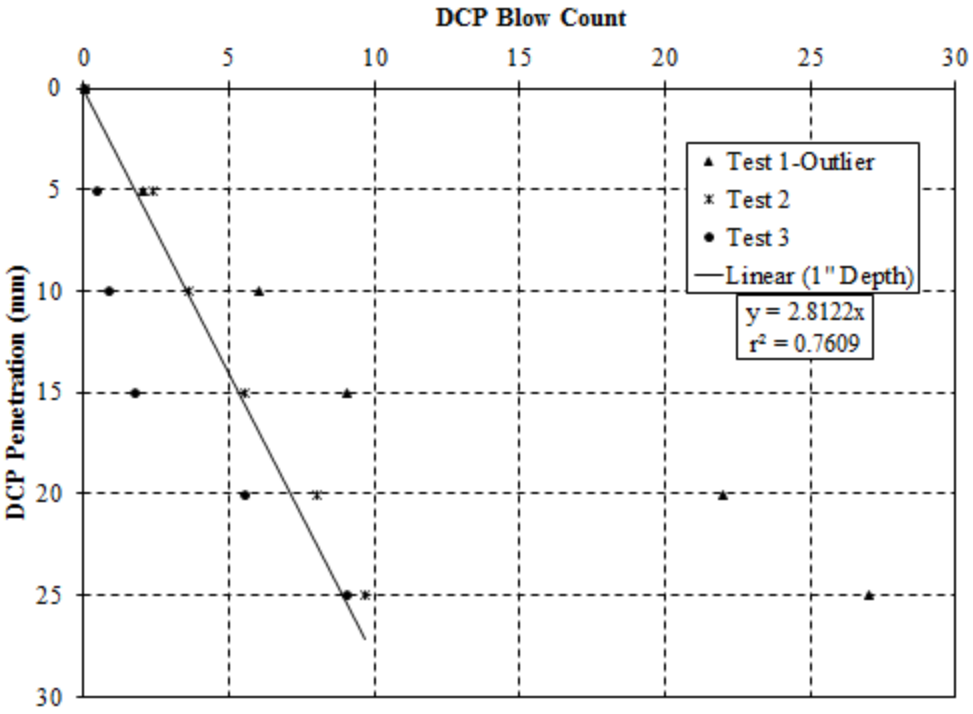

Figure D.14: Test conducted on March 23, 2017 Location 18 – compressive strength of 160 psi

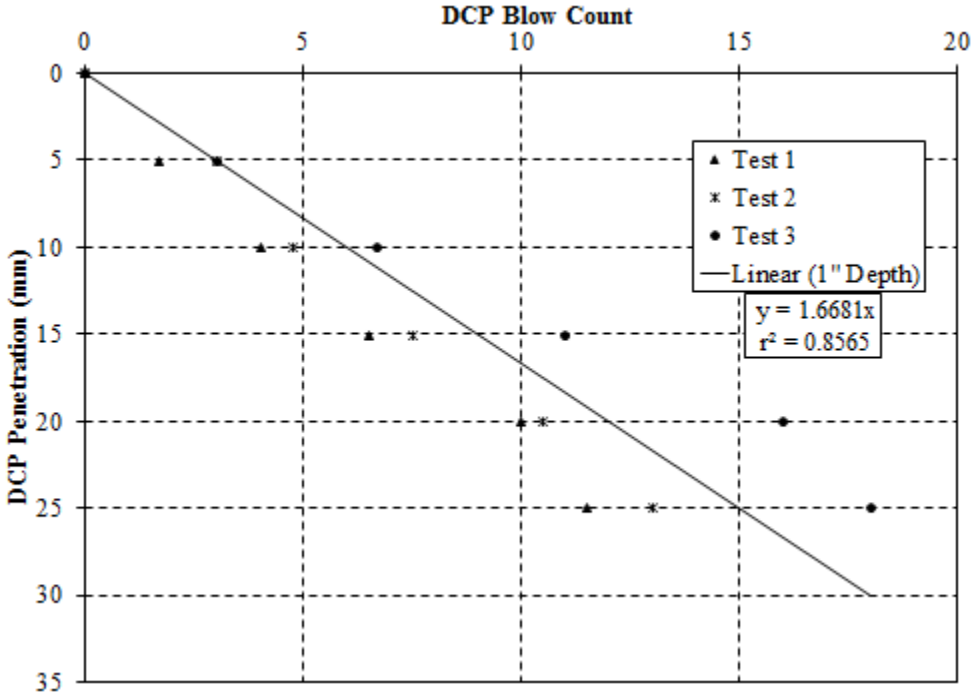

Figure D.15: Test conducted on March 23, 2017 Location 19 – compressive strength of 330 psi

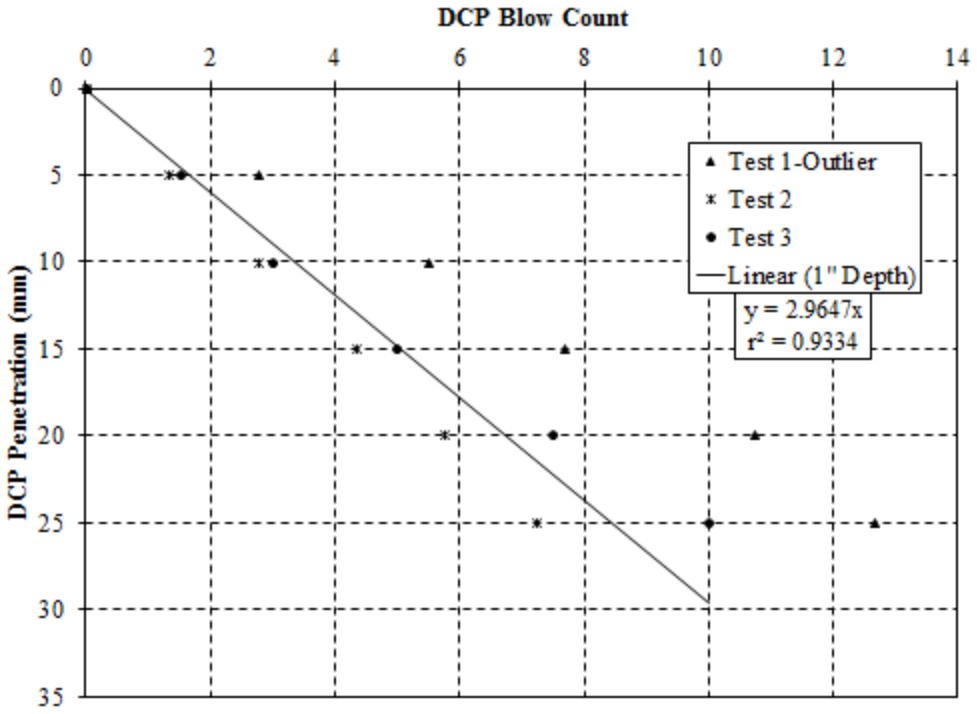

Figure D.16: Test conducted on March 27, 2017 Location 20– compressive strength of 150 psi

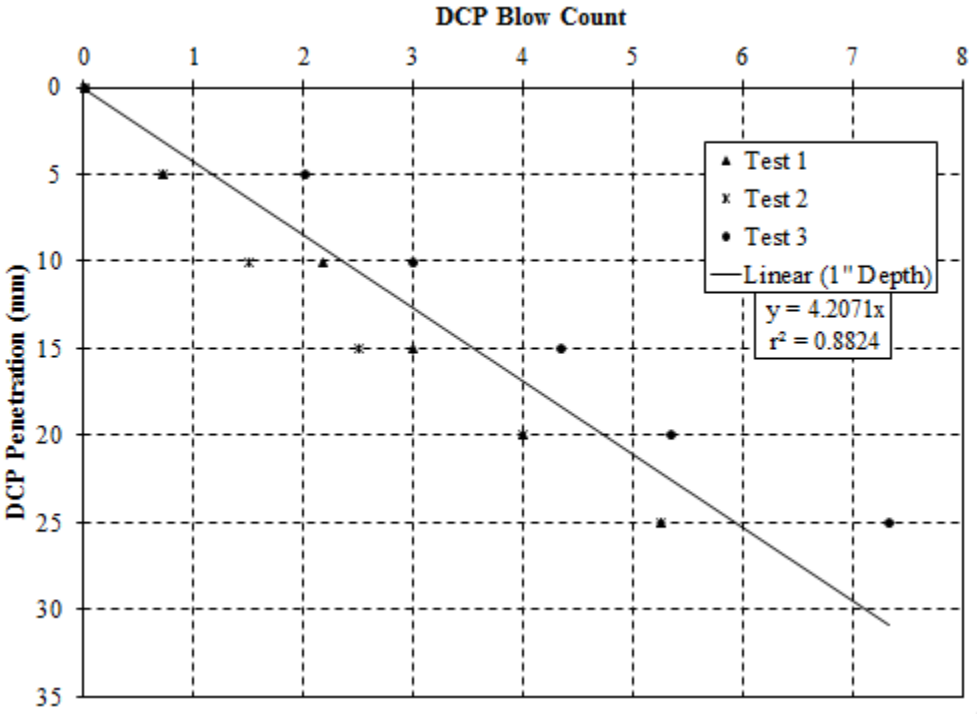

Figure D.17: Test conducted on March 27, 2017 Location 21– compressive strength of 70 psi

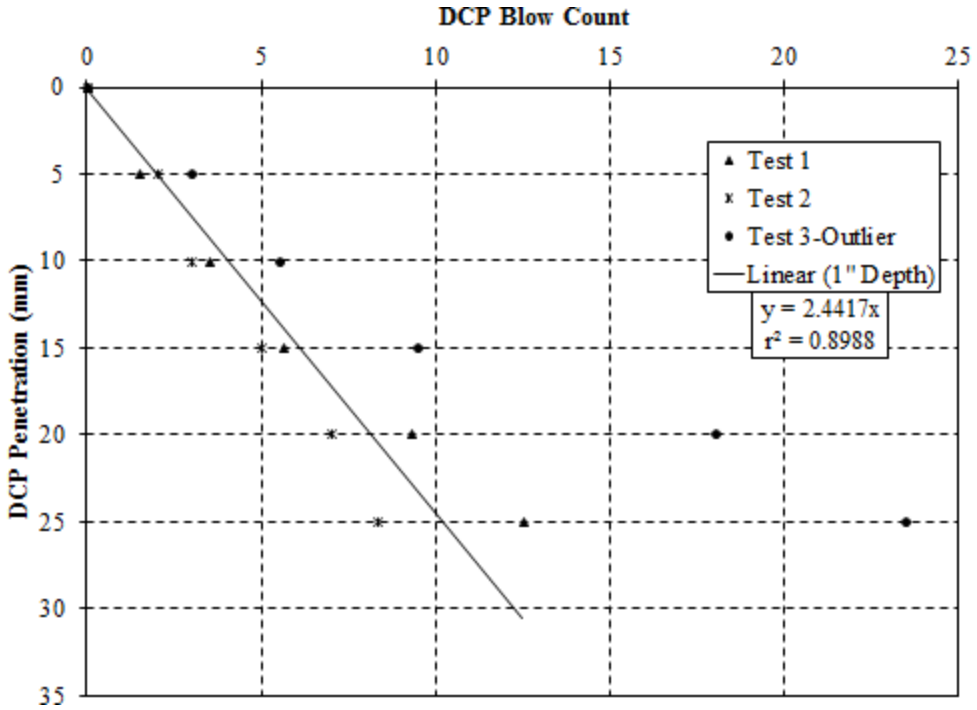

Figure D.18: Test conducted on March 27, 2017 Location 22 – compressive strength of 210 psi

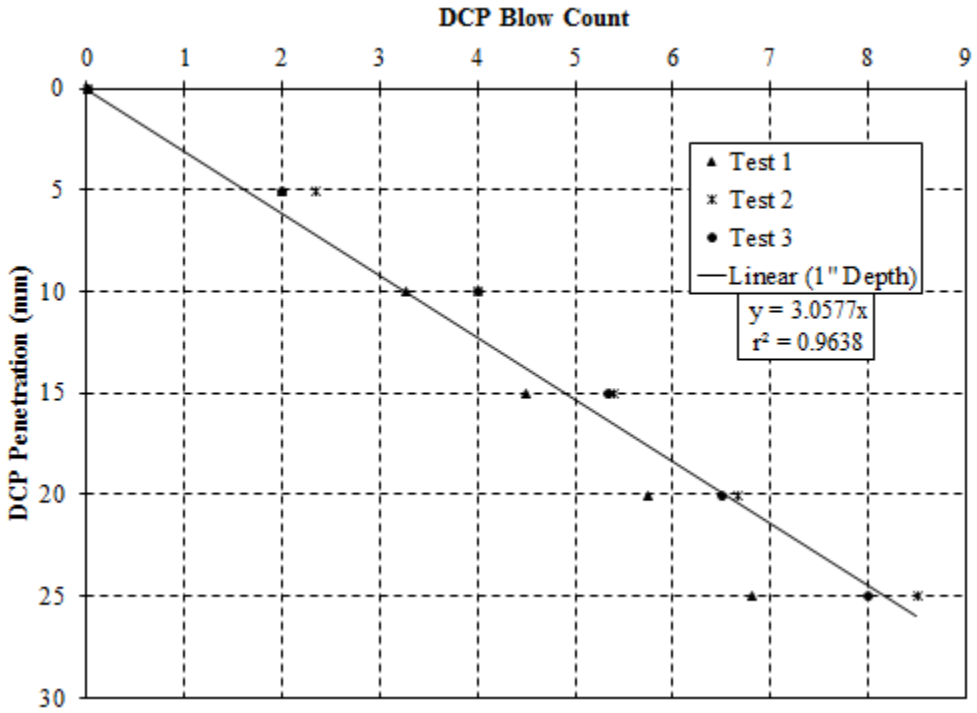

Figure D.19: Test conducted on March 30, 2017 Location 23 – compressive strength of 140 psi

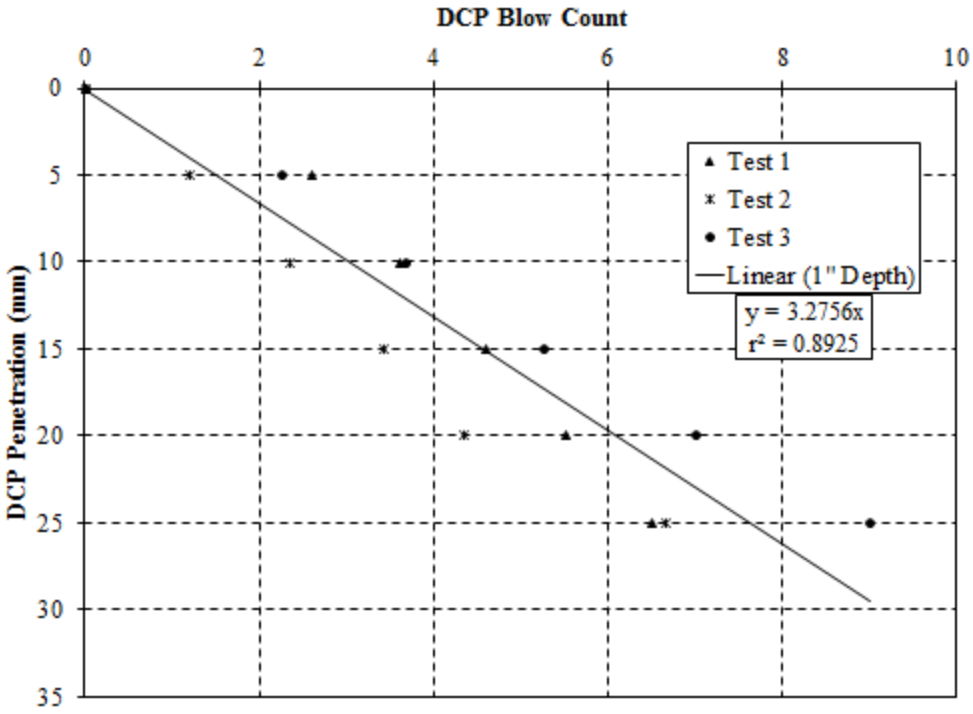

Figure D.20: Test conducted on March 30, 2017 Location 24 – compressive strength of 120 psi

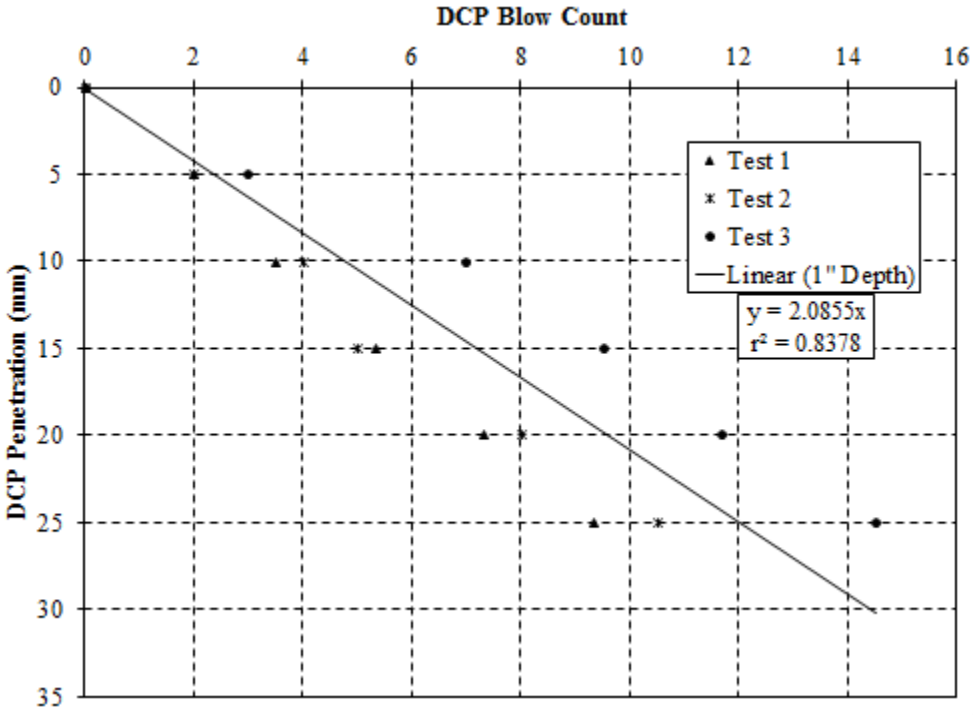

Figure D.21: Test conducted on March 30, 2017 Location 25 – compressive strength of 260 psi

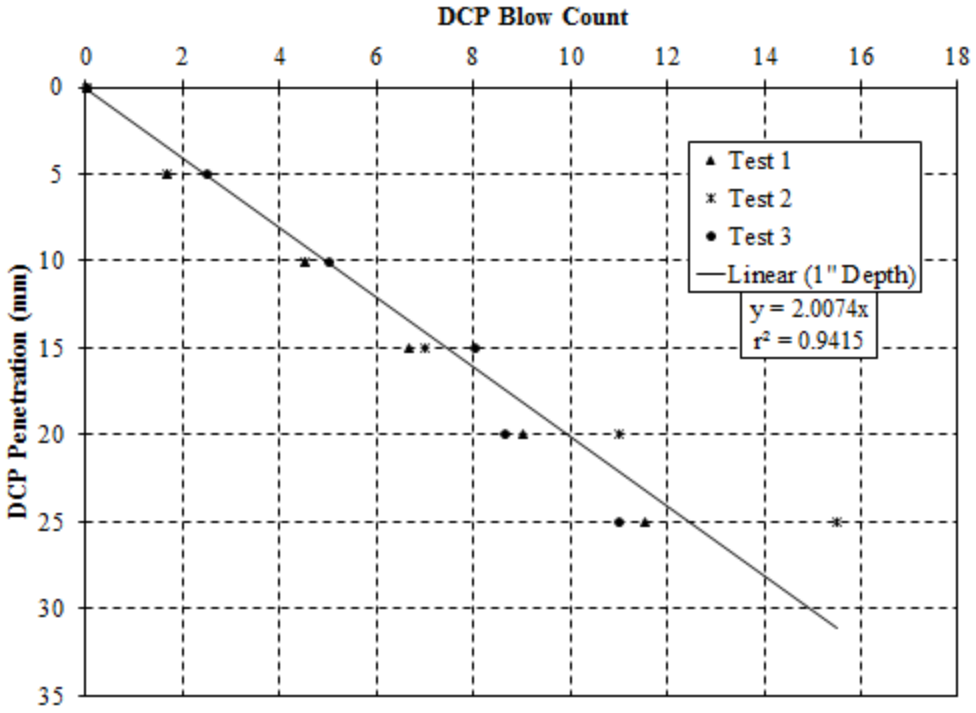

Figure D.22: Test conducted on March 31, 2017 Location 26 – compressive strength of 270 psi

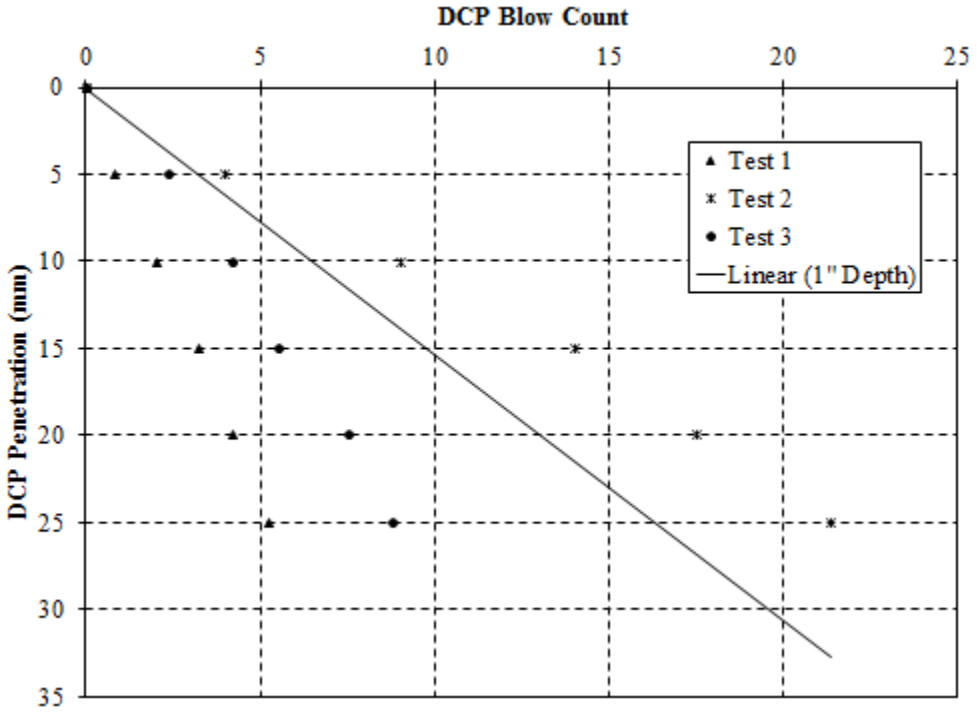

Figure D.23: Test conducted on March 31, 2017 Location 27 – range greater than 50%

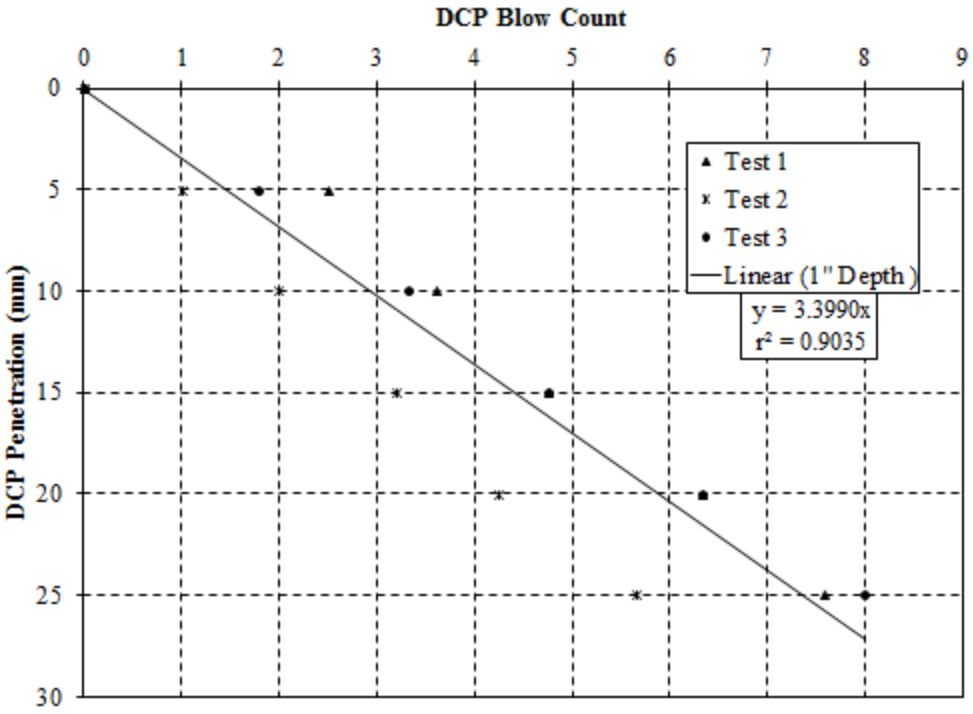

Figure D.24: Test conducted on March 31, 2017 Location 28 – compressive strength of 110 psi

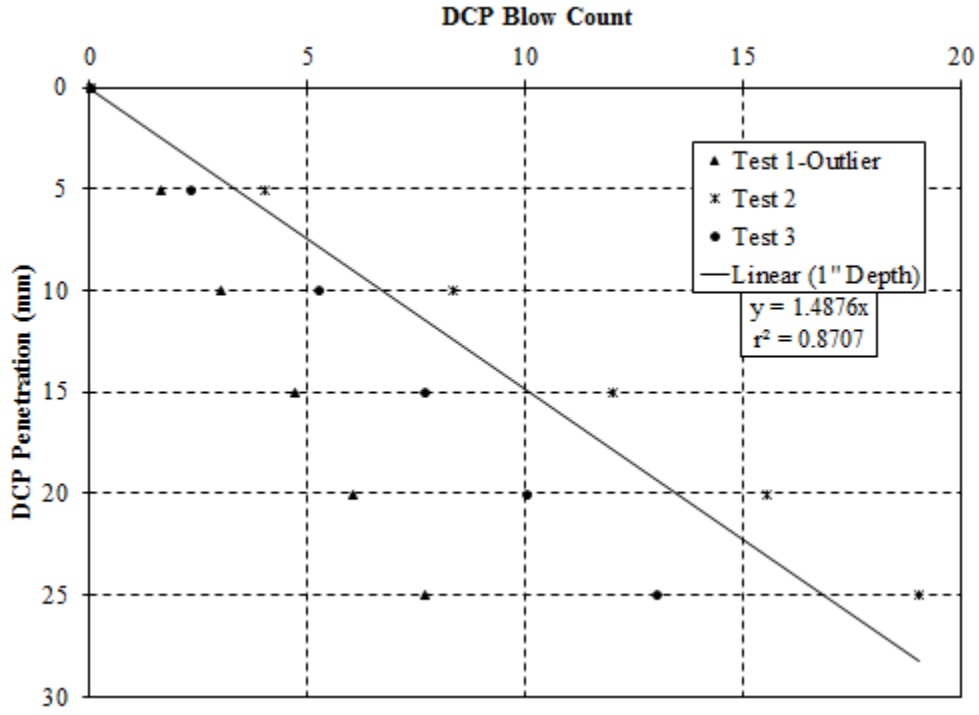

Figure D.25: Test conducted on April 3, 2017 Location 29 – compressive strength of 370 psi

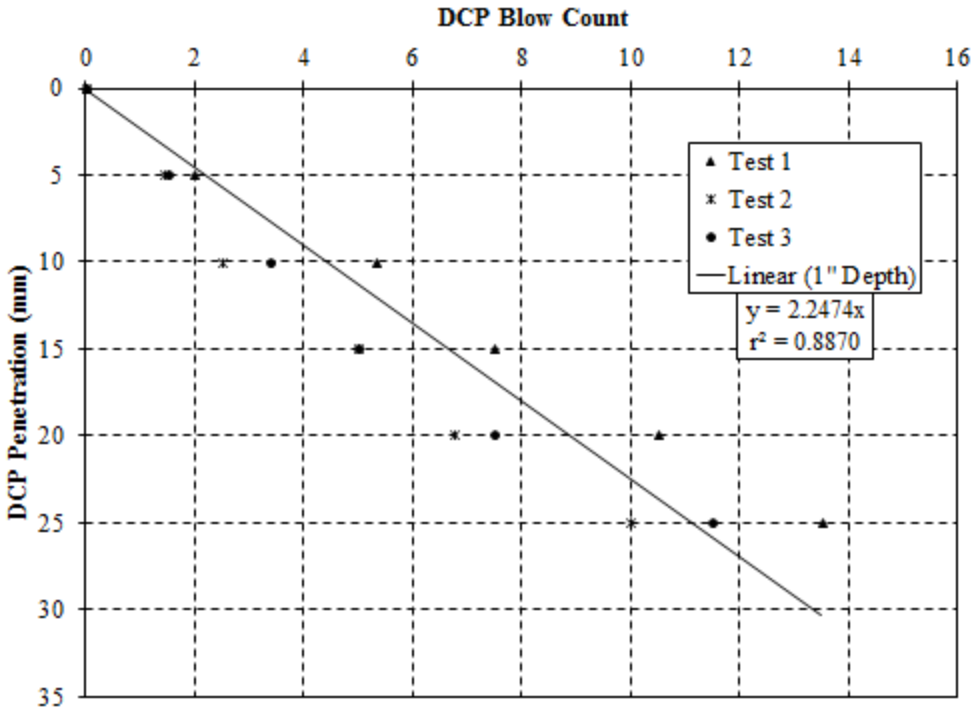

Figure D.26: Test conducted on April 3, 2017 Location 30 – compressive strength of 230 psi

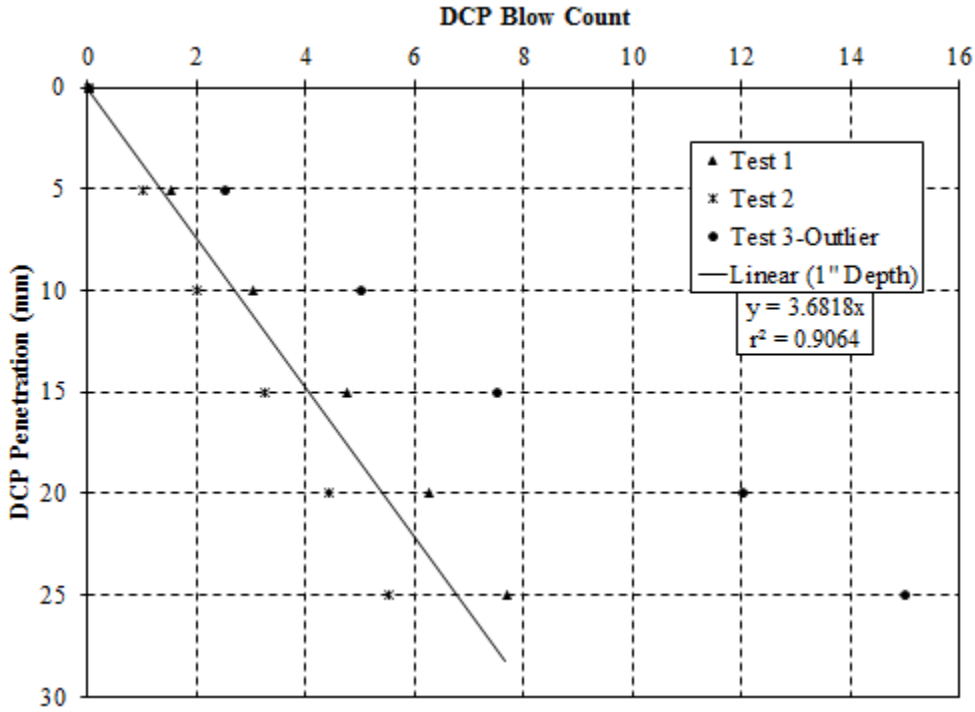

Figure D.27: Test conducted on April 3, 2017 Location 31 – compressive strength of 100 psi

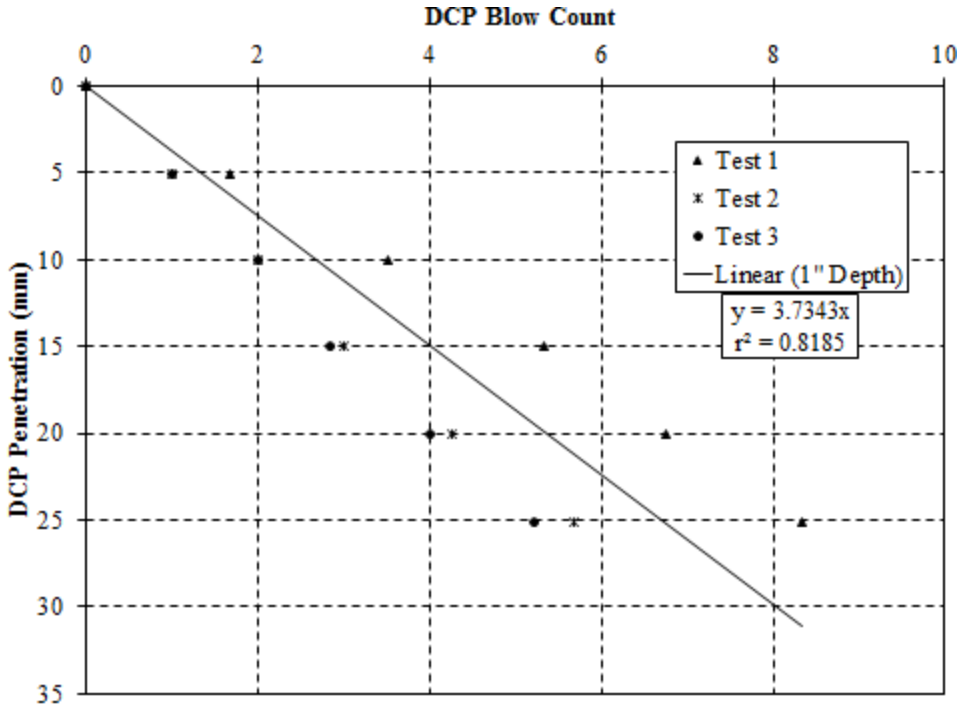

Figure D.28: Test conducted on April 5, 2017 Location 32 – compressive strength of 90 psi

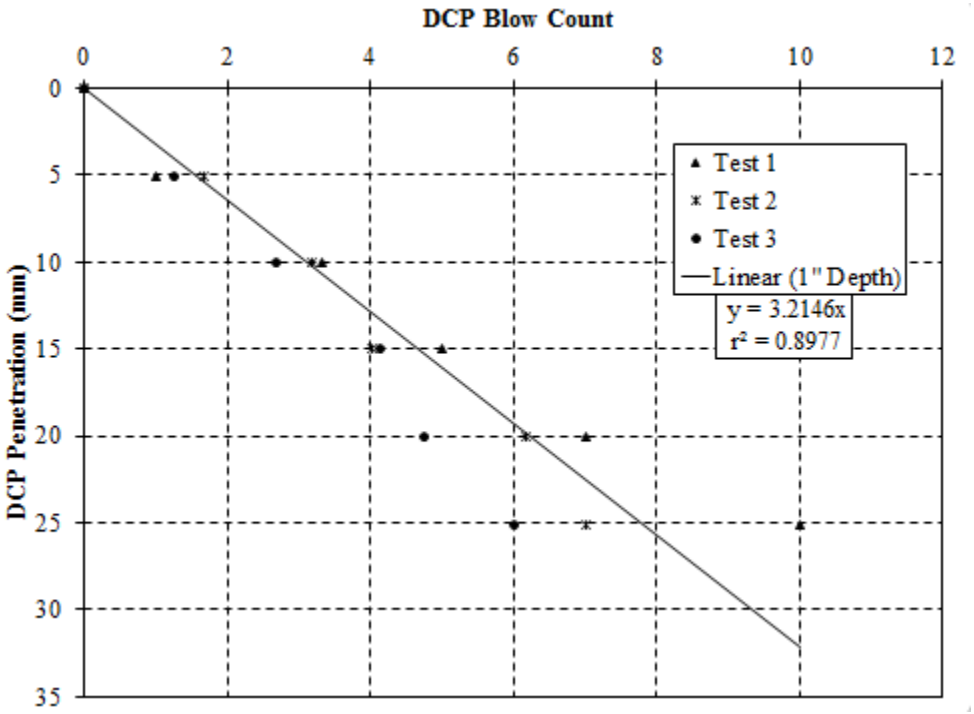

Figure D.29: Test conducted on April 5, 2017 Location 33 – compressive strength of 130 psi

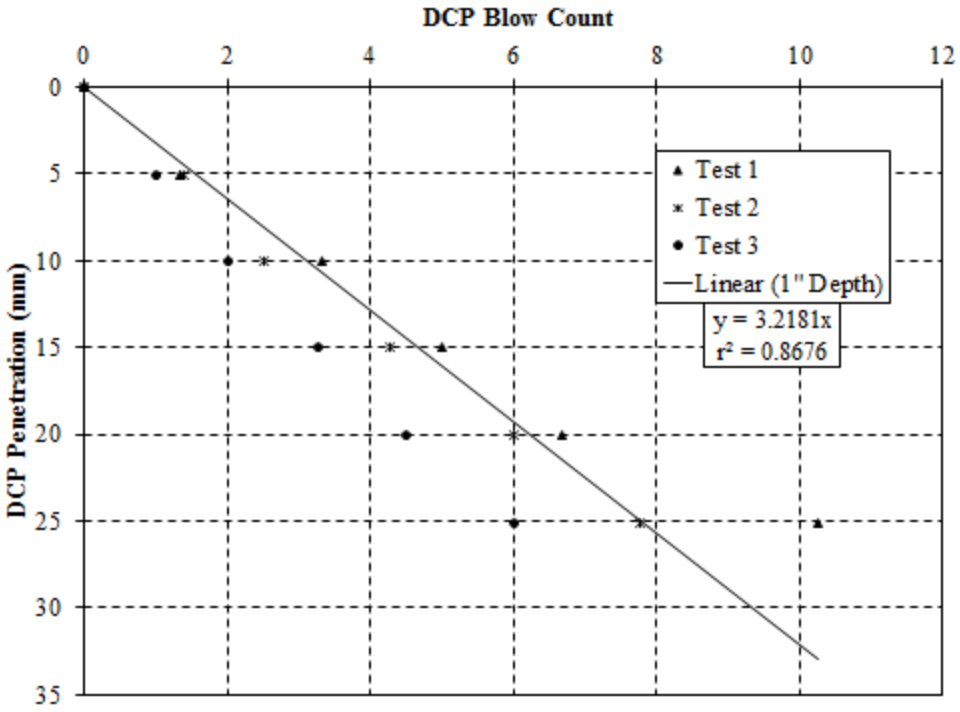

Figure D.30: Test conducted on April 5, 2017 Location 34 – compressive strength of 130 psi

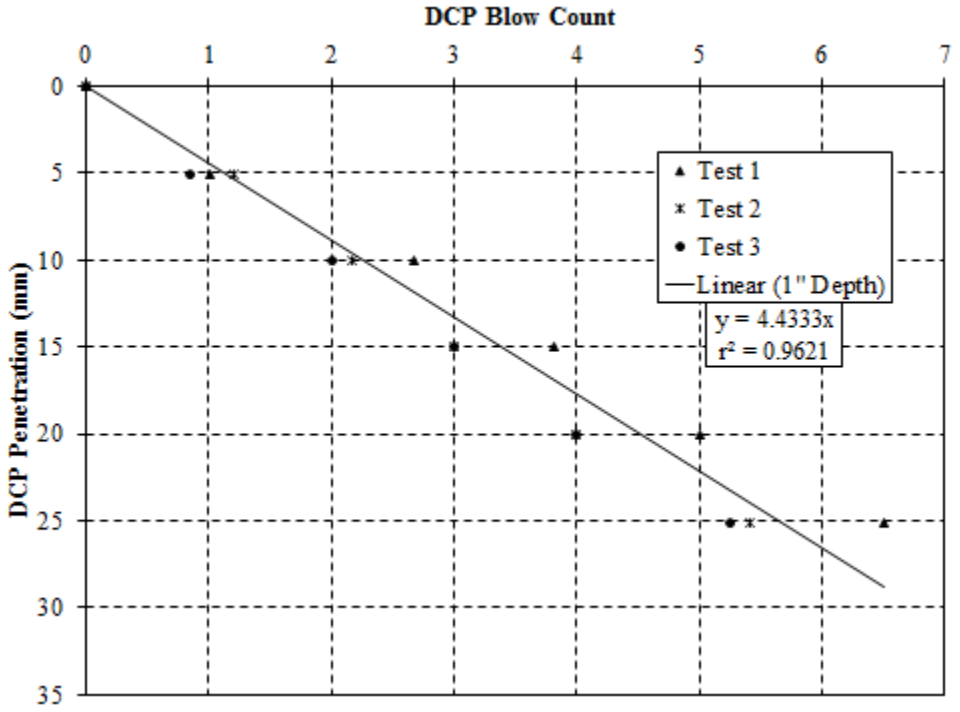

Figure D.31: Test conducted on April 5, 2017 Location 35 – compressive strength of 60 psi

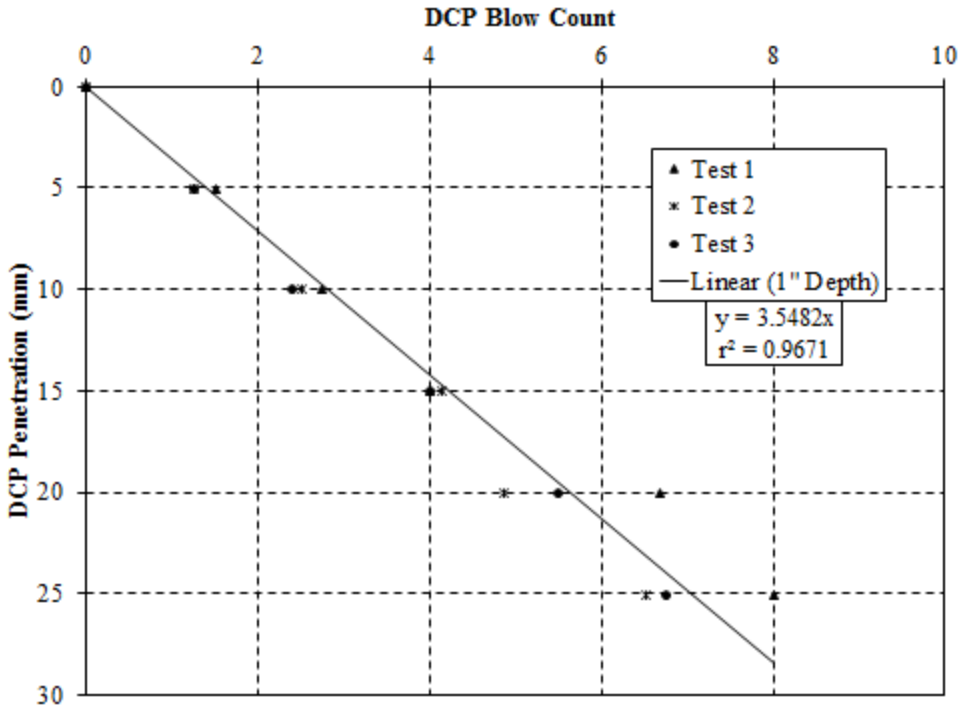

Figure D.32: Test conducted on April 5, 2017 Location 36 – compressive strength of 100 psi

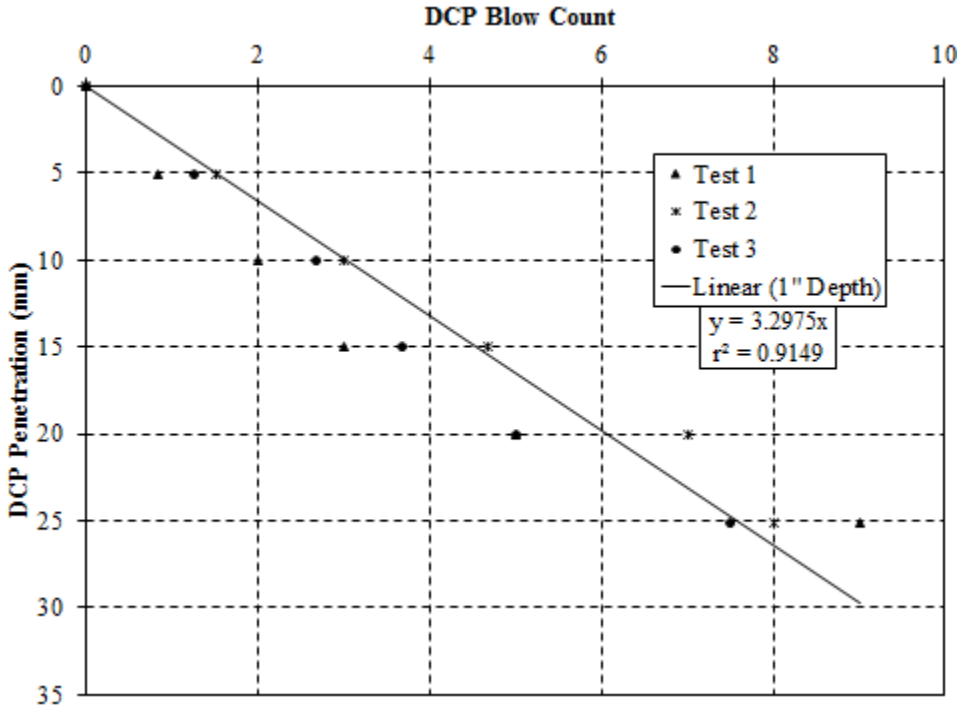

Figure D.33: Test conducted on April 5, 2017 Location 37 – compressive strength of 120 psi

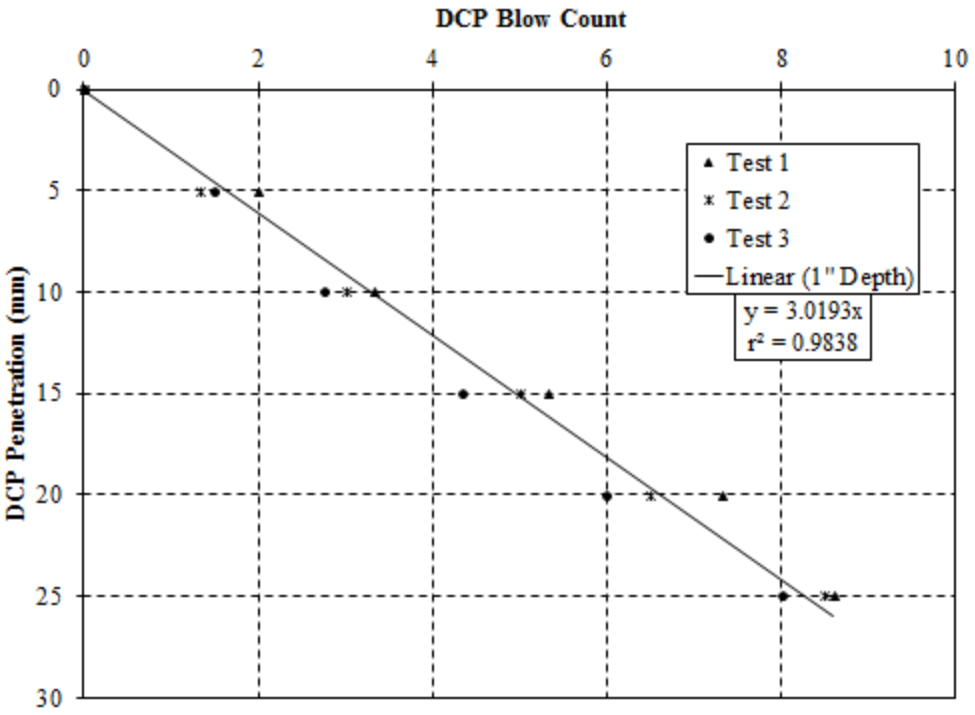

Figure D.34: Test conducted on April 6, 2017 Location 38 – compressive strength of 140 psi

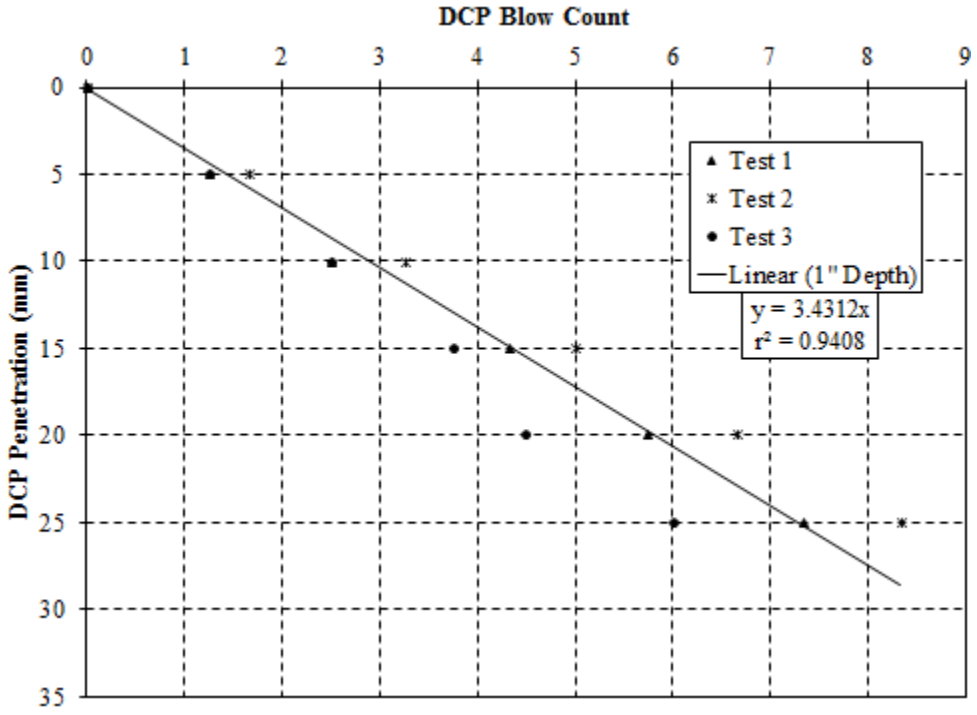

Figure D.35: Test conducted on April 6, 2017 Location 40 – compressive strength of 110 psi

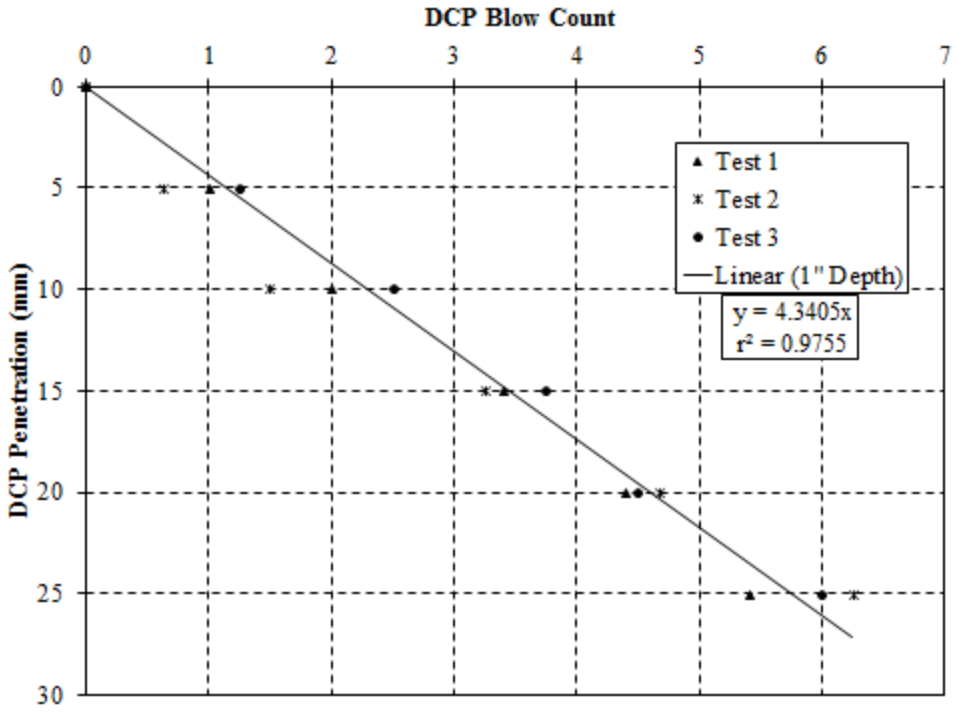

Figure D.36: Test conducted on April 19, 2017 Location 41 – compressive strength of 60 psi

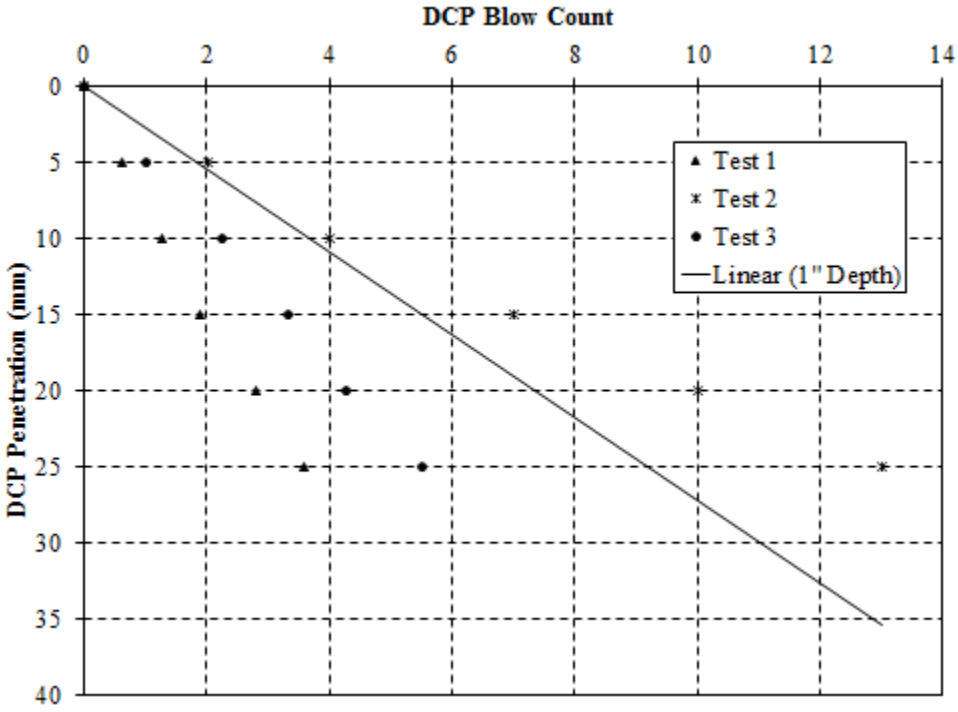

Figure D.37: Test conducted on April 19, 2017 Location 42 – range greater than 50%

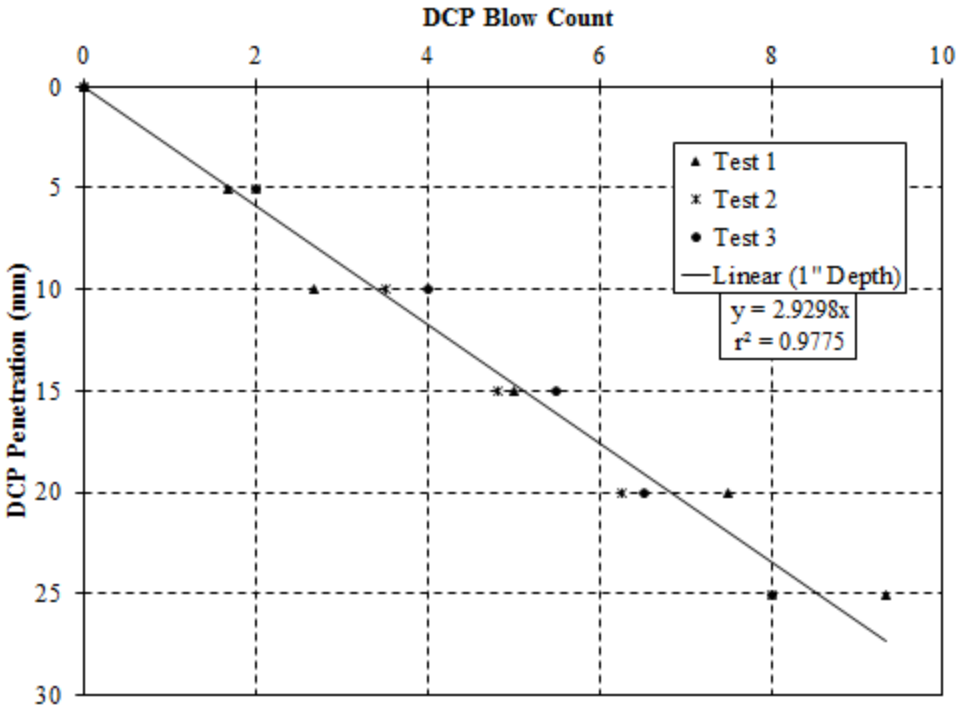

Figure D.38: Test conducted on April 19, 2017 Location 43 – compressive strength of 150 psi

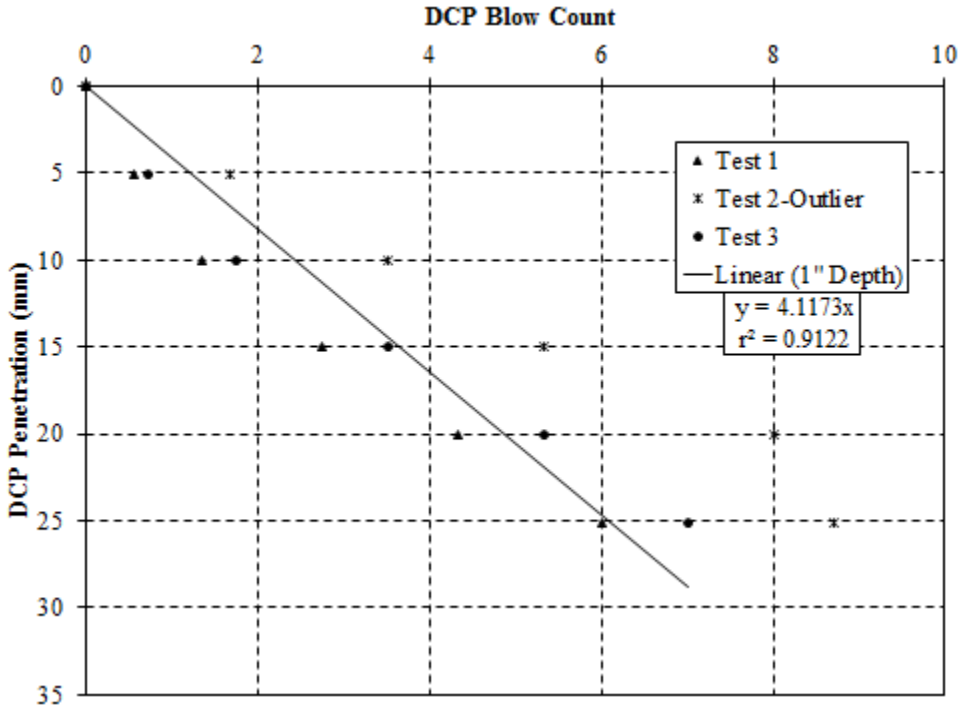

Figure D.39: Test conducted on April 19, 2017 Location 44 – compressive strength of 70 psi

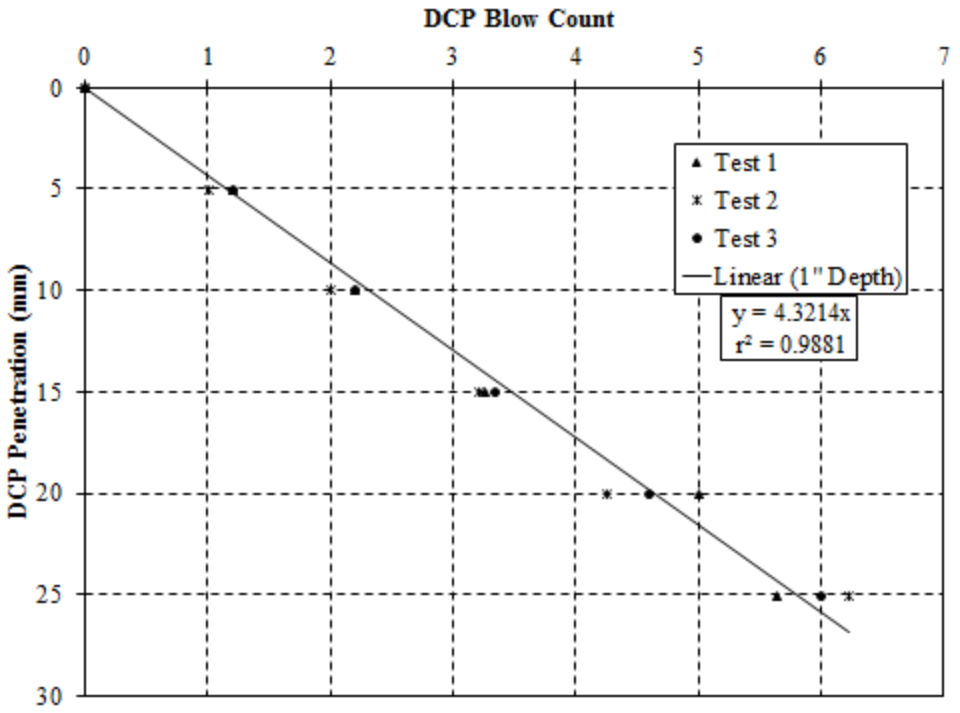

Figure D.40: Test conducted on April 19, 2017 Location 45 – compressive strength of 60 psi

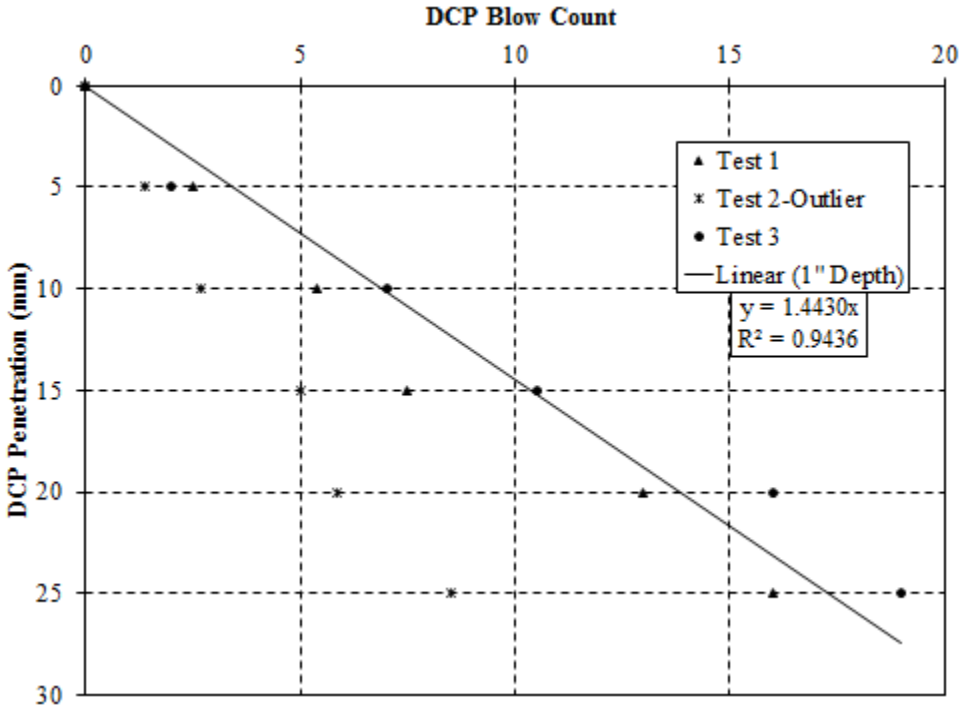

Figure D.41: Test conducted on April 19, 2017 Location 46 – compressive strength of 380 psi

Appendix E

50 mm Penetration

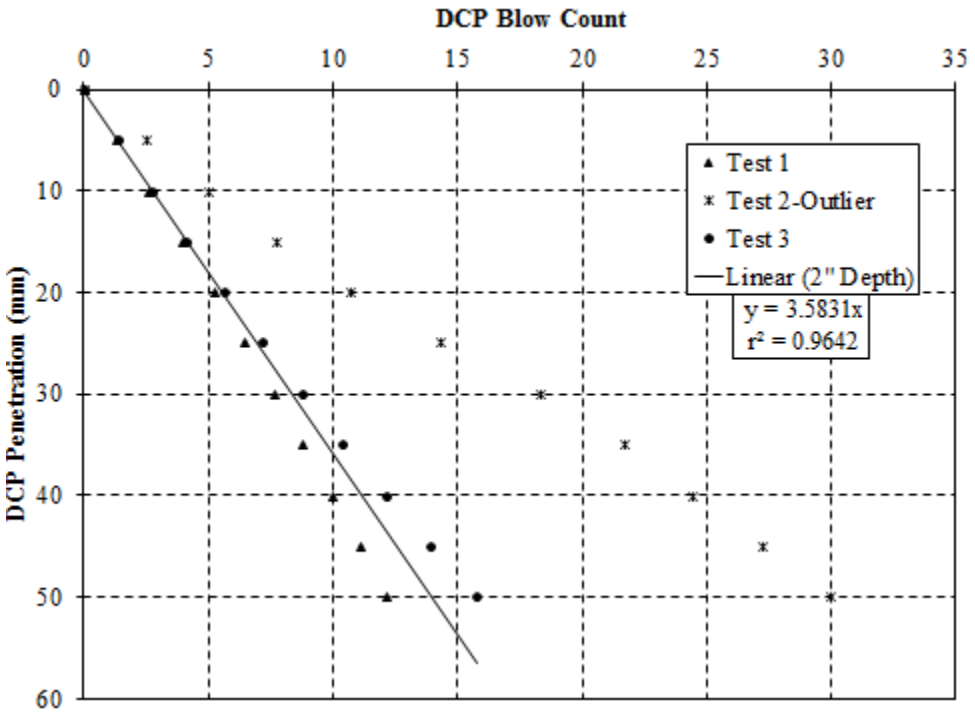

Figure E.1: Test conducted on November 1, 2016 Location 1 – compressive strength of 100 psi

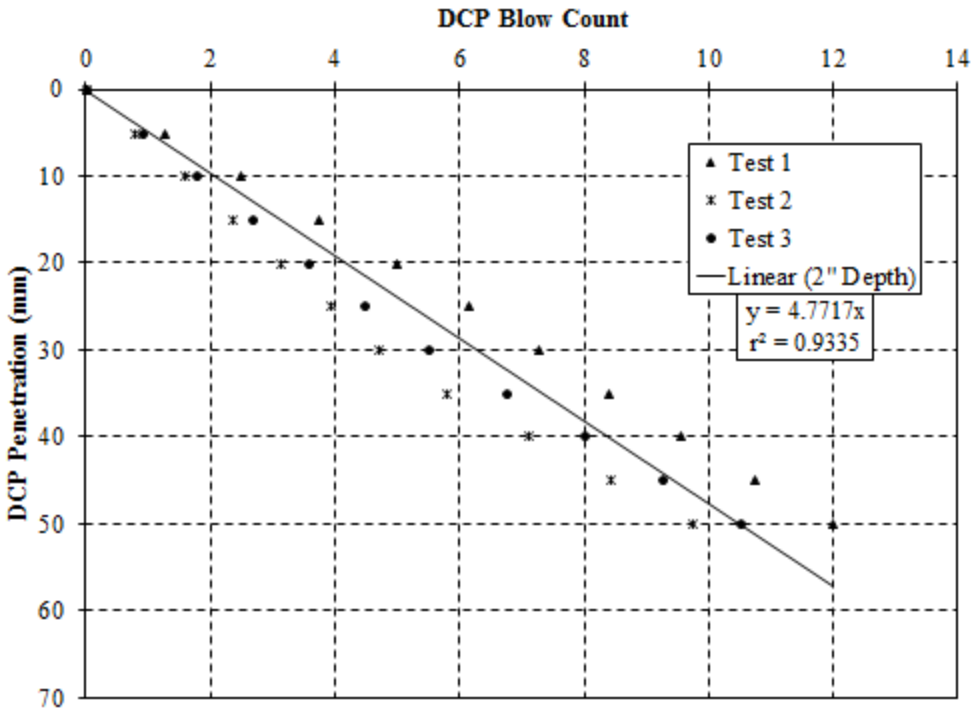

Figure E.2: Test conducted on November 1, 2016 Location 2 – compressive strength of 50 psi

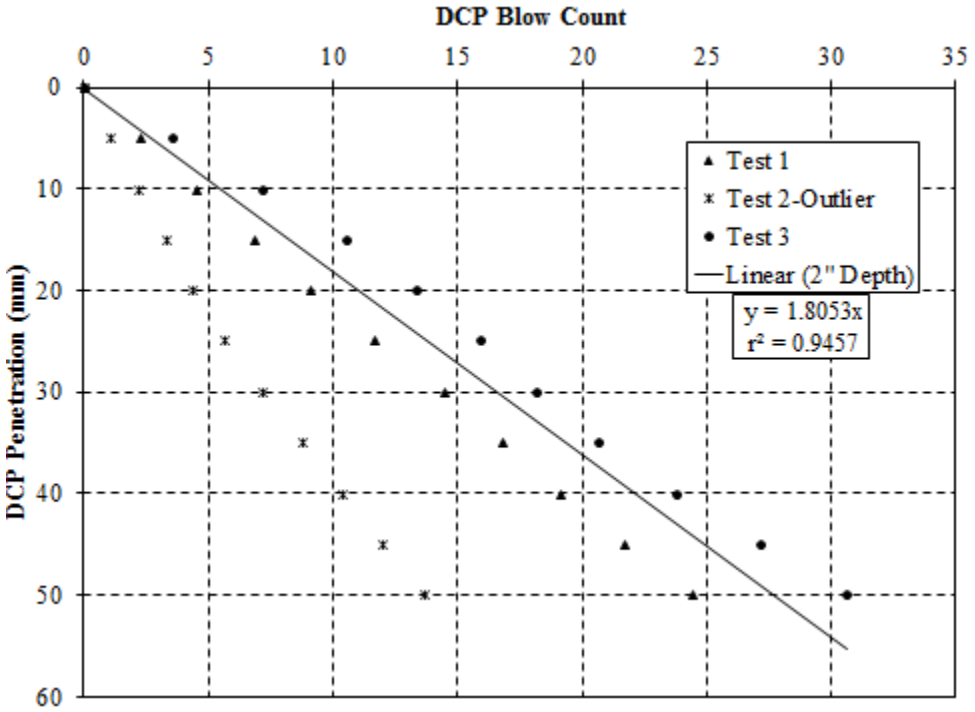

Figure E.3: Test conducted on November 7, 2016 Location 6 – compressive strength of 310 psi

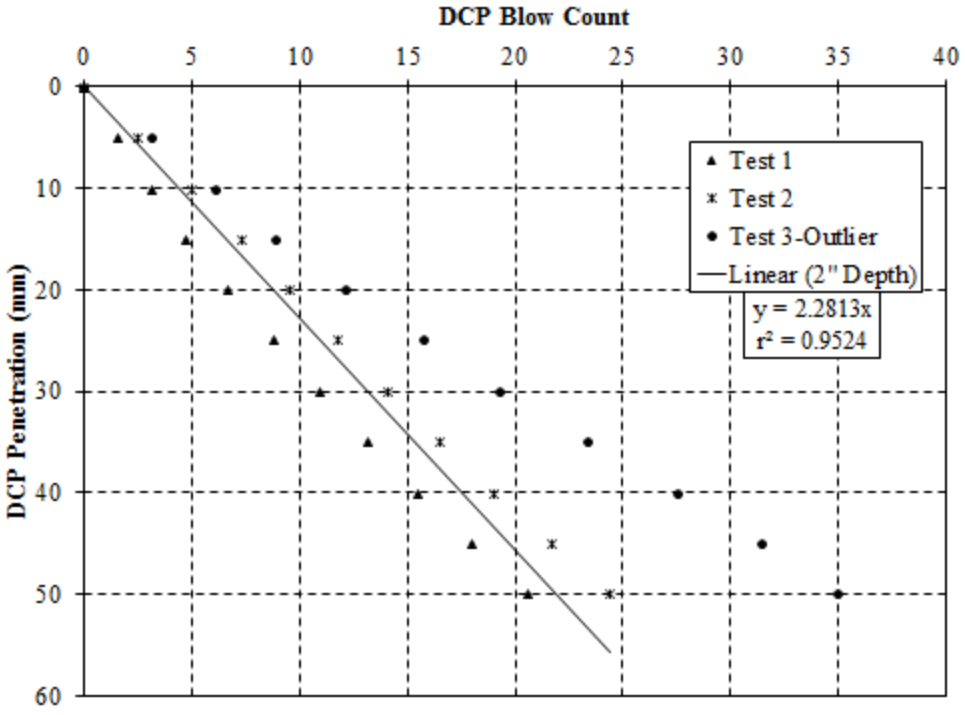

Figure E.4: Test conducted on November 7, 2016 Location 7– compressive strength of 230 psi

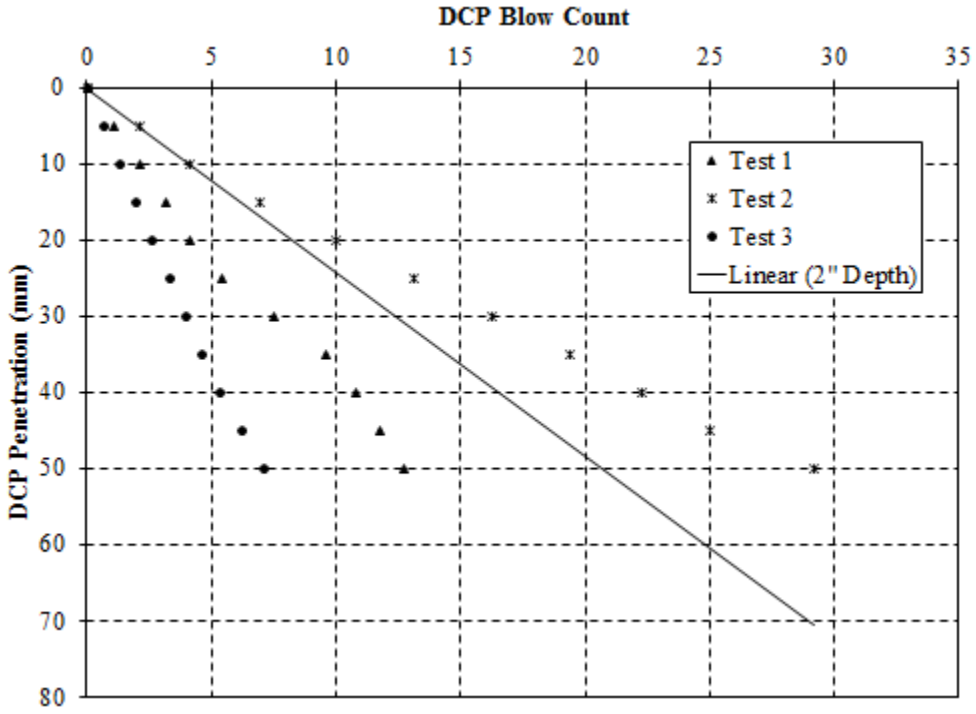

Figure E.5: Test conducted on November 22, 2016 Location 8 – range greater than 50 %

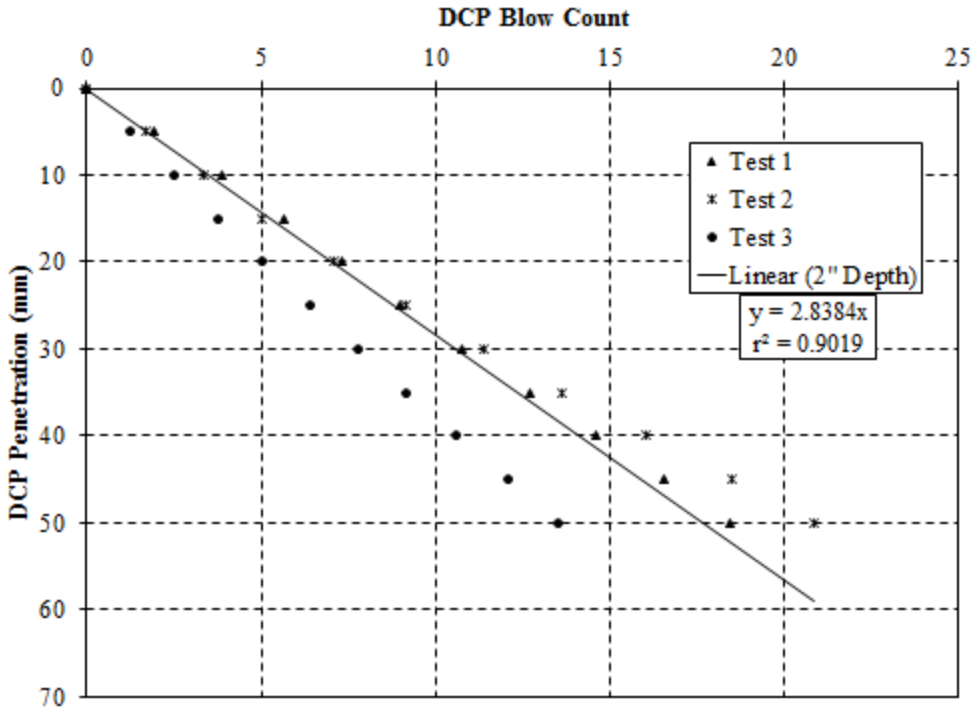

Figure E.6: Test conducted on November 22, 2016 Location 9 – compressive strength of 160 psi

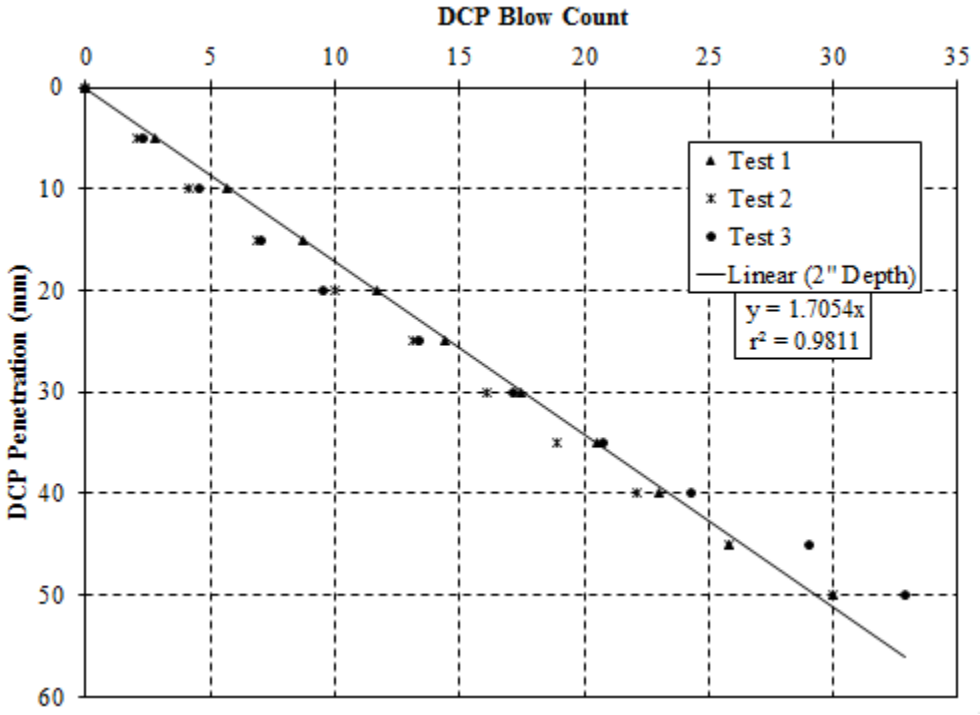

Figure E.7: Test Conducted on November 22, 2016 Location 10– compressive strength of 320 psi

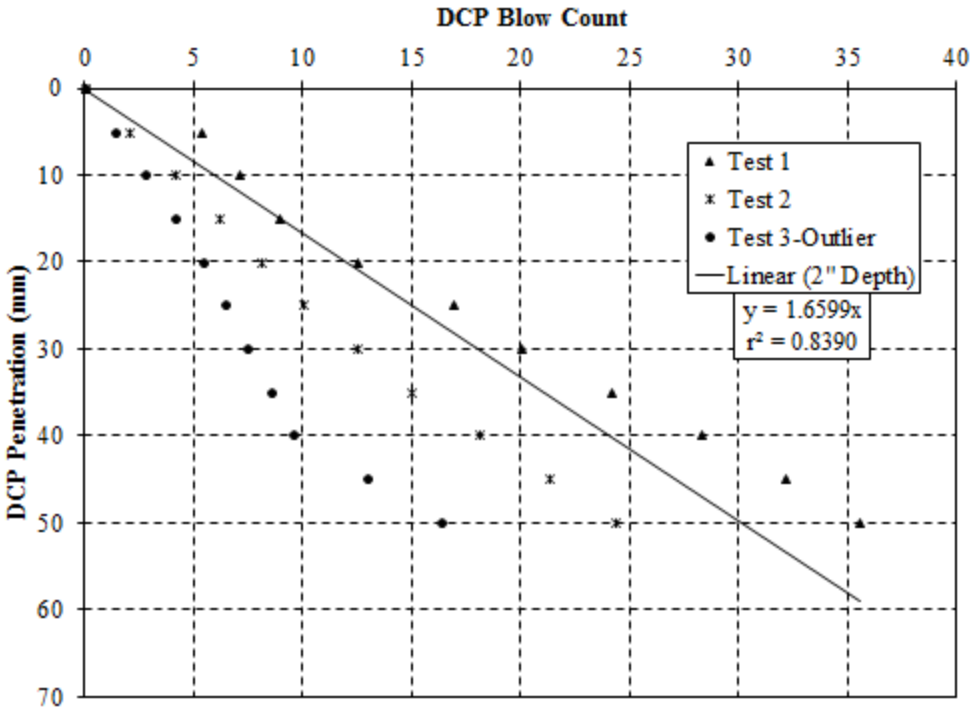

Figure E.8: Test conducted on November 22, 2016 Location 12–compressive strength of 330 psi

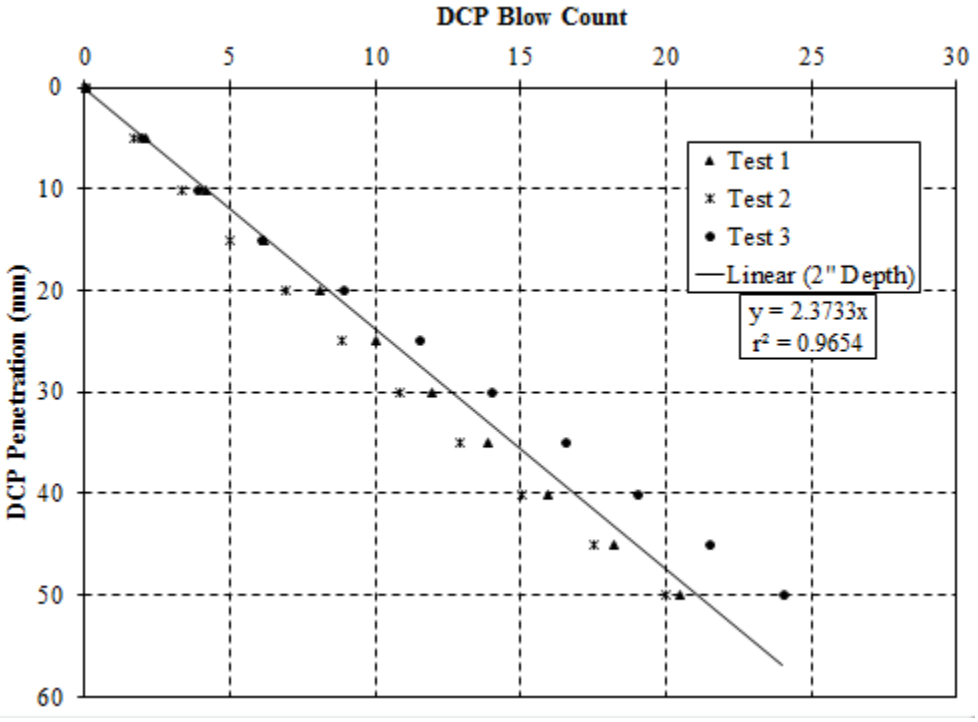

Figure E.9: Test conducted on November 22, 2016 Location 13–compressive strength of 220 psi

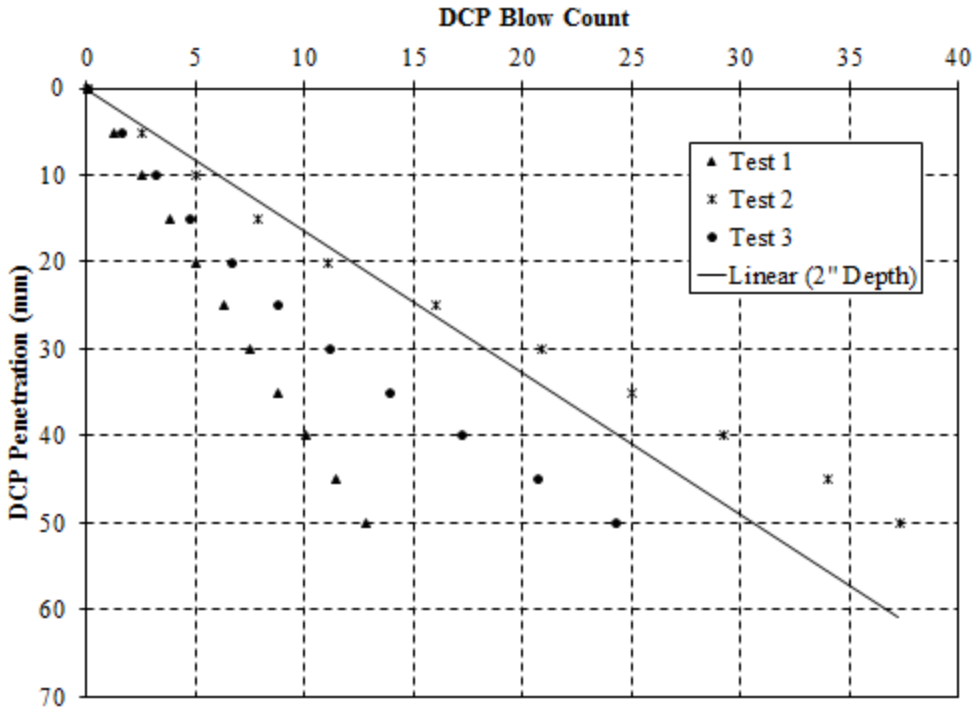

Figure E.10: Test conducted on November 23, 2016 Location 14 – range greater than 50 %

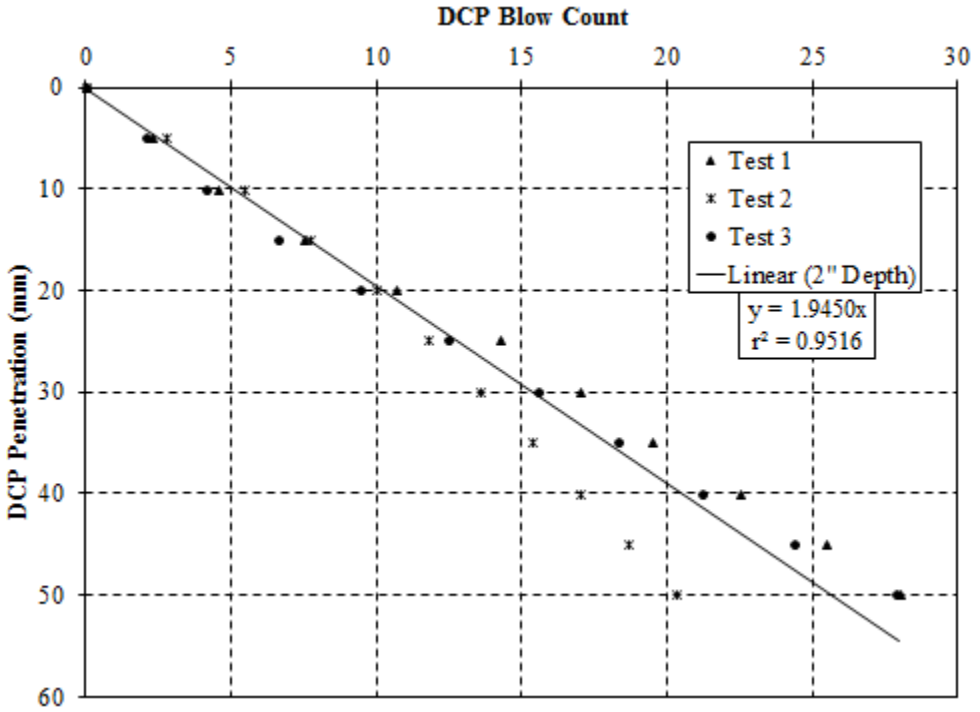

Figure E.11: Test conducted on November 23, 2016 Location 15–compressive strength of 280 psi

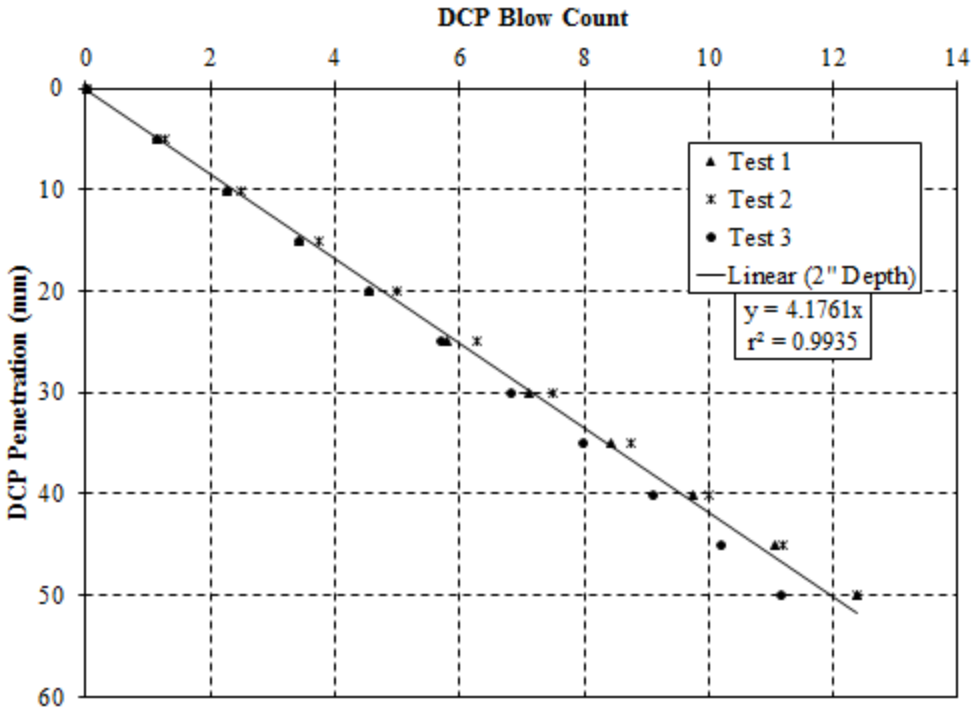

Figure E.12: Test conducted on November 23, 2016 Location 16–compressive strength of 70 psi

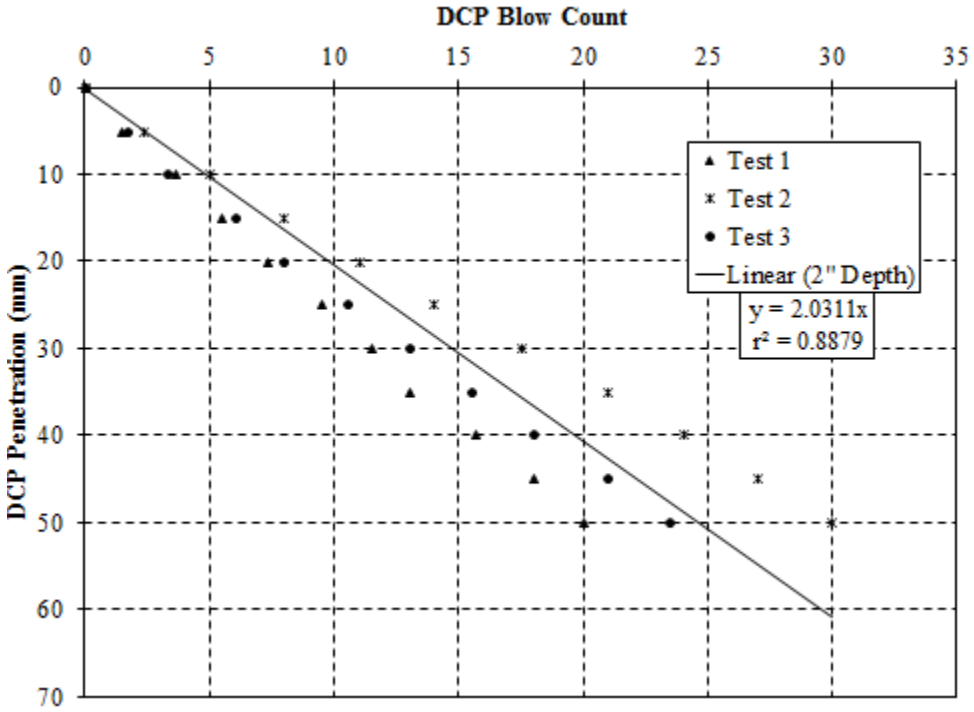

Figure E.13: Test conducted on March 23, 2017 Location 17 – compressive strength of 270 psi

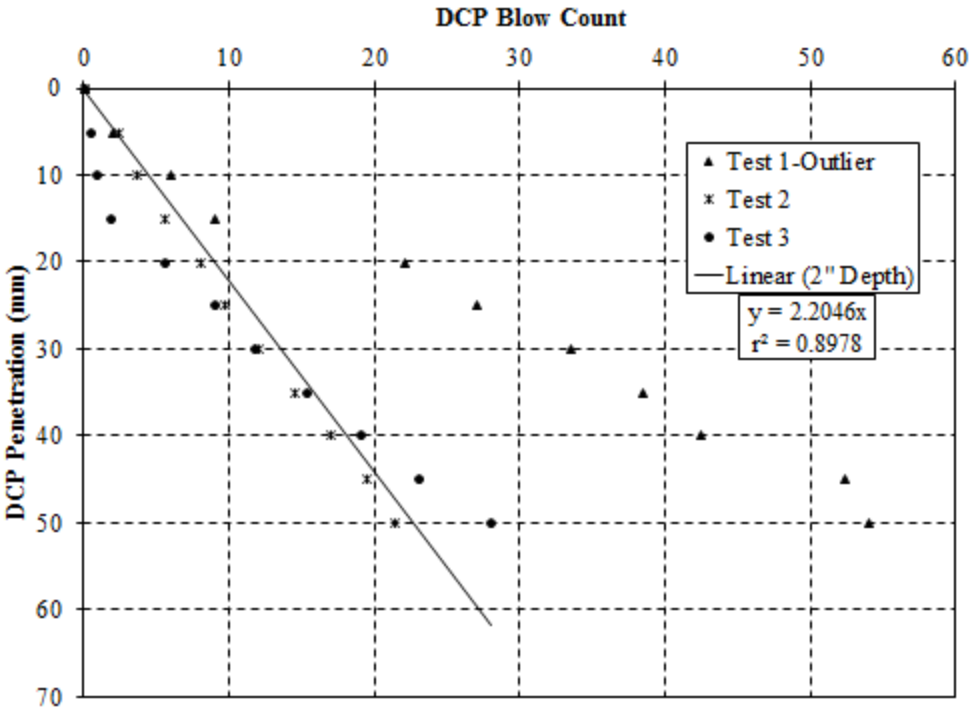

Figure E.14: Test conducted on March 23, 2017 Location 18 – compressive strength of 240 psi

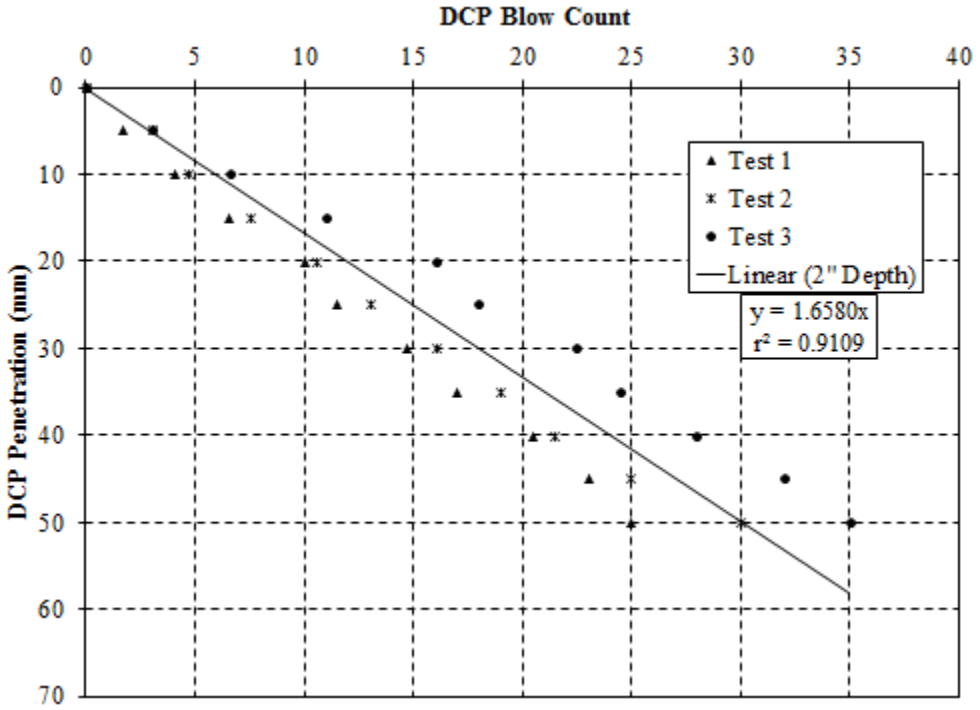

Figure E.15: Test conducted on March 23, 2017 Location 19 – compressive strength of 330 psi

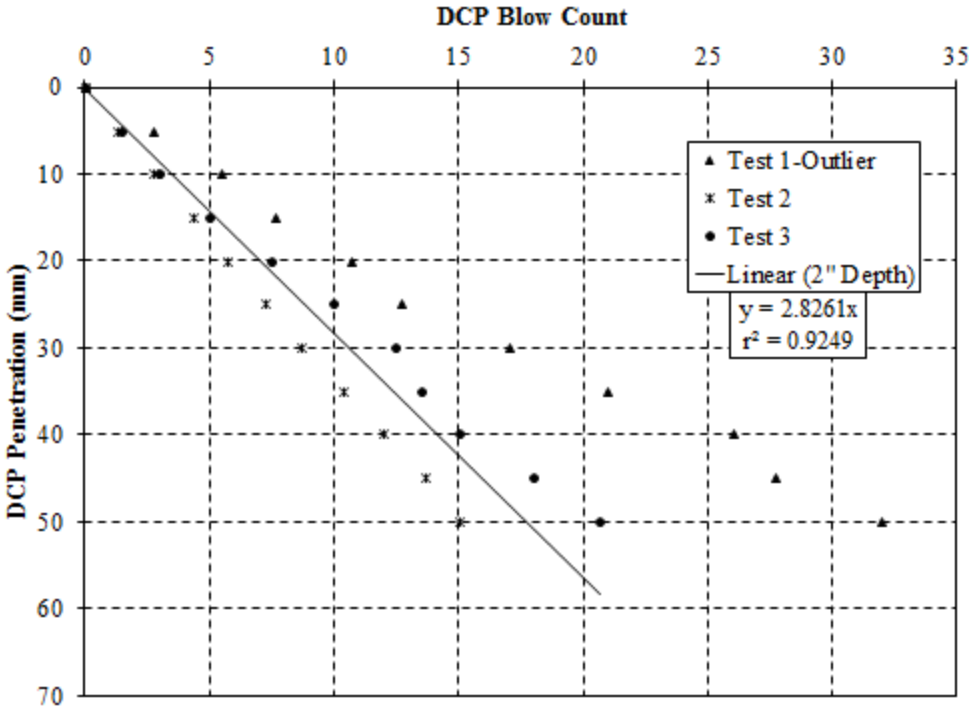

Figure E.16: Test conducted on March 27, 2017 Location 20 – compressive strength of 160 psi

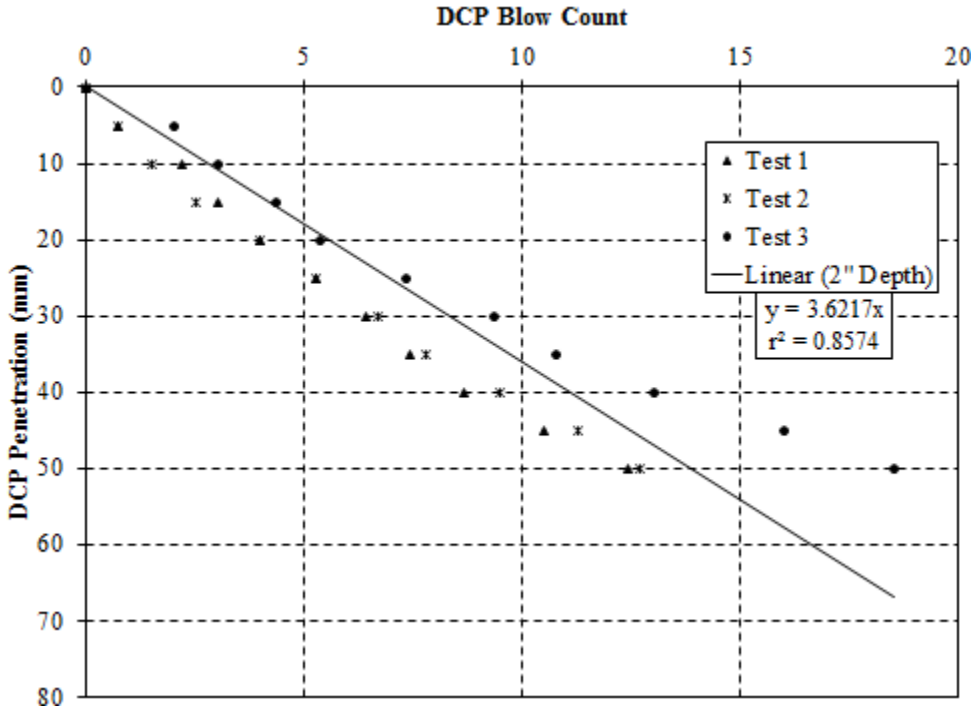

Figure E.17: Test conducted on March 27, 2017 Location 21 – compressive strength of 100 psi

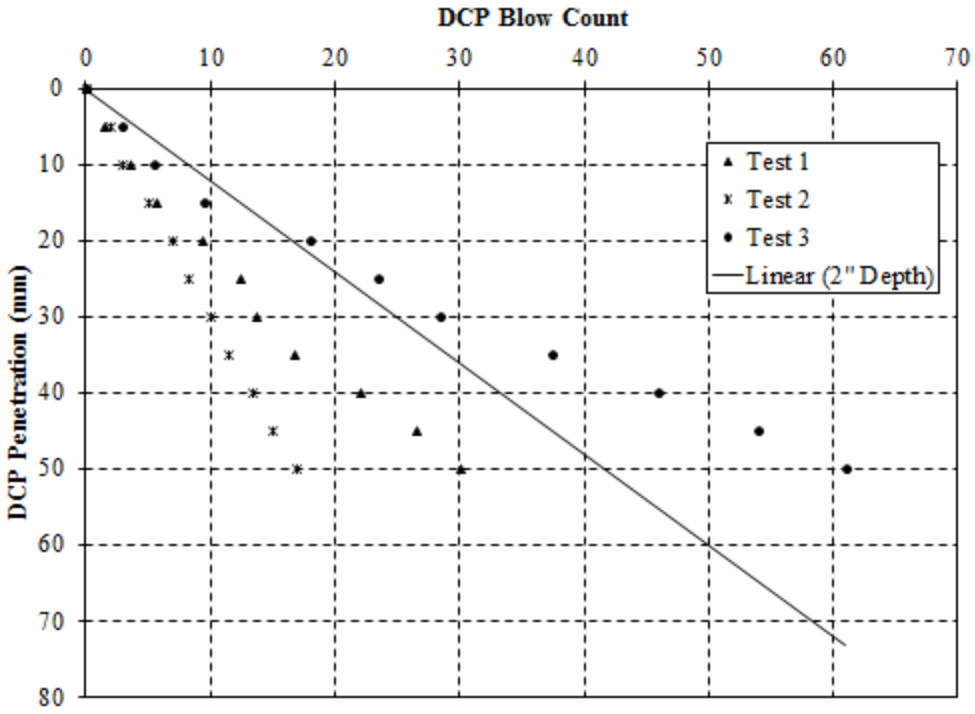

Figure E.18: Test conducted on March 27, 2017 Location 22 – range greater than 50 %

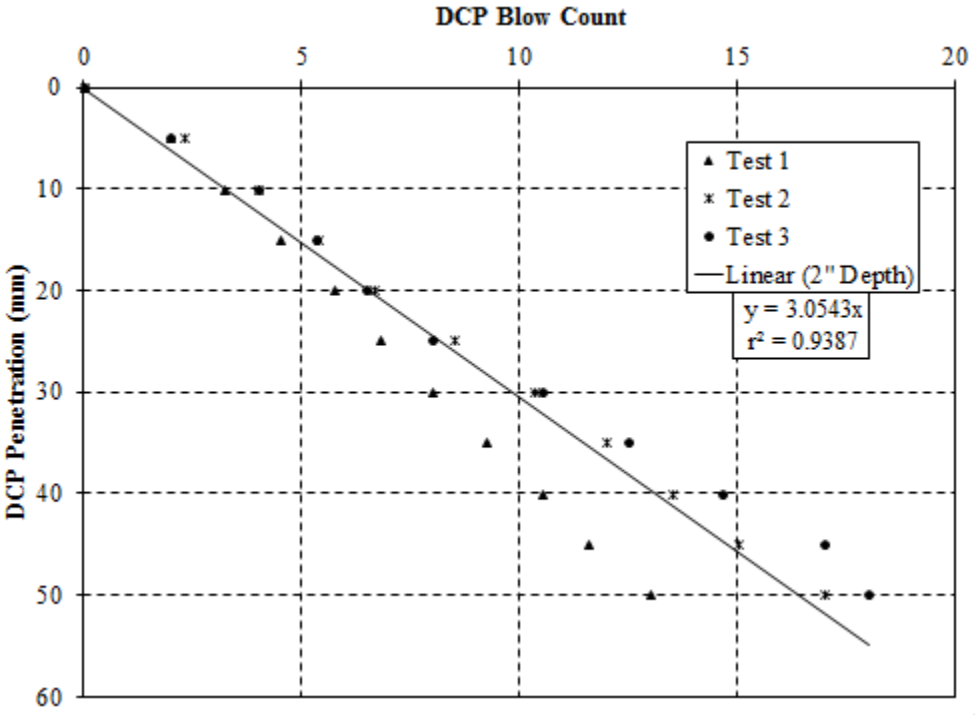

Figure E.19: Test conducted on March 30, 2017 Location 23 – compressive strength of 140 psi

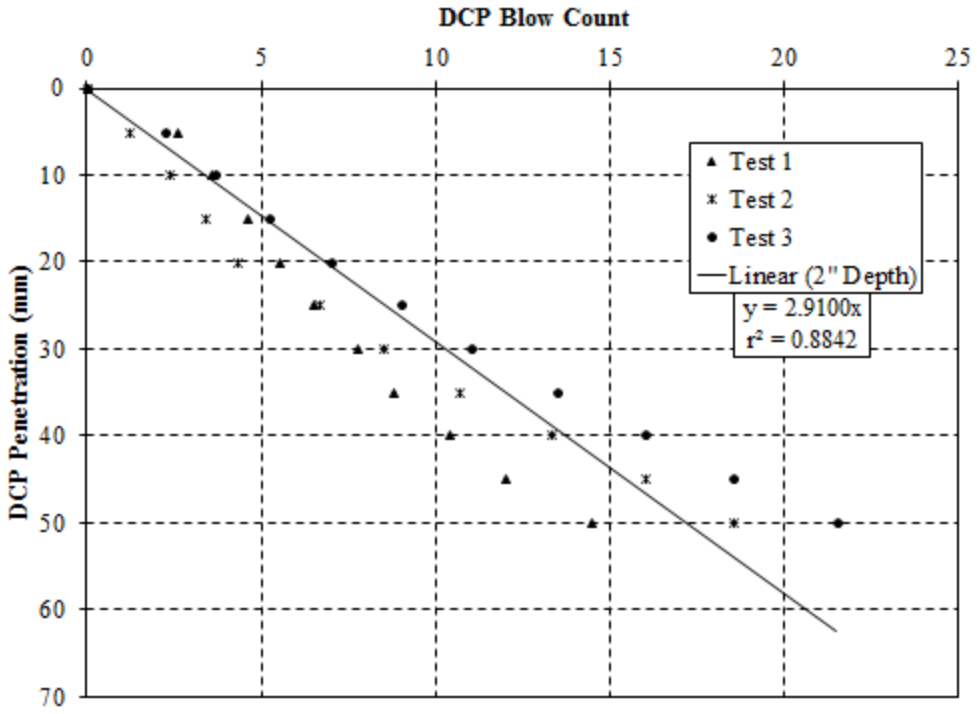

Figure E.20: Test conducted on March 30, 2017 Location 24 – compressive strength of 150 psi

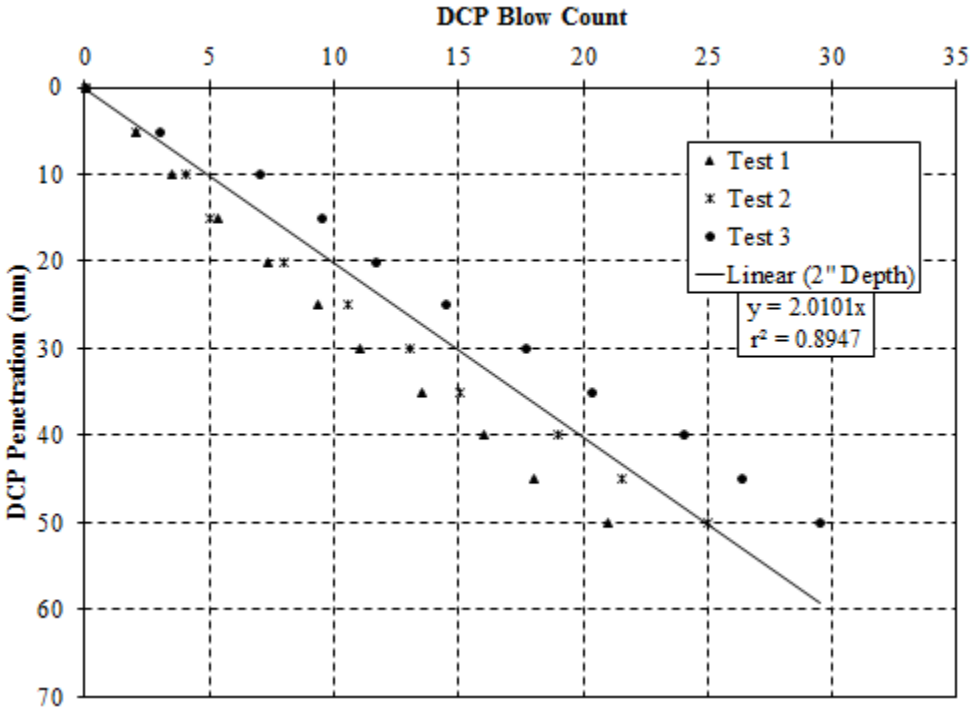

Figure E.21: Test conducted on March 30, 2017 Location 25 – compressive strength of 270 psi

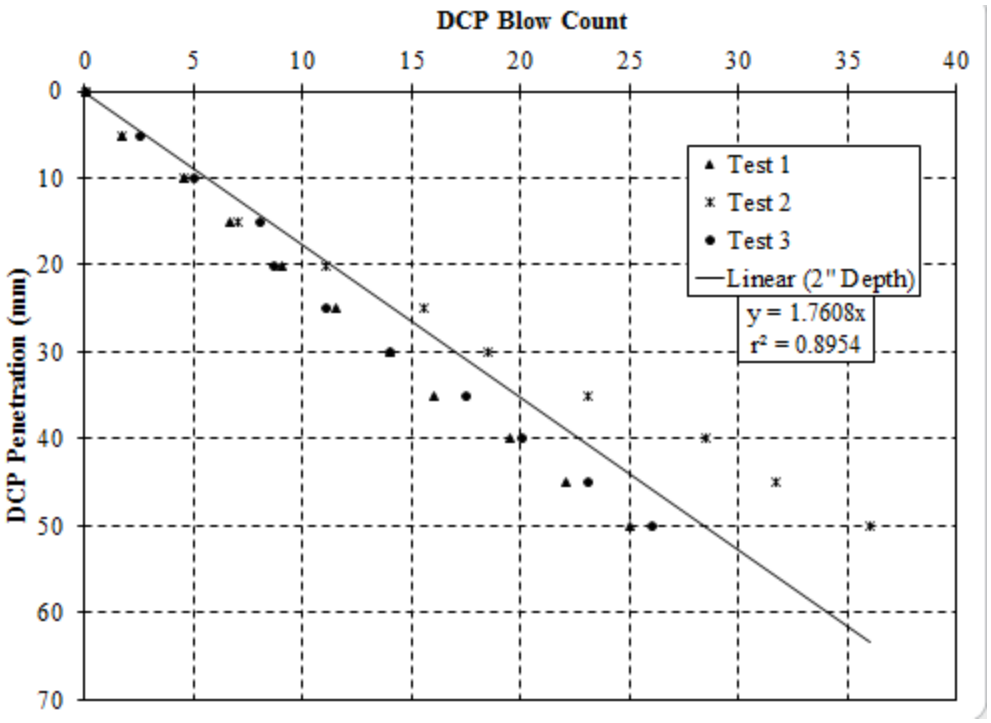

Figure E.22: Test conducted on March 31, 2017 Location 26 – compressive strength of 310 psi

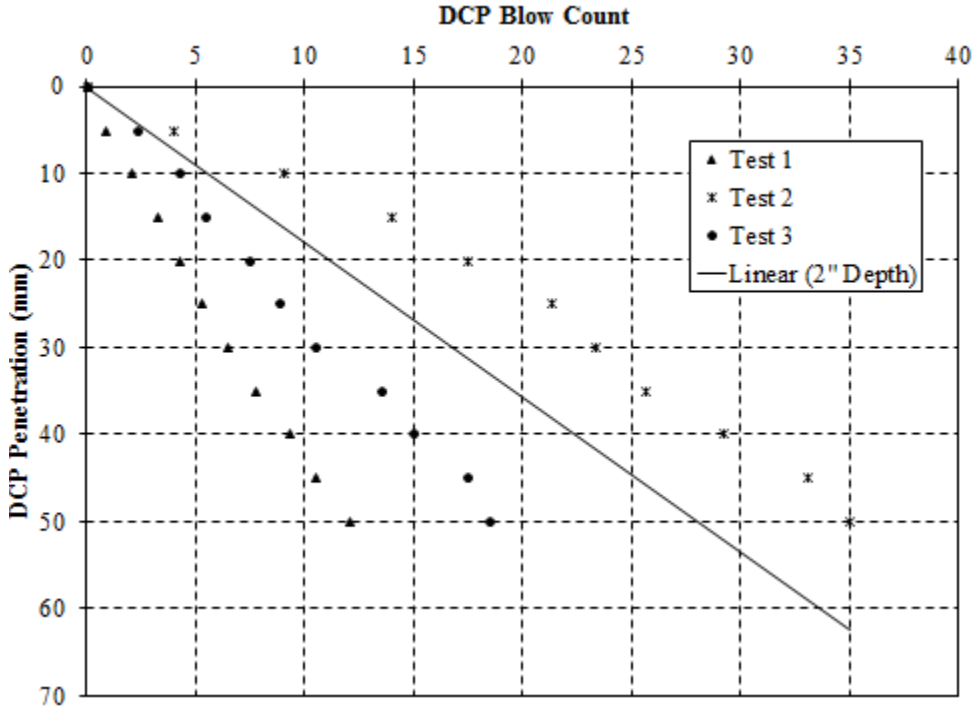

Figure E.23: Test conducted on March 31, 2017 Location 27 – range greater than 50 %

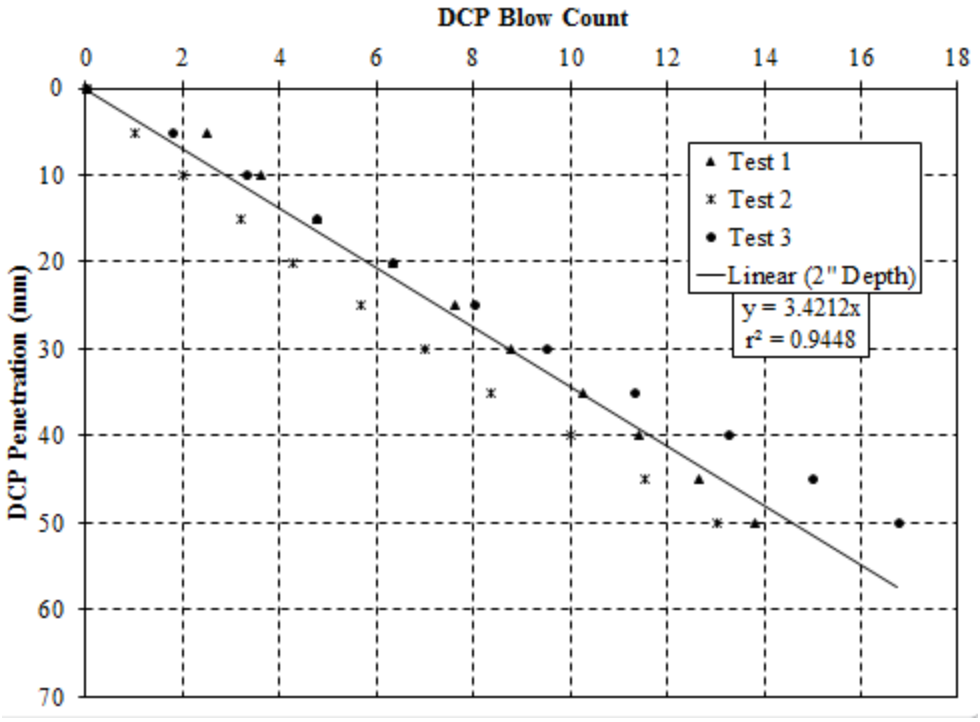

Figure E.24: Test conducted on March 31, 2017 Location 28 – compressive strength of 110 psi

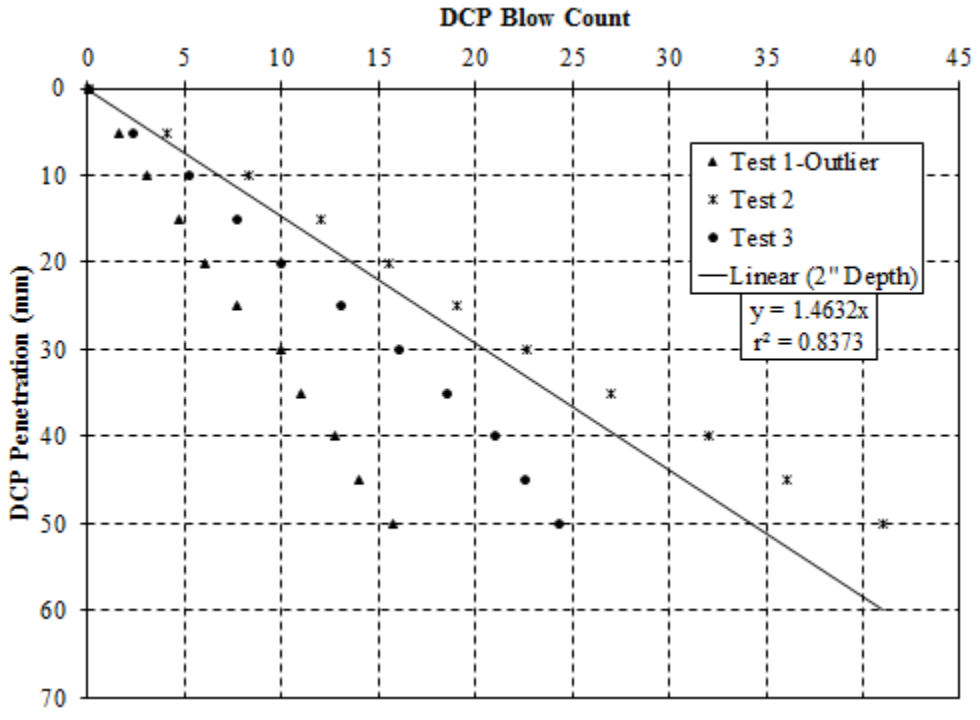

Figure E.25: Test conducted on April 3, 2017 Location 29– compressive strength of 380 psi

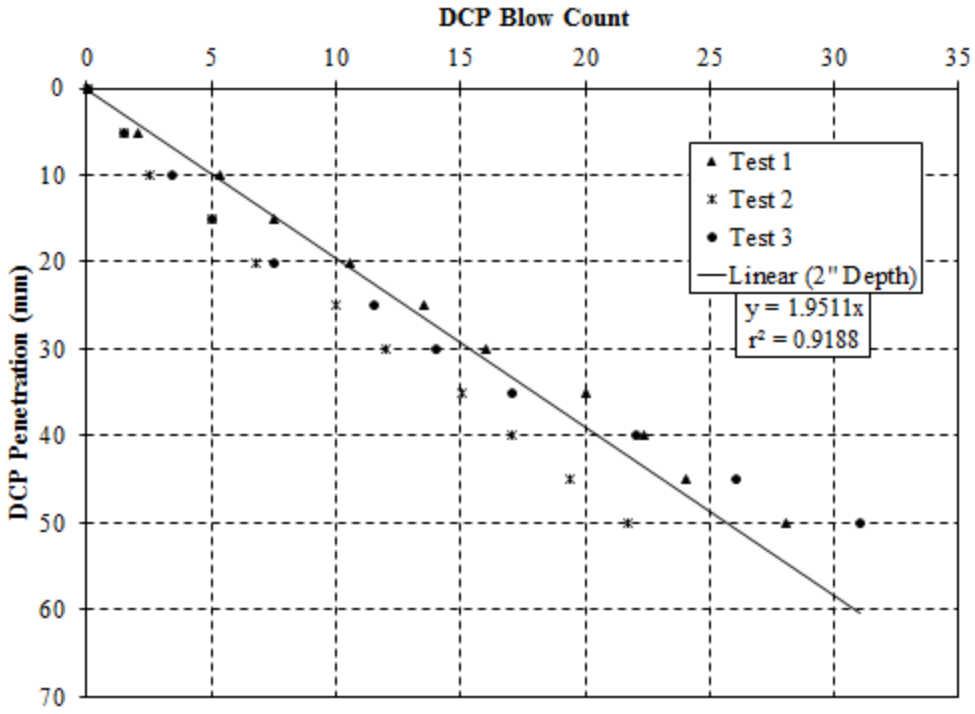

Figure E.26: Test conducted on April 3, 2017 Location 30 – compressive strength of 280 psi

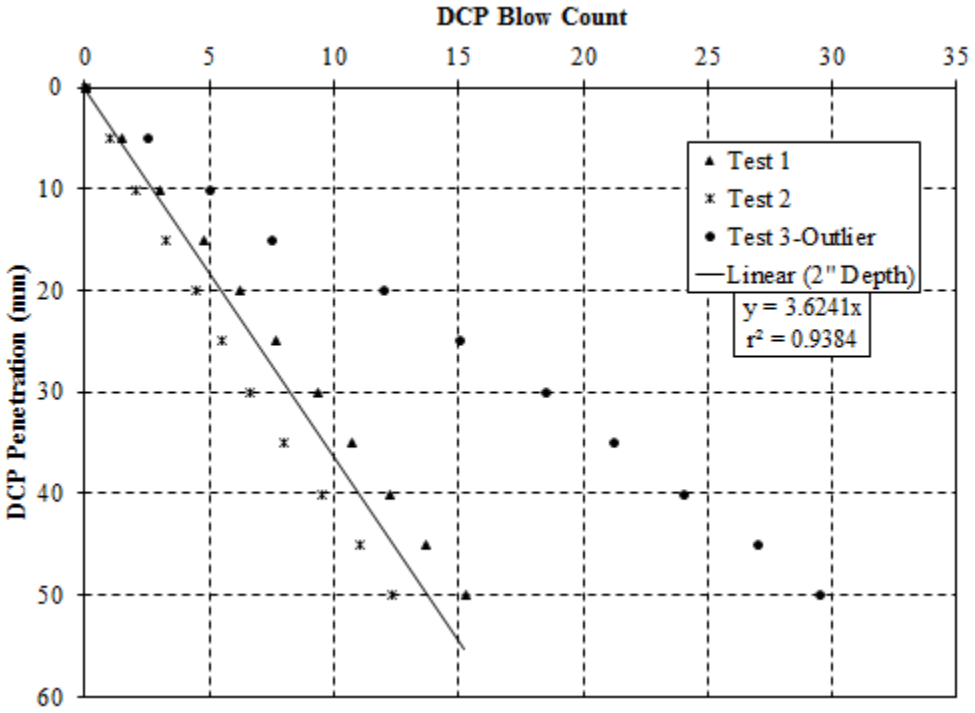

Figure E.27: Test conducted on April 3, 2017 Location 31 – compressive strength of 100 psi

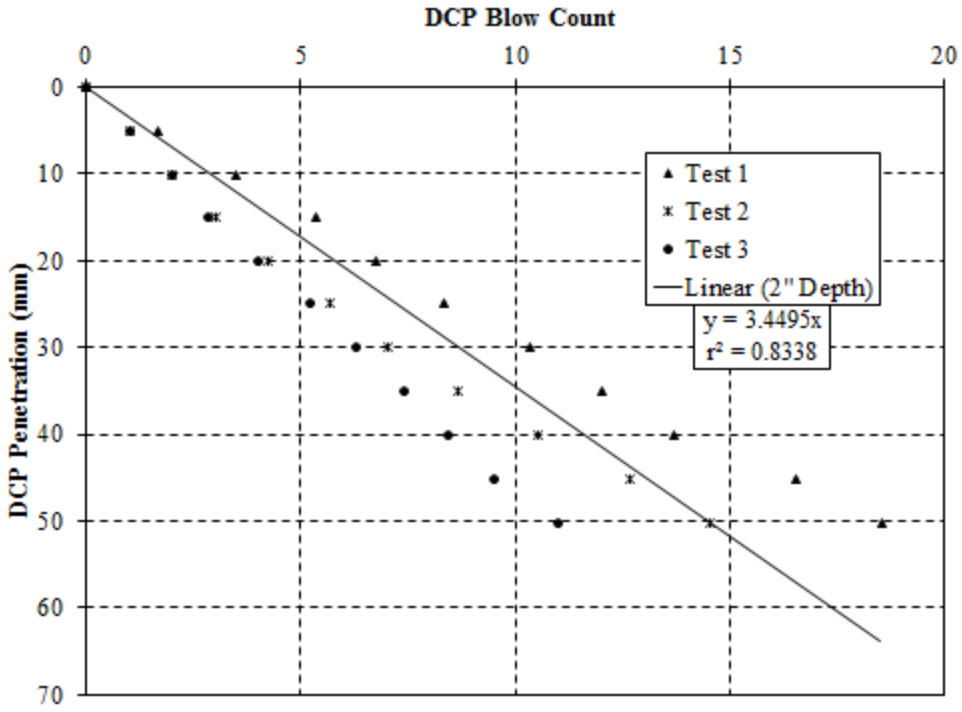

Figure E.28: Test conducted on April 5, 2017 Location 32 – compressive strength of 110 psi

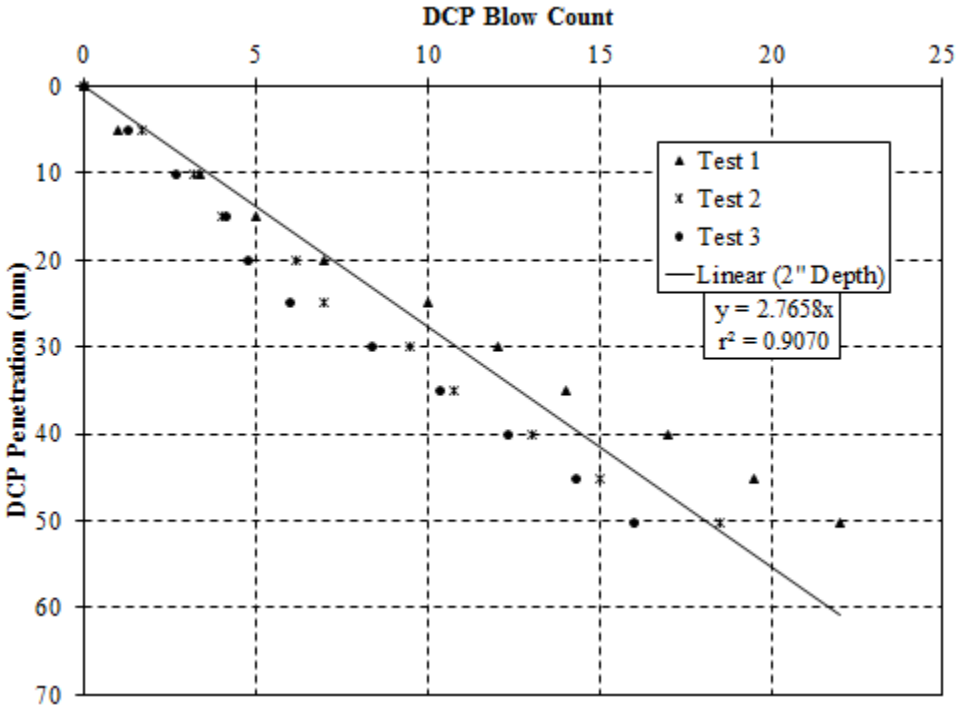

Figure E.29: Test conducted on April 5, 2017 Location 33 – compressive strength of 170 psi

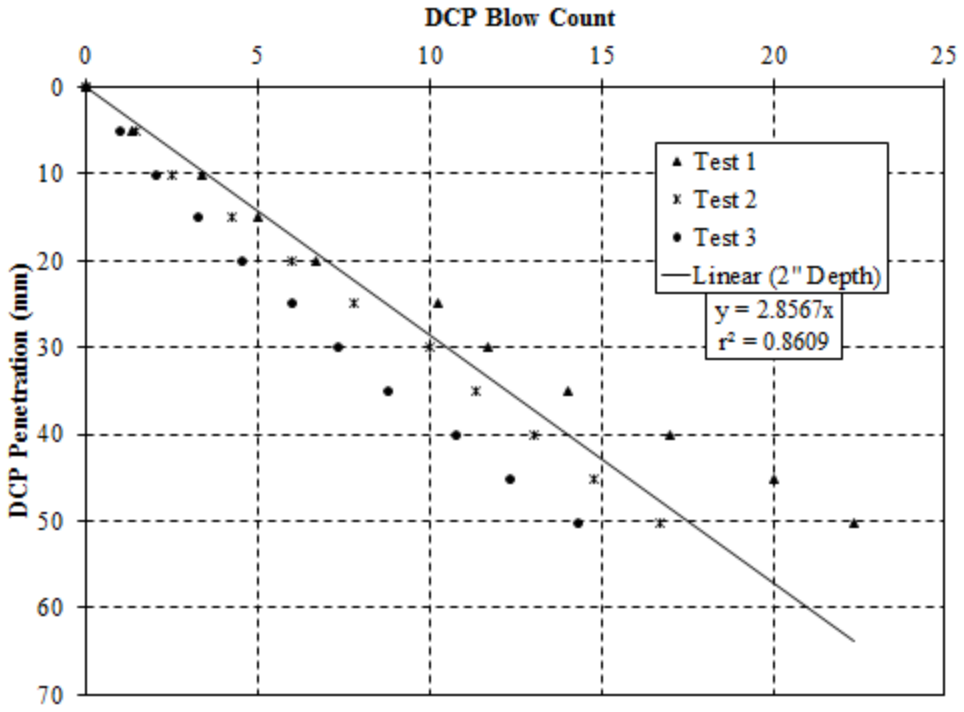

Figure E.30: Test conducted on April 5, 2017 Location 34 – compressive strength of 160 psi

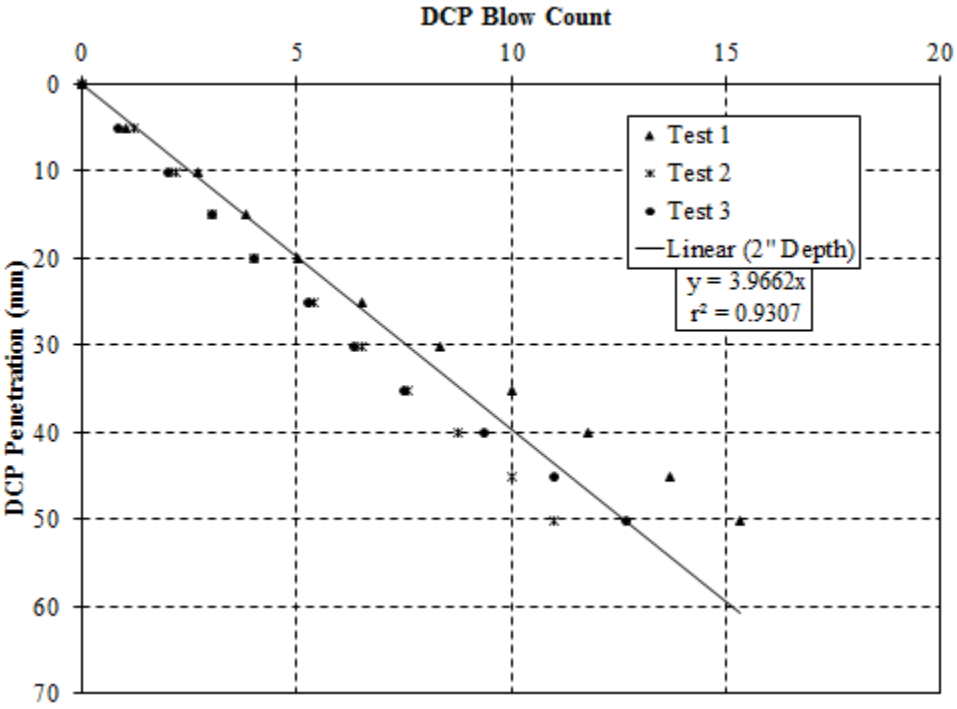

Figure E.31: Test conducted on April 5, 2017 Location 35 – compressive strength of 80 psi

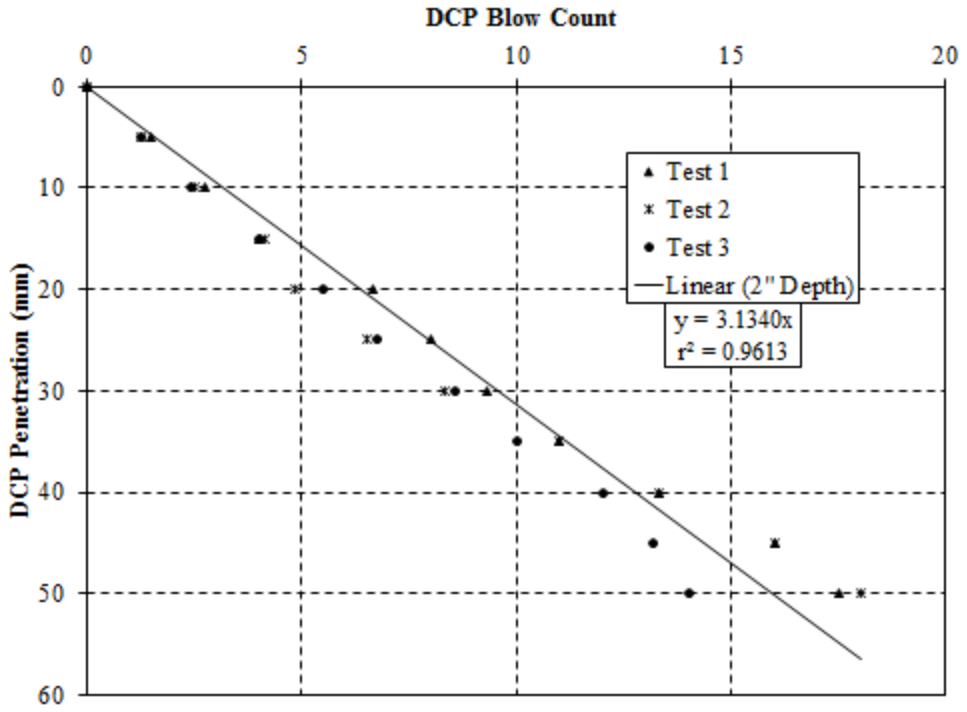

Figure E.32: Test conducted on April 5, 2017 Location 36 – compressive strength of 130 psi

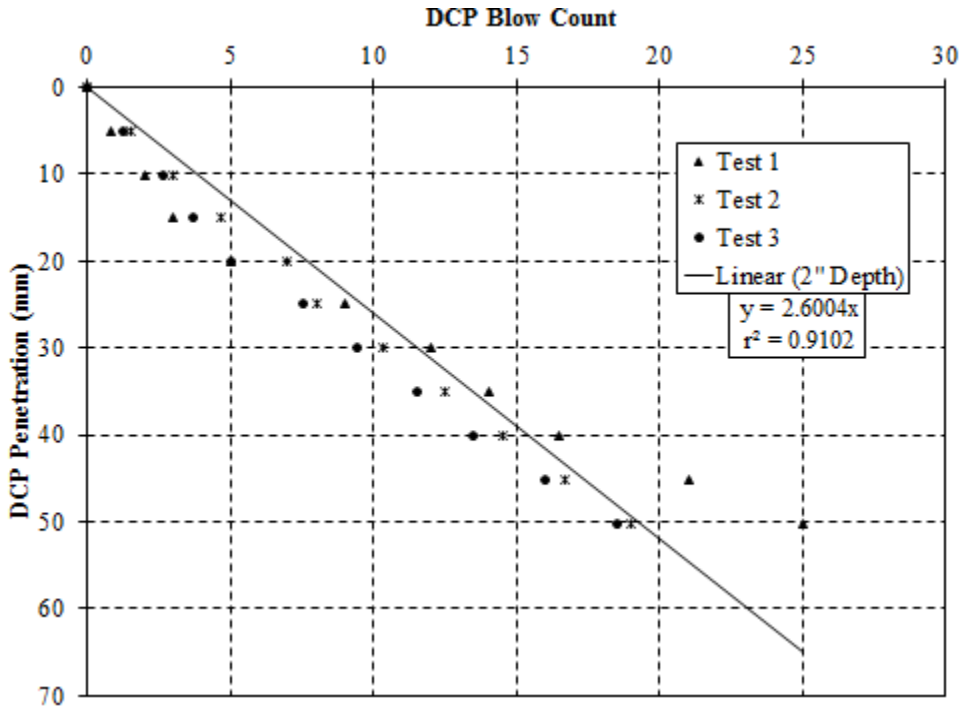

Figure E.33: Test conducted on April 5, 2017 Location 37 – compressive strength of 190 psi

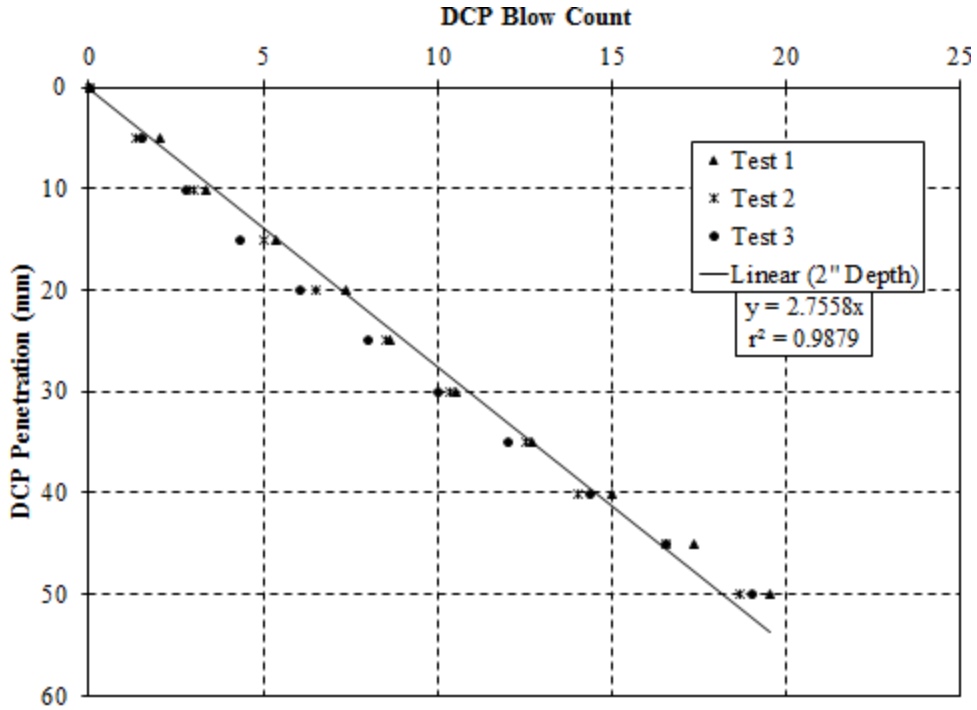

Figure E.34: Test conducted on April 6, 2017 Location 38 – compressive strength of 170 psi

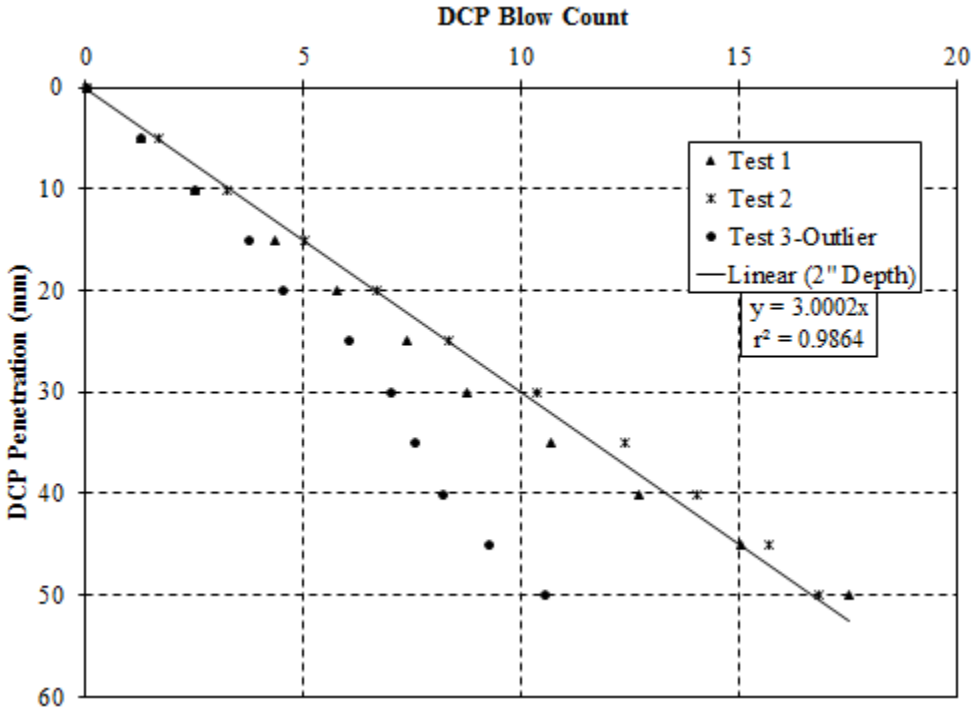

Figure E.35: Test conducted on April 6, 2017 Location 40 – compressive strength of 150 psi

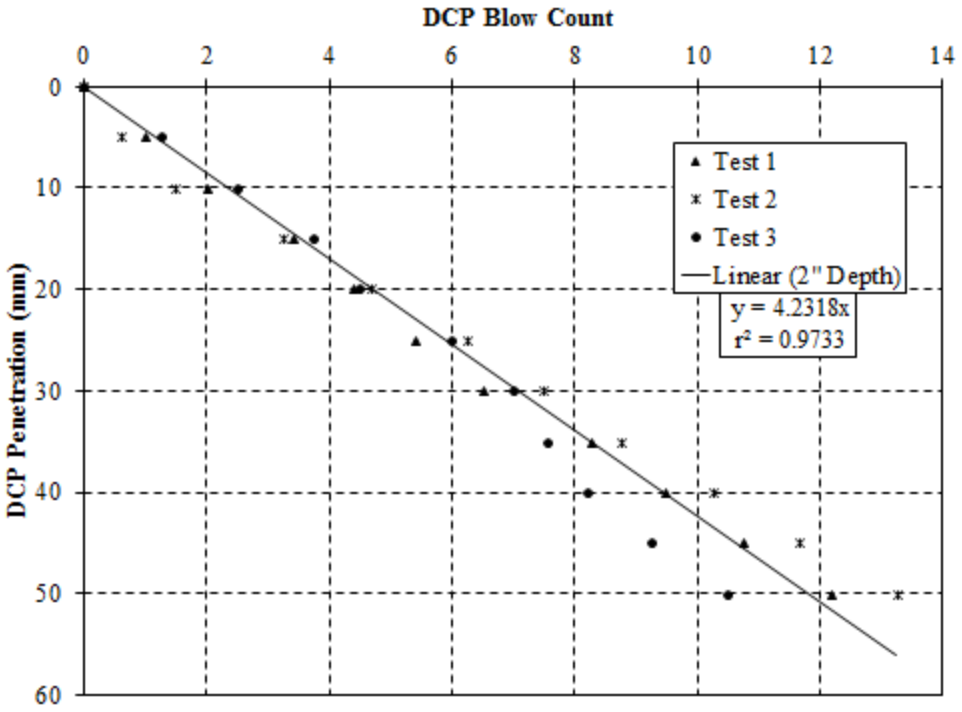

Figure E.36: Test conducted on April 19, 2017 Location 41 – compressive strength of 70 psi

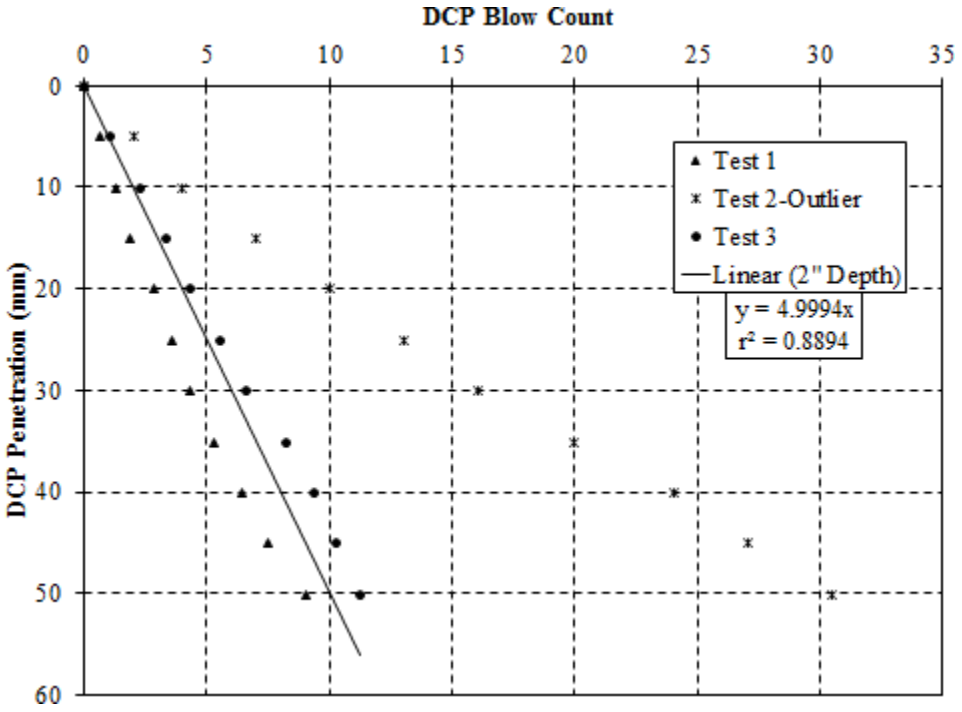

Figure E.37: Test conducted on April 19, 2017 Location 42 – compressive strength of 40 psi

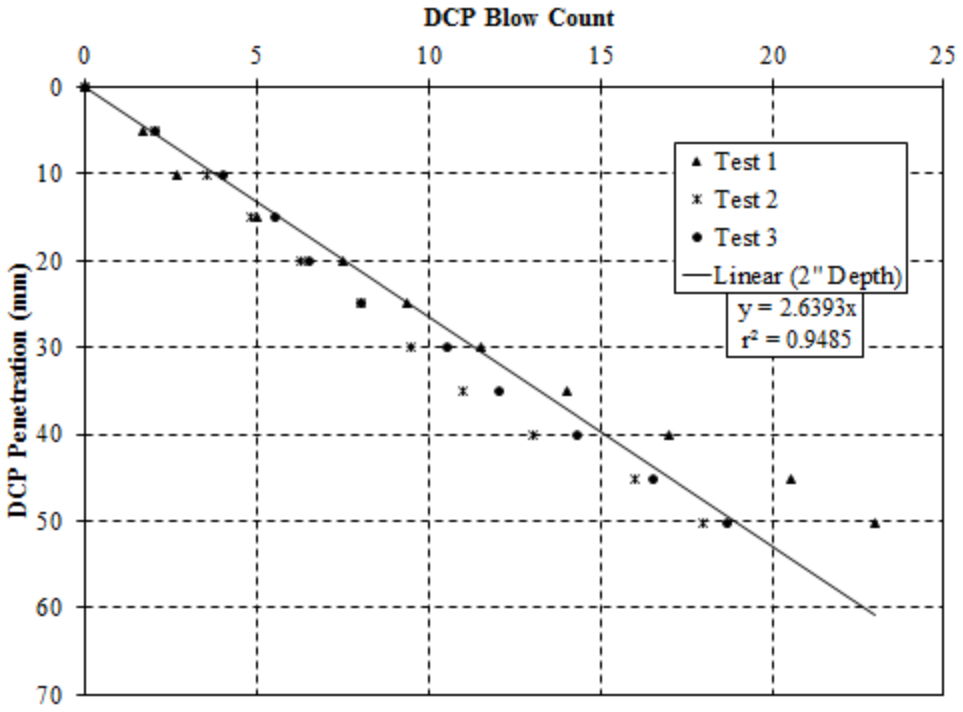

Figure E.38: Test conducted on April 19, 2017 Location 43 – compressive strength of 180 psi

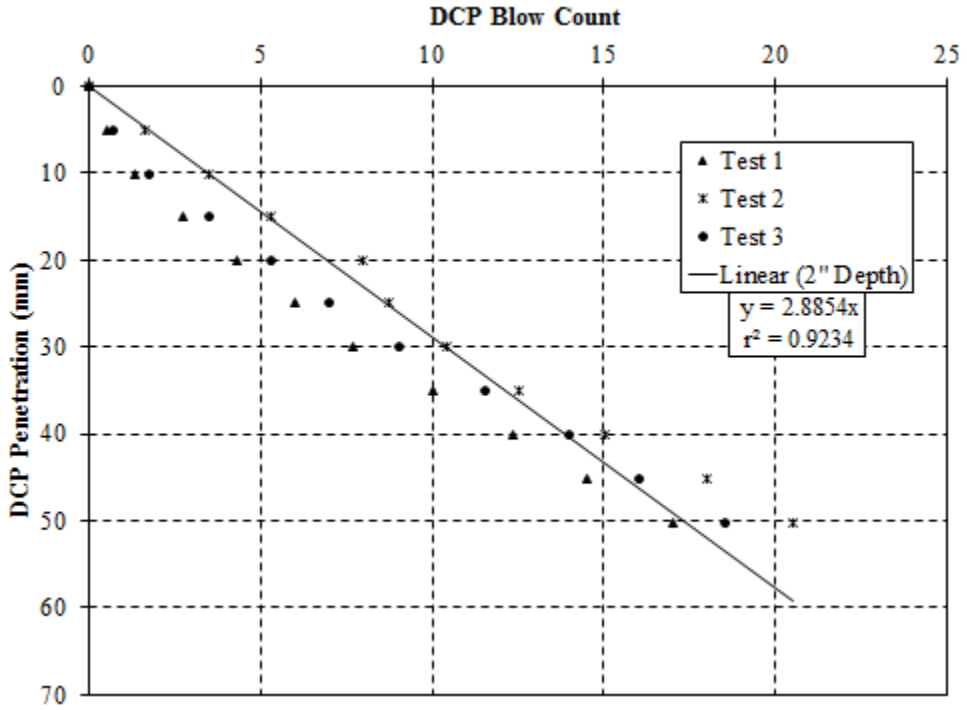

Figure E.39: Test conducted on April 19, 2017 Location 44 – compressive strength of 160 psi

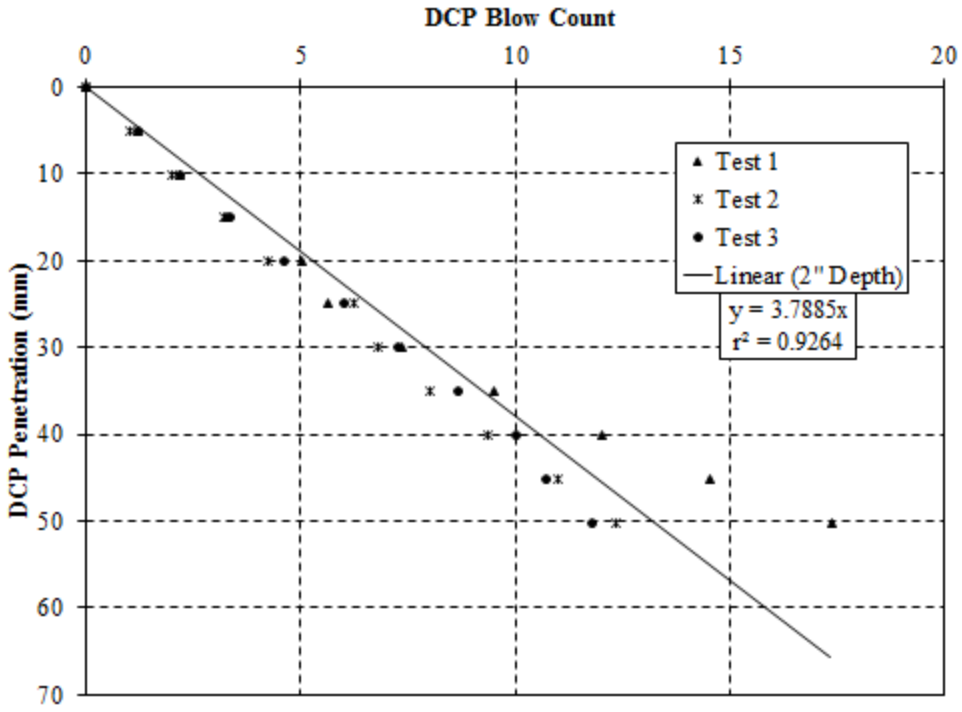

Figure E.40: Test conducted on April 19, 2017 Location 45 – compressive strength of 90 psi

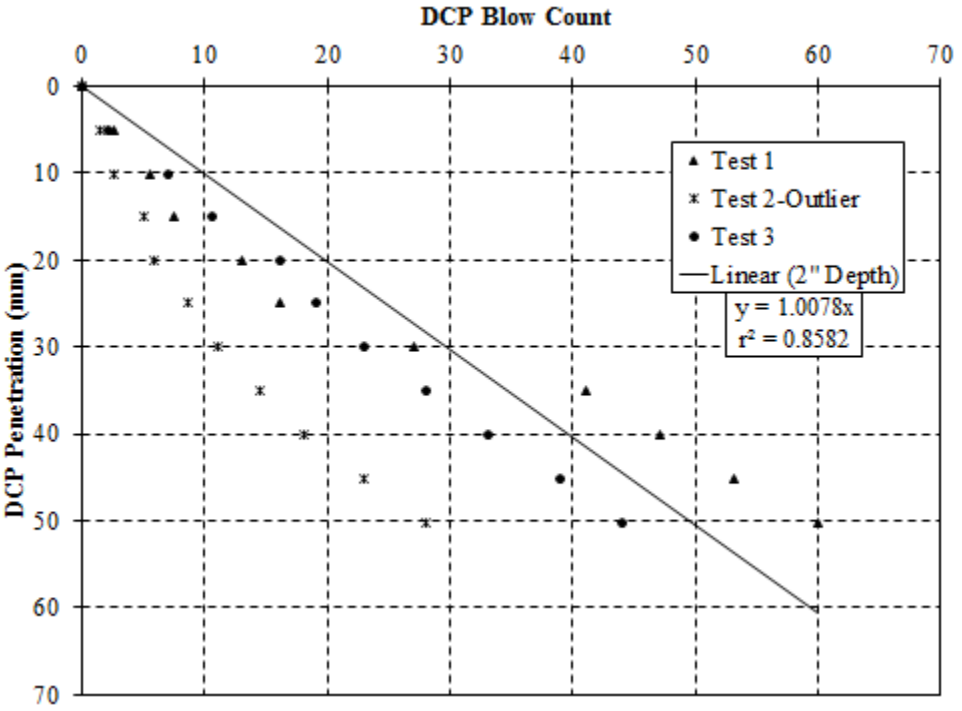

Figure E.41: Test conducted on April 19, 2017 Location 46 – compressive strength of 500 psi

Appendix F

75 mm Penetration

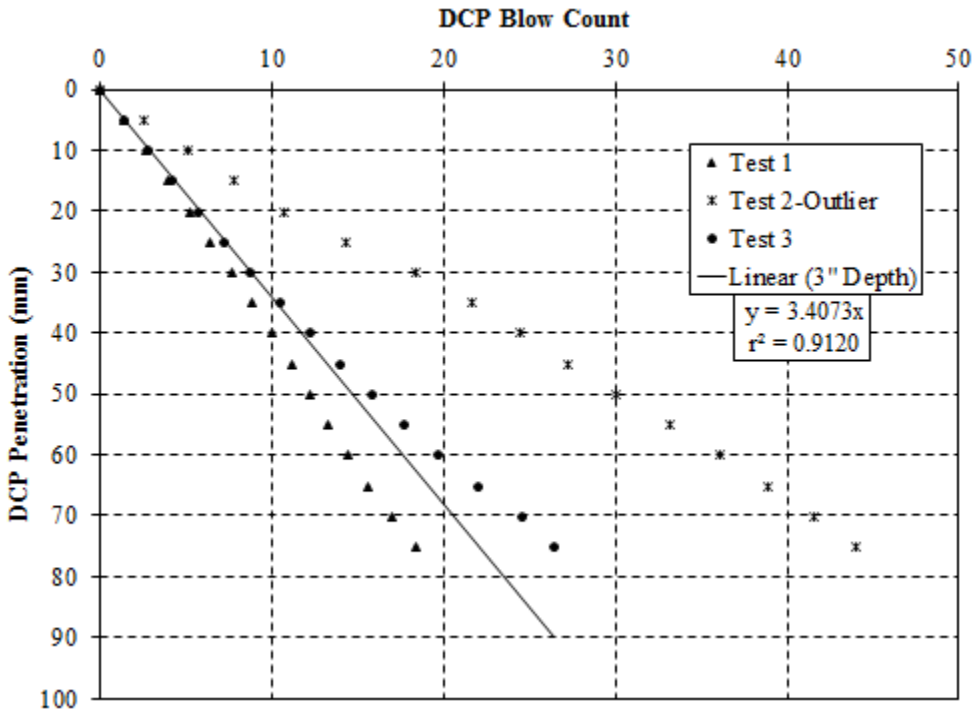

Figure F.1: Test conducted on November 1, 2016 Location 1 – compressive strength of 110 psi

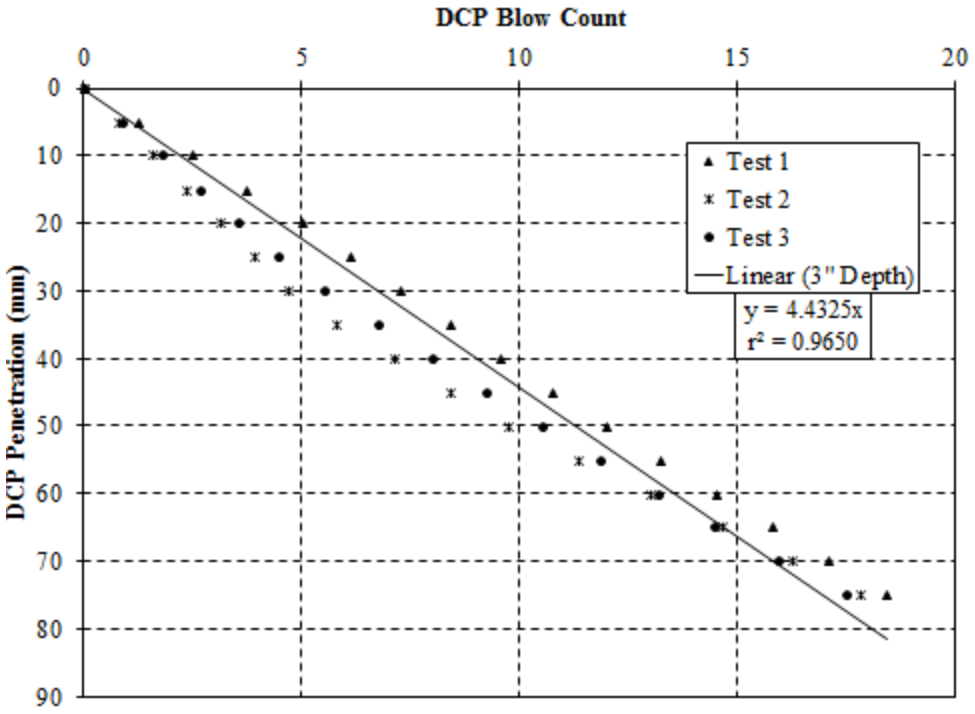

Figure F.2: Test conducted on November 1, 2016 Location 2– compressive strength of 60 psi

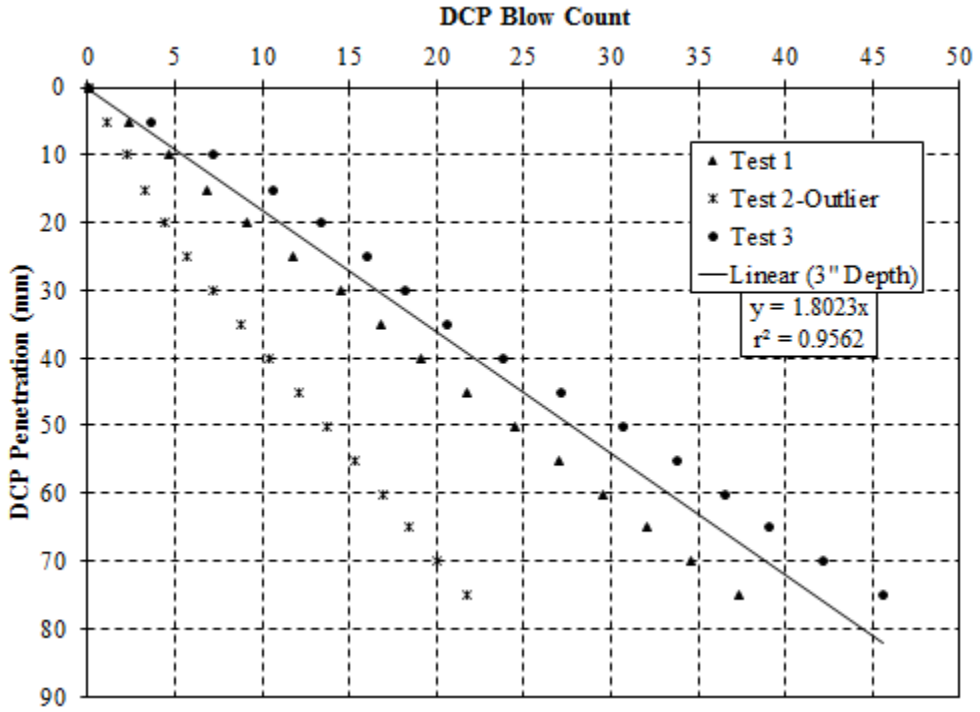

Figure F.3: Test conducted on November 7, 2016 Location 6 – compressive strength of 310 psi

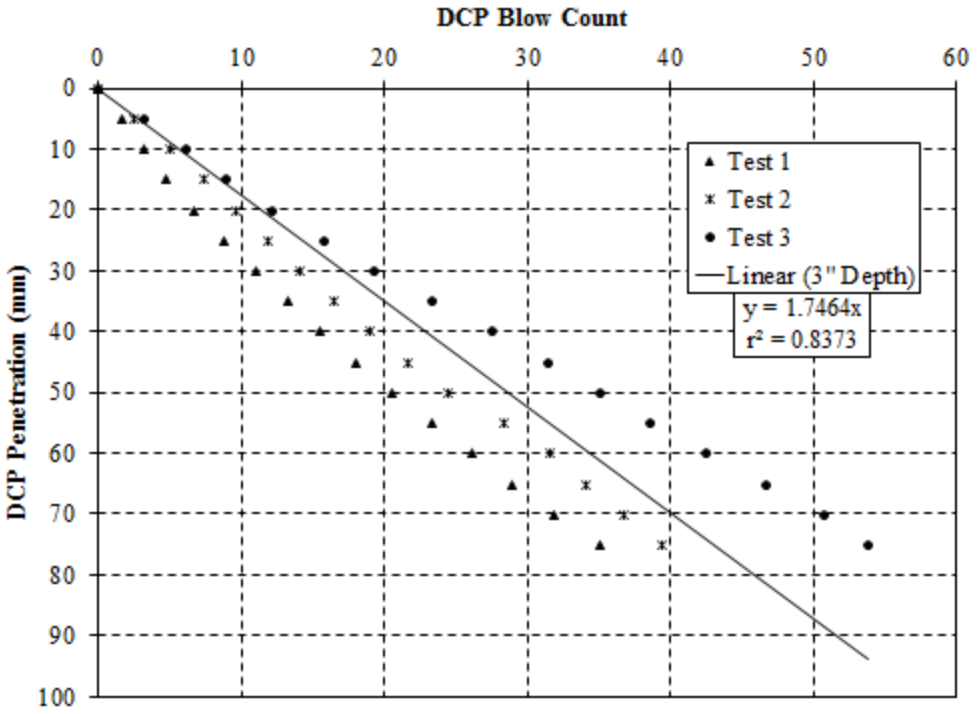

Figure F.4: Test conducted on November 7, 2016 Location 7 – compressive strength of 320 psi

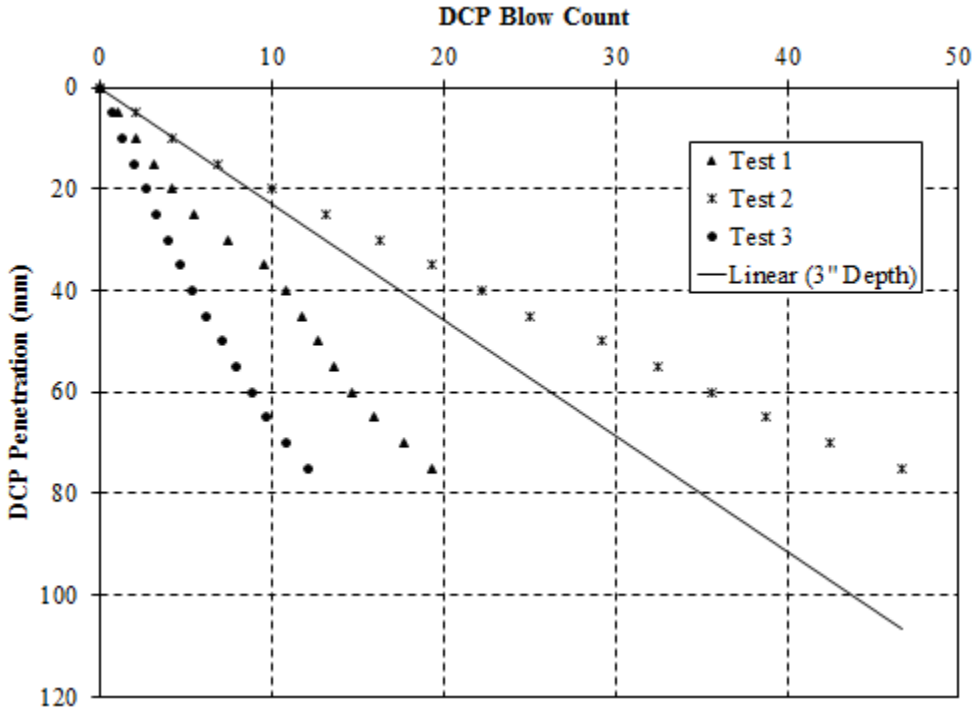

Figure F.5: Test conducted on November 22, 2016 Location 8 – range greater than 50 %

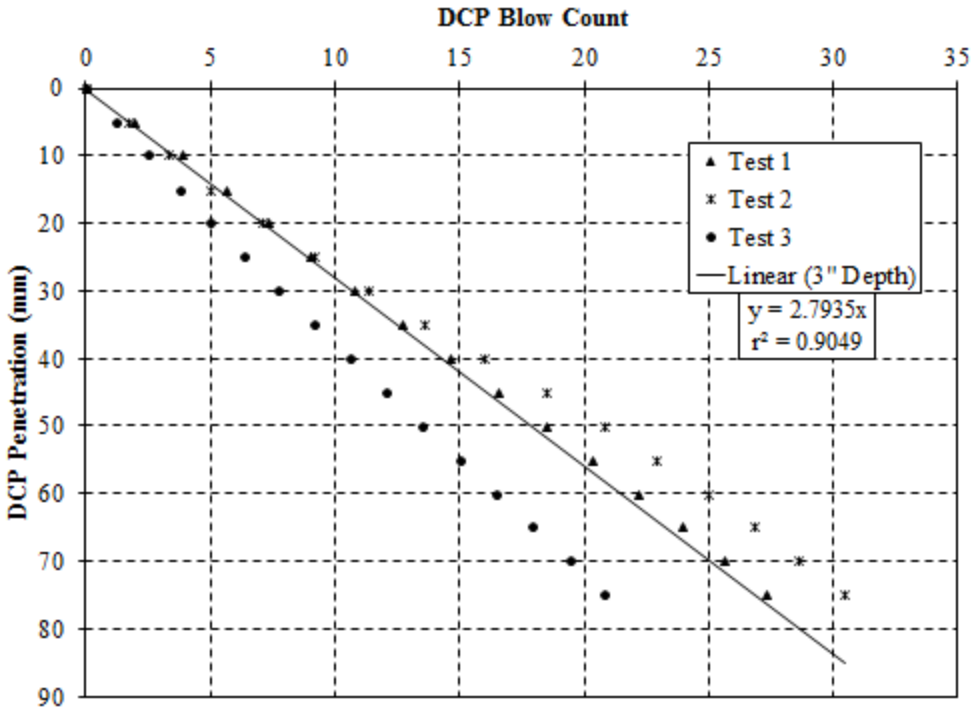

Figure F.6: Test conducted on November 22, 2016 Location 9 – compressive strength of 170 psi

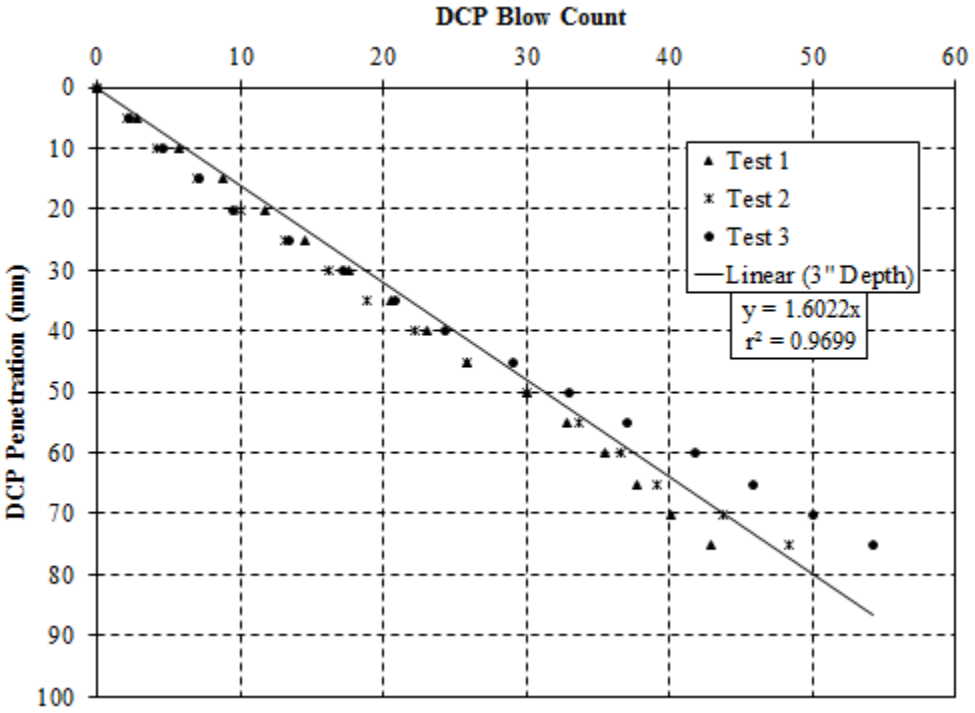

Figure F.7: Test conducted on November 22, 2016 Location 10–compressive strength of 350 psi

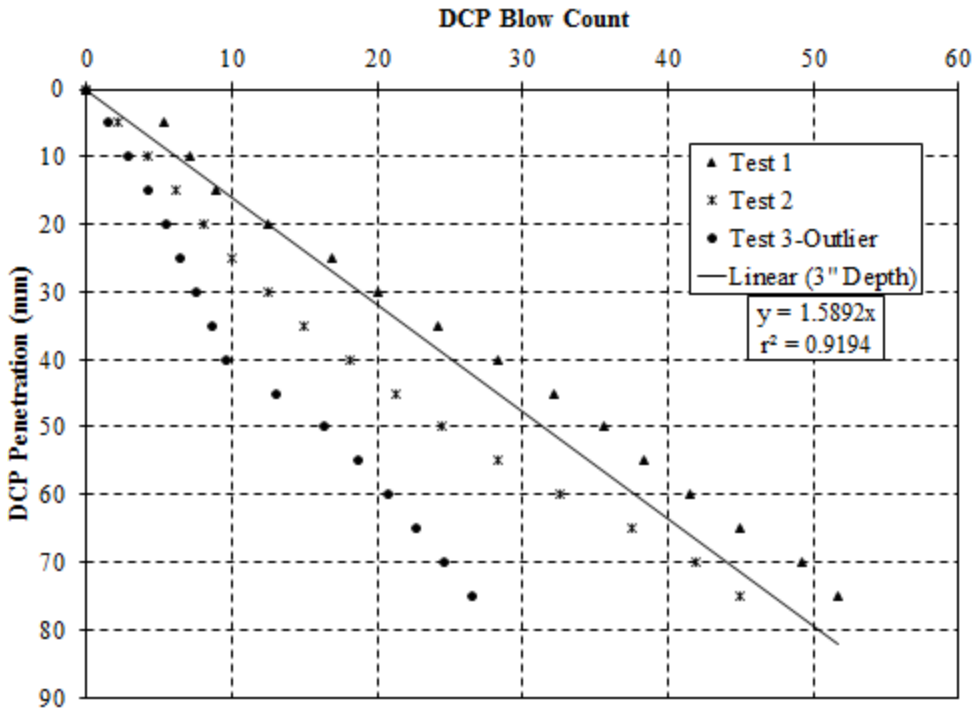

Figure F.8: Test conducted on November 22, 2016 Location 12–compressive strength of 350 psi

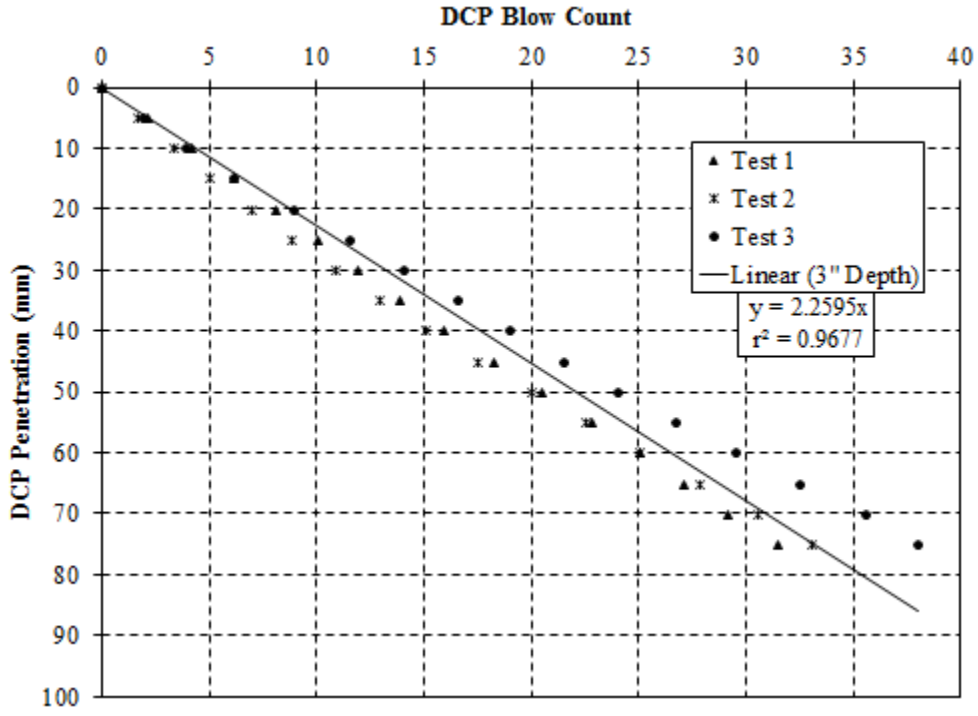

Figure F.9: Test conducted on November 22, 2016 Location 13–compressive strength of 230 psi

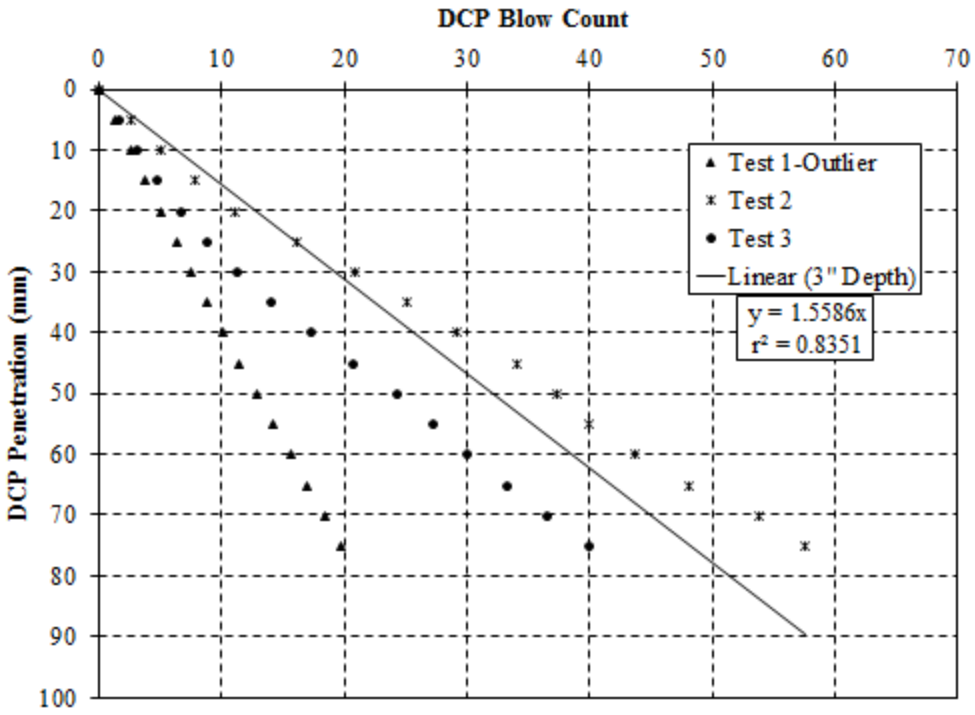

Figure F.10: Test conducted on November 23, 2016 Location 14–compressive strength of 360 psi

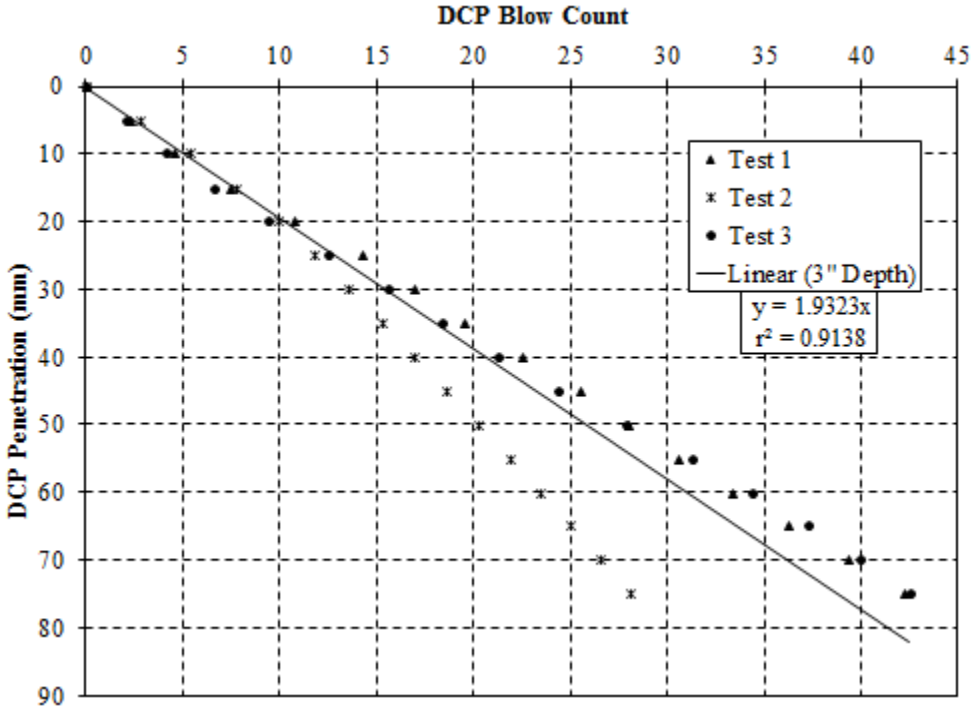

Figure F.11: Test conducted on November 23, 2016 Location 15–compressive strength of 280 psi

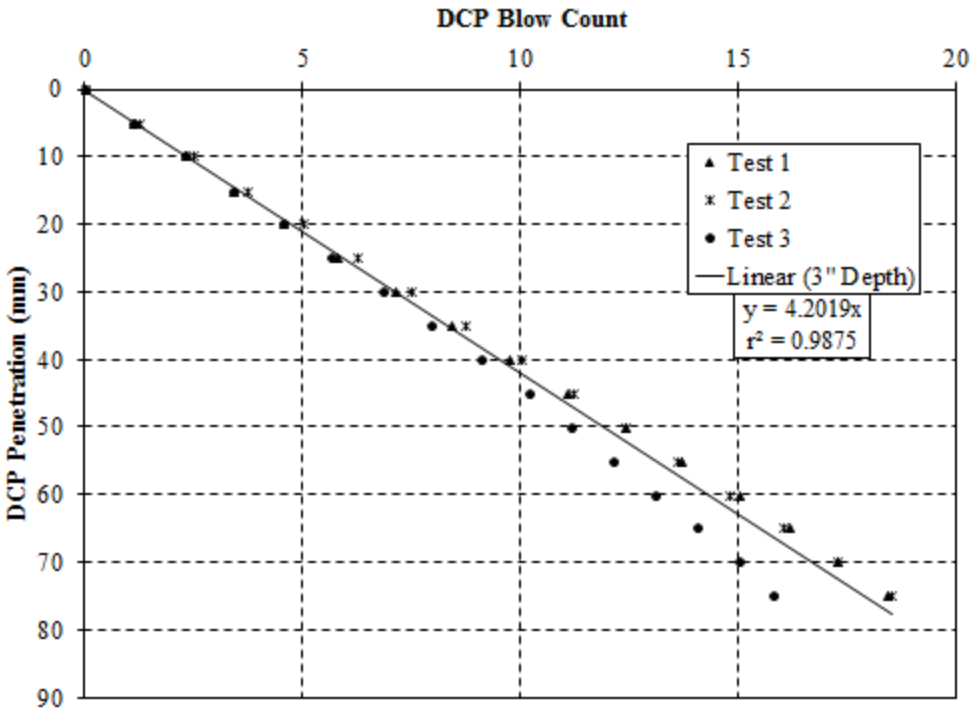

Figure F.12: Test conducted on November 23, 2016 Location 16–compressive strength of 70 psi

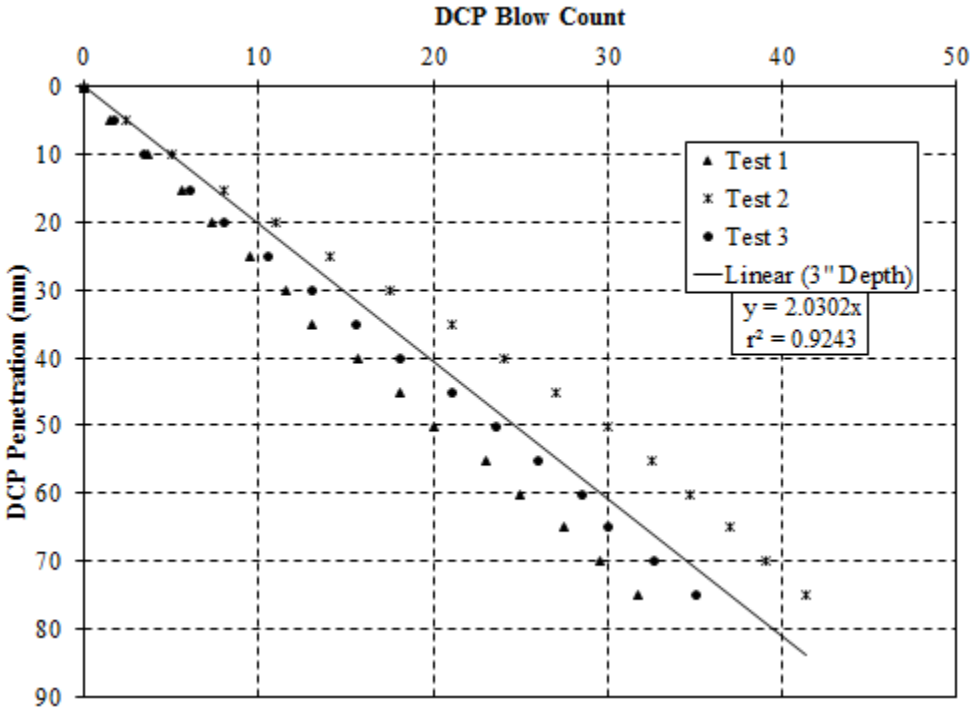

Figure F.13: Test conducted on March 23, 2017 Location 17 – compressive strength of 270 psi

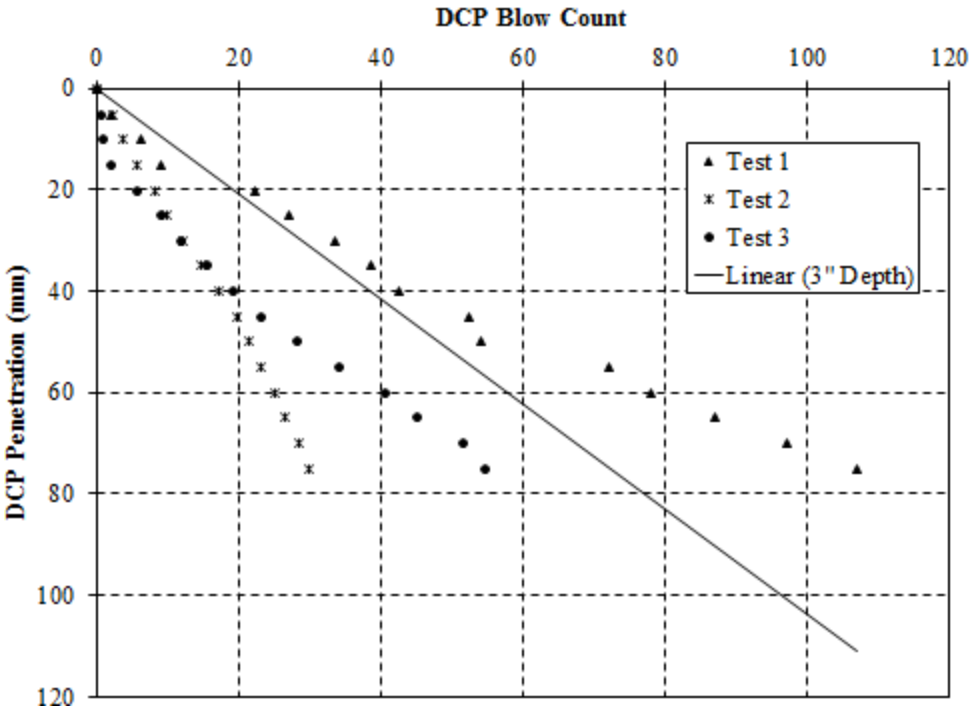

Figure F.14: Test conducted on March 23, 2017 Location 18 – range greater than 50 %

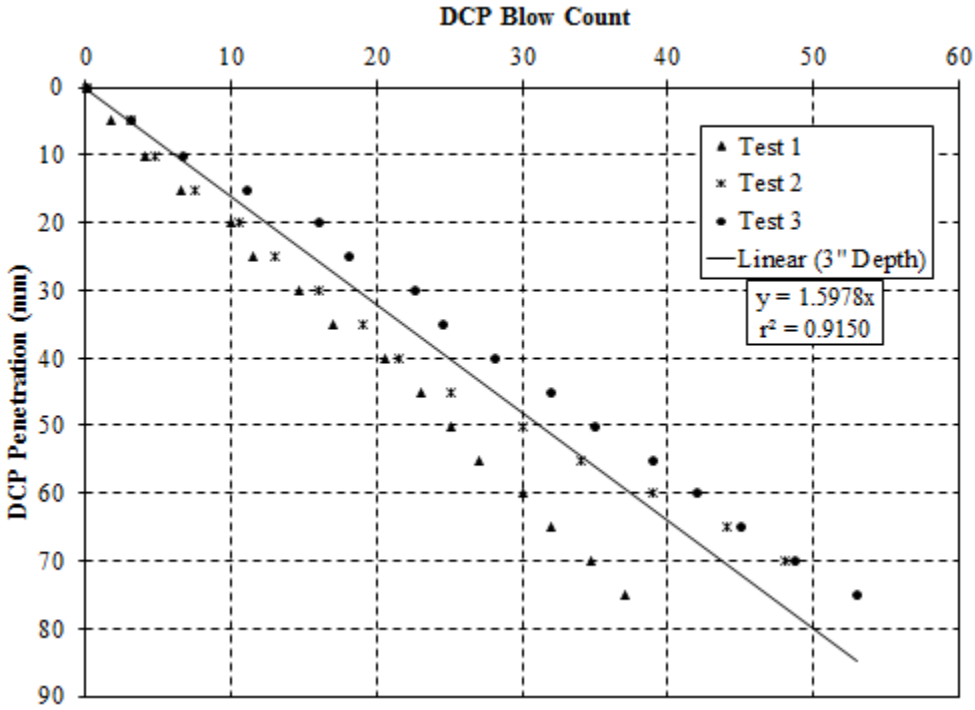

Figure F.15: Test conducted on March 23, 2017 Location 19 – compressive strength of 350 psi

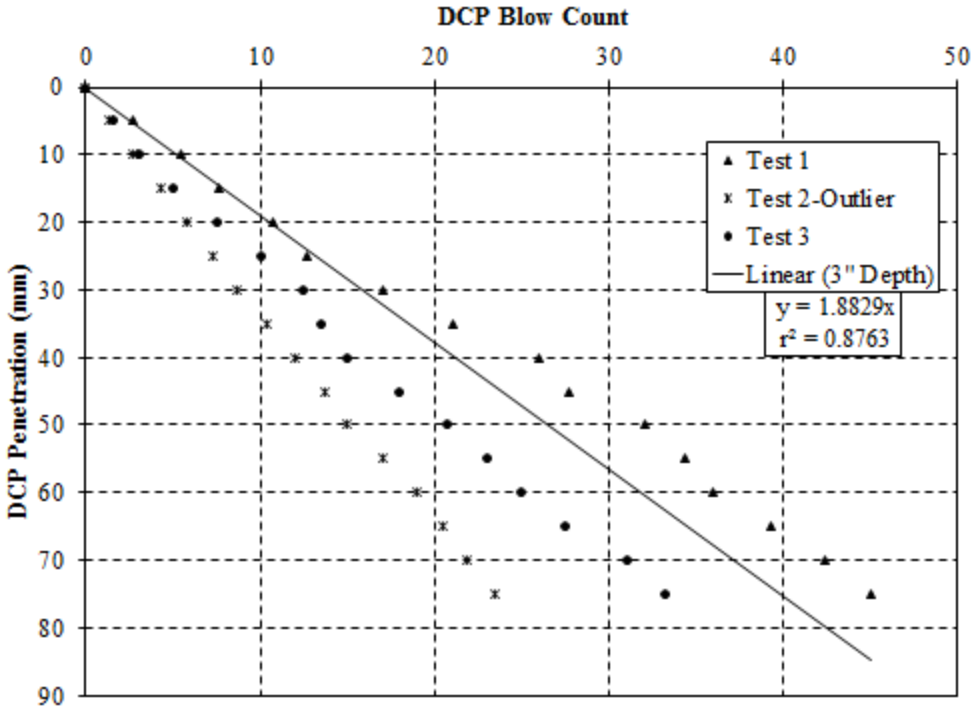

Figure F.16: Test conducted on March 27, 2017 Location 20 – compressive strength of 290 psi

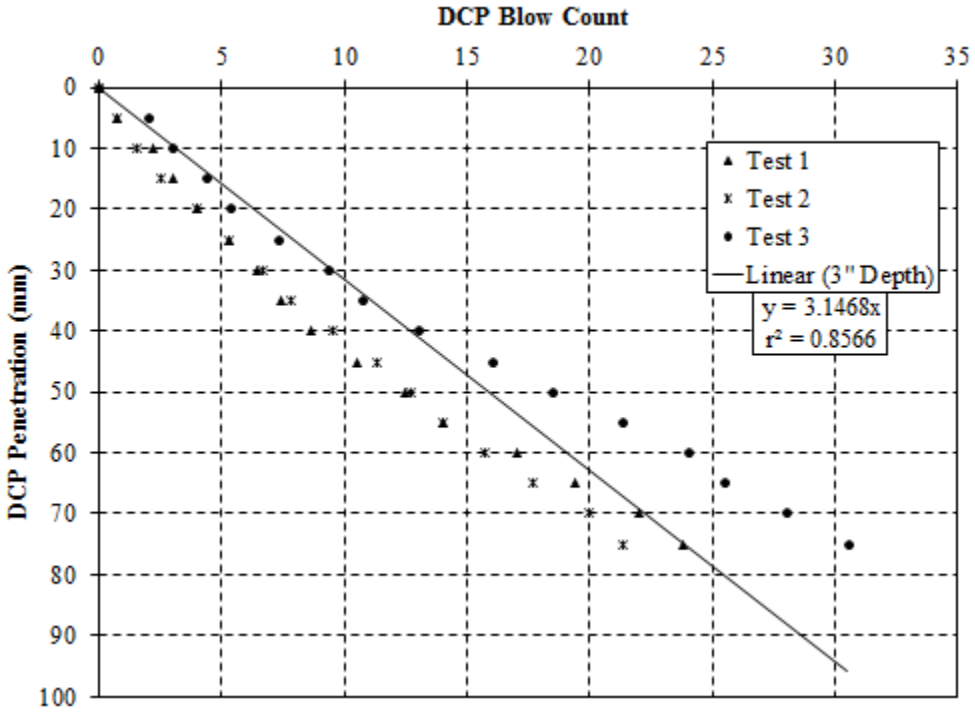

Figure F.17: Test conducted on March 27, 2017 Location 21 – compressive strength of 130 psi

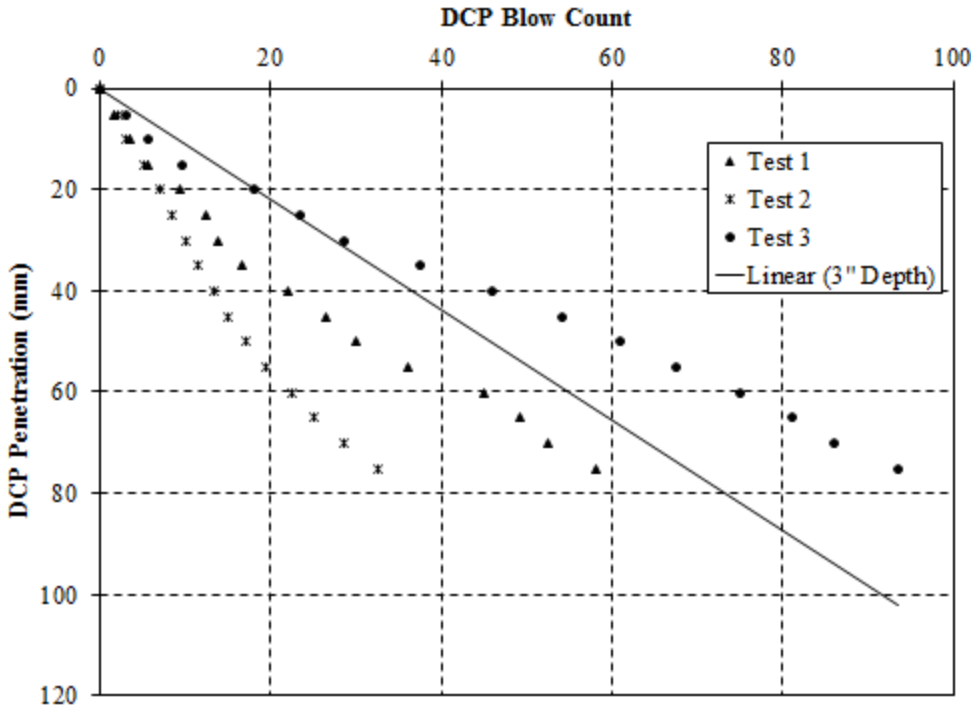

Figure F.18: Test conducted on March 27, 2017 Location 22 – range greater than 50 %

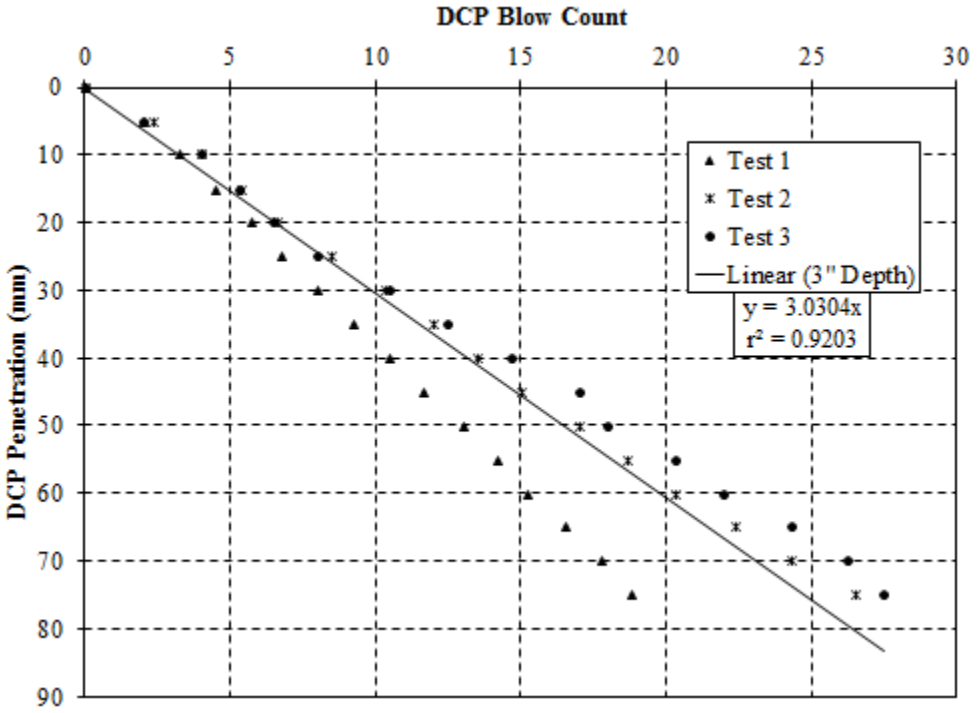

Figure F.19: Test conducted on March 30, 2017 Location 23 – compressive strength of 140 psi

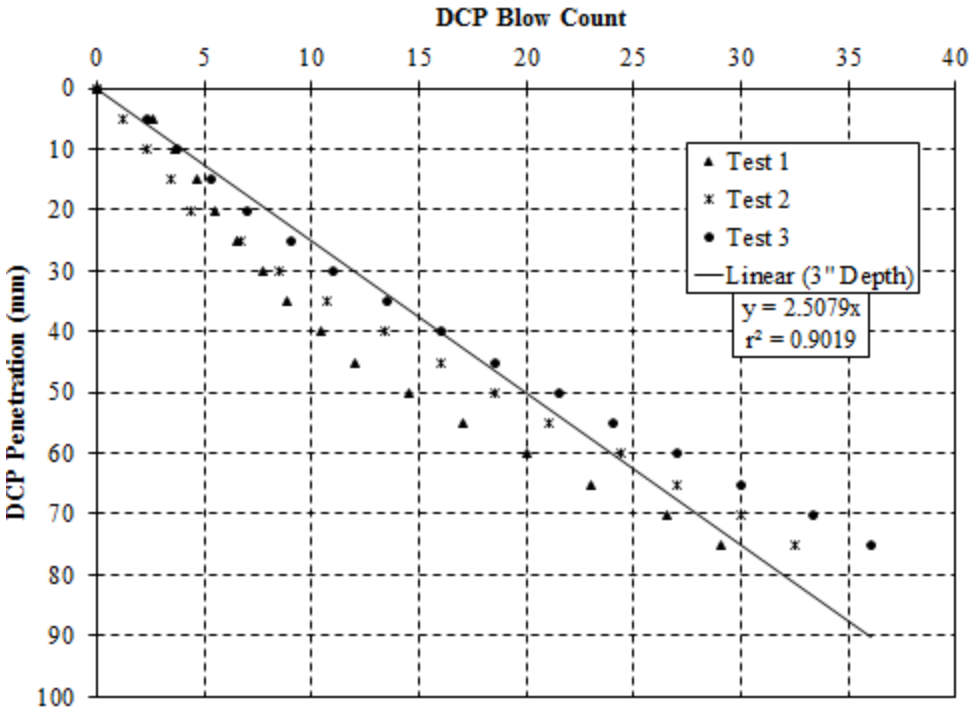

Figure F.20: Test conducted on March 30, 2017 Location 24 – compressive strength of 200 psi

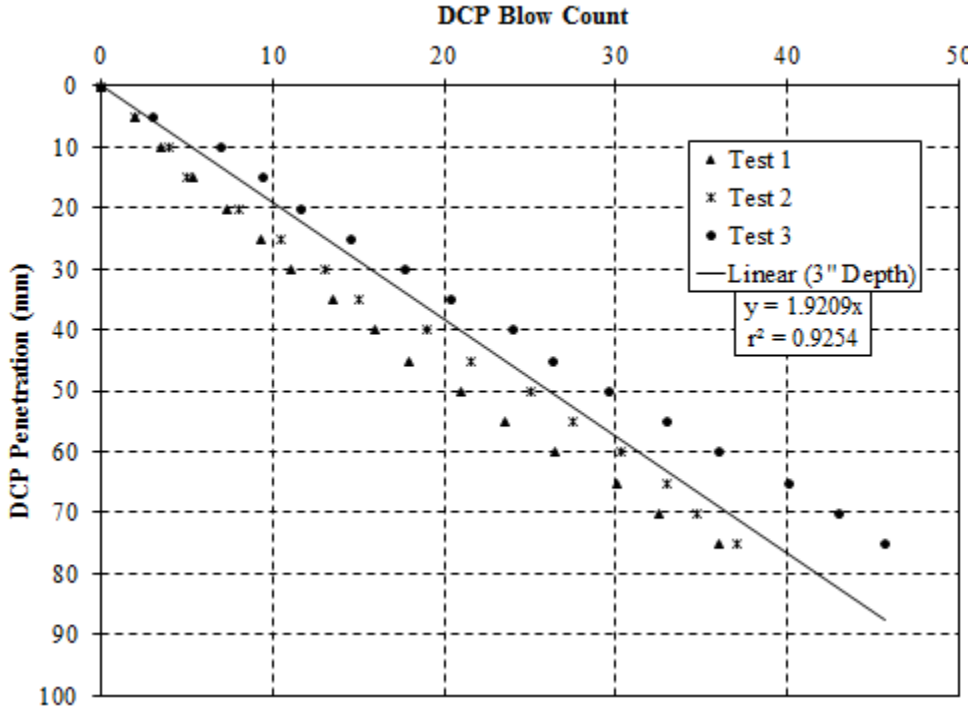

Figure F.21: Test conducted on March 30, 2017 Location 25 – compressive strength of 280 psi

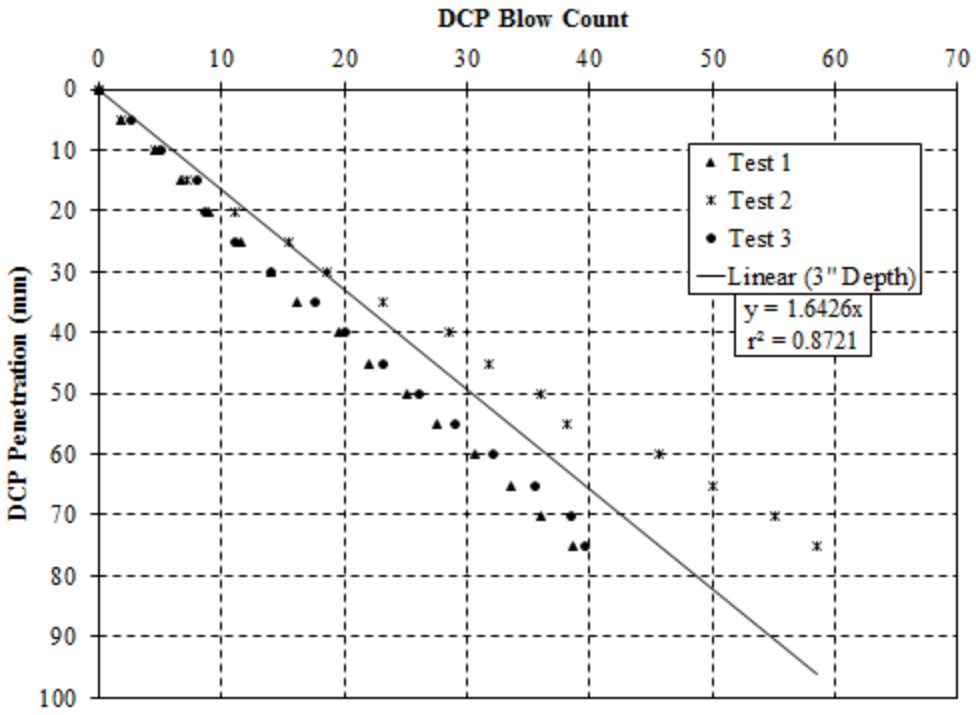

Figure F.22: Test conducted on March 31, 2017 Location 26 – compressive strength of 340 psi

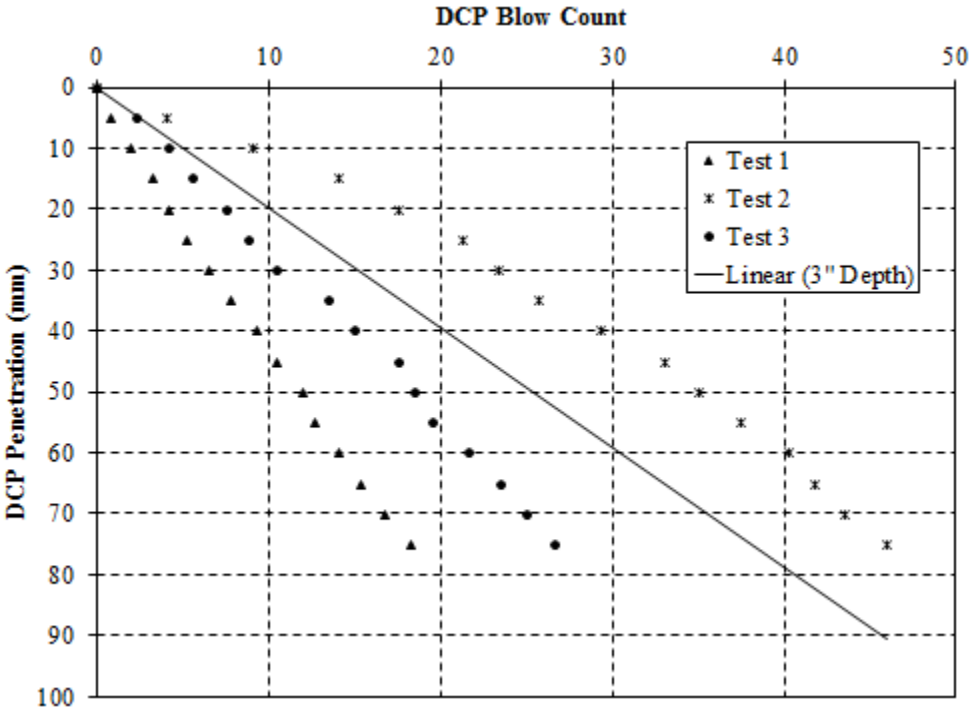

Figure F.23: Test conducted on March 31, 2017 Location 27 – range greater than 50 %

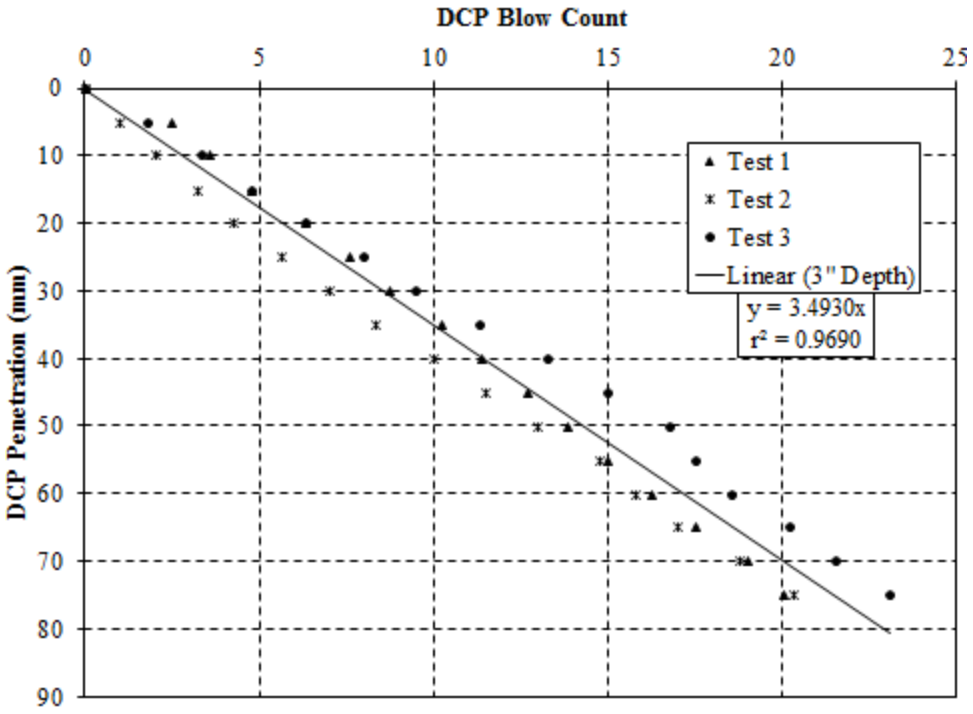

Figure F.24: Test conducted on March 31, 2017 Location 28 – compressive strength of 130 psi

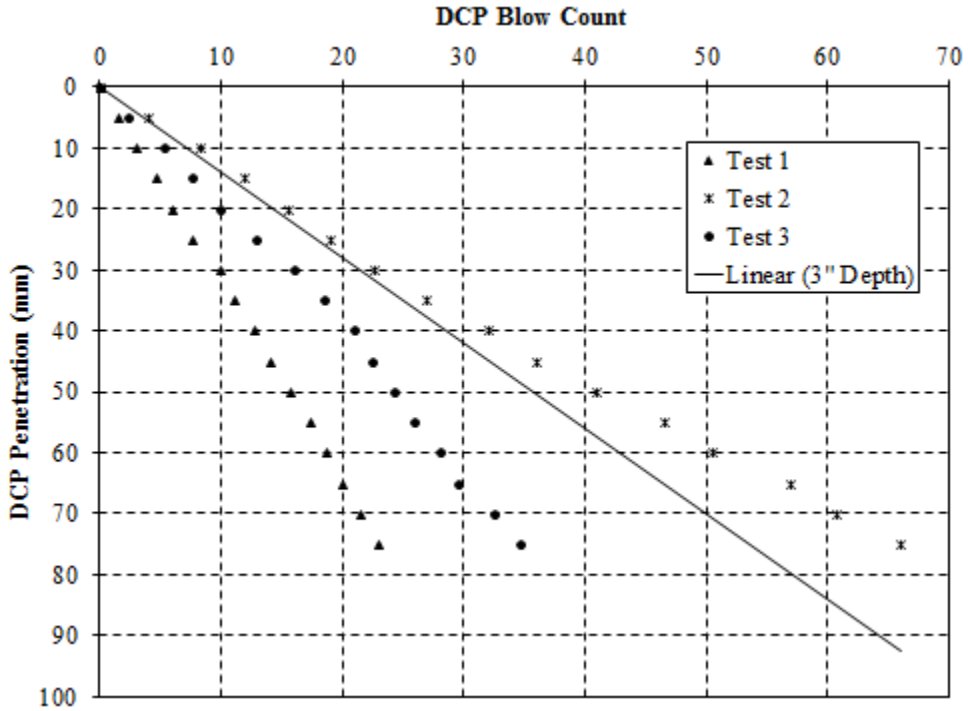

Figure F.25: Test conducted on April 3, 2017 Location 29 – range greater than 50 %

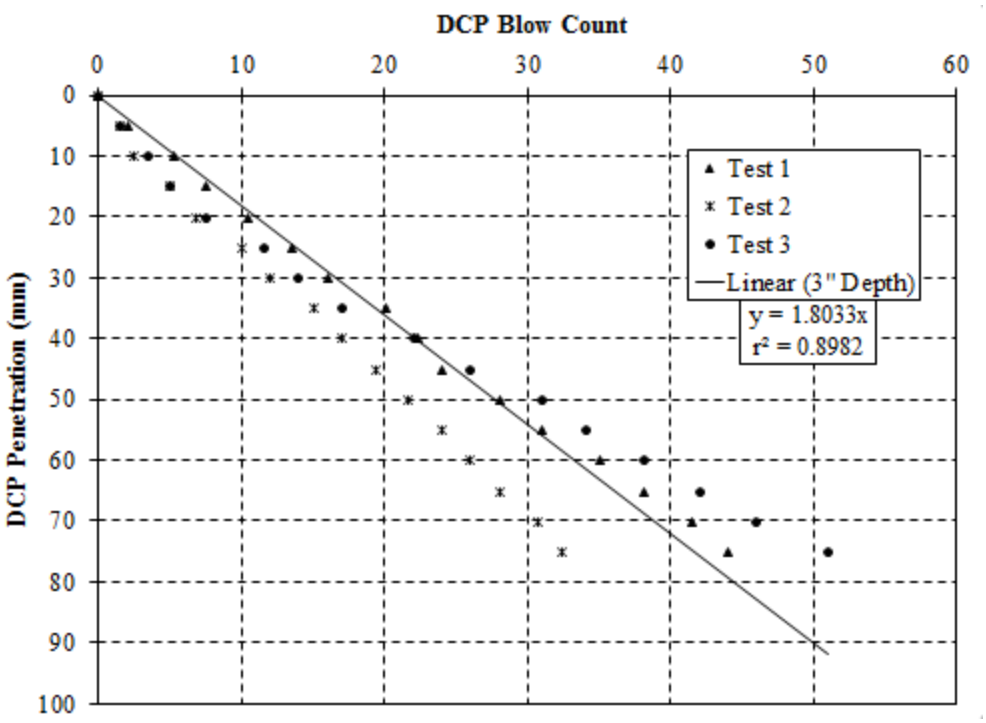

Figure F.26: Test conducted on April 3, 2017 Location 30 – compressive strength of 310 psi

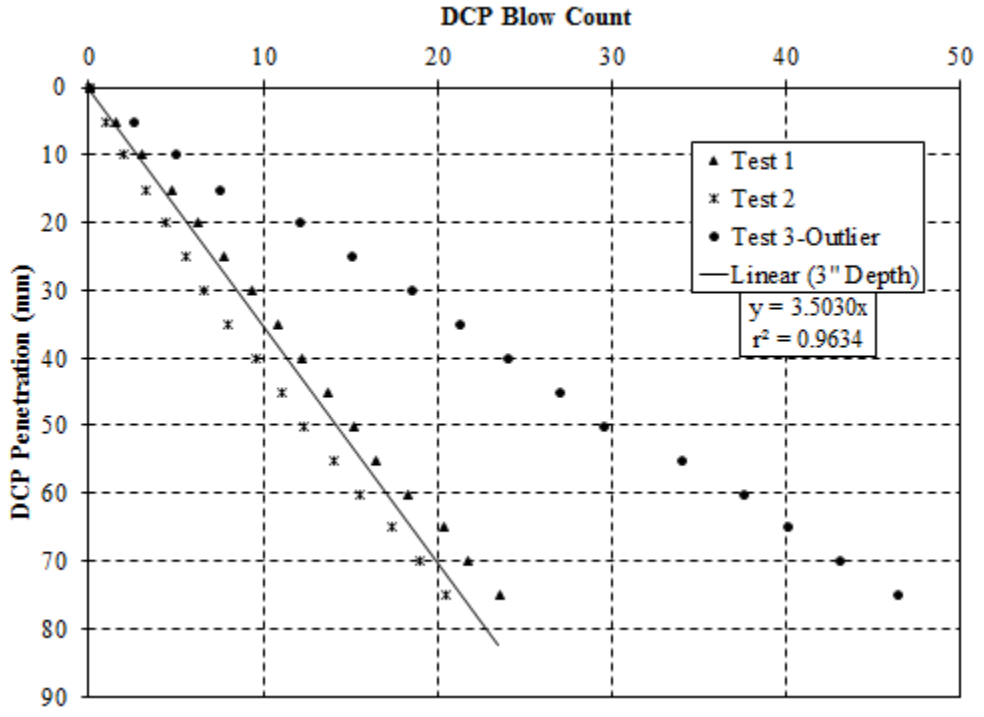

Figure F.27: Test conducted on April 3, 2017 Location 31 – compressive strength of 110 psi

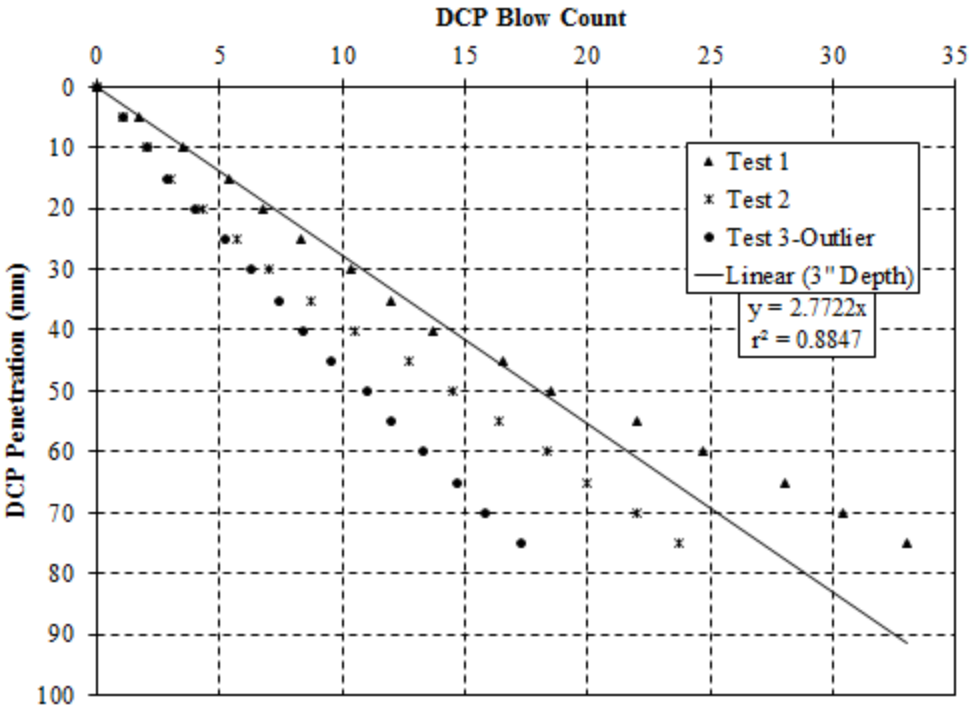

Figure F.28: Test conducted on April 5, 2017 Location 32 – compressive strength of 170 psi

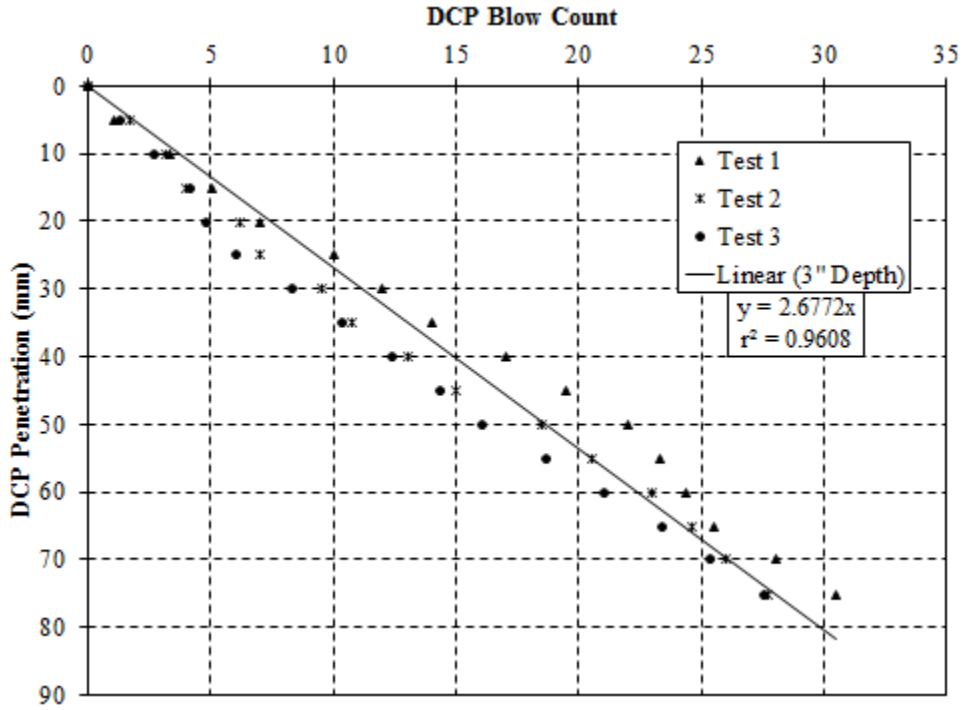

Figure F.29: Test conducted on April 5, 2017 Location 33 – compressive strength of 180 psi

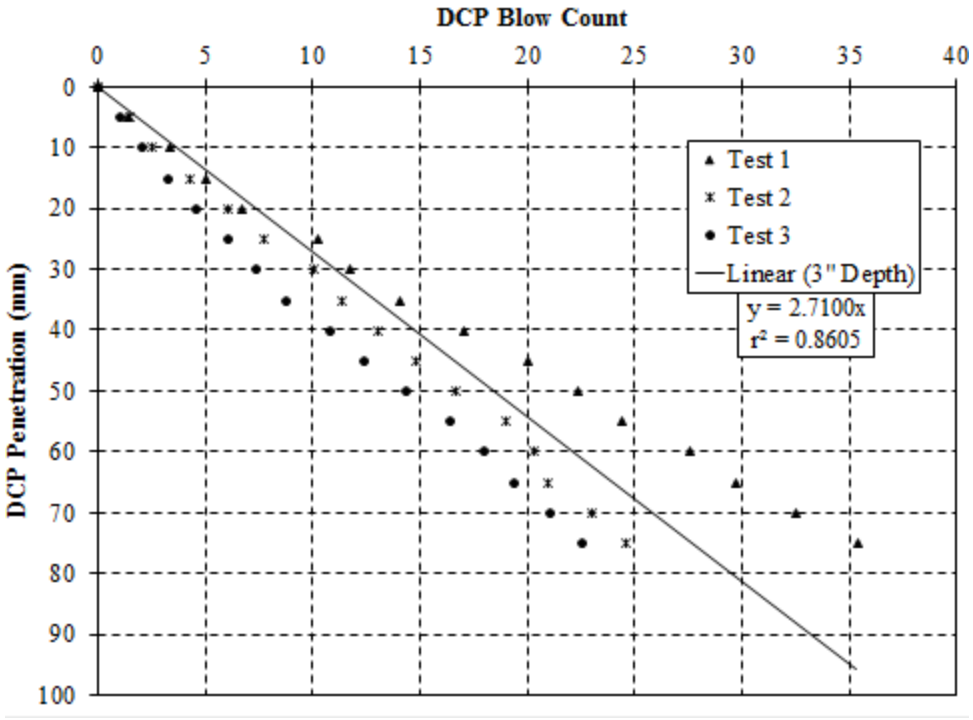

Figure F.30: Test conducted on April 5, 2017 Location 34 – compressive strength of 170 psi

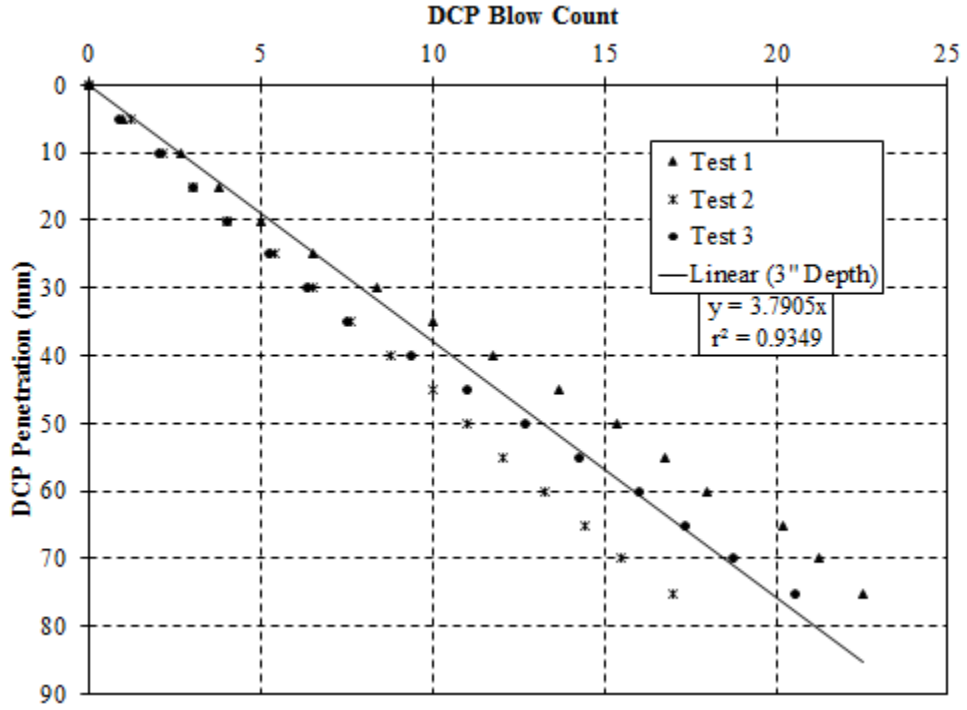

Figure F.31: Test conducted on April 5, 2017 Location 35 – compressive strength of 90 psi

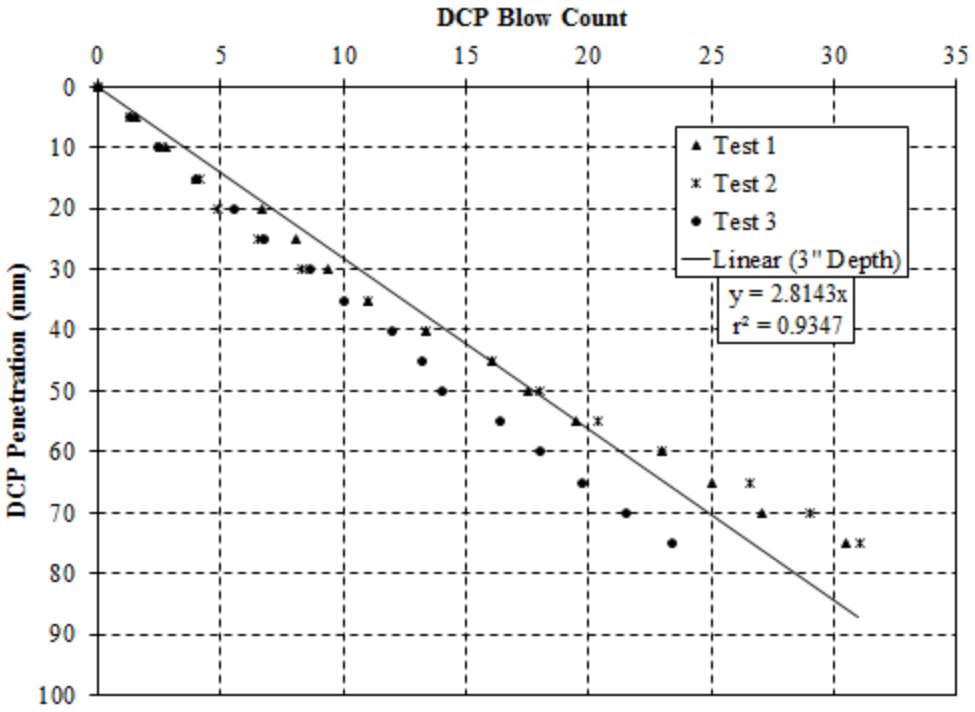

Figure F.32: Test conducted on April 5, 2017 Location 36 – compressive strength of 160 psi

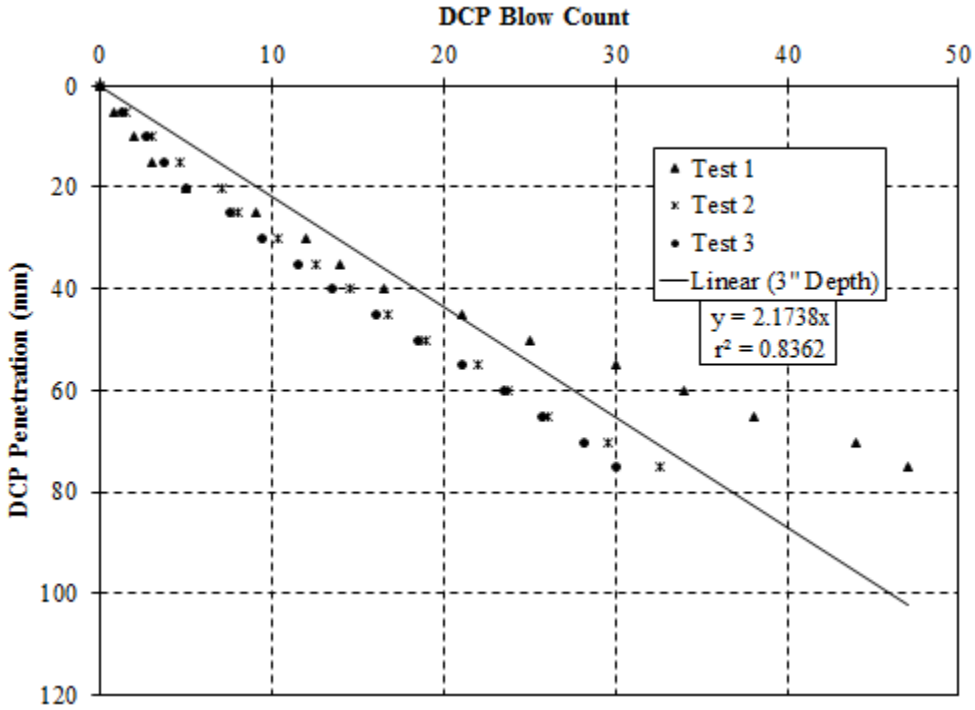

Figure F.33: Test conducted on April 5, 2017 Location 37 – compressive strength of 240 psi

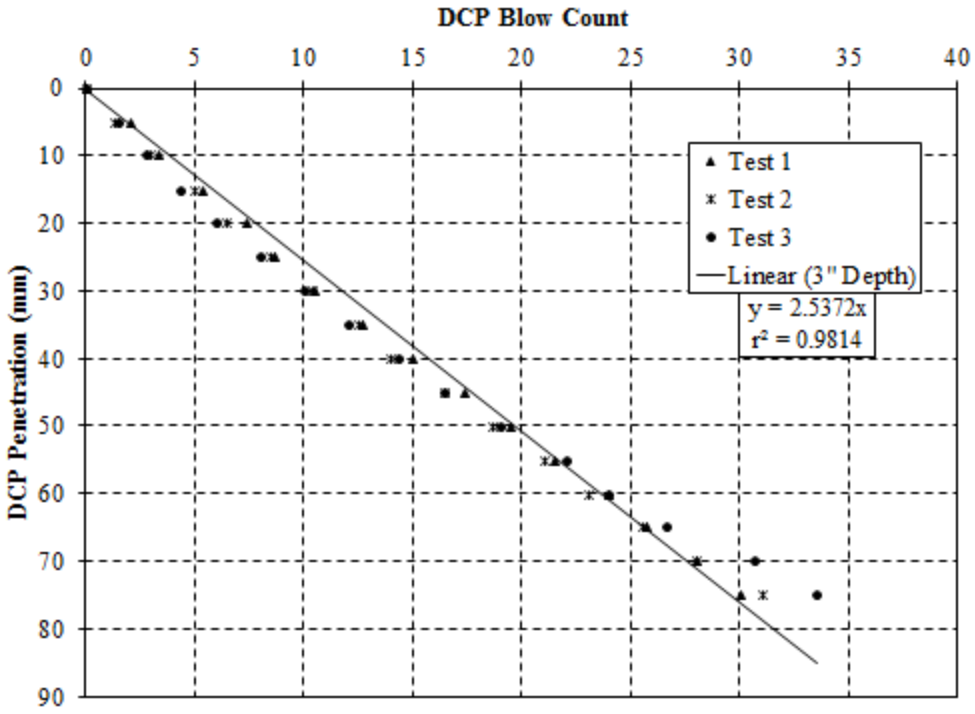

Figure F.34: Test conducted on April 6, 2017 Location 38 – compressive strength of 190 psi

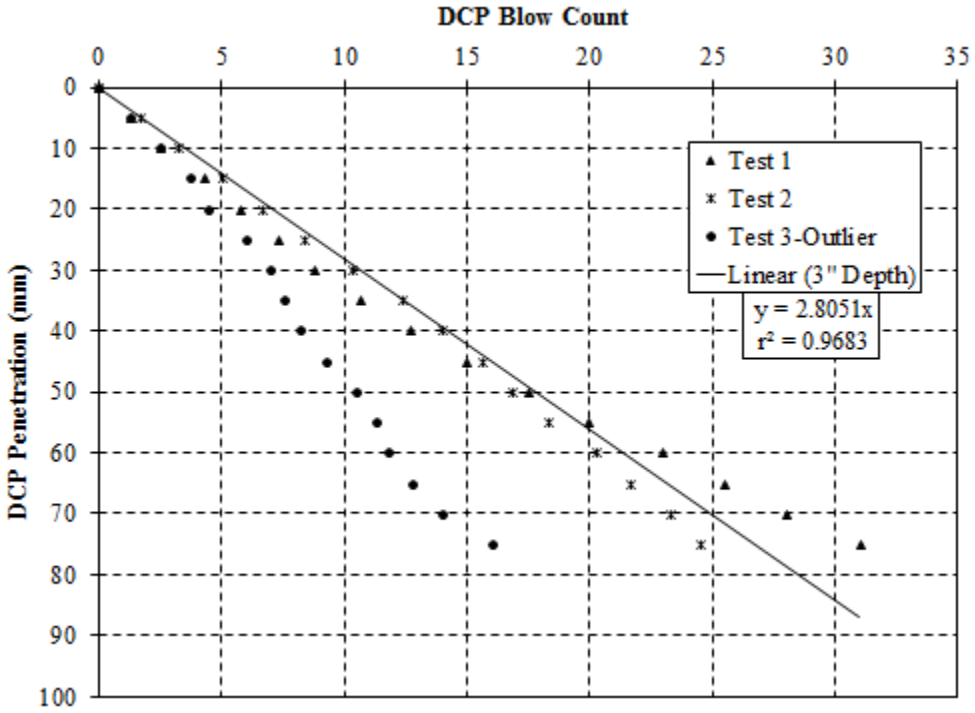

Figure F.35: Test conducted on April 6, 2017 Location 40 – compressive strength of 160 psi

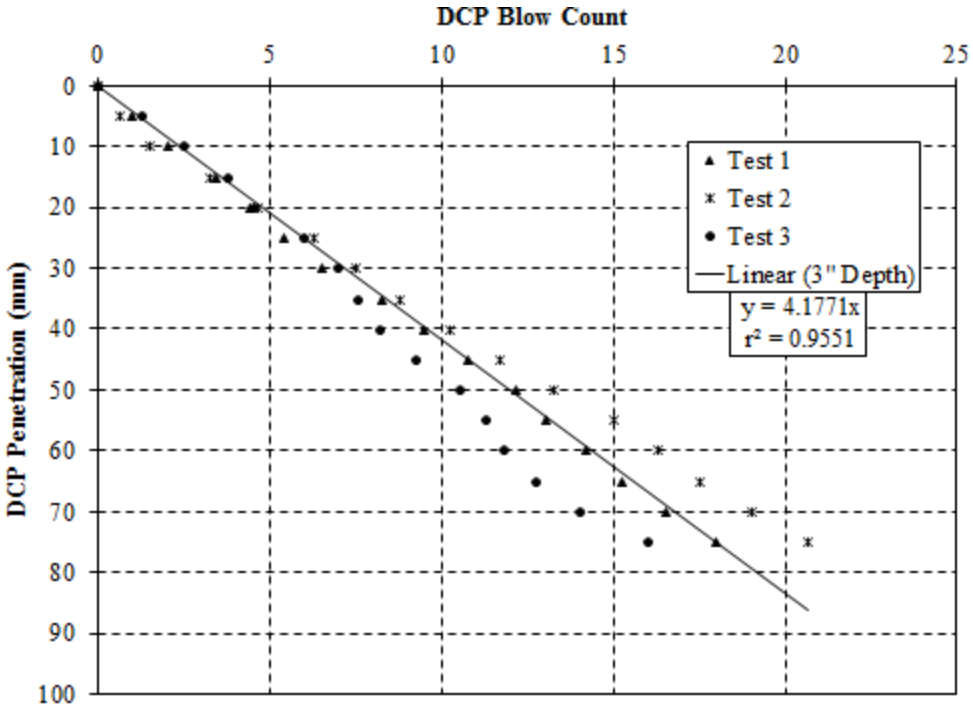

Figure F.36: Test conducted on April 19, 2017 Location 41 – compressive strength of 70 psi

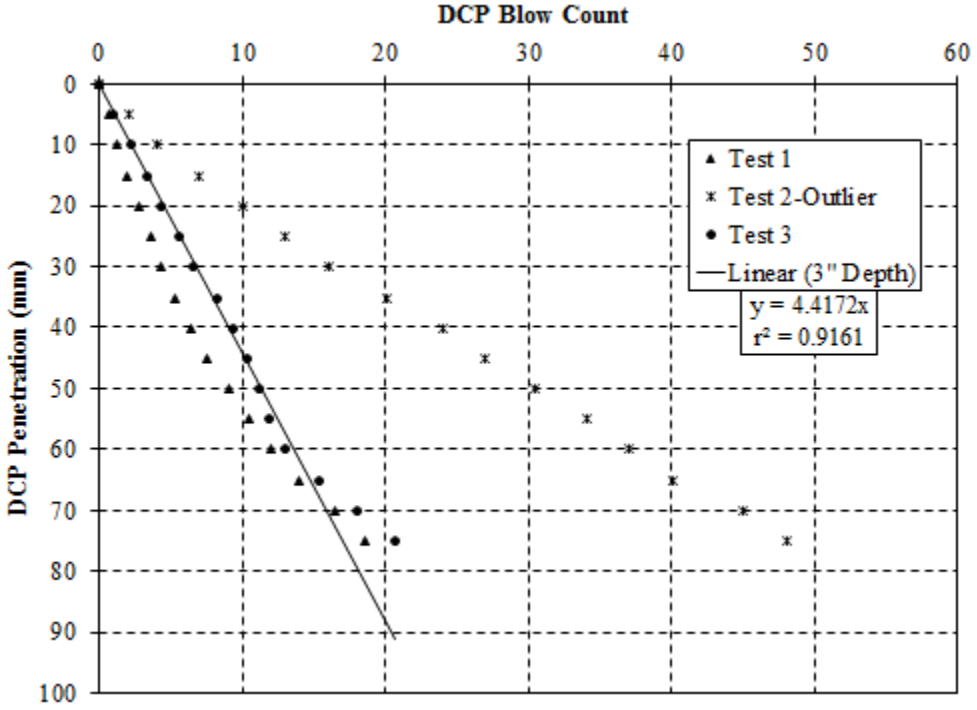

Figure F.37: Test conducted on April 19, 2017 Location 42 – compressive strength of 60 psi

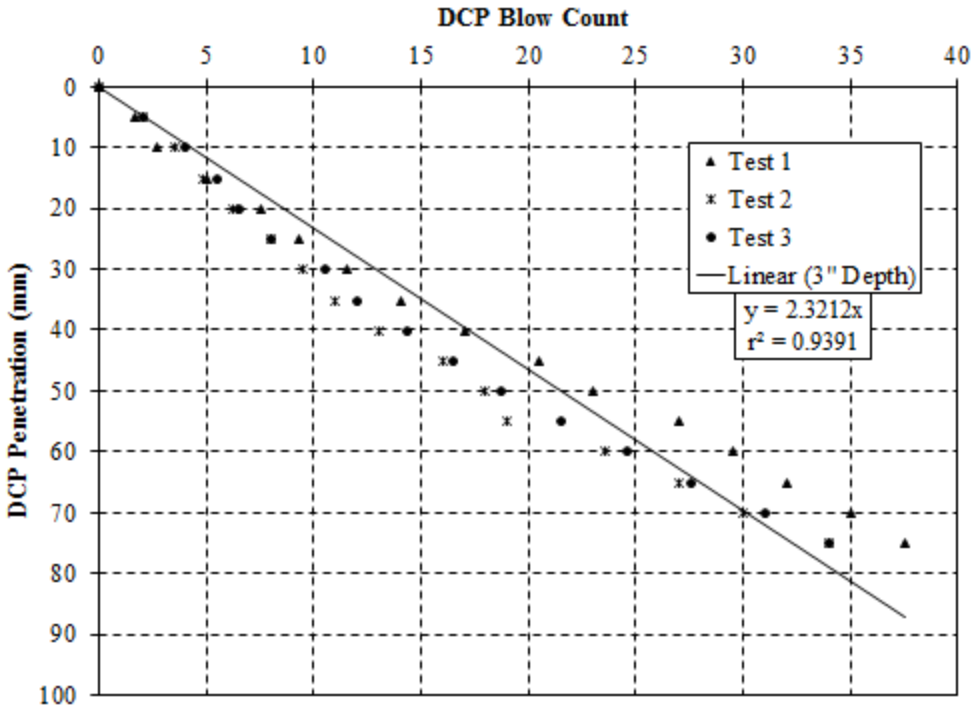

Figure F.38: Test conducted on April 19, 2017 Location 43 – compressive strength of 220 psi

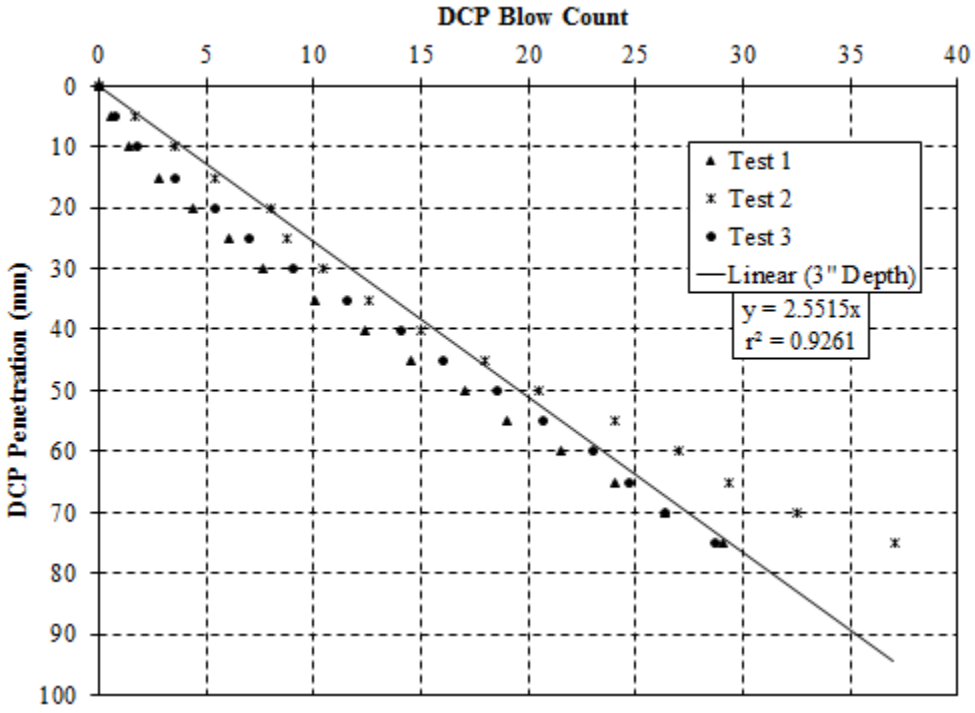

Figure F.39: Test conducted on April 19, 2017 Location 44 – compressive strength of 190 psi

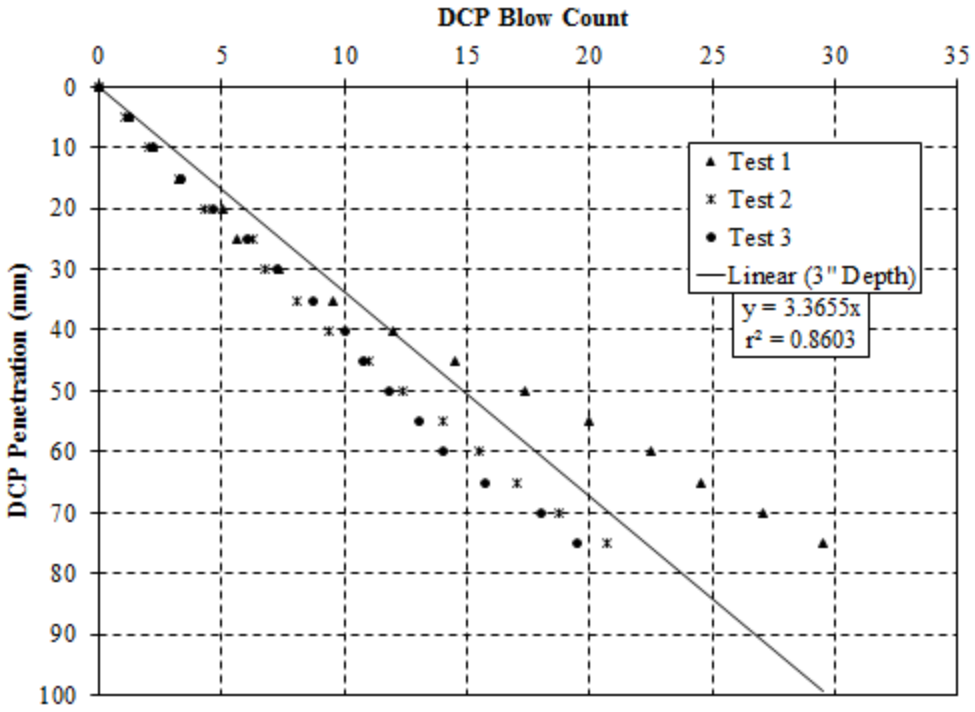

Figure F.40: Test conducted on April 19, 2017 Location 45 – compressive strength of 120 psi

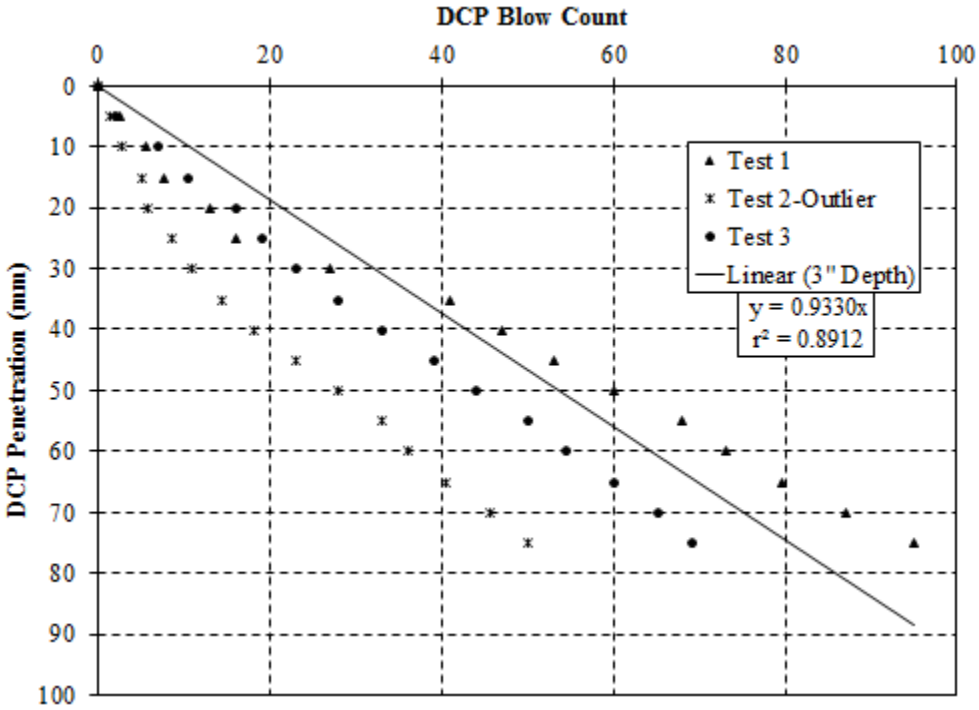

Figure F.41: Test conducted on April 19, 2017 Location 46 – compressive strength of 520 psi

Appendix G

100 mm Penetration

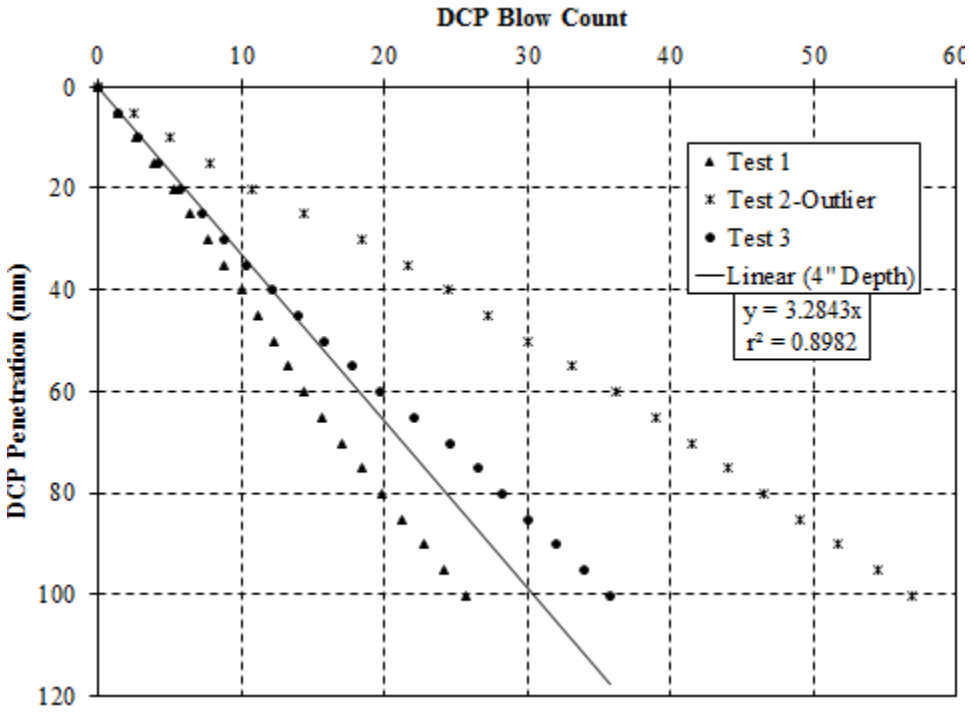

Figure G.1: Test conducted on November 1, 2016 Location 1 – compressive strength of 120 psi

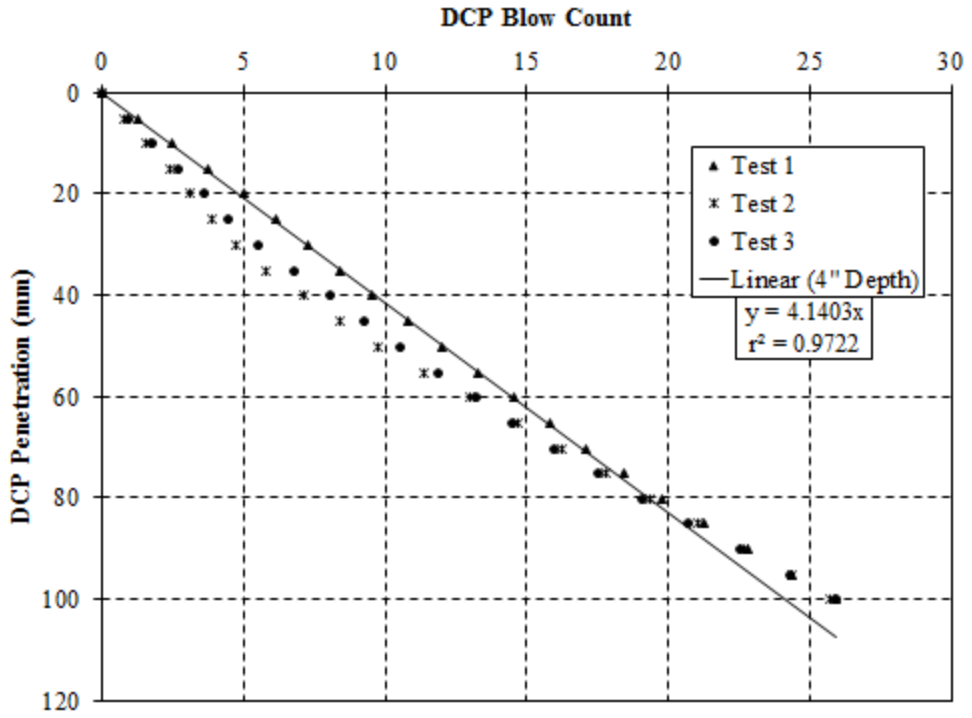

Figure G.2: Test conducted on November 1, 2016 Location 2– compressive strength of 70 psi

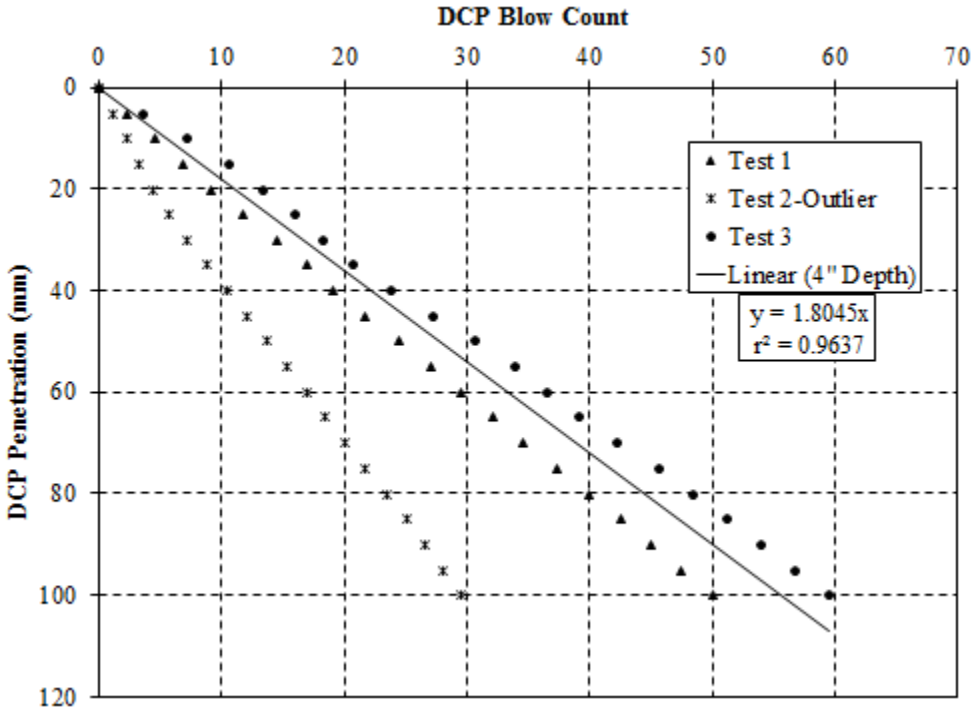

Figure G.3: Test conducted on November 7, 2016 Location 6 – compressive strength of 310 psi

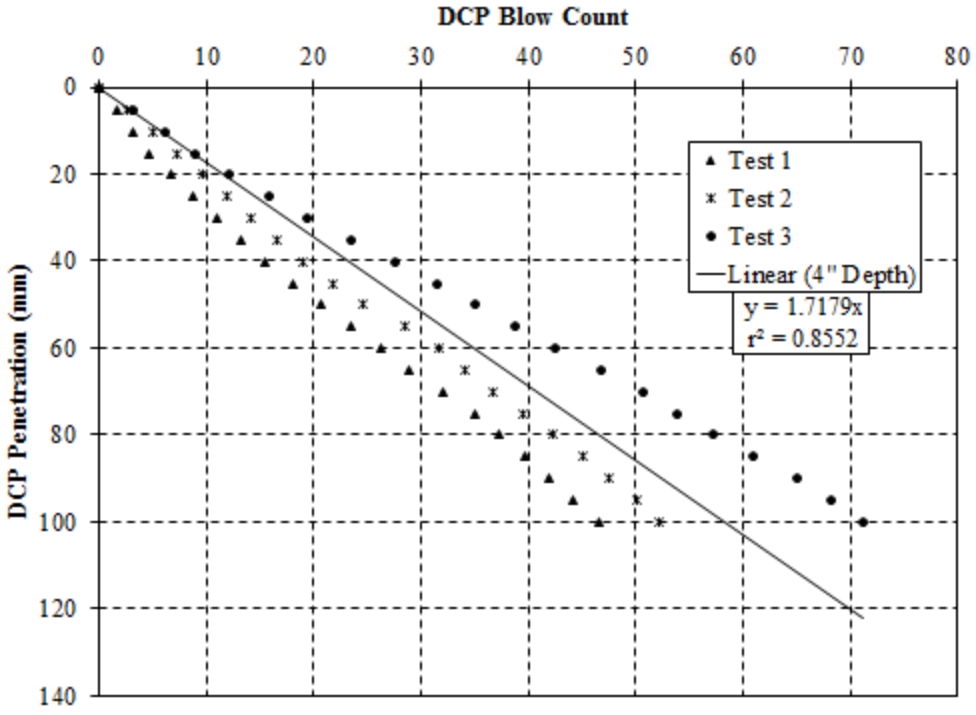

Figure G.4: Test conducted on November 7, 2016 Location 7 – compressive strength of 320 psi

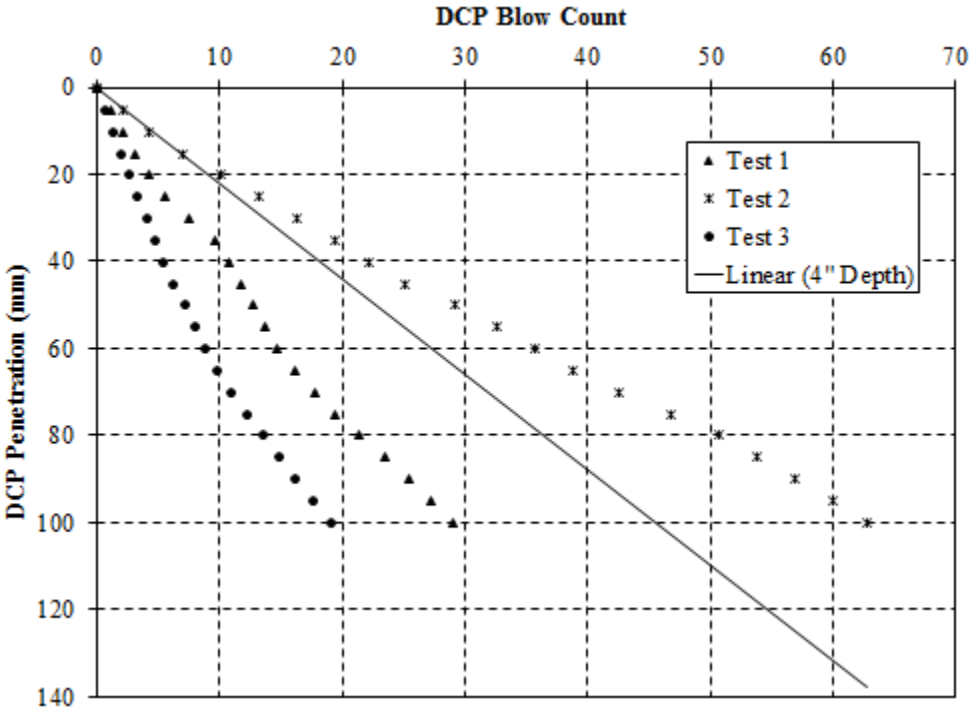

Figure G.5: Test conducted on November 22, 2016 Location 8 – range greater than 50 %

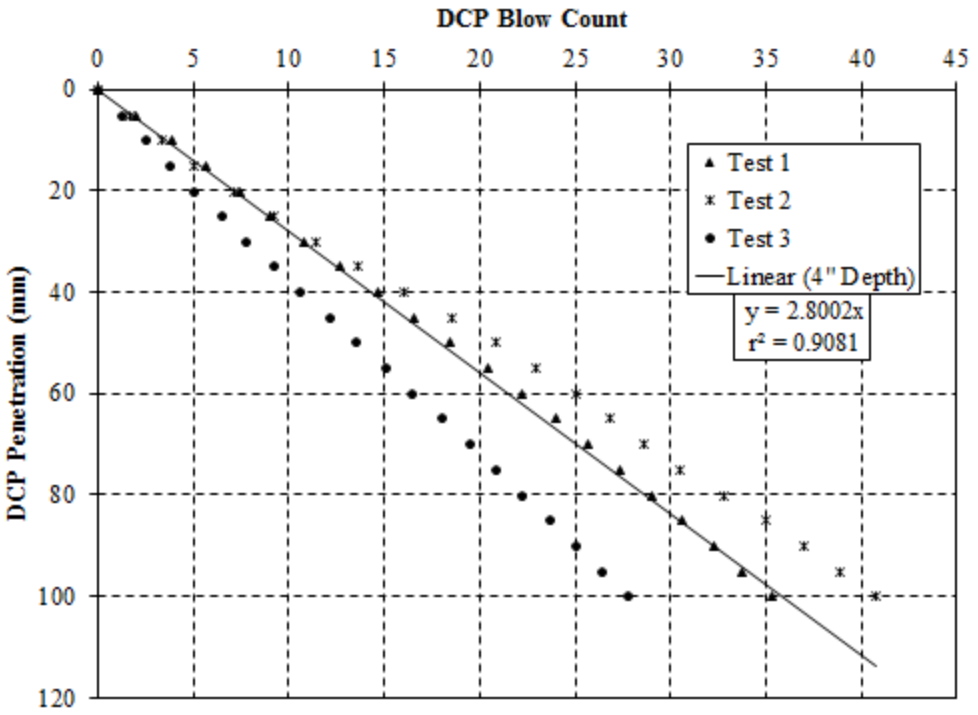

Figure G.6: Test conducted on November 22, 2016 Location 9 –compressive strength of 170 psi

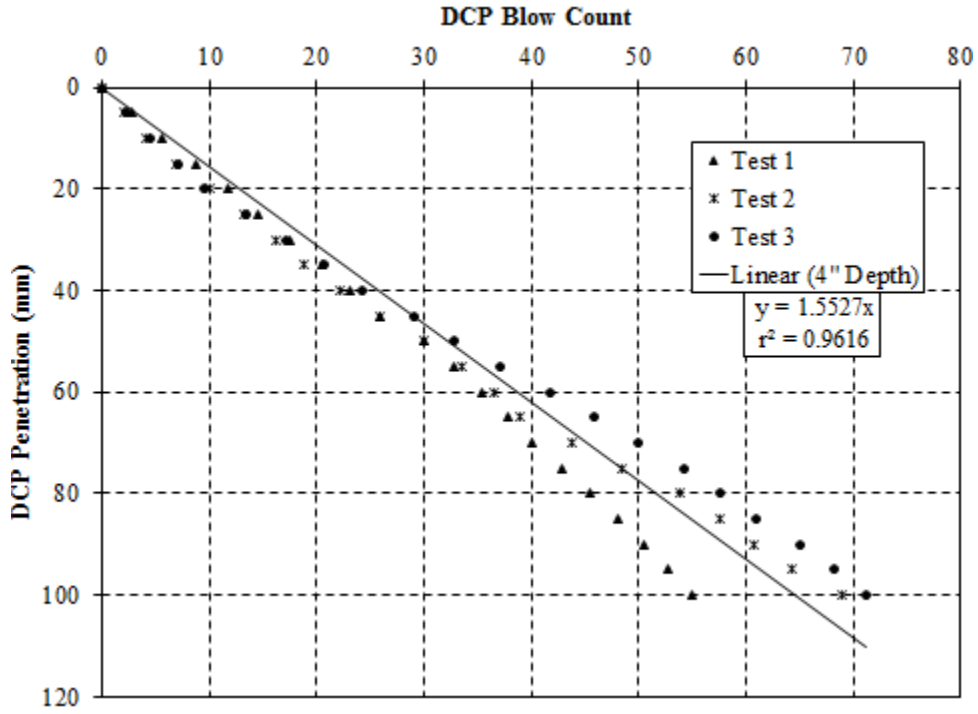

Figure G.7: Test conducted on November 22, 2016 Location 10–compressive strength of 360 psi

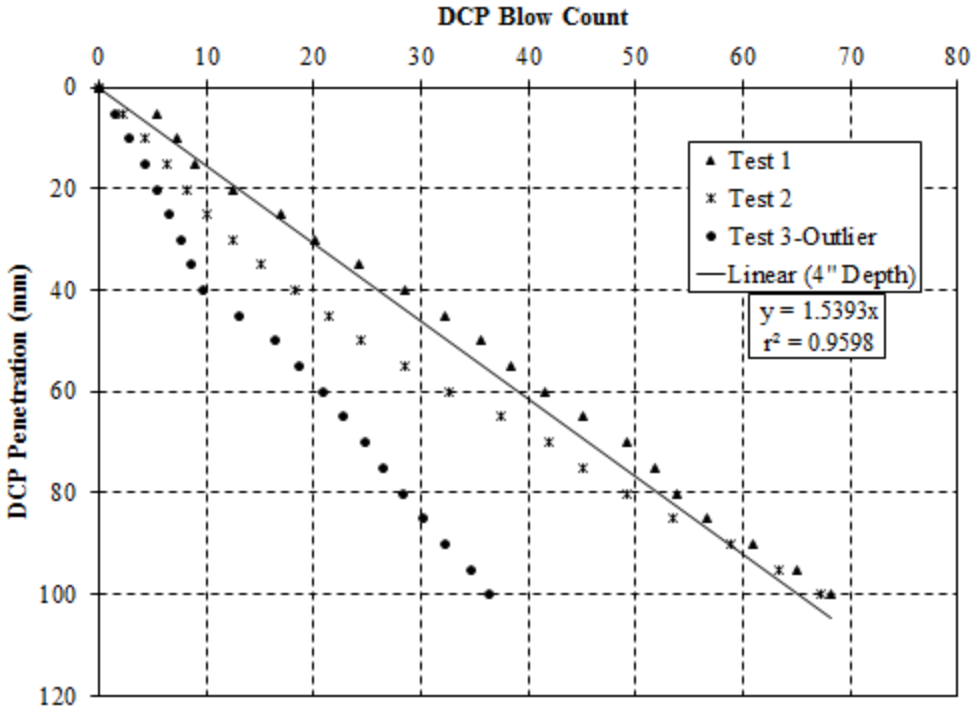

Figure G.8: Test conducted on November 22, 2016 Location 12–compressive strength of 360 psi

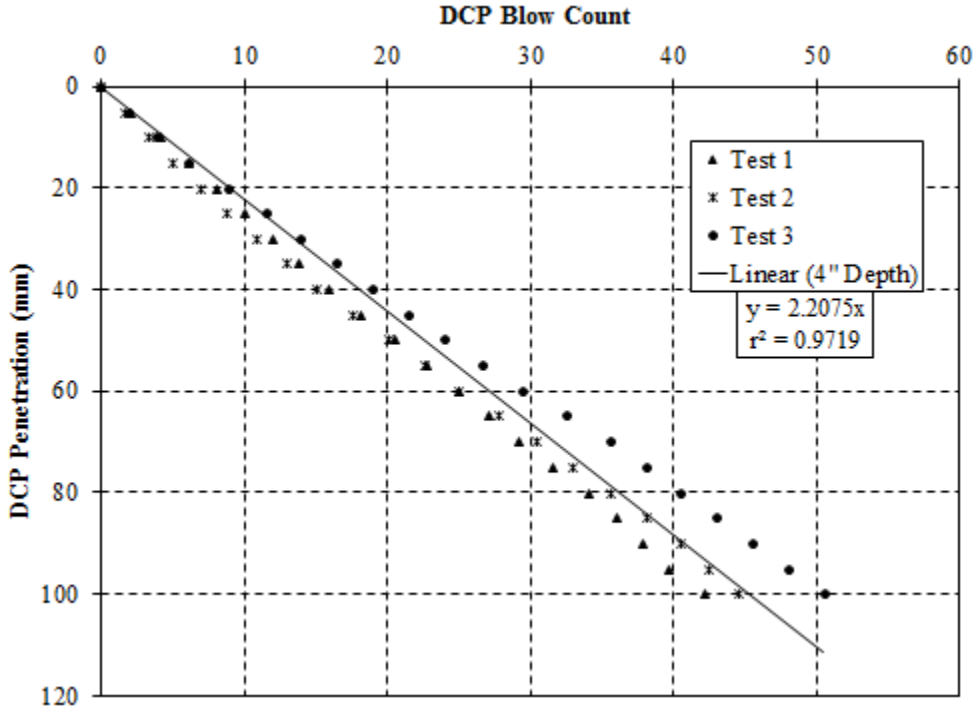

Figure G.9: Test conducted on November 22, 2016 Location 13–compressive strength of 240 psi

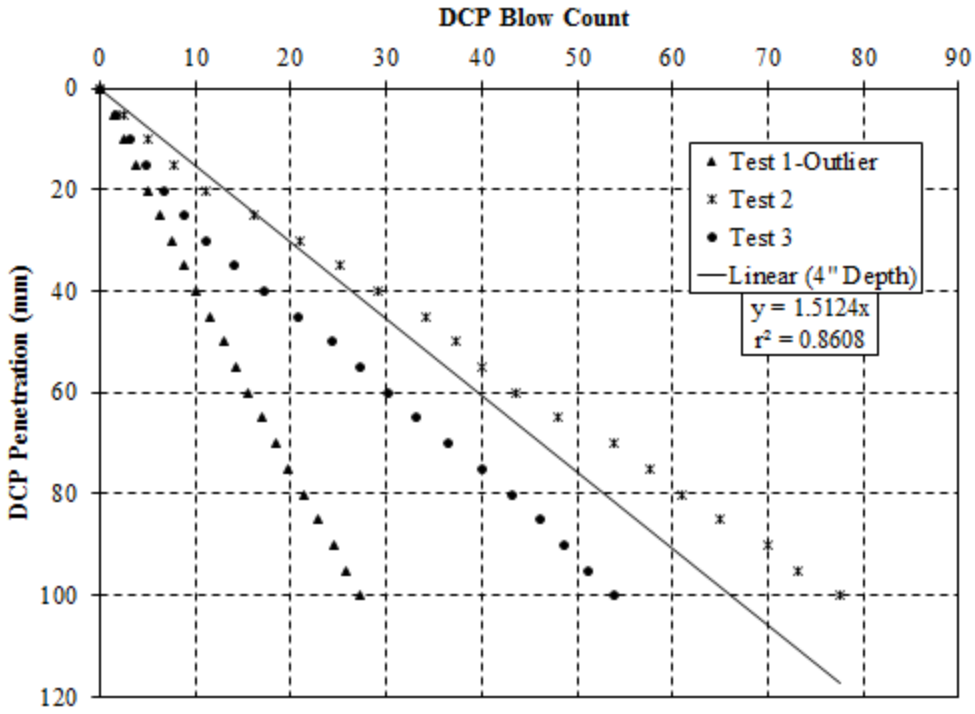

Figure G.10: Test conducted on November 23, 2016 Location 14–compressive strength of 370 psi

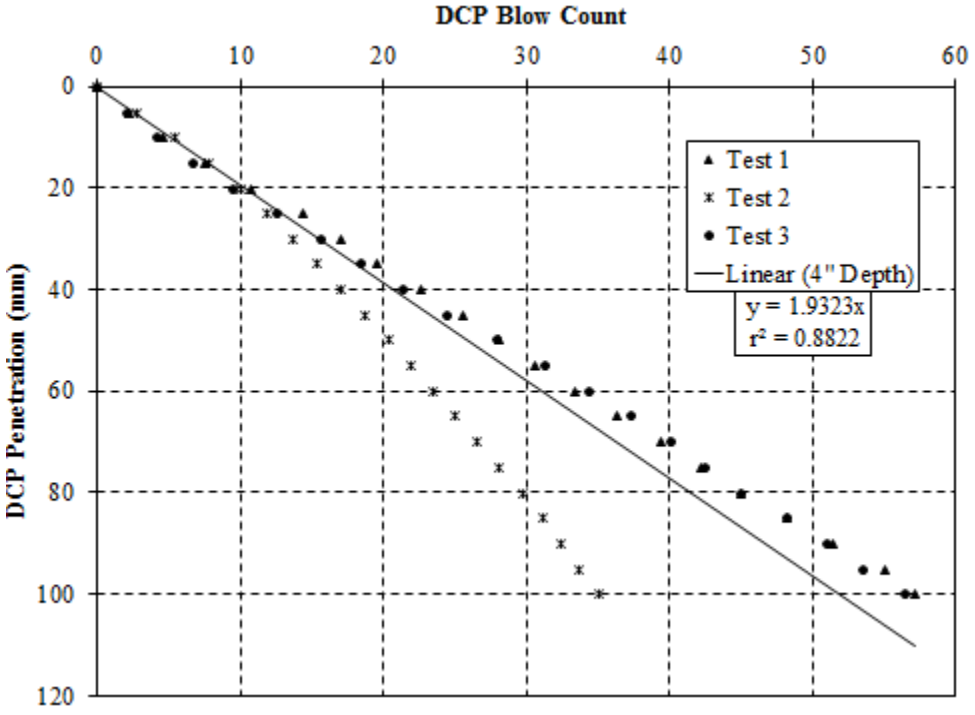

Figure G.11: Test conducted on November 23, 2016 Location 15 – compressive strength of 280 psi

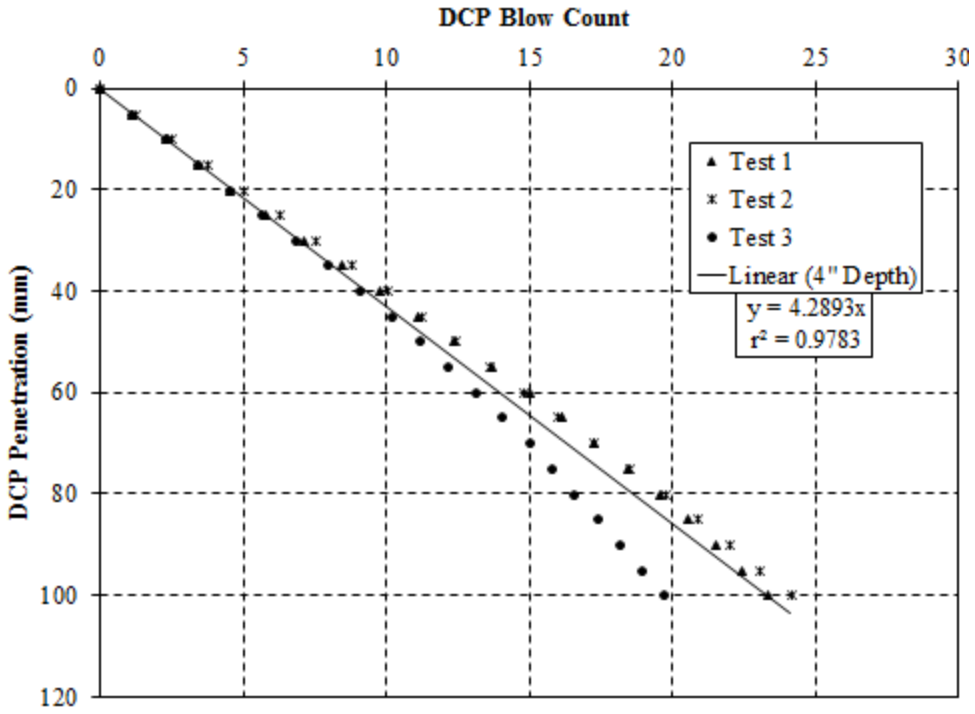

Figure G.12: Test conducted on November 23, 2016 Location 16 – compressive strength of 70 psi

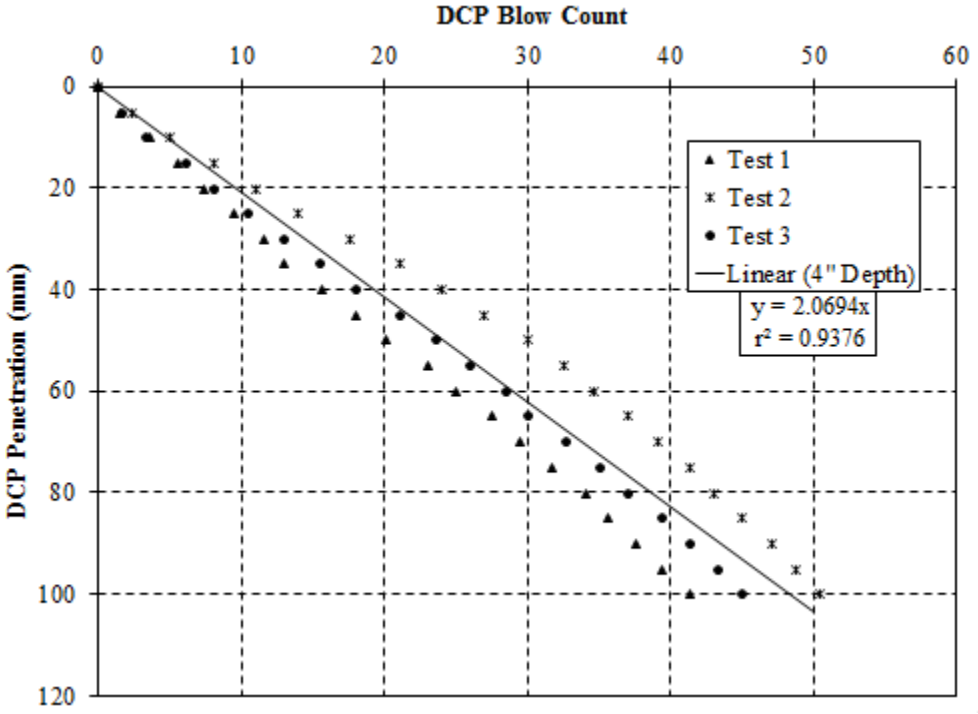

Figure G.13: Test conducted on March 23, 2017 Location 17 – compressive strength of 260 psi

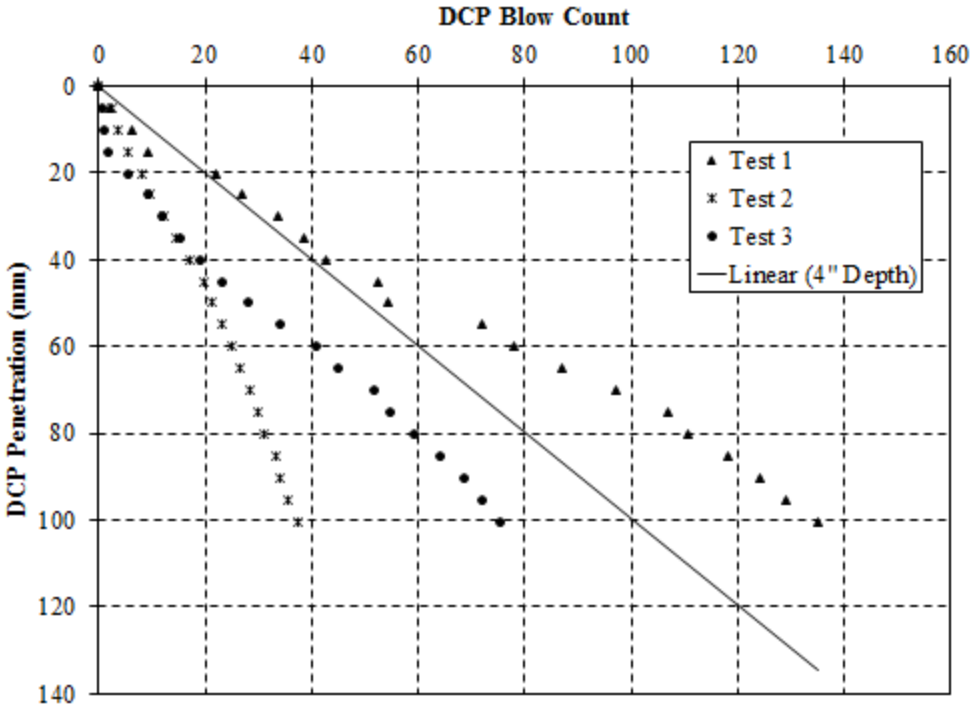

Figure G.14: Test conducted on March 23, 2017 Location 18 – range greater than 50 %

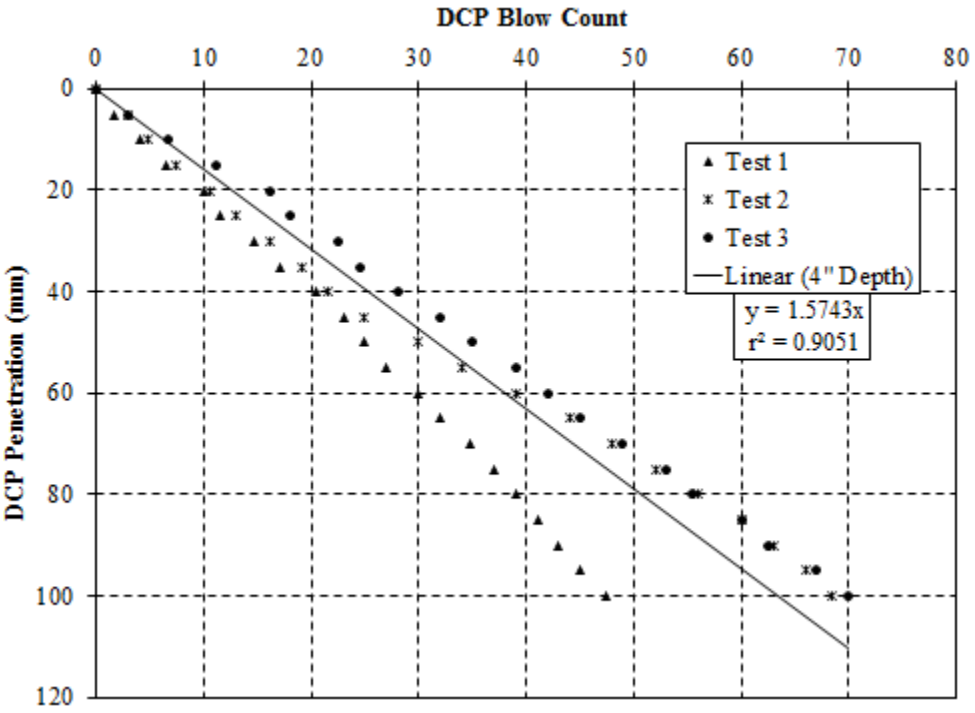

Figure G.15: Test conducted on March 23, 2017 Location 19 – compressive strength of 350 psi

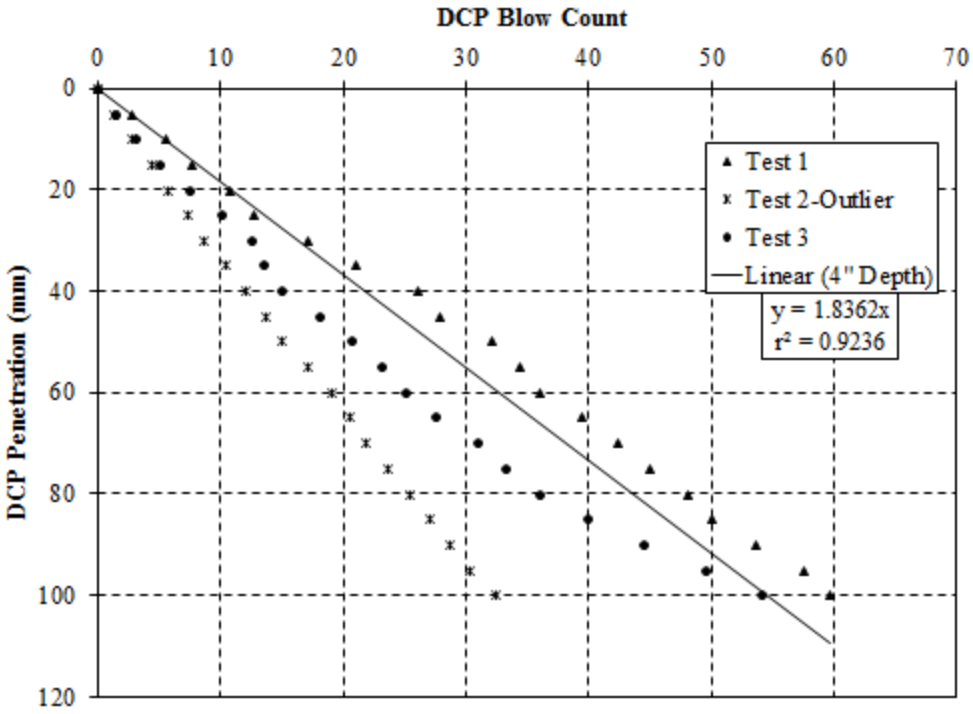

Figure G.16: Test conducted on March 27, 2017 Location 20 – compressive strength of 300 psi

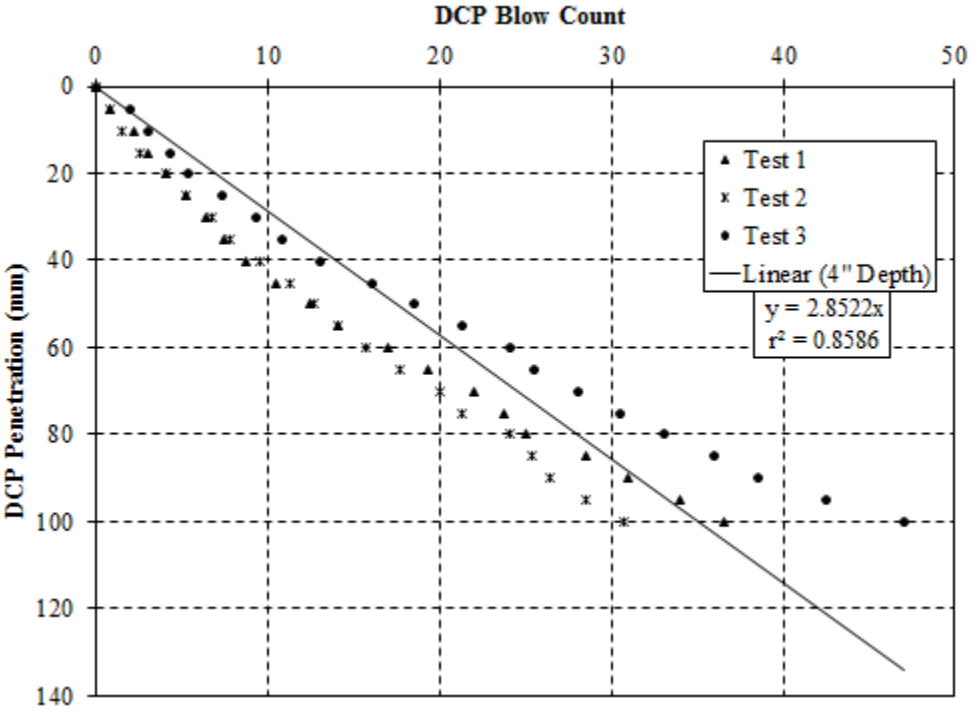

Figure G.17: Test conducted on March 27, 2017 Location 21 – compressive strength of 160 psi

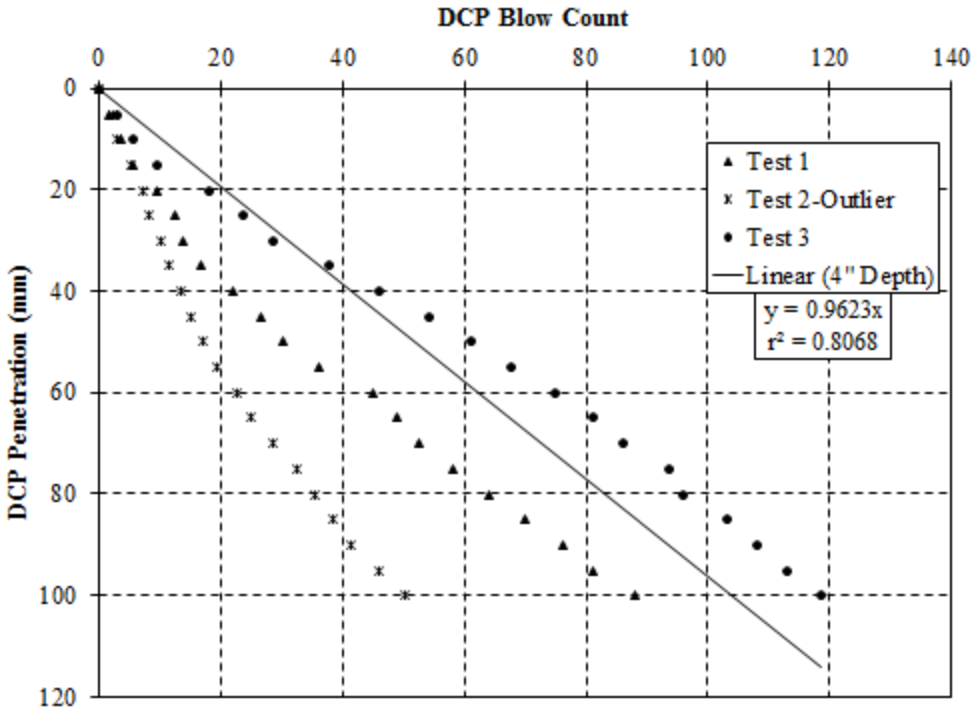

Figure G.18: Test conducted on March 27, 2017 Location 22 – compressive strength of 510 psi

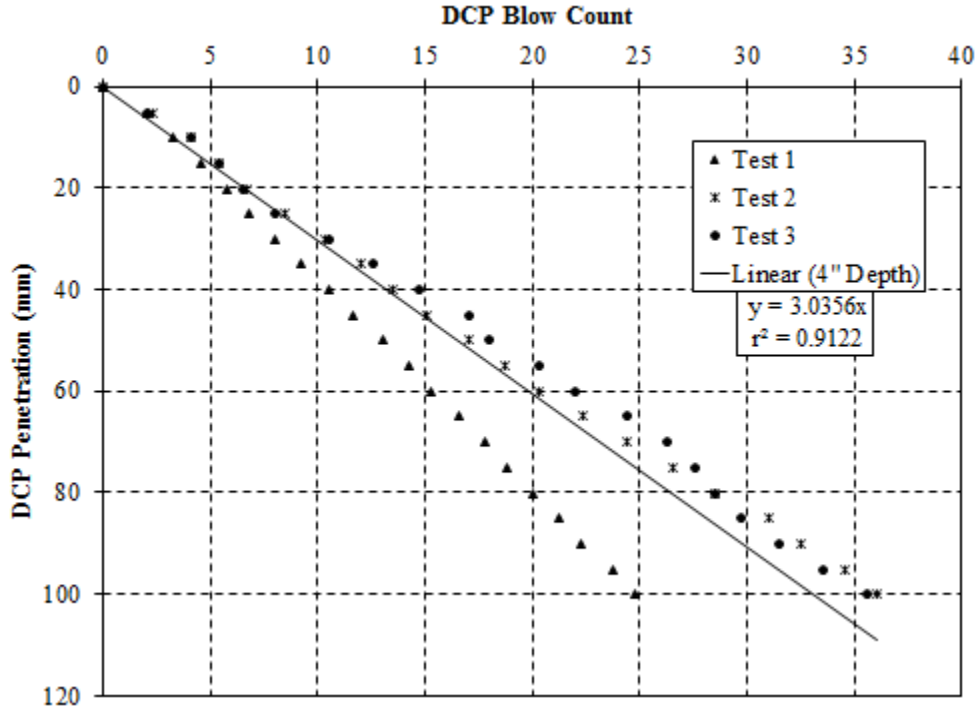

Figure G.19: Test conducted on March 30, 2017 Location 23 – compressive strength of 140 psi

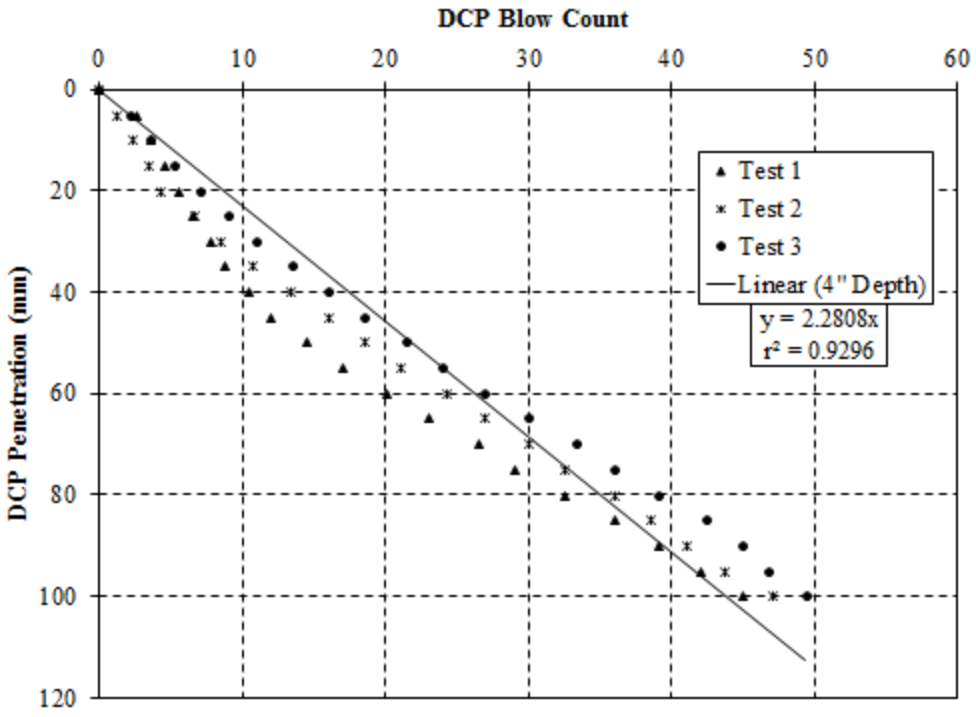

Figure G.20: Test conducted on March 30, 2017 Location 24 – compressive strength of 230 psi

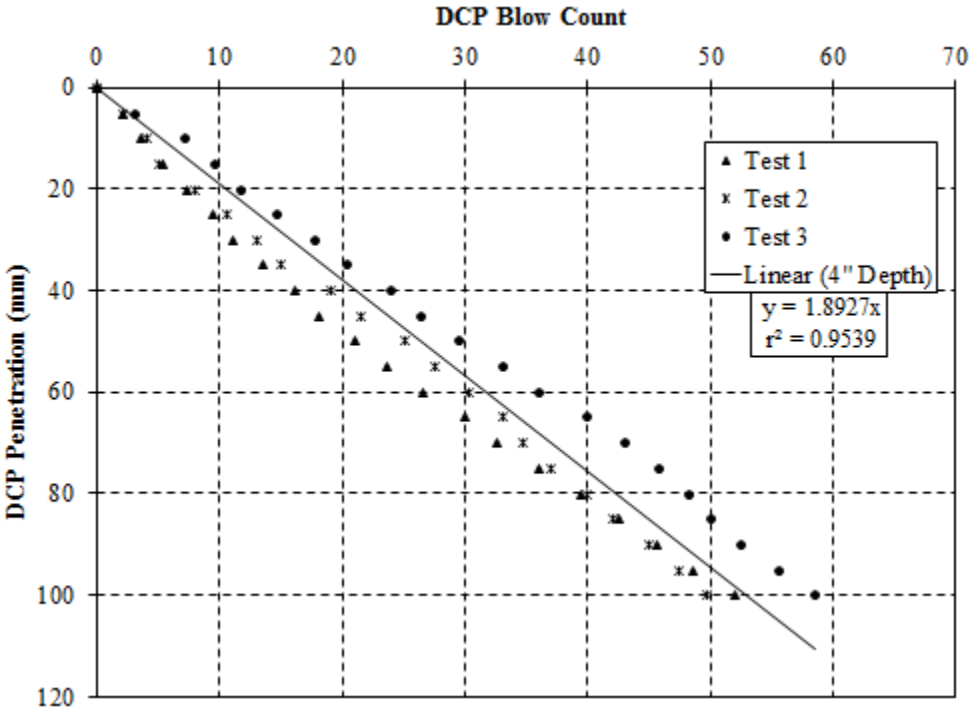

Figure G.21: Test conducted on March 30, 2017 Location 25 – compressive strength of 290 psi

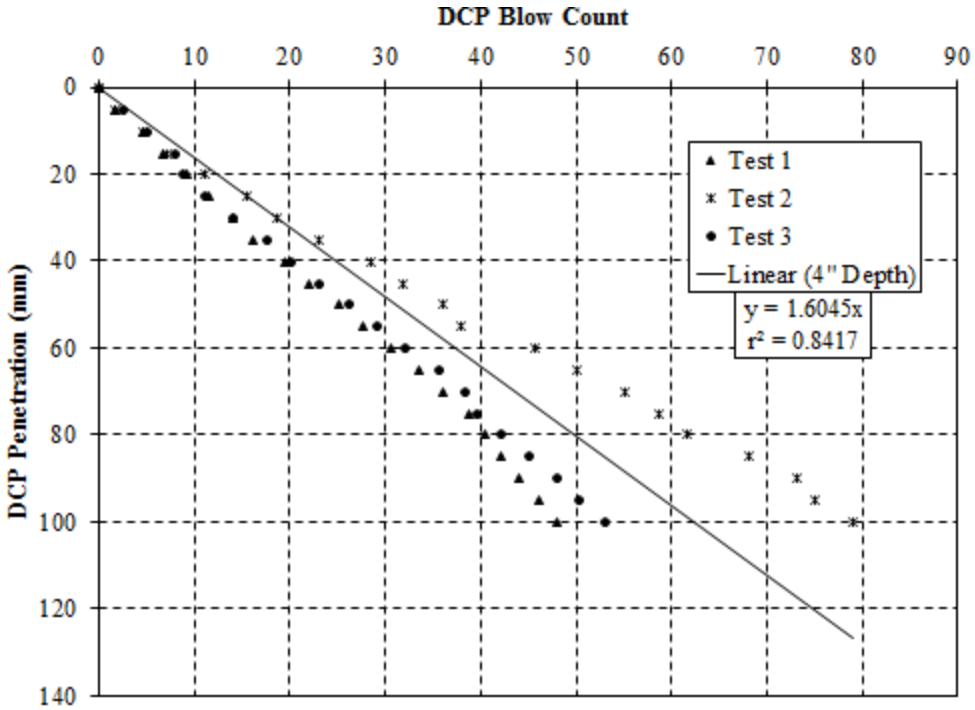

Figure G.22: Test conducted on March 31, 2017 Location 26 – compressive strength of 350 psi

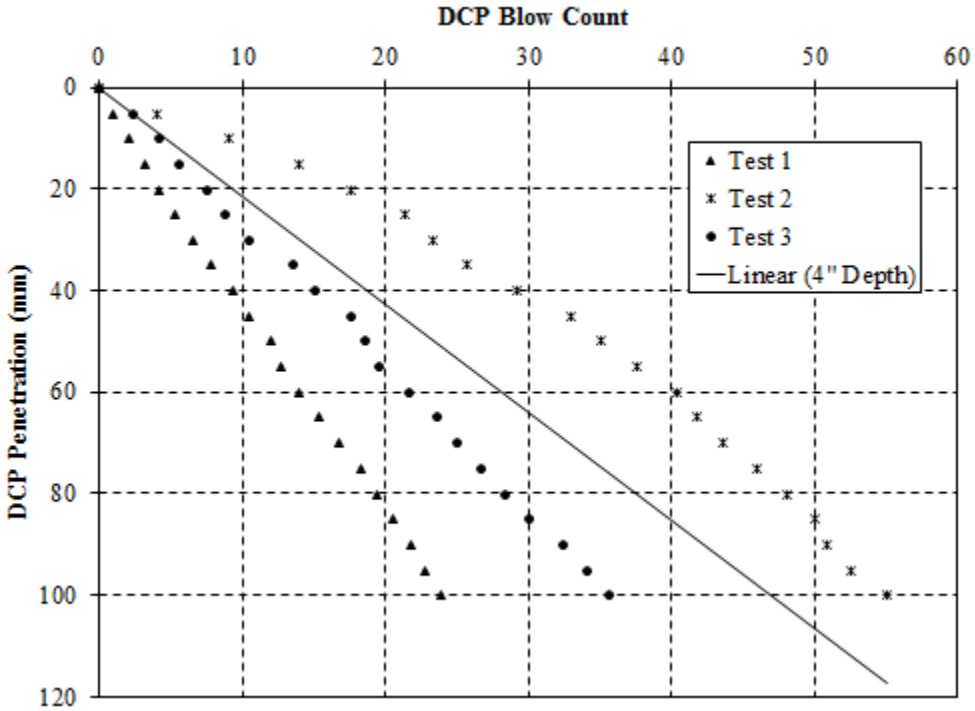

Figure G.23: Test conducted on March 31, 2017 Location 27 – range greater than 50 %

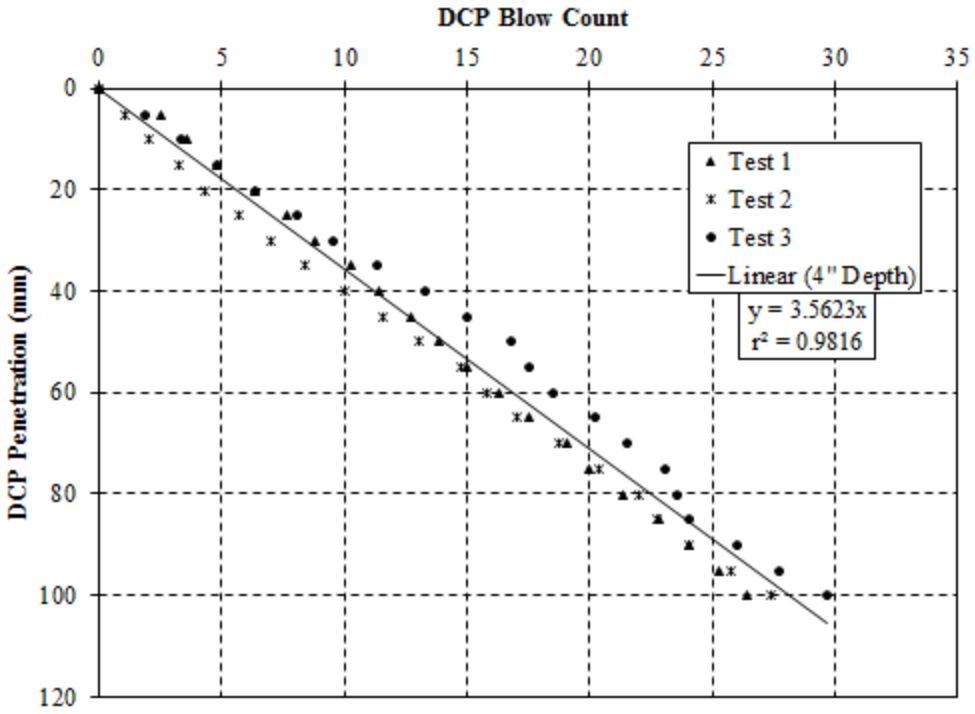

Figure G.24: Test conducted on March 31, 2017 Location 28 – compressive strength of 100 psi

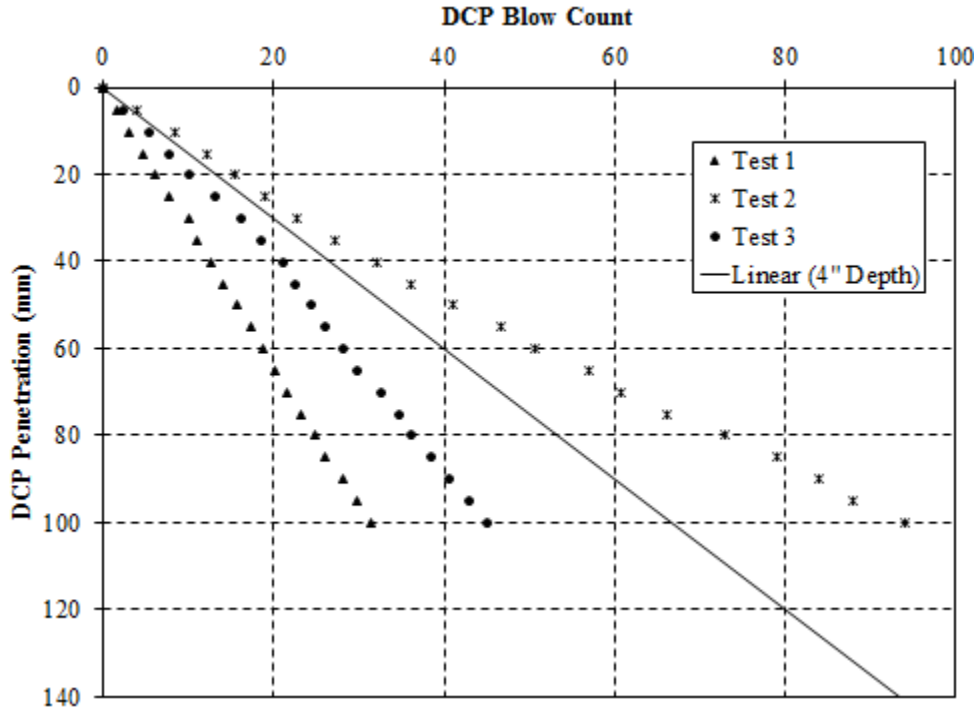

Figure G.25: Test conducted on April 3, 2017 Location 29 – range greater than 50 %

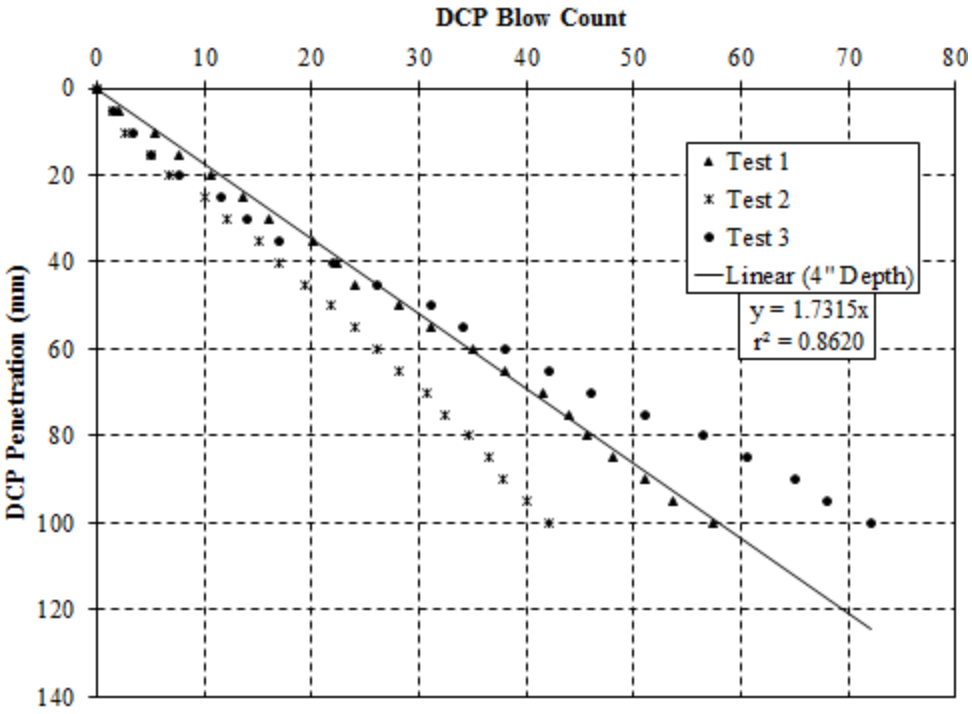

Figure G.26: Test conducted on April 3, 2017 Location 30 – compressive strength of 320 psi

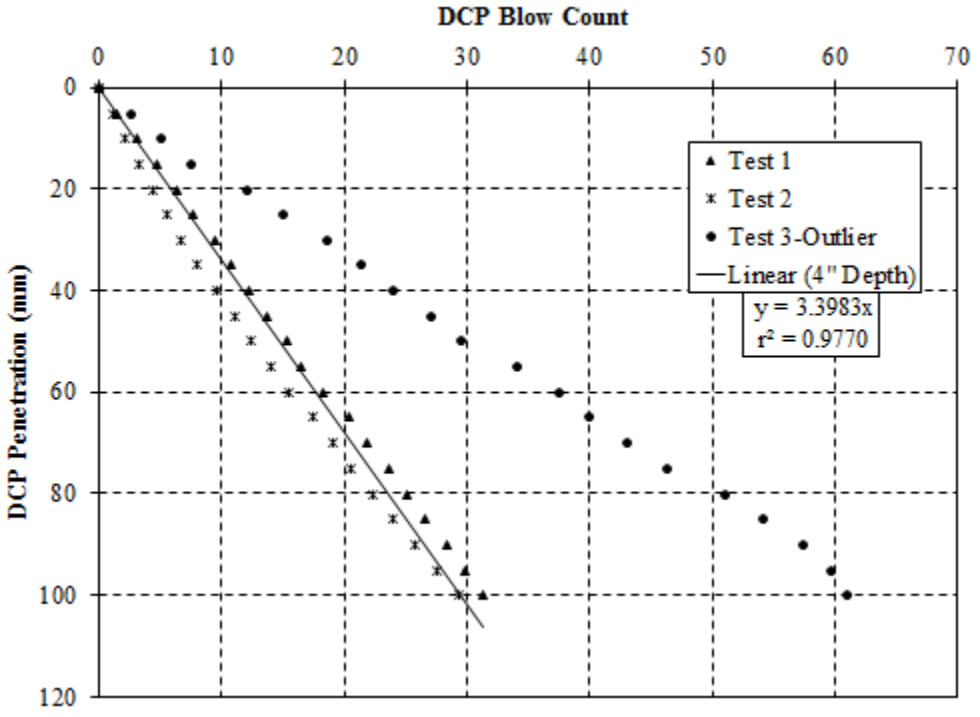

Figure G.27: Test conducted on April 3, 2017 Location 31 – compressive strength of 110 psi

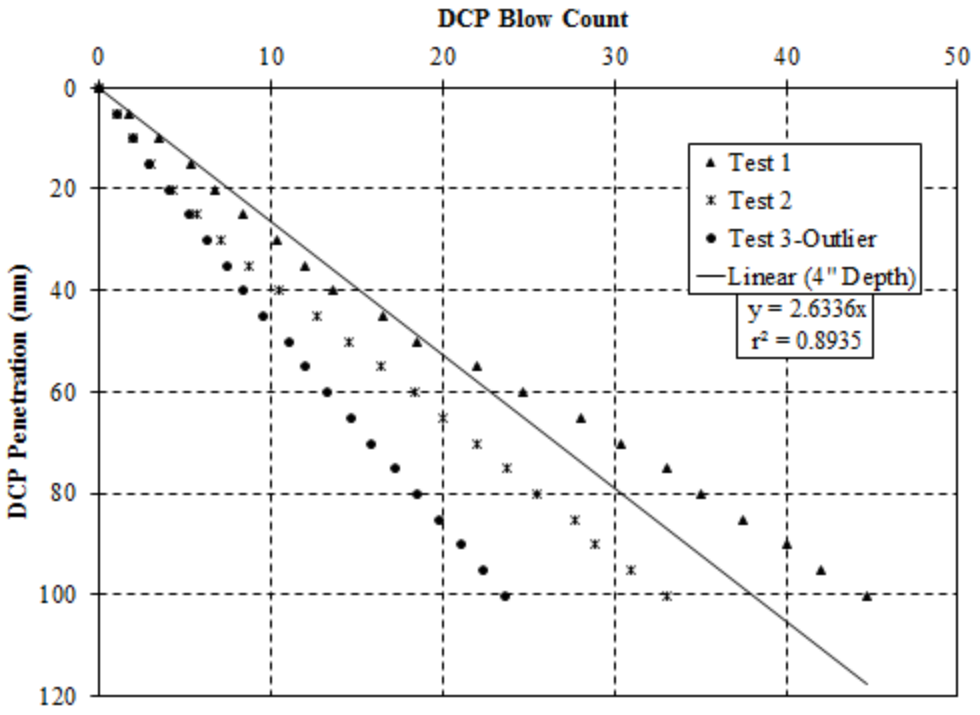

Figure G.28: Test conducted on April 5, 2017 Location 32 – compressive strength of 180 psi

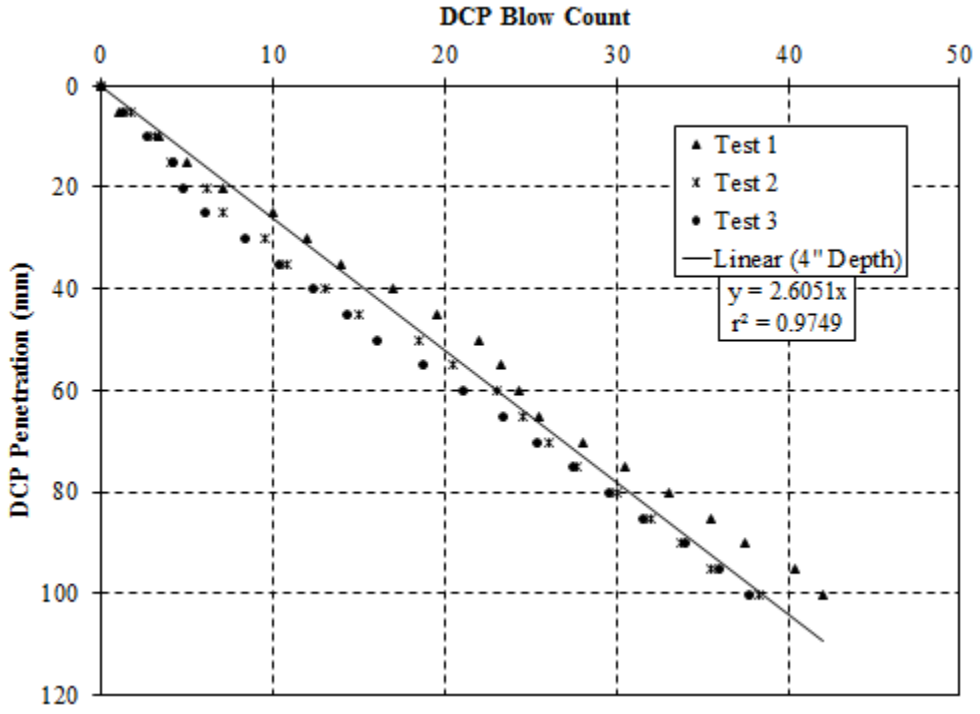

Figure G.29: Test conducted on April 5, 2017 Location 33 – compressive strength of 190 psi

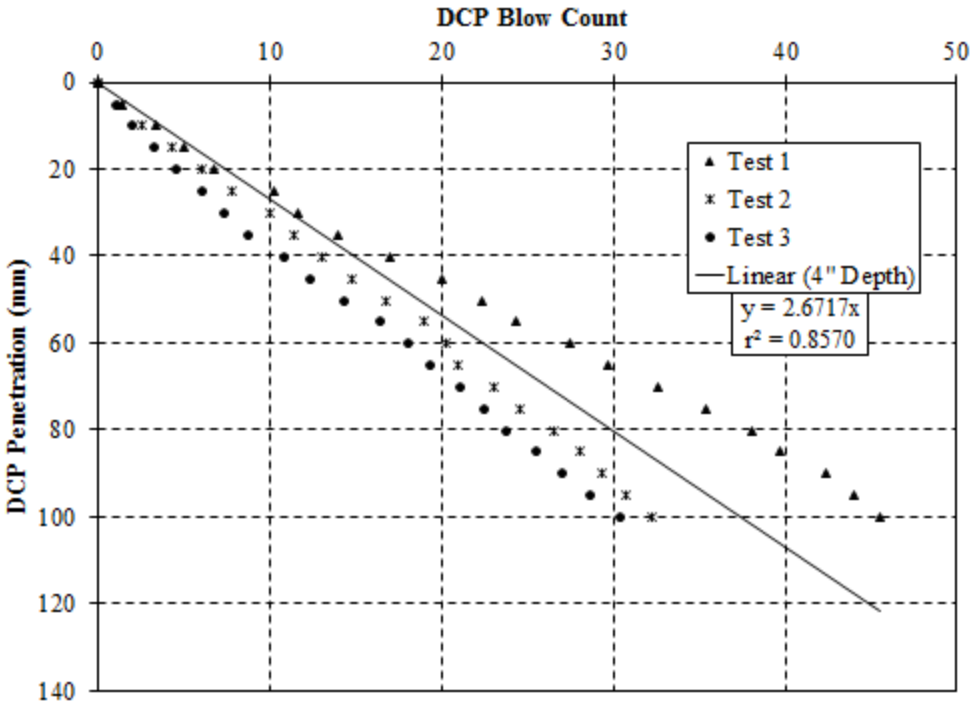

Figure G.30: Test conducted on April 5, 2017 Location 34 – compressive strength of 180 psi

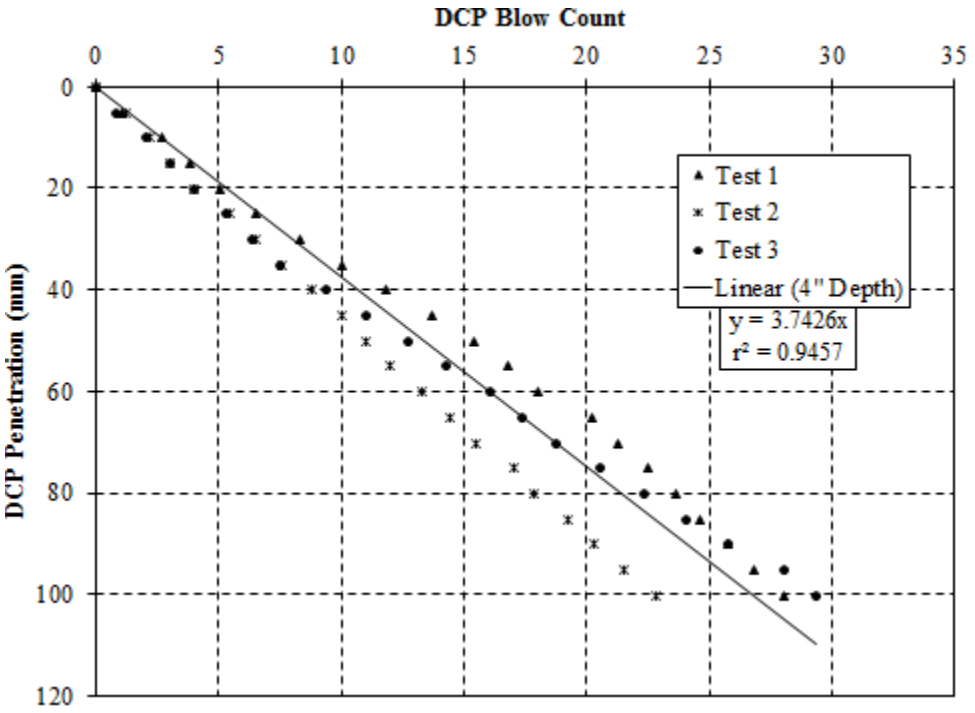

Figure G.31: Test conducted on April 5, 2017 Location 35 – compressive strength of 90 psi

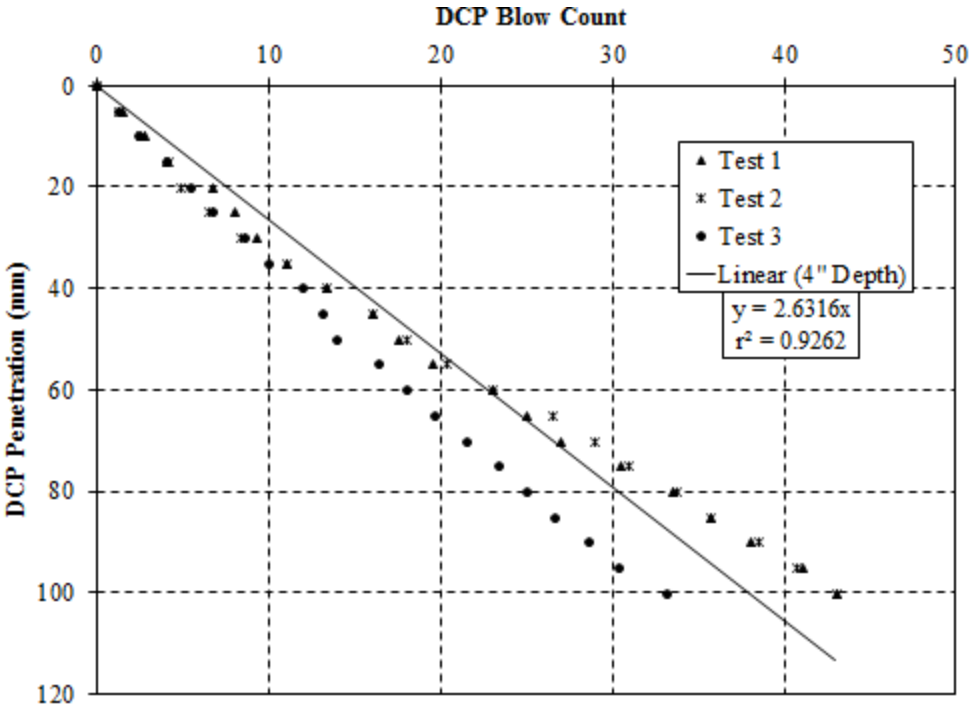

Figure G.32: Test conducted on April 5, 2017 Location 36 – compressive strength of 180 psi

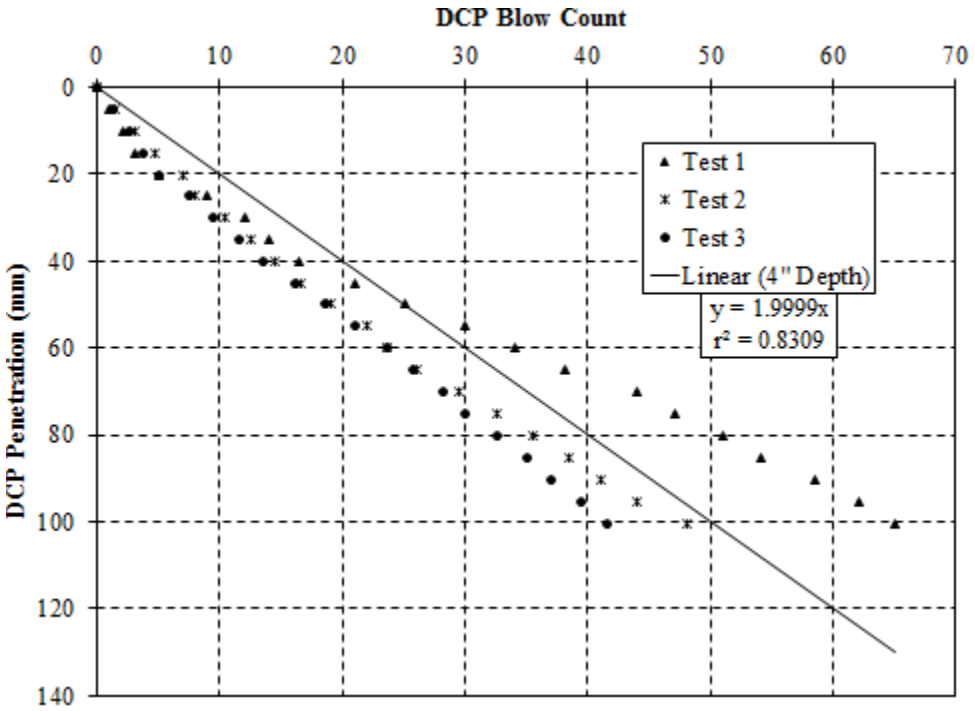

Figure G.33: Test conducted on April 5, 2017 Location 37 – compressive strength of 270 psi

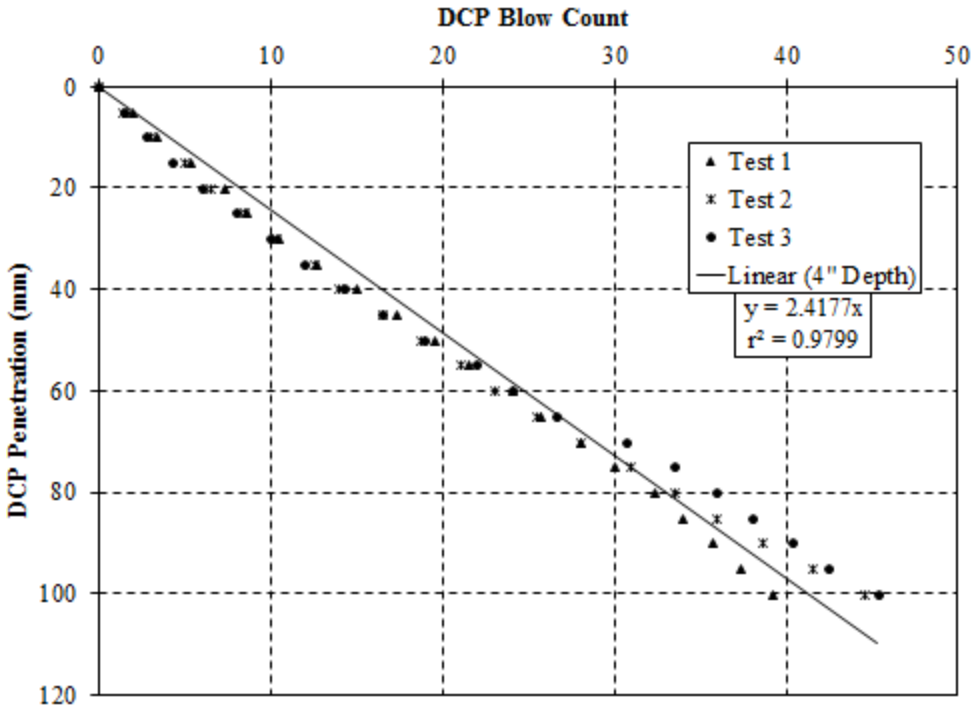

Figure G.34: Test conducted on April 6, 2017 Location 38 – compressive strength of 210 psi

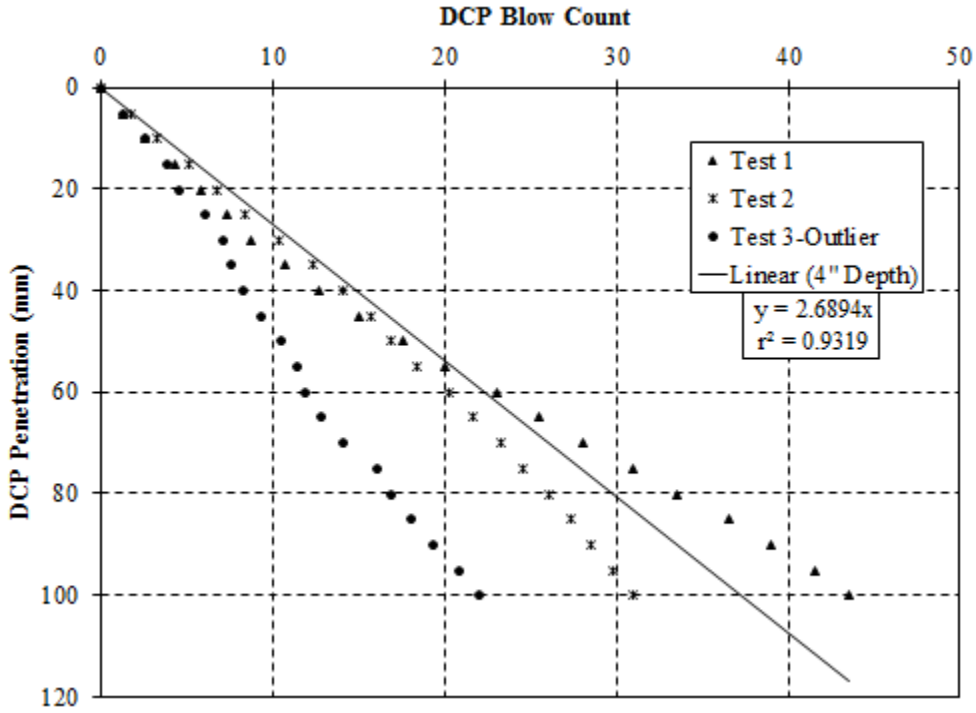

Figure G.35: Test conducted on April 6, 2017 Location 40 – compressive strength of 180 psi

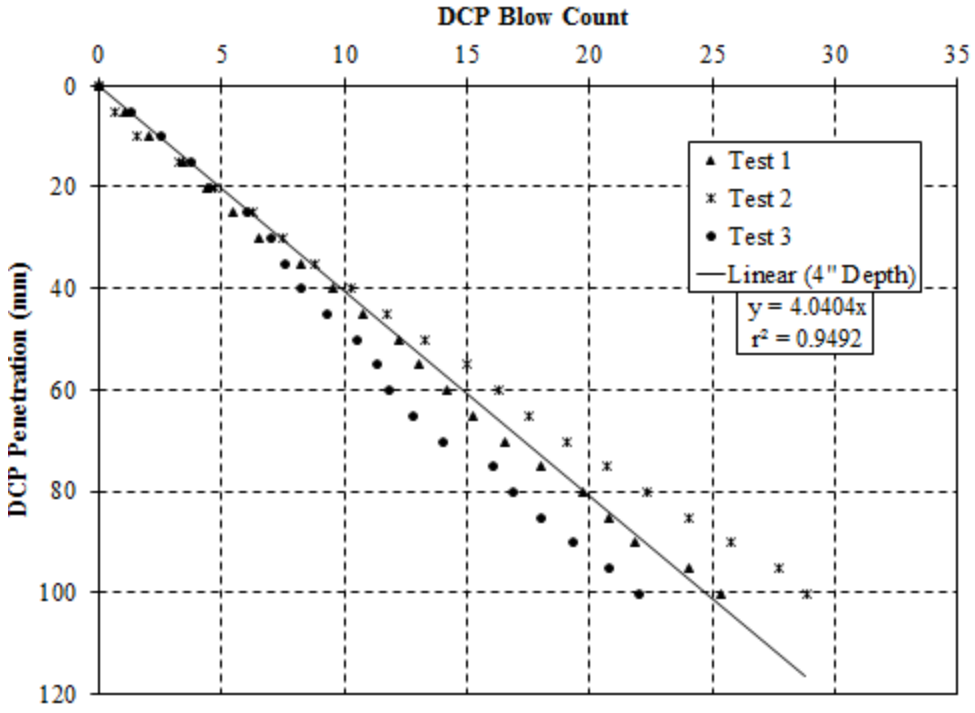

Figure G.36: Test conducted on April 19, 2017 Location 41 – compressive strength of 80 psi

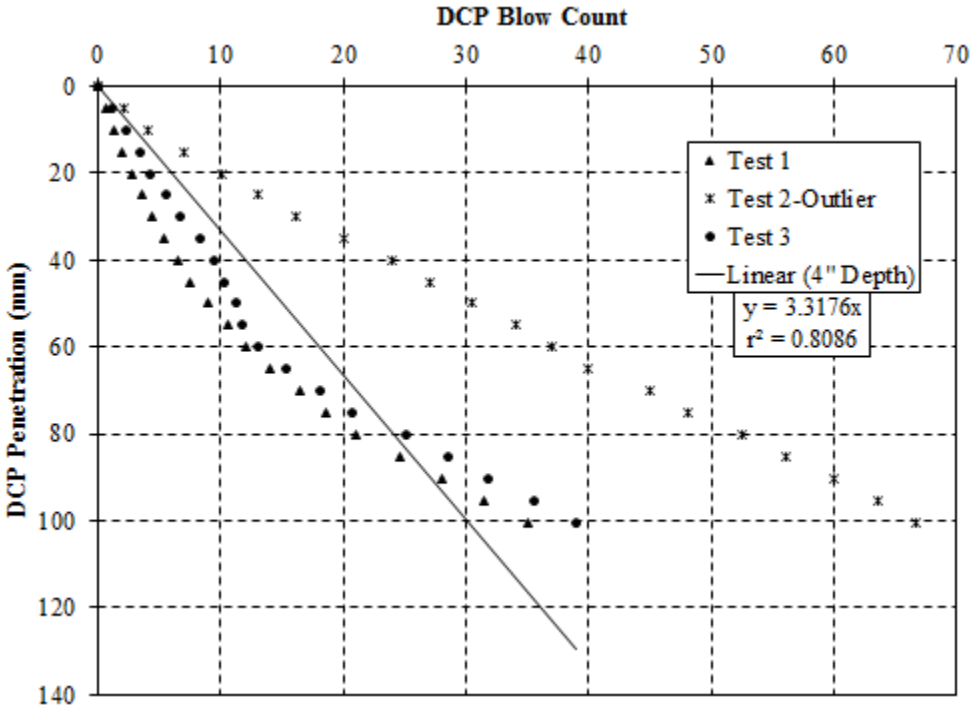

Figure G.37: Test conducted on April 19, 2017 Location 42 – compressive strength of 120 psi

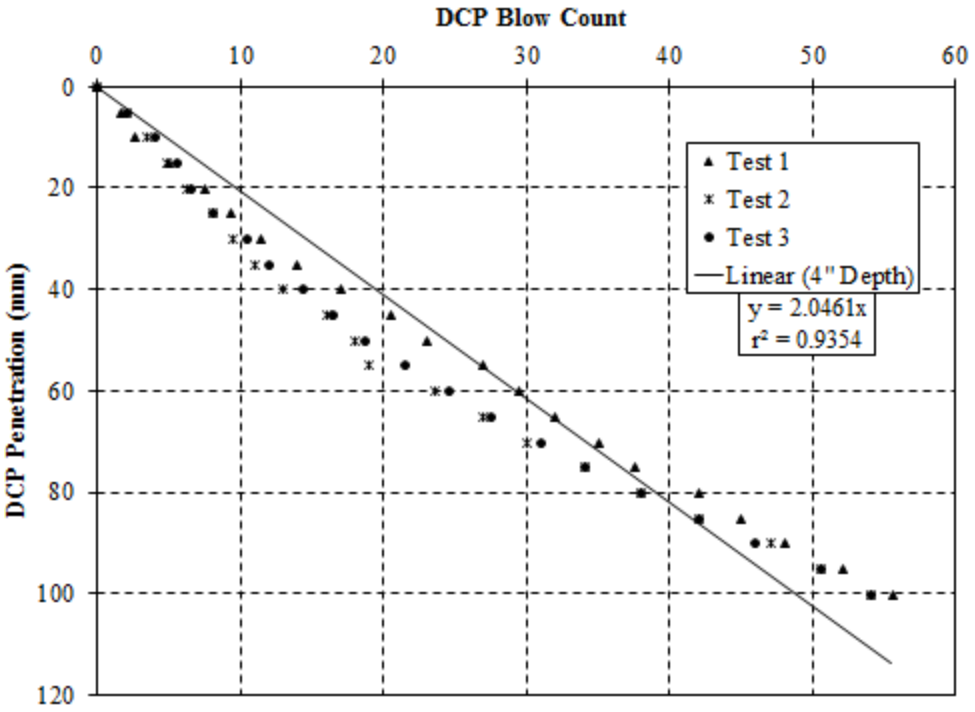

Figure G.38: Test conducted on April 19, 2017 Location 43 – compressive strength of 260 psi

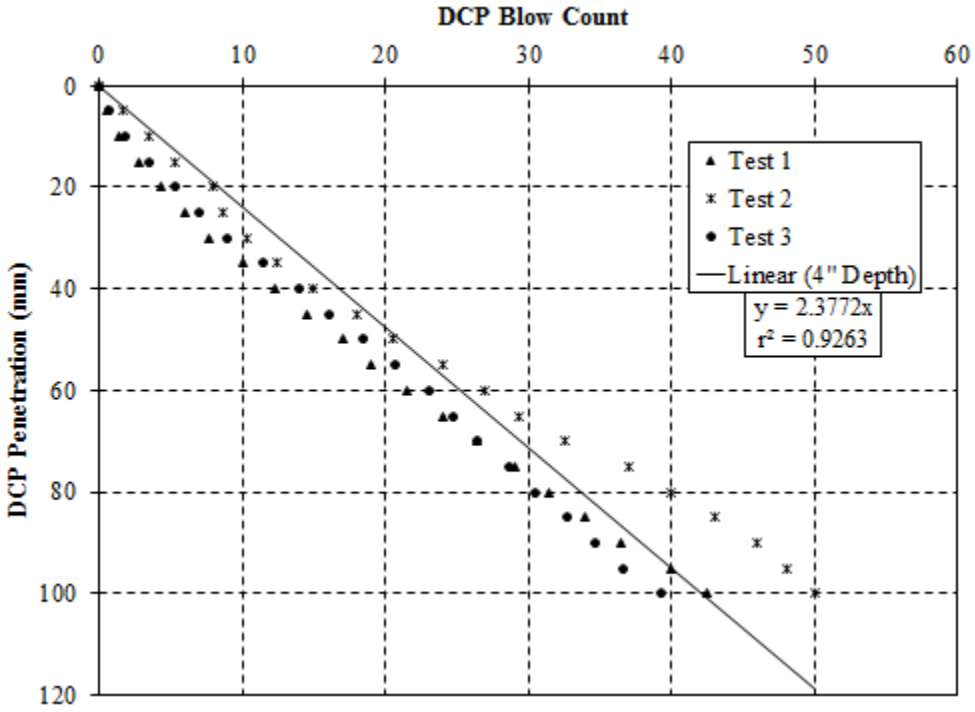

Figure G.39: Test conducted on April 19, 2017 Location 44 – compressive strength of 210 psi

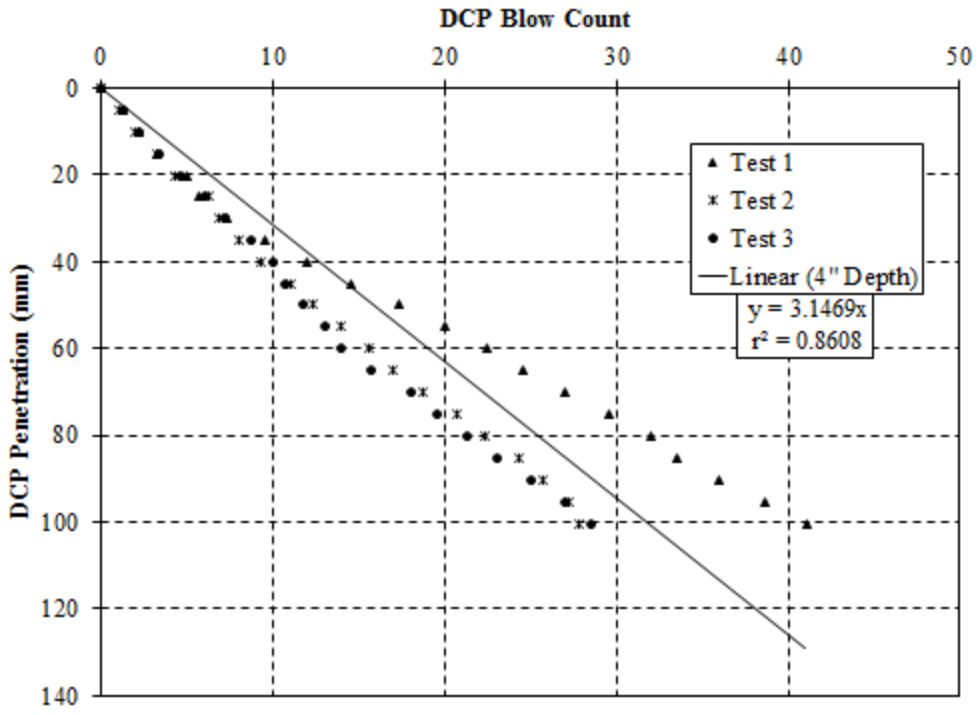

Figure G.40: Test conducted on April 19, 2017 Location 45 – compressive strength of 130 psi

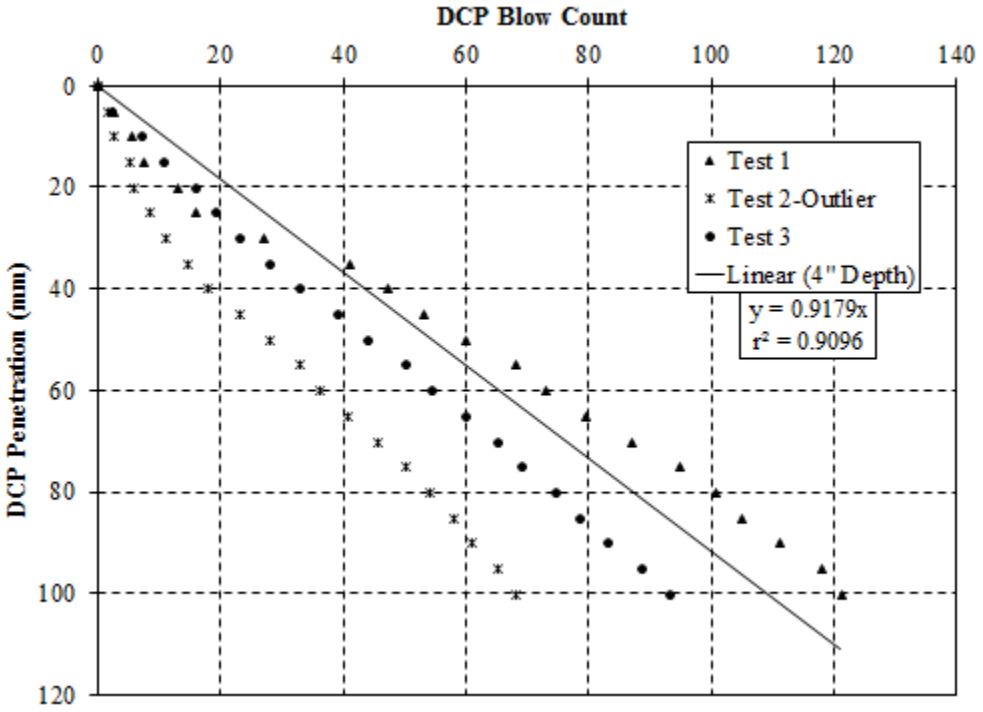

Figure G.41: Test conducted on April 19, 2017 Location 46 – compressive strength of 530 psi

Appendix H

Full Depth (175 mm) Penetration

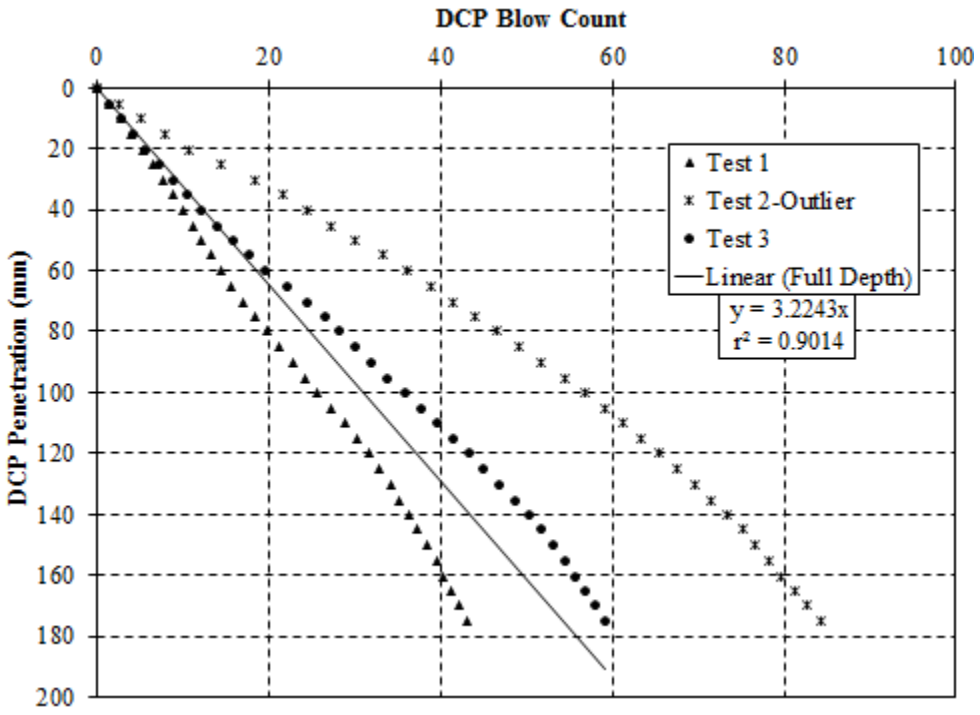

Figure H.1: Test conducted on November 1, 2016 Location 1 – compressive strength of 130 psi

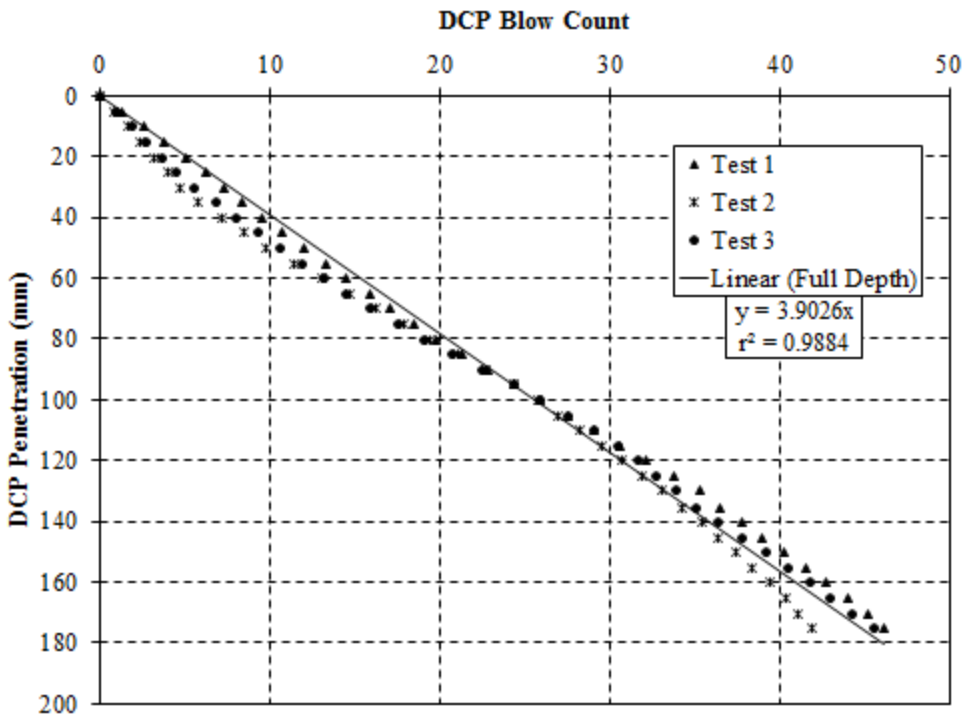

Figure H.2: Test conducted on November 1, 2016 Location 2 – compressive strength of 80 psi

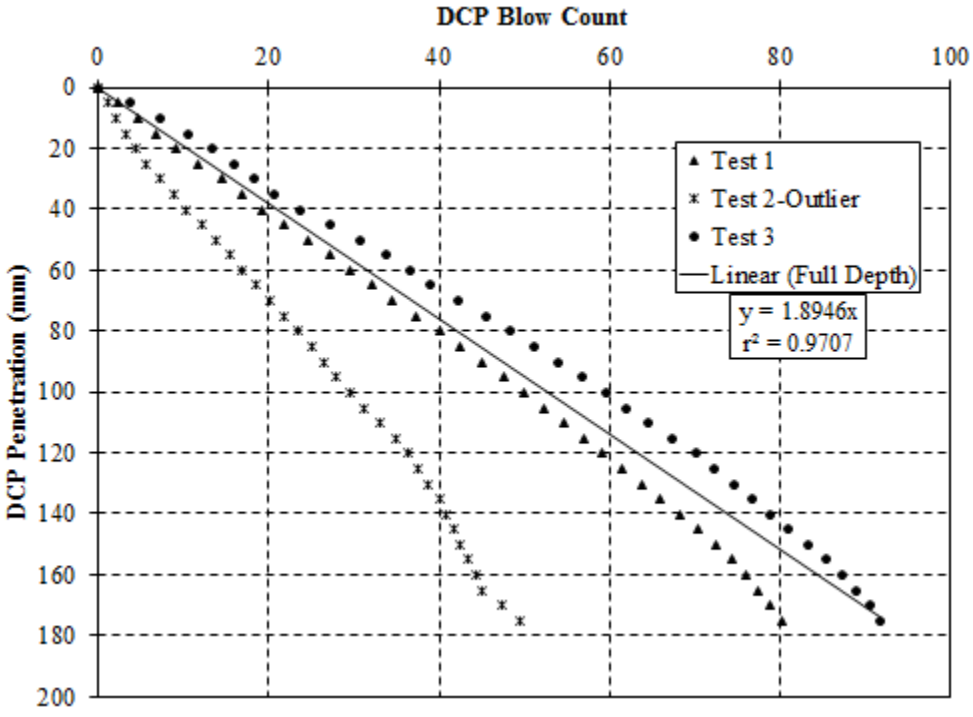

Figure H.3: Test conducted on November 7, 2016 Location 6 – compressive strength of 290 psi

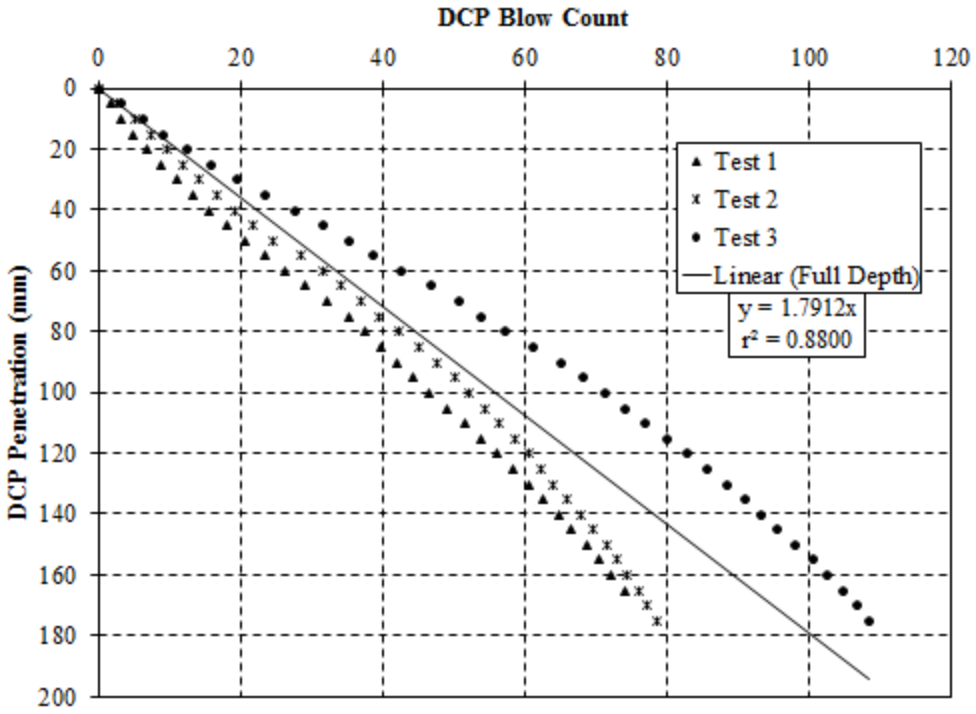

Figure H.4: Test conducted on November 7, 2016 Location 7 – compressive strength of 310 psi

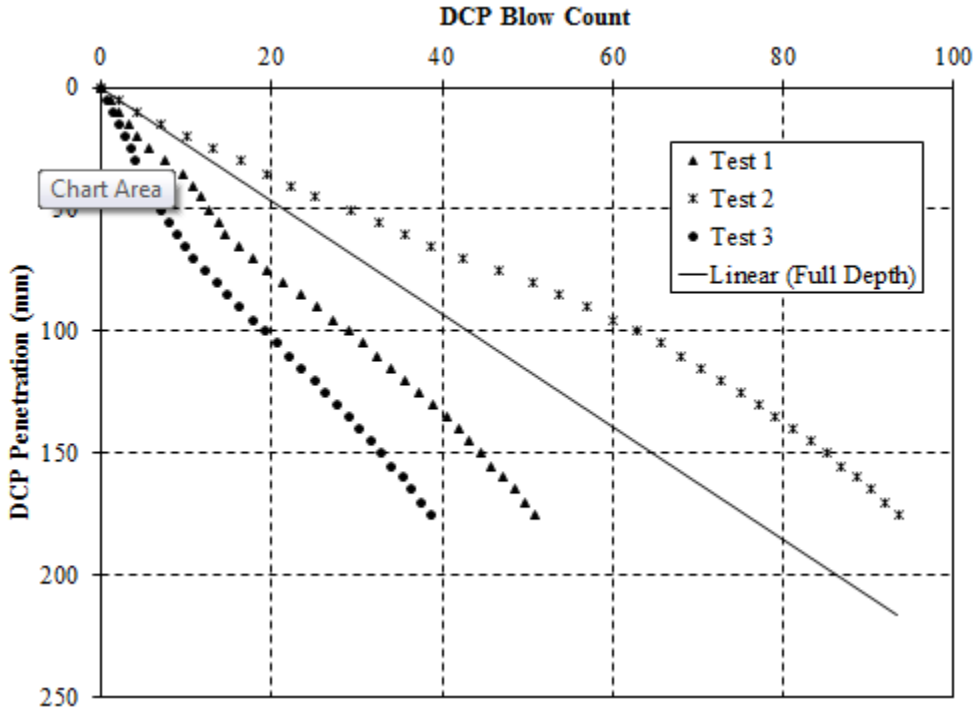

Figure H.5: Test conducted on November 22, 2017 Location 8 – range greater than 50 %

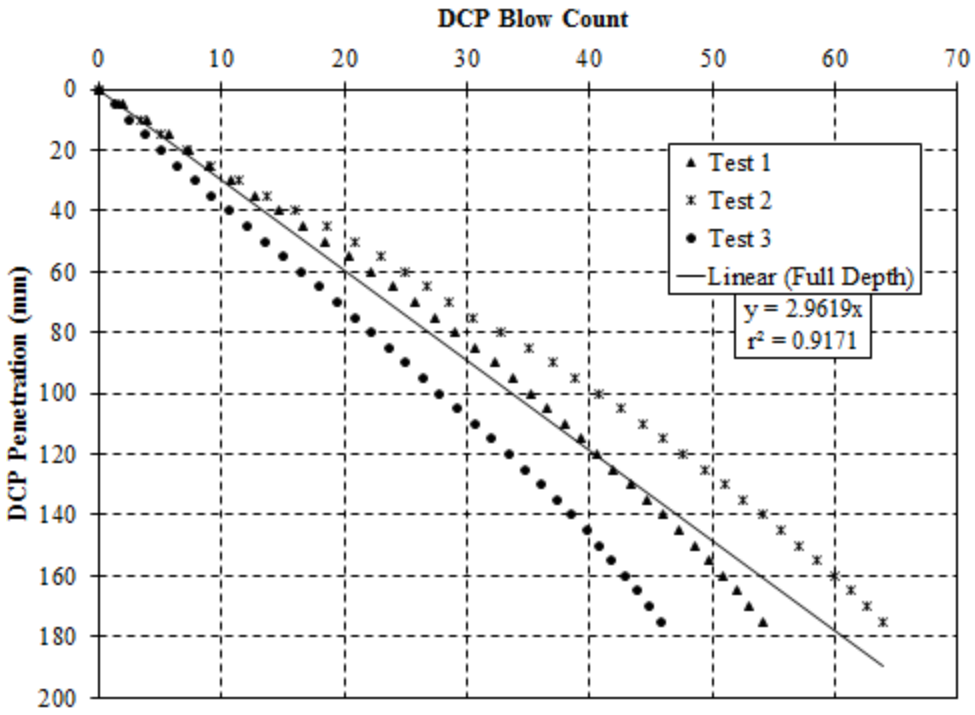

Figure H.6: Test conducted on November 22, 2017 Location 9 –compressive strength of 150 psi

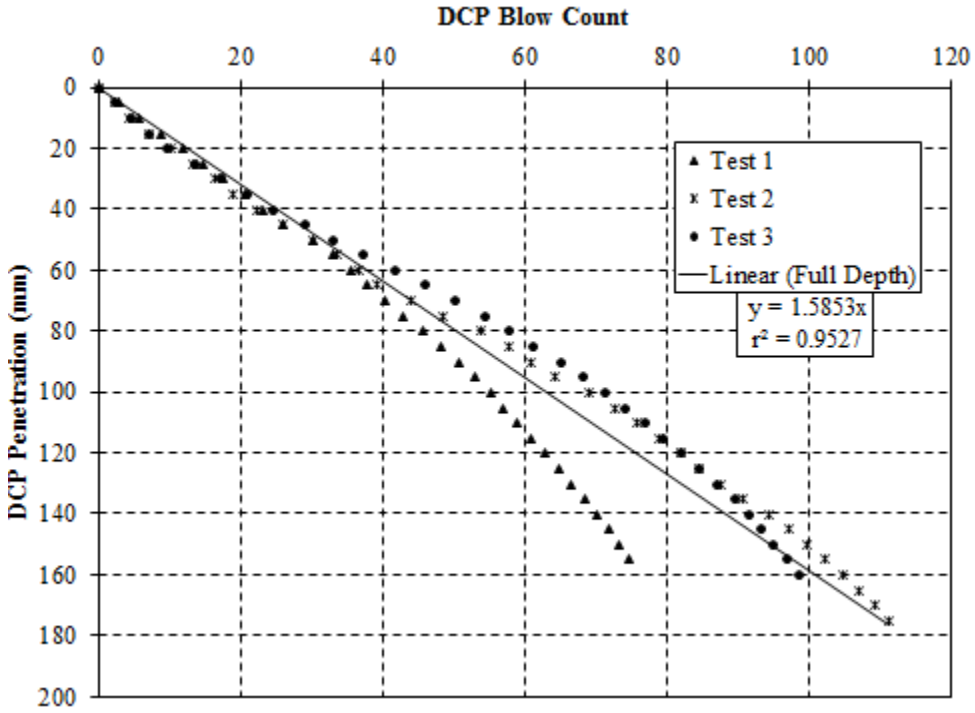

Figure H.7: Test conducted on November 22, 2017 Location 10 – compressive strength of 350 psi

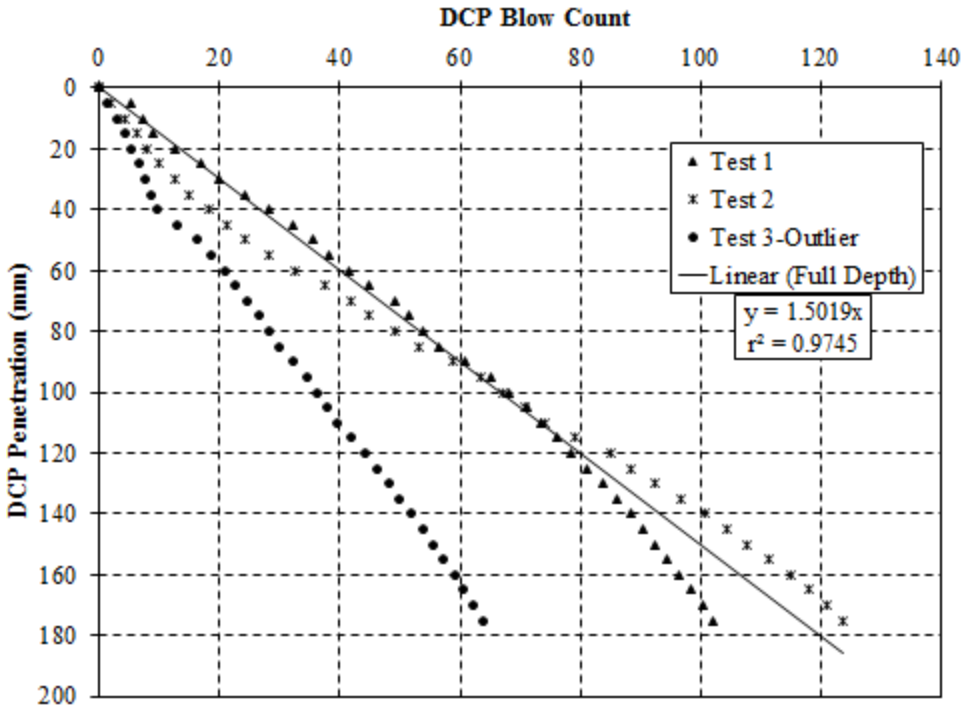

Figure H.8: Test conducted on November 22, 2016 Location 12–compressive strength of 370psi

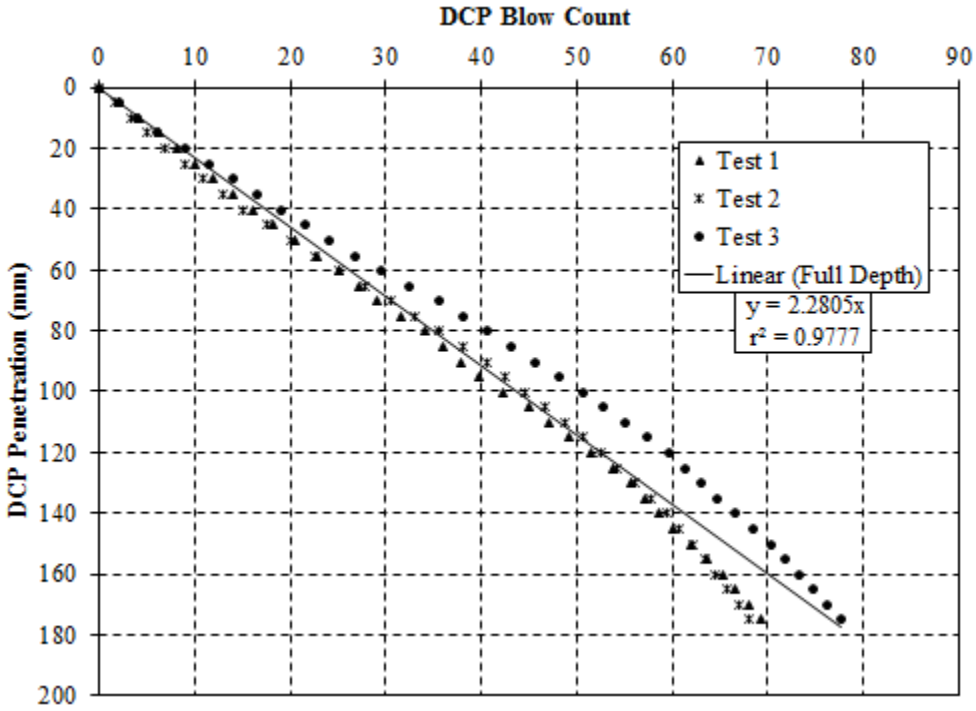

Figure H.9: Test conducted on November 22, 2016 Location 13–compressive strength of 230psi

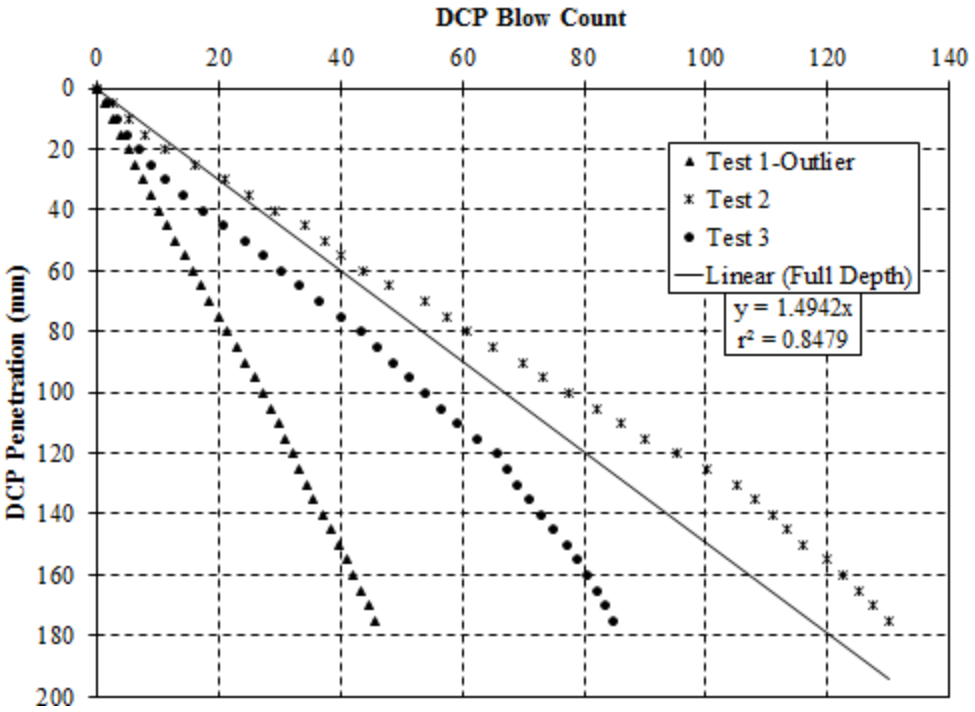

Figure H.10: Test conducted on November 23, 2016 Location 14-compressive strength of 370psi

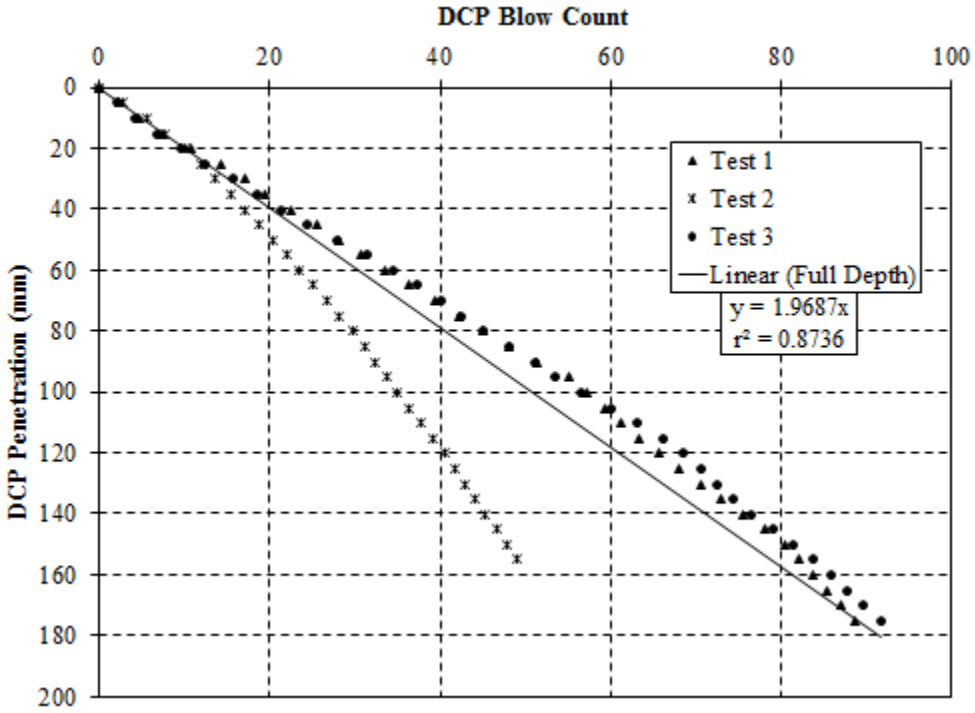

Figure H.11: Test conducted on November 23, 2016 Location 15-compressive strength of 280psi

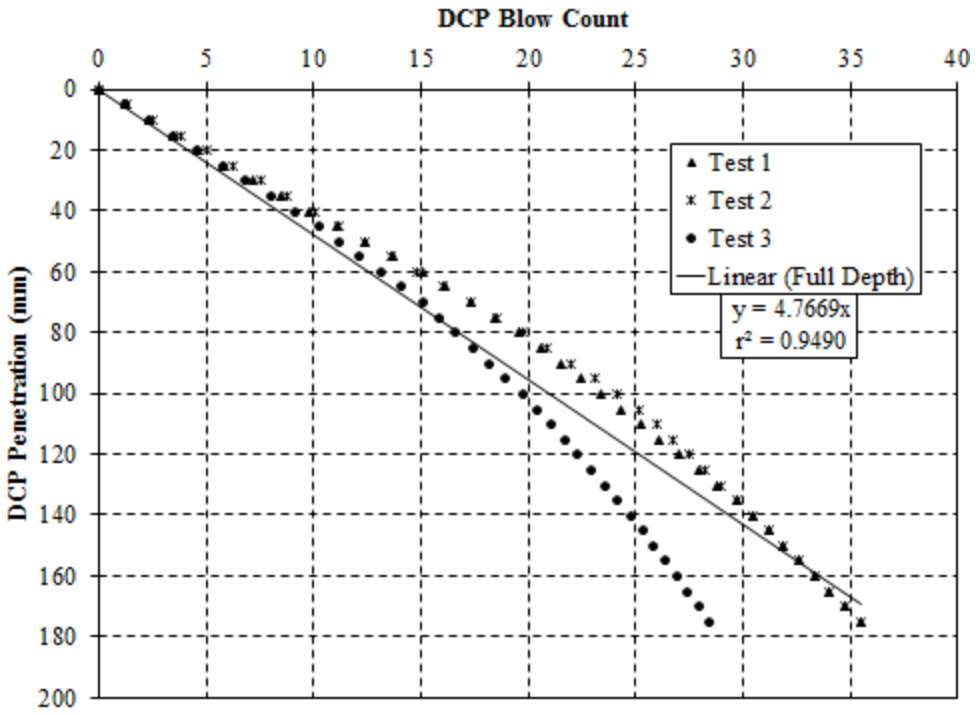

Figure H.12: Test conducted on November 23, 2016 Location 16-compressive strength of 50psi

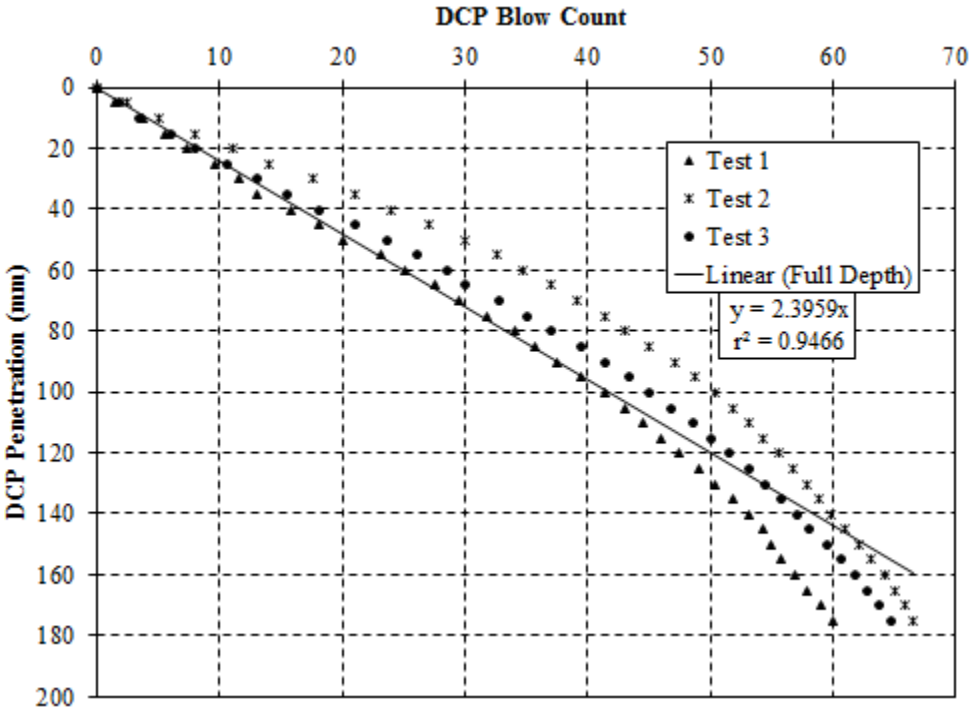

Figure H.13: Test conducted on March 23, 2017 Location 17– compressive strength of 210 psi

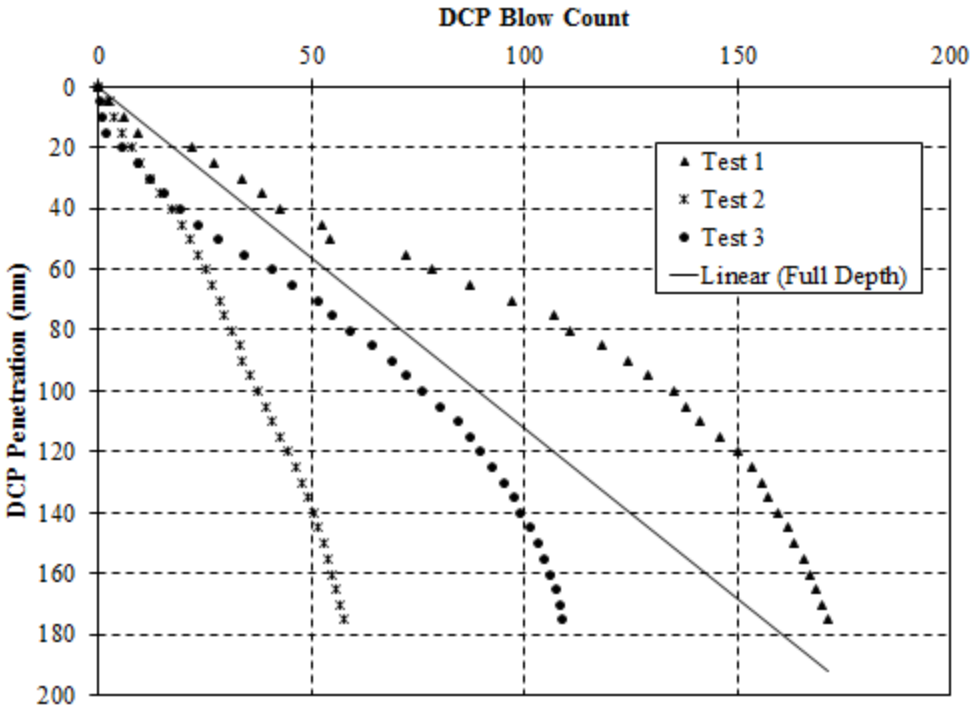

Figure H.14: Test conducted on March 23, 2017 Location 18 – range value greater than 50 %

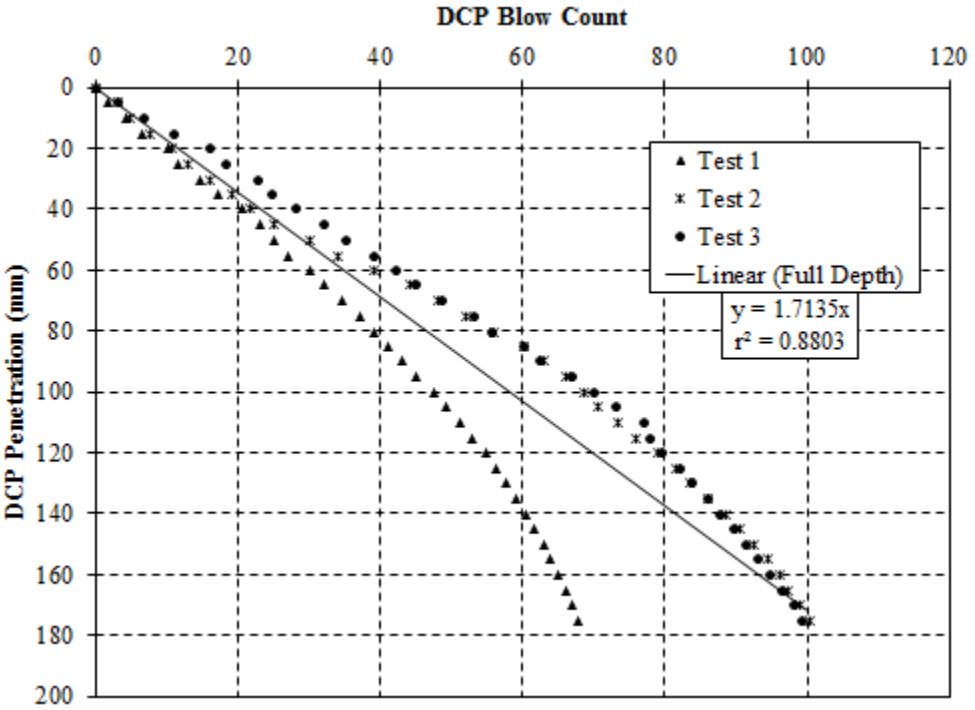

Figure H.15: Test conducted on March 23, 2017 Location 19 – compressive strength of 320 psi

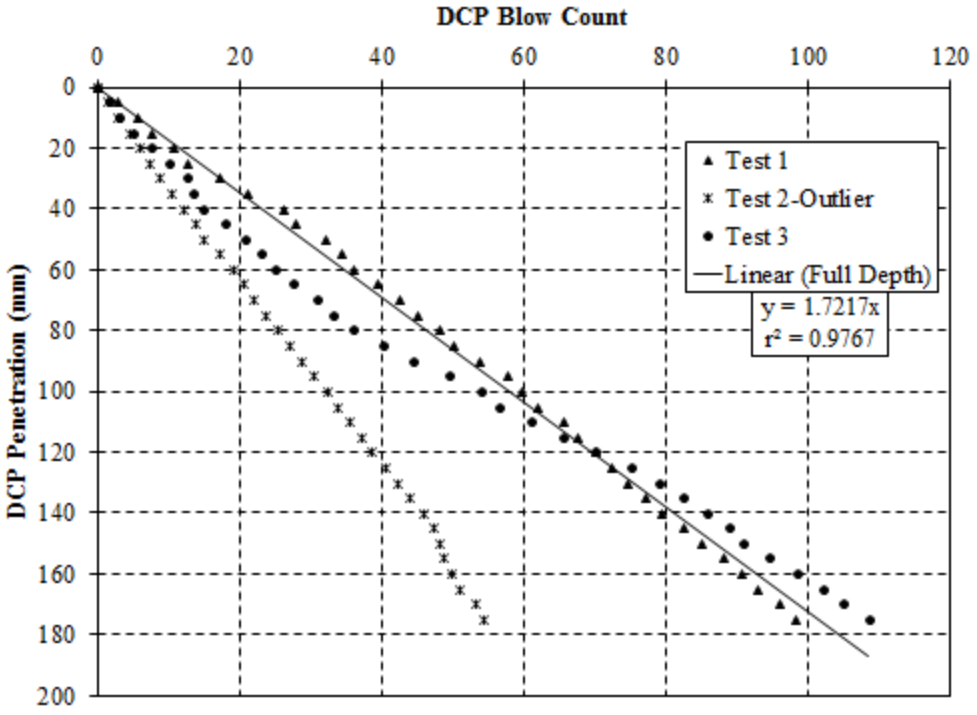

Figure H.16: Test conducted on March 27, 2017 Location 20 – compressive strength of 320 psi

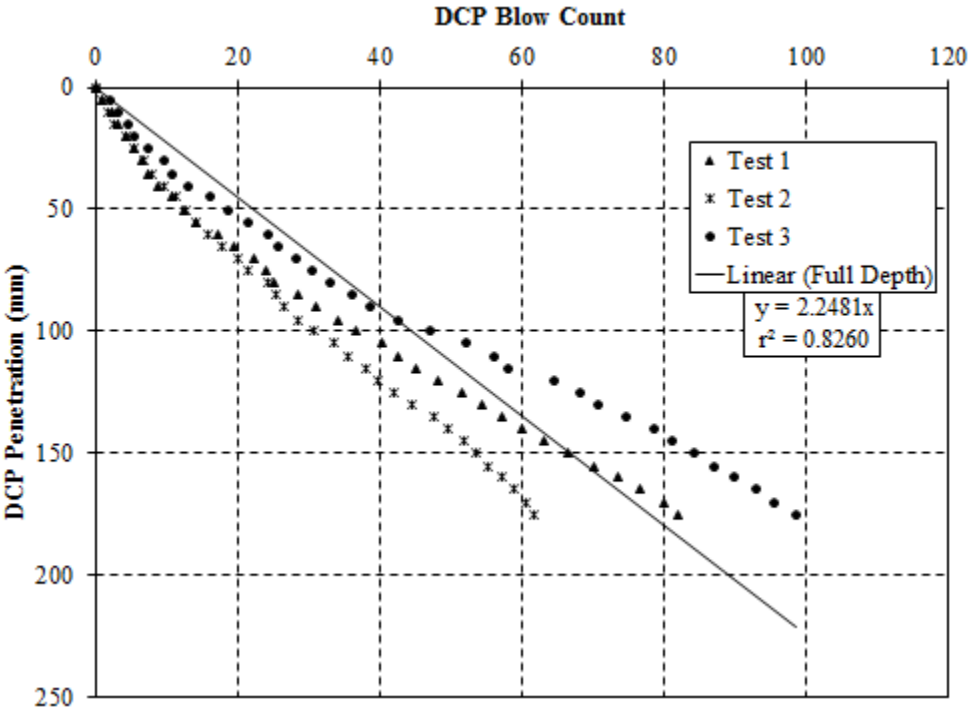

Figure H.17: Test conducted on March 27, 2017 Location 21 – compressive strength of 230 psi

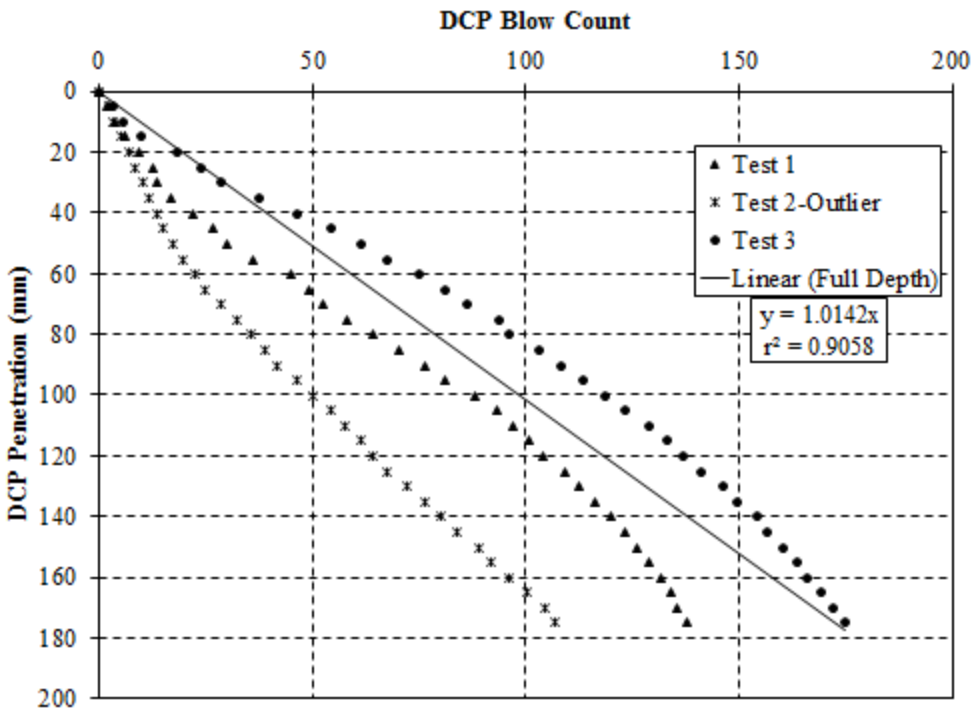

Figure H.18: Test conducted on March 27, 2017 Location 22 – compressive strength of 500 psi

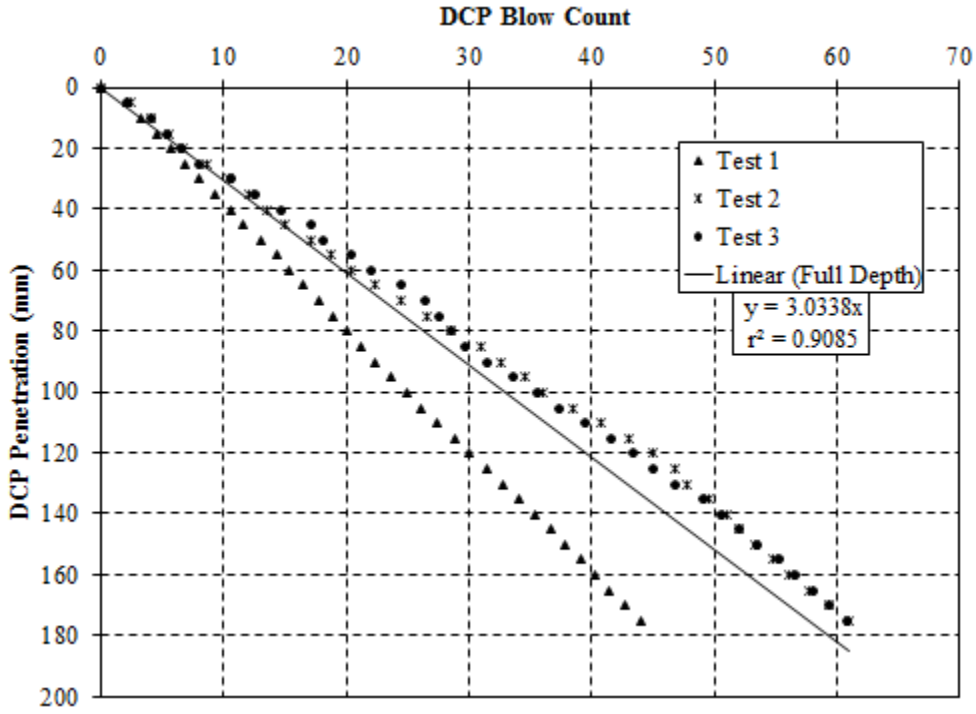

Figure H.19: Test conducted on March 30, 2017 Location 23 – compressive strength of 140 psi

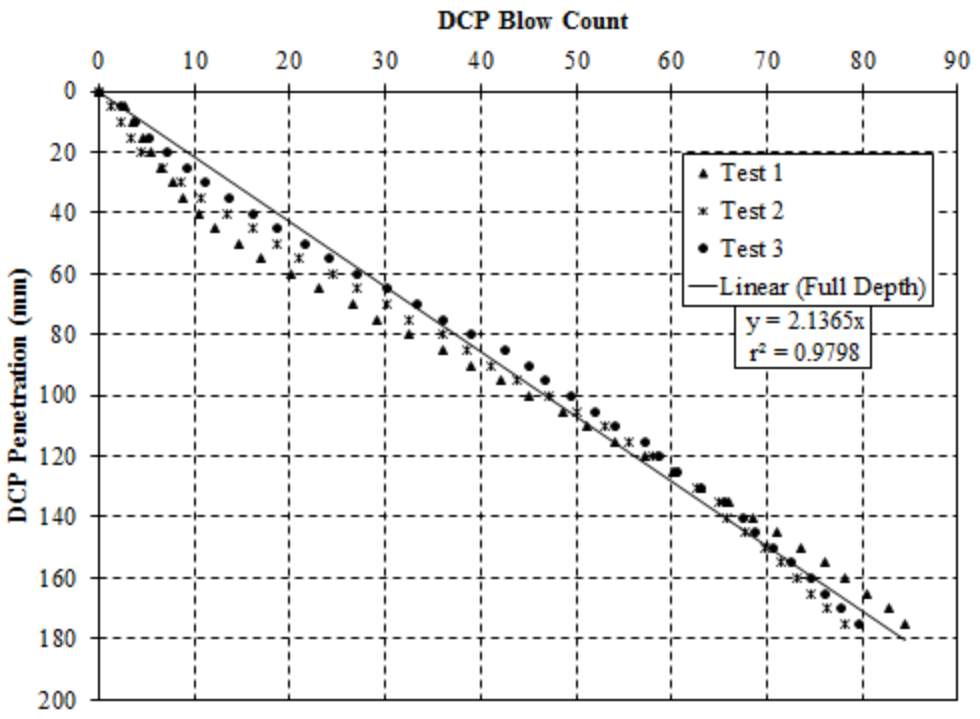

Figure H.20: Test conducted on March 30, 2017 Location 24 – compressive strength of 250 psi

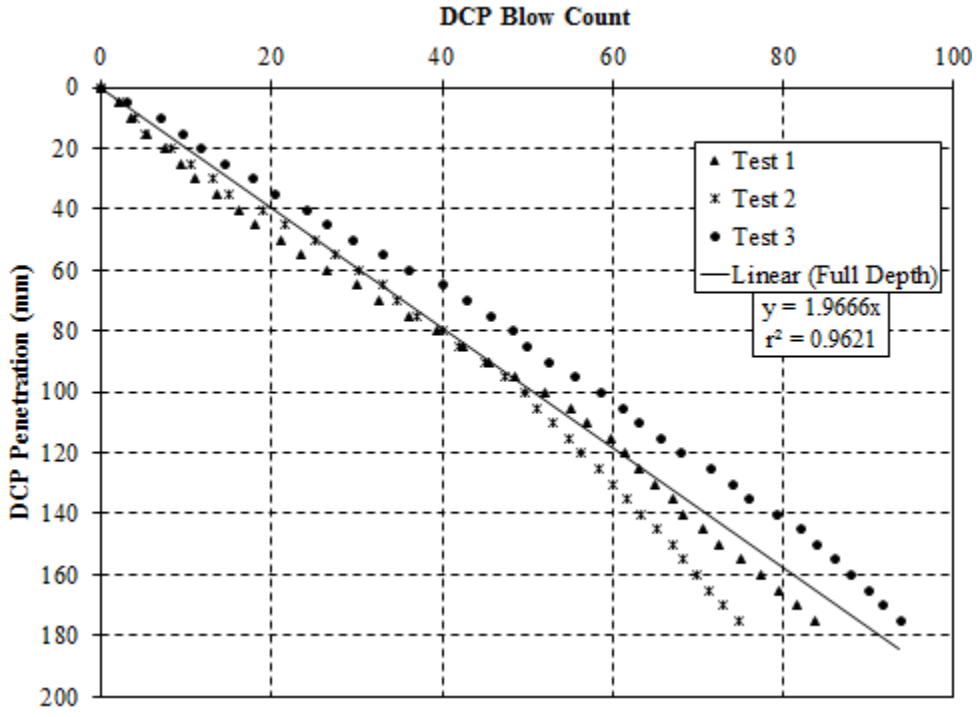

Figure H.21: Test conducted on March 30, 2017 Location 25 – compressive strength of 280 psi

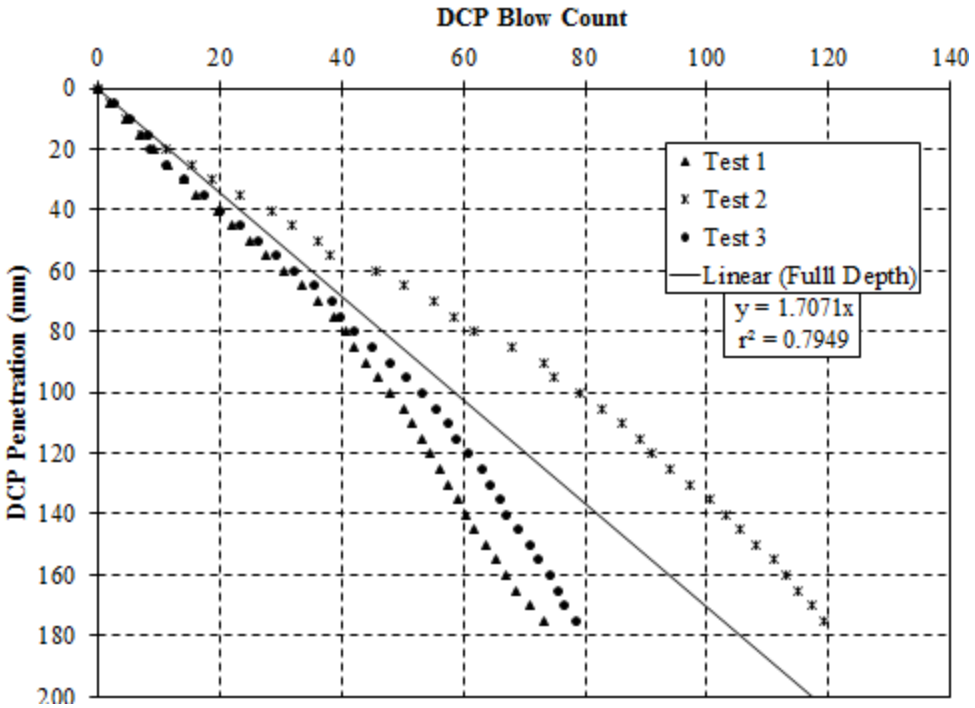

Figure H.22: Test conducted on March 31, 2017 Location 26 – compressive strength of 320 psi

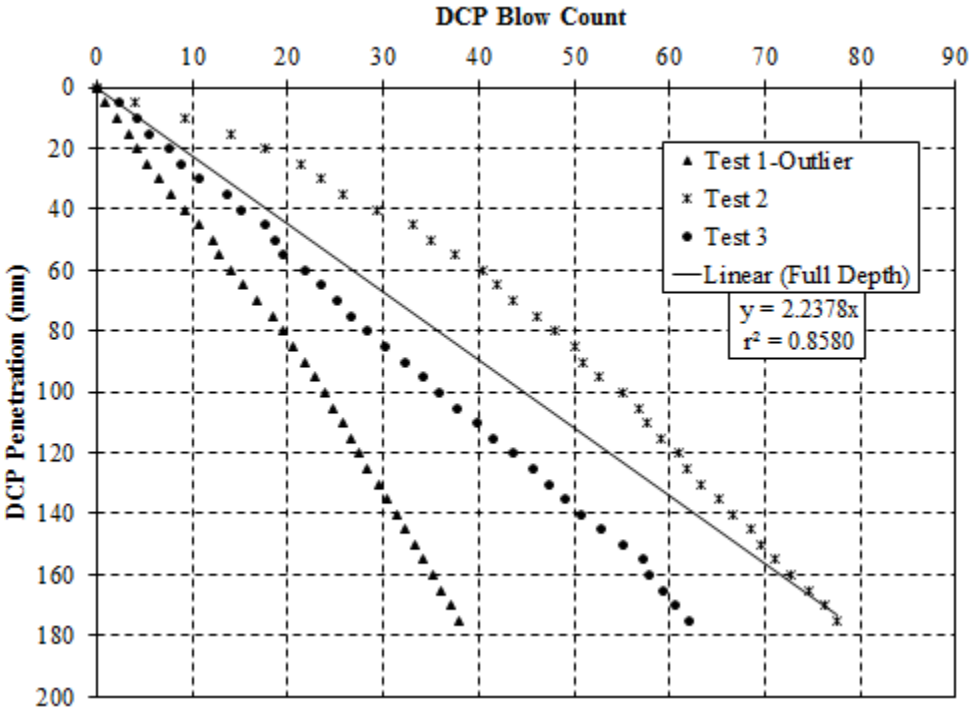

Figure H.23: Test conducted on March 31, 2017 Location 27 – compressive strength of 230 psi

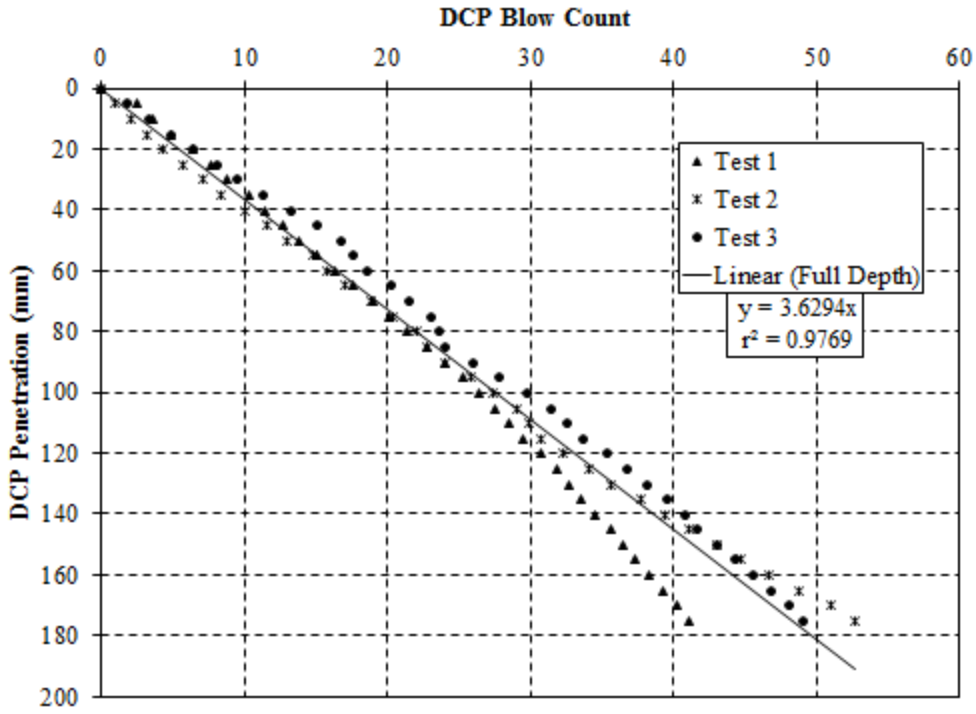

Figure H.24: Test conducted on March 31, 2017 Location 28 – compressive strength of 100 psi

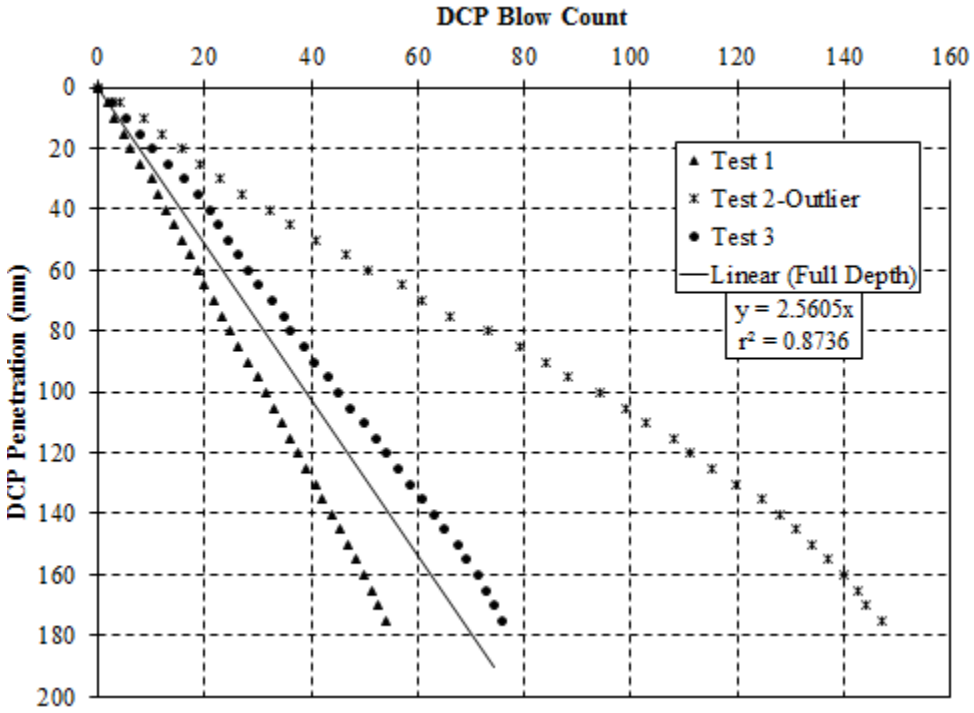

Figure H.25: Test conducted on April 3, 2017 Location 29 – compressive strength of 190 psi

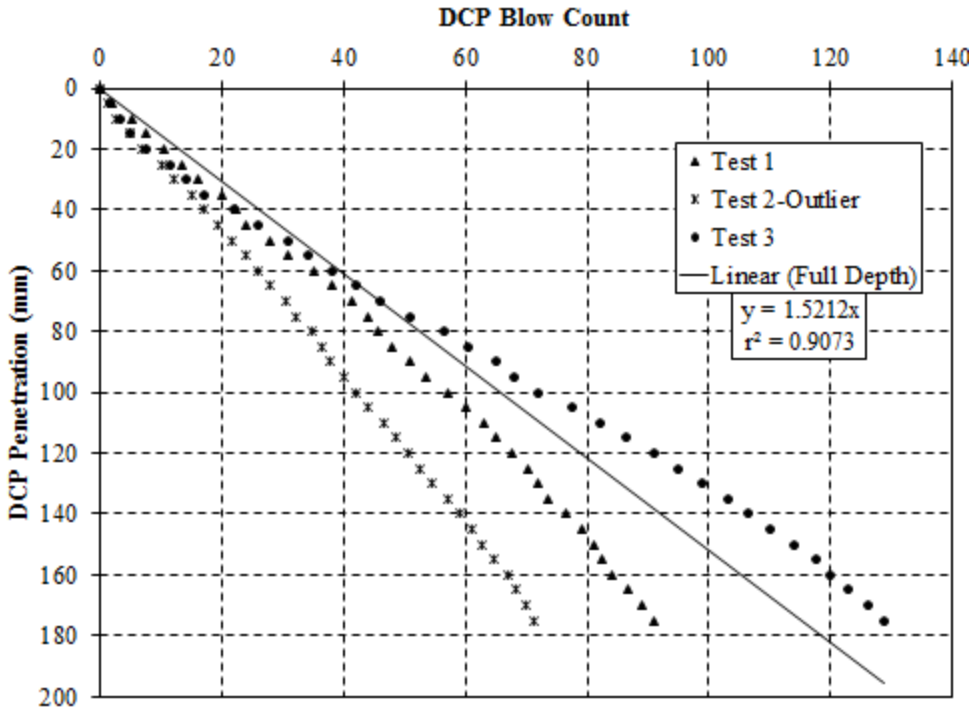

Figure H.26: Test conducted on April 3, 2017 Location 30 – compressive strength of 360 psi

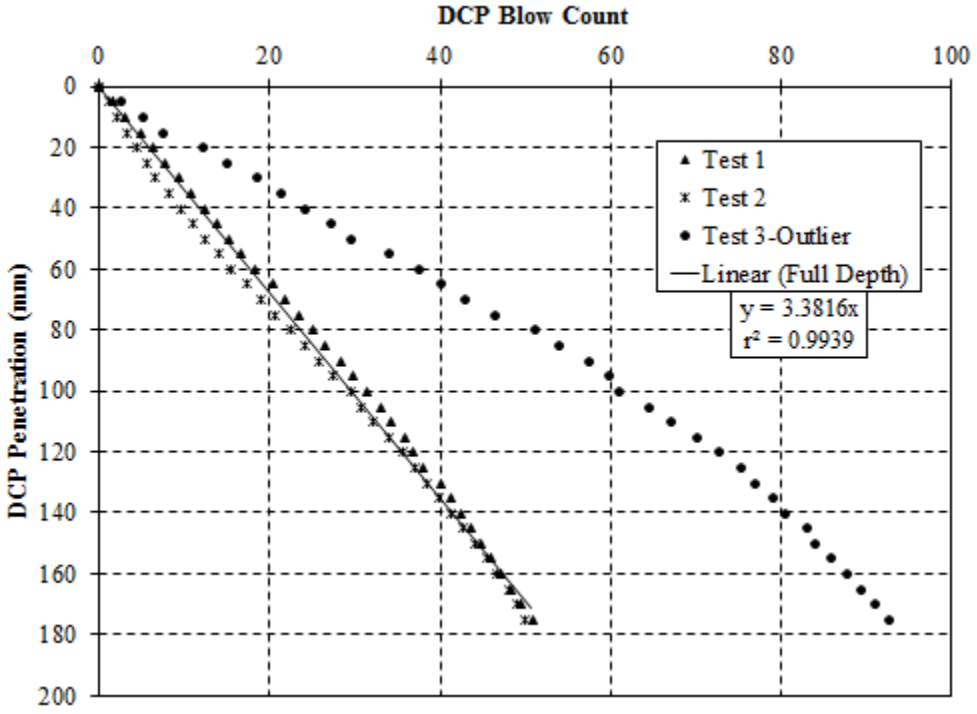

Figure H.27: Test conducted on April 3, 2017 Location 31 – compressive strength of 120 psi

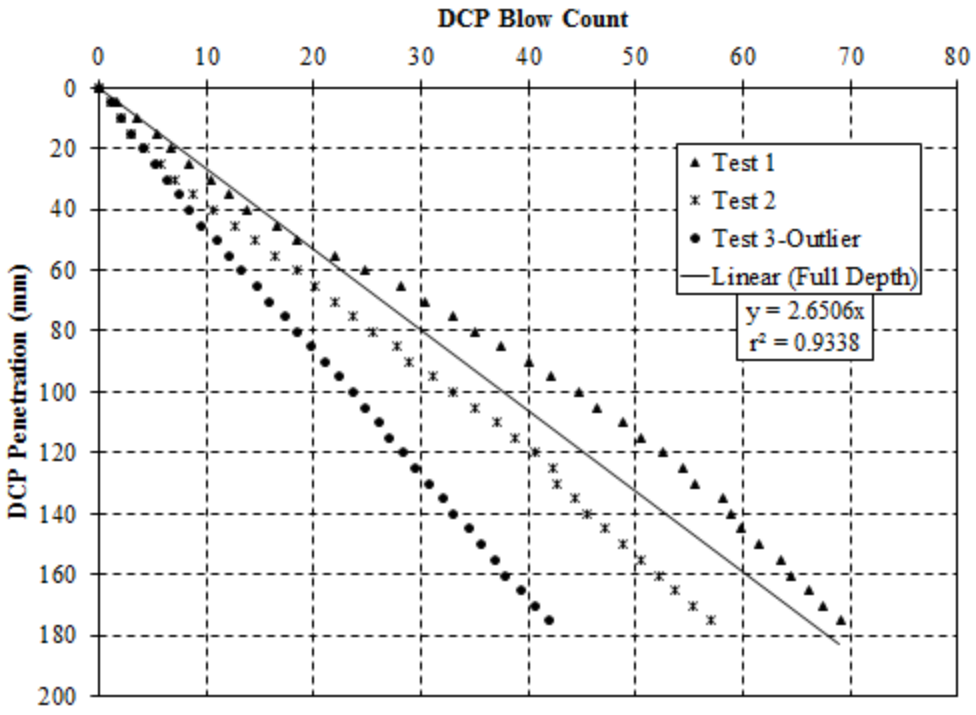

Figure H.28: Test conducted on April 5, 2017 Location 32 – compressive strength of 180 psi

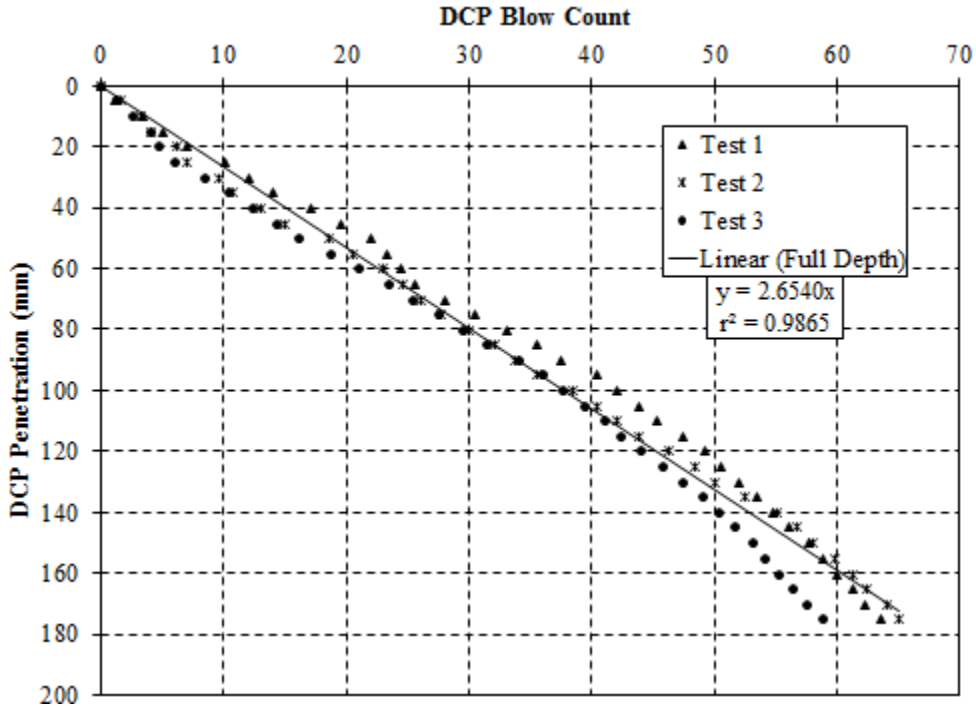

Figure H.29: Test conducted on April 5, 2017 Location 33 – compressive strength of 180 psi

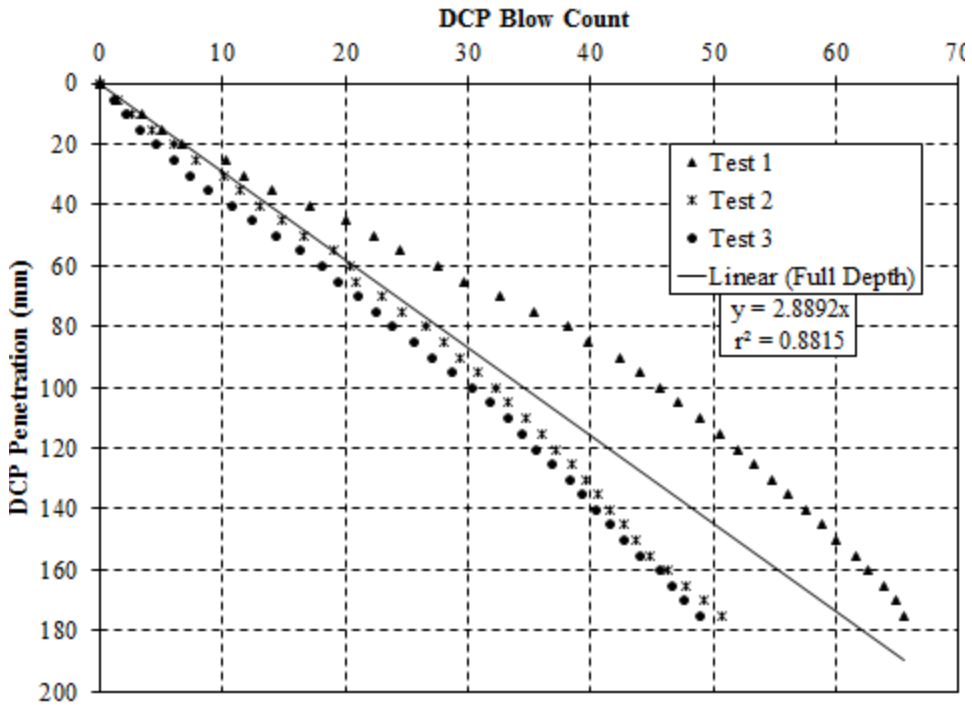

Figure H.30: Test conducted on April 5, 2017 Location 34 – compressive strength of 160 psi

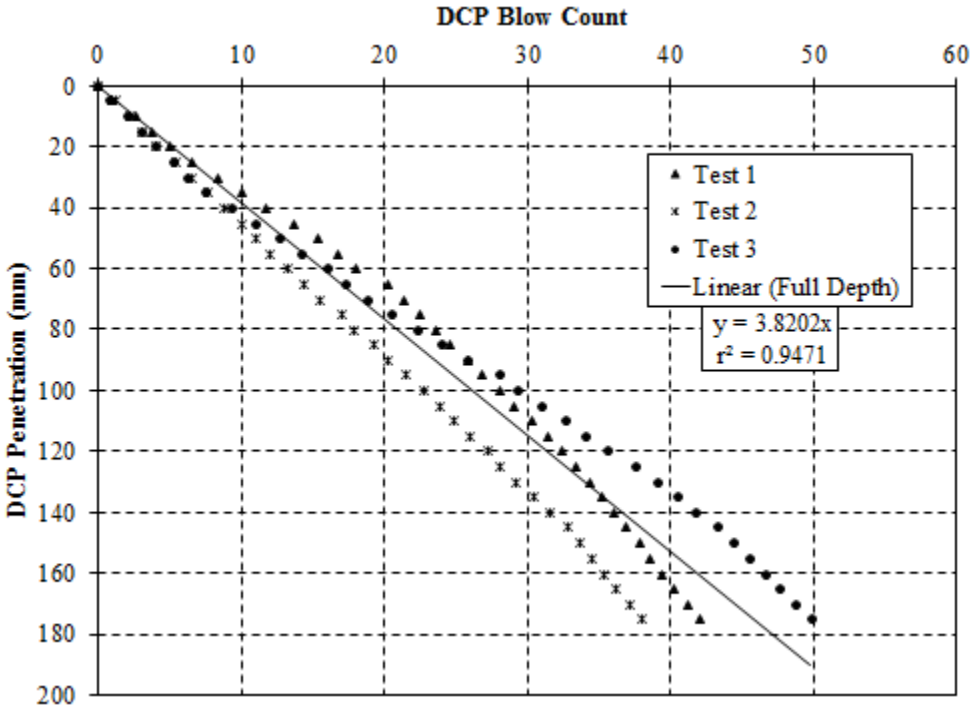

Figure H.31: Test conducted on April 5, 2017 Location 35 – compressive strength of 90 psi

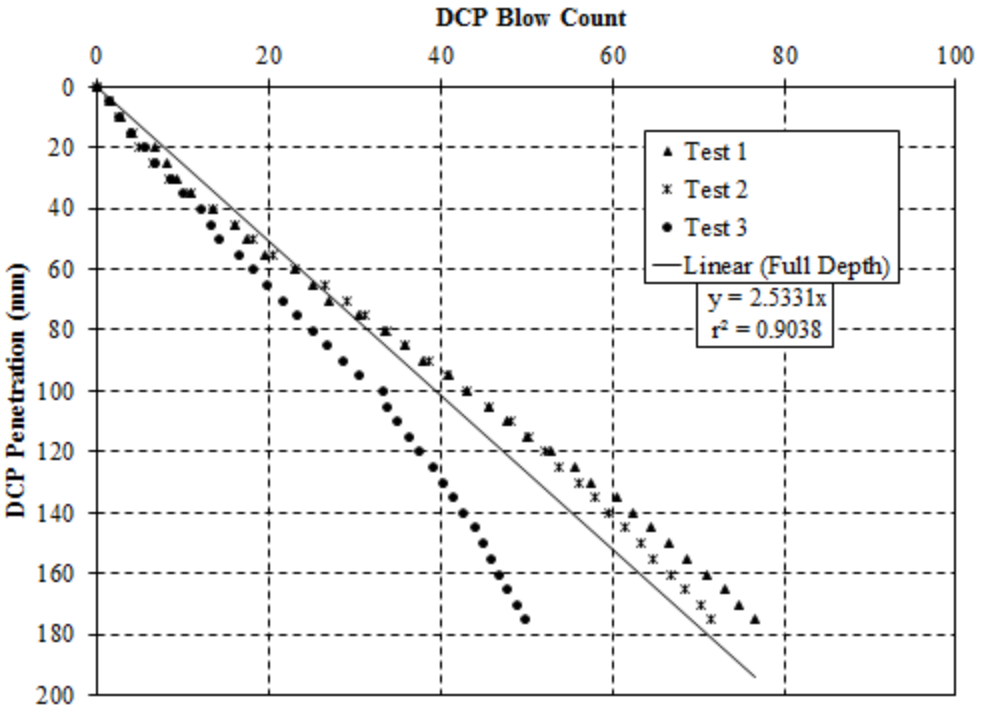

Figure H.32: Test conducted on April 5, 2017 Location 36 – compressive strength of 200 psi

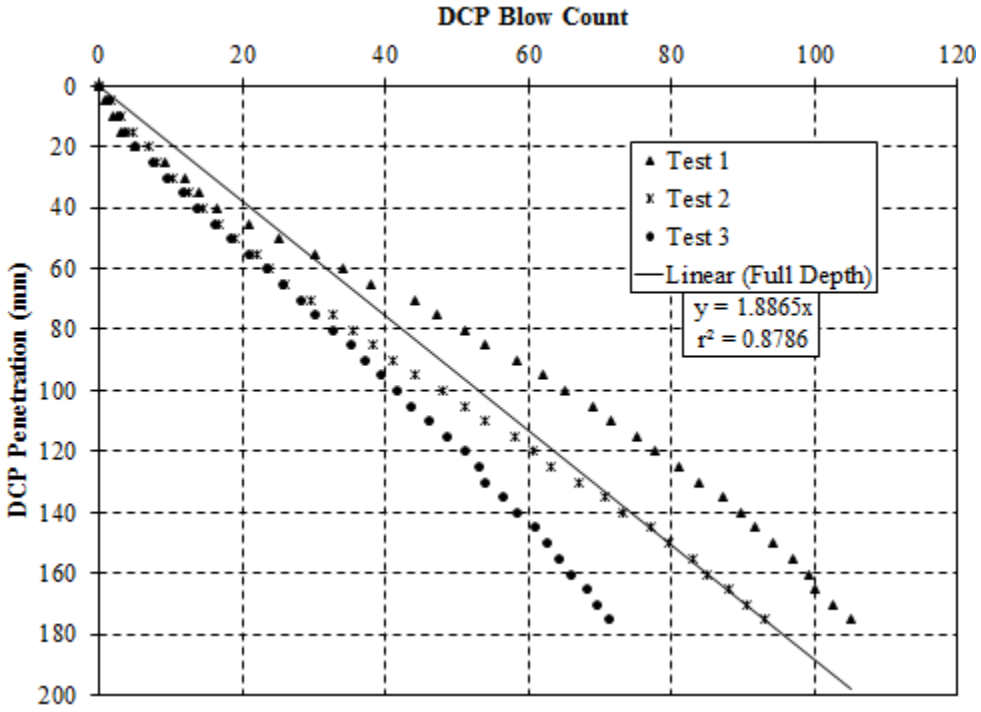

Figure H.33: Test conducted on April 5, 2017 Location 37 – compressive strength of 290 psi

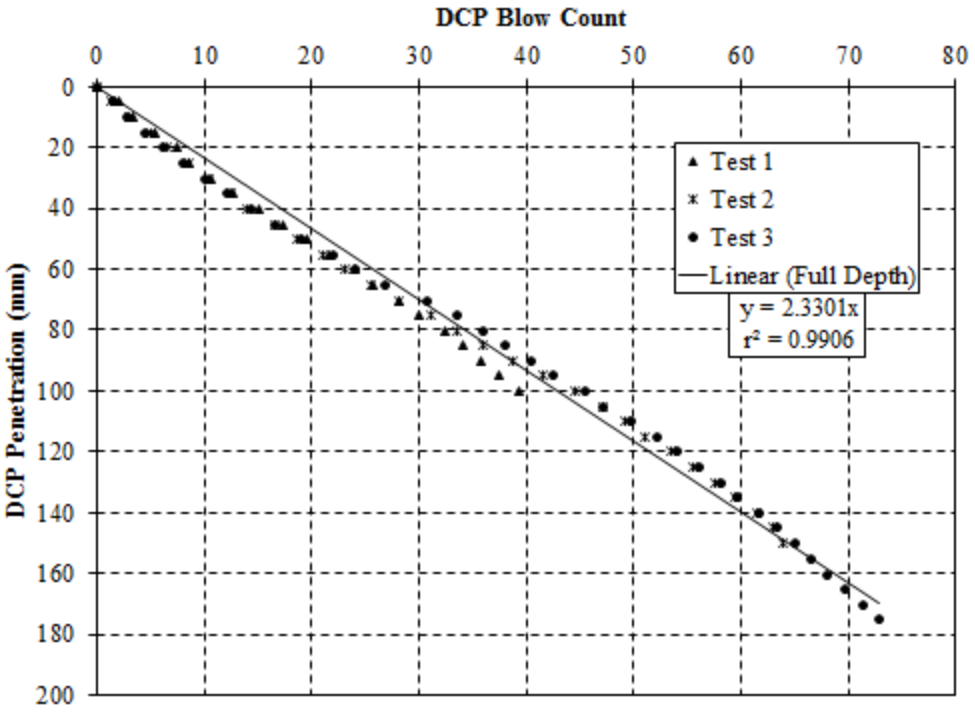

Figure H.34: Test conducted on April 6, 2017 Location 38 – compressive strength of 220 psi

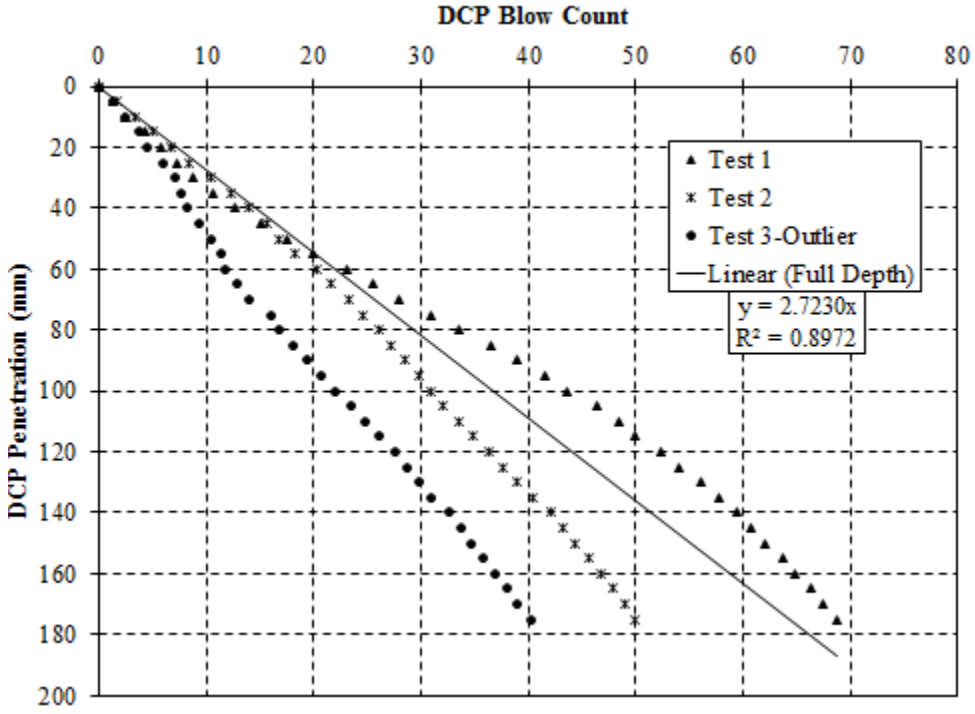

Figure H.35: Test conducted on April 6, 2017 Location 40 – compressive strength of 170 psi

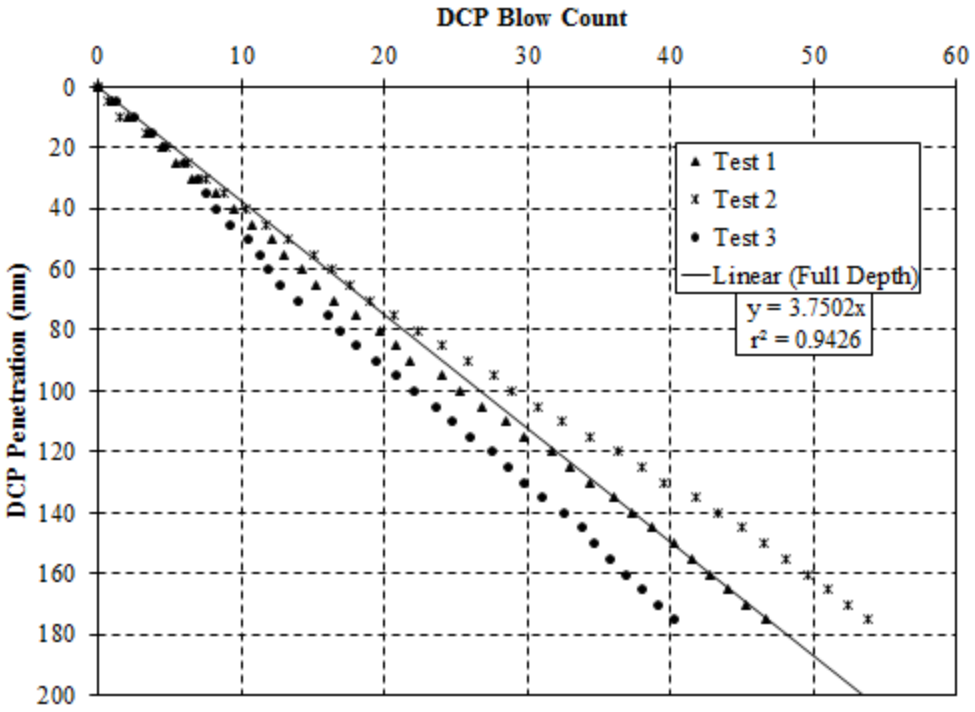

Figure H.36: Test conducted on April 19, 2017 Location 41 – compressive strength of 90 psi

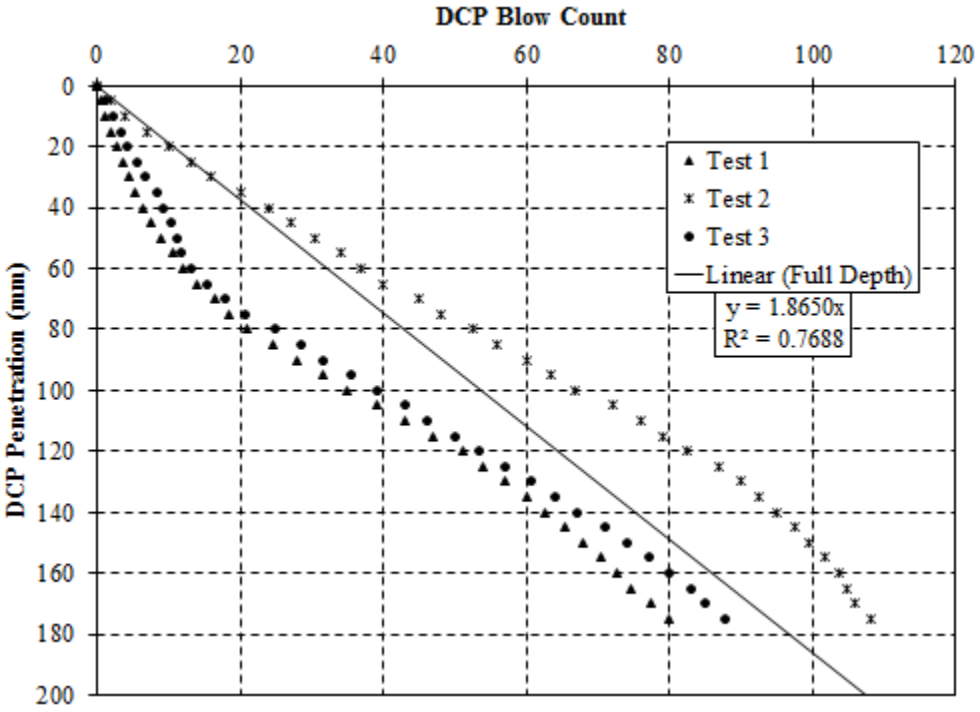

Figure H.37: Test conducted on April 19, 2017 Location 42 – compressive strength of 290 psi

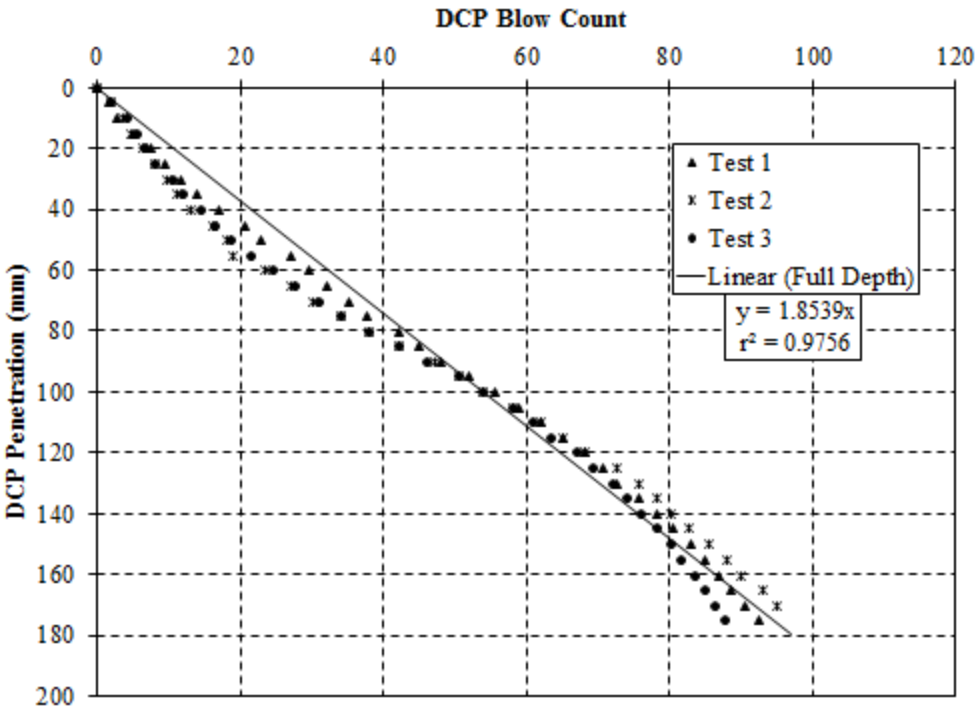

Figure H.38: Test conducted on April 19, 2017 Location 43 – compressive strength of 300 psi

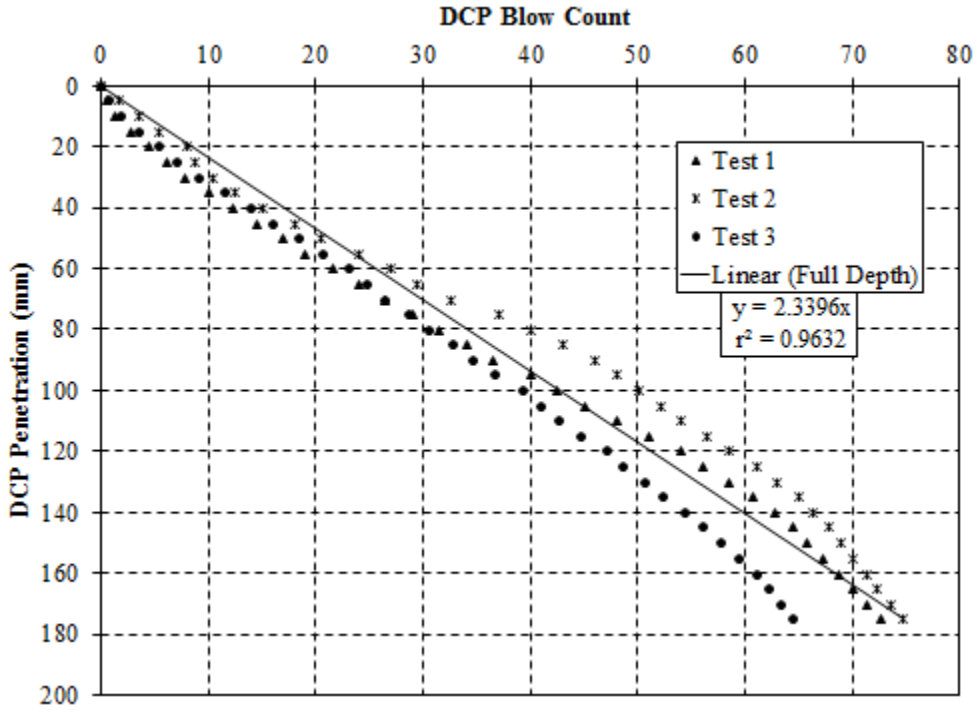

Figure H.39: Test conducted on April 19, 2017 Location 44 – compressive strength of 220 psi

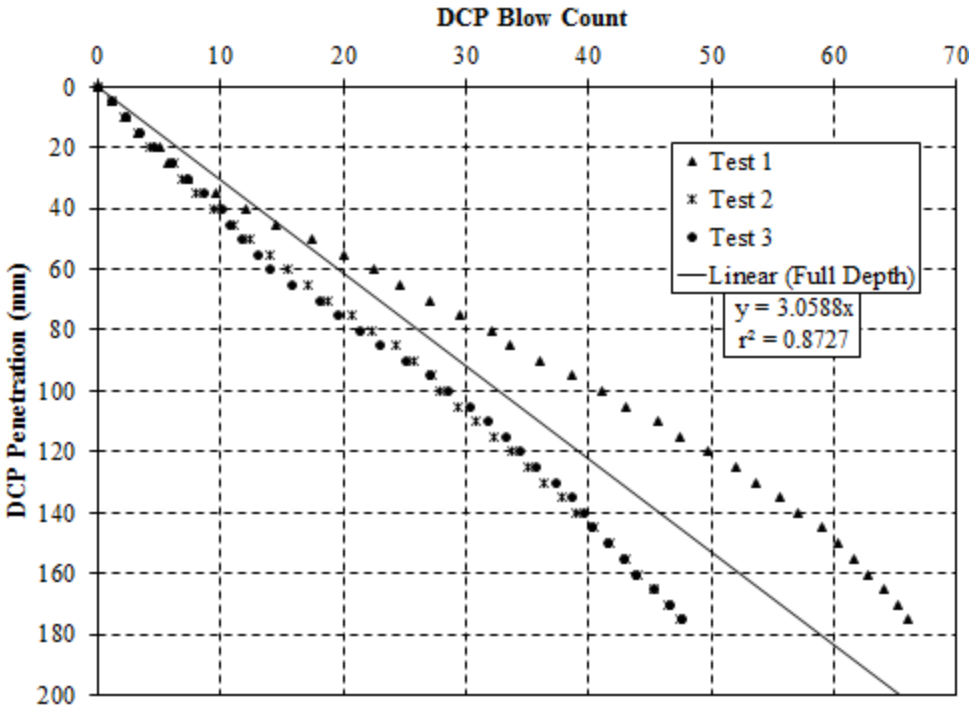

Figure H.40: Test conducted on April 19, 2017 Location 45 – compressive strength of 140 psi

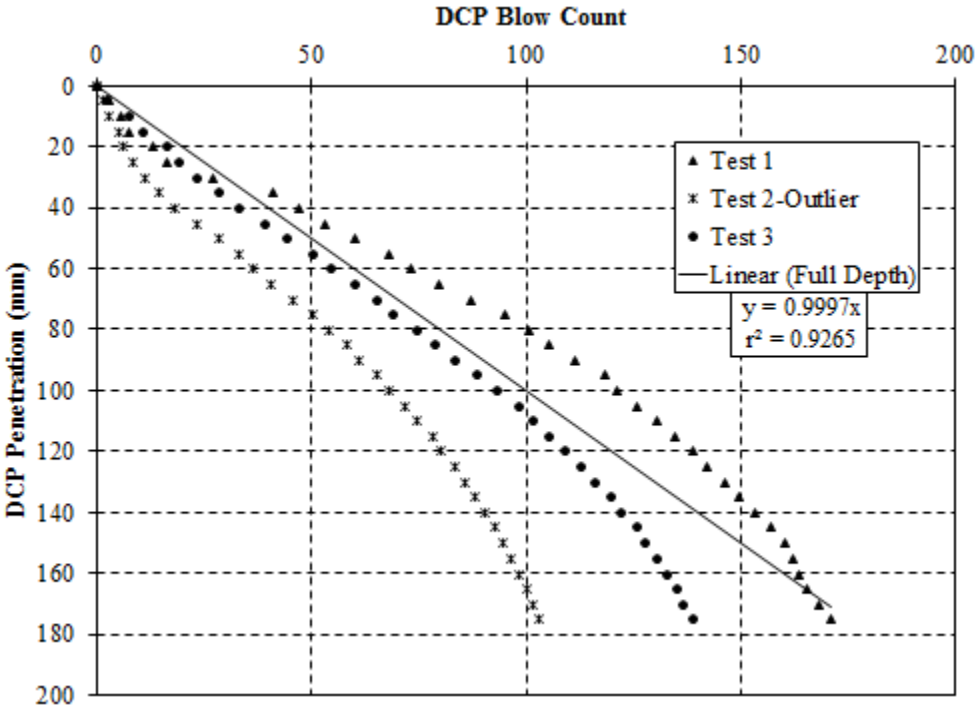

Figure H.41: Test conducted on April 19, 2017 Location 46 – compressive strength of 500 psi

Appendix I

Core Results